

**Transition metal complexes of some bis(thiosemicarbazones) derived  
from 2,6-diacetylpyridine and  $N^4$ -substituted thiosemicarbazides:  
Synthesis, spectral and structural studies**

*Thesis submitted to*

**COCHIN UNIVERSITY OF SCIENCE AND TECHNOLOGY**

*In partial fulfillment of the requirements  
for the degree of*

**DOCTOR OF PHILOSOPHY**

**Under the Faculty of Science**

by

**Suja Krishnan**



**DEPARTMENT OF APPLIED CHEMISTRY  
COCHIN UNIVERSITY OF SCIENCE AND TECHNOLOGY  
KOCHI 682 022  
INDIA**

**June 2008**

**Transition metal complexes of some bis(thiosemicarbazones) derived from 2,6-diacetylpyridine and  $N^4$ -substitutedthiosemicarbazides: Synthesis, spectral and structural studies**

**Ph. D. Thesis under the Faculty of Science**

**Author:**

**Suja Krishnan**

Research fellow, Department of Applied Chemistry

Cochin university of Science and Technology

Kochi, India

E mail: sujakrishnan@cusat.ac.in

**Research advisor:**

**Dr. M. R. Prathapachandra Kurup**

Professor

Department of Applied Chemistry

Cochin University of Science and Technology

Kochi, India

Email: mrp@cusat.ac.in

Department of Applied Chemistry,  
Cochin University of Science and Technology  
Kochi, India

June 2008

**Front cover:** Crystal Structure of zinc (II) complex of 2,6-diacetylpyridine bis( $N^4$ -cyclohexylthiosemicarbazone)

*... to my*

*Achan*



Phone Off. 0484-2575804  
Phone Res. 0484-2576904  
Telex: 885-5019 CUIN  
Fax: 0484-2577595  
Email: [mrp@cusat.ac.in](mailto:mrp@cusat.ac.in)  
[mrp\\_k@yahoo.com](mailto:mrp_k@yahoo.com)

**DEPARTMENT OF APPLIED CHEMISTRY  
COCHIN UNIVERSITY OF SCIENCE AND  
TECHNOLOGY  
KOCHI 682 022, INDIA**

---

**Dr. M.R. Prathapachandra Kurup  
Professor**

04<sup>th</sup> June 2008

---

**CERTIFICATE**

This is to certify that the thesis entitled “**Transition metal complexes of some bis(thiosemicarbazones) derived from 2,6-diacetylpyridine and  $N^4$ -substituted thiosemicarbazides: Synthesis, spectral and structural studies**” submitted by Ms. Suja Krishnan, in partial fulfillment of the requirements for the degree of Doctor of Philosophy, to the Cochin University of Science and Technology, Kochi-22, is an authentic record of the original research work carried out by her under my guidance and supervision. The results embodied in this thesis, in full or in part, have not been submitted for the award of any other degree.

**M. R. Prathapachandra Kurup**

## DECLARATION

I hereby declare that the work presented in this thesis entitled **“Transition metal complexes of some bis(thiosemicarbazones) derived from 2,6-diacetylpyridine and  $N^4$ -substituted thiosemicarbazides: Synthesis, spectral and structural studies”** is entirely original and was carried out independently under the supervision of Professor M. R. Prathapachandra Kurup, Department of Applied Chemistry, Cochin University of Science and Technology and has not been included in any other thesis submitted previously for the award of any other degree.

04-06-'08

Kochi 22

  
Suja Krishnan

## ACKNOWLEDGEMENTS

*I remember with gratitude ...*

*My supervising guide, Dr. M. R. Prathapachandra Kurup, Professor, for his guidance, valuable suggestions and comments. His sincerity and commitment to work and tremendous support has been a steady source of inspiration for me. I was able to persevere, complete the research and deliver this thesis because of his able guidance and immense patience. I cherish the period of learning under him. He is a real supervisor and a great teacher.*

*Dr. K. Girish Kumar, Head of the department, for his support and valuable suggestions.*

*Dr. P.V. Mohanan, for his support as my doctoral committee member.*

*The support received from all the teaching and non-teaching staff of the Dept. of Applied Chemistry, CUSAT.*

*Dr. E. Suresh, CSMCRJ, Gujarat, for single crystal X-ray diffraction studies.*

*Head of the Institutions, SAIK Kochi, IISc Bangalore, IIT Roorkee and IIT Bombay, for the services rendered the institutions in sample analyses.*

*My dearest seniors, Dr. Rohit P. John, Dr. Sreeja P.B., Dr. Suni V., Dr. Seena E.B., Dr. P.F. Rapheal, Mini, Bessy, Sreesha, Manoj, Leji and Binu, for their help and valuable suggestions throughout my research work,*

*My labmates, Sheeja, Nancy, Laly miss, Renjusha, Reena, Neema, Sarika, Dhanya, Jessy miss, Anie miss, Jayakumar sir, Shimi and Ananya, for providing a friendly work atmosphere.*

*All my friends, especially Manju, Reshmi, Roshini, Arun, Kannan, Prem, Kala miss, Ajitha miss, Jitha, Ananthan and Prajas, for their friendship and support.*

*My Prabha chechy, for her sisterly affection, help and encouragement. She had been always with me, whenever I needed help and for making my life in CUSAT memorable.*

*My parents and brother, for their prayers and support that kept and still keep on going. The pains they have taken all through these long years, is beyond words.*

*My in-laws, for their love, affection and encouragement.*

*My husband Shine, for being there always as a source of energy, all through these years and for letting me persevere. I would not have been able to complete this work without his wholehearted support and constant encouragement.*

*Above all, I kneel down before God Almighty, for the blessings showering over me.*

*Suja Krishnan*

## PREFACE

---

The importance of coordination complexes in our day to day life is increasing due to their complex structures and interesting magnetic, electronic and optical properties. Twentieth century witnessed the development of Alfred Werner's coordination chemistry as one of the most productive areas of research. He developed the modern theory of coordination compounds in 1892, explaining two types of valencies for the metal. Since then the field of coordination chemistry has been widely explored. The number, variety and complexity of coordination compounds still continue to grow. The stereochemistry of coordination compounds is one of the major interests of the coordination chemist. Coordination complexes can assume a wide variety of structures depending on the metal ion, its coordination number and the denticity of the ligands used. The ligands also range from monodentate to polydentate based on the potential donor sites available in their structural skeleton.

Metal complexes of thiosemicarbazones with aldehydes and ketones have been widely reported. But there have been fewer reports on potential pentadentate bis(thiosemicarbazones) formed from 2,6-diacetylpyridine. This work stems from our interests in the coordination behaviour as well as the structure of the metal complexes of bis(thiosemicarbazones). The primary aim of this investigation was to synthesize and characterize some transition metal complexes using the ligands 2,6-diacetylpyridine bis(*N*<sup>4</sup>-substitutedthiosemicarbazones). Complexation with metal ions like copper, manganese, nickel, palladium, zinc and cadmium were tried. Various spectral techniques were employed for characterization. The structure of one complex has been well established by single crystal X-ray diffraction studies.



The work is presented in six chapters and the last section deals with summary and conclusion. Chapter 1 involves a brief foreword of the metal complexes of bis(thiosemicarbazones) including their bonding, stereochemistry and biological activities. The different analytical and spectroscopic techniques used for the analysis of the ligands and their complexes are discussed in this chapter. Chapter 2 deals with the synthesis and spectral characterization of the bis(thiosemicarbazones). Chapter 3 describes the synthesis, and spectral characterization of copper(II) complexes with SNNNS donor bis(thiosemicarbazones). Chapter 4 deals with the synthesis and spectral characterization of manganese(II) complexes. Chapter 5 contains the synthesis and spectral characterization of the nickel(II) and palladium(II) complexes. Chapter 6 includes the synthesis, structural and spectral characterization of zinc(II) and cadmium(II) complexes with SNNNS donor bis(thiosemicarbazones).

# CONTENTS

Page No.

## CHAPTER 1

<b>A prologue on the chemistry of bis(thiosemicarbazones)</b>		1
1.1	Importance of bis(thiosemicarbazones)	2
1.2	Bonding and stereochemistry	4
1.3	Characterization techniques	10
1.3.1	Elemental analyses	10
1.3.2	Magnetic susceptibility measurements	10
1.3.3	IR spectroscopy	12
1.3.4	Electronic spectroscopy	12
1.3.5	EPR spectroscopy	14
1.3.6	NMR spectroscopy	15
1.3.7	X-ray crystallography	16
	Objectives of the present work	16
	References	18

## CHAPTER 2

<b>Synthesis and spectral characterization of bis(thiosemicarbazones)</b>		24
2.1	Introduction	24
2.2.	Experimental	27
2.2.1	Materials	27
2.2.2	Synthesis of Ligands	27
2.3	Physical measurements	32
2.4	Results and discussion	32
2.4.1	IR spectral studies	33
2.4.2	Electronic spectral studies	37
2.4.3	<sup>1</sup> H NMR spectral studies	39
	Concluding remarks	44
	References	44

### **CHAPTER 3**

<b>Synthesis and spectral characterization of Cu(II) complexes of bis(<i>N</i><sup>4</sup>-substitutedthiosemicarbazones) of 2,6-diacetylpyridine</b>	<b>48</b>
3.1 Introduction	48
3.2 Experimental	49
3.2.1 Materials	49
3.2.2 Syntheses of complexes	49
3.3 Physical measurements	51
3.4 Results and discussion	52
3.4.1 IR spectral studies	54
3.4.2 Electronic spectral studies	62
3.4.3 EPR Spectral studies	70
Concluding remarks	95
References	96

### **CHAPTER 4**

<b>Synthesis and spectral characterization of Mn(II) complexes of bis(<i>N</i><sup>4</sup>-substitutedthiosemicarbazones) of 2,6-diacetylpyridine</b>	<b>101</b>
4.1 Introduction	101
4.2 Experimental	102
4.2.1 Materials	102
4.2.2 Synthesis of complexes	103
4.3 Physical measurements	104
4.4 Results and discussion	105
4.4.1 IR spectral studies	107
4.4.2 Electronic spectral studies	113
4.4.3 EPR spectral studies	116
Concluding remarks	127
References	127

<b>CHAPTER 5</b>		131
<b>Synthesis and spectral characterization of Ni(II) and Pd(II) complexes of bis(<i>N</i><sup>4</sup>-substitutedthiosemicarbazones) of 2,6-diacetyl-pyridine</b>		
5.1	Introduction	131
5.2	Experimental	132
5.2.1	Materials	132
5.2.2	Syntheses of ligands	132
5.2.3	Synthesis of Ni(II) complexes	132
5.2.4	Synthesis of Pd(II) complexes	134
5.3	Physical measurements	135
5.4	Results and discussion	135
5.4.1	Spectral characteristics of nickel complexes	138
5.4.1a	IR spectral studies	138
5.4.1b	Electronic spectral studies	145
5.4.2	Spectral characteristics of palladium complexes	148
5.4.2a	IR spectral studies	148
5.4.2b	Electronic spectral studies	152
5.4.2c	<sup>1</sup> H NMR spectral studies	153
	Concluding remarks	162
	References	163

<b>CHAPTER 6</b>		
<b>Synthesis and spectral characterization of Zn(II) and Cd(II) complexes of bis(<i>N</i><sup>4</sup>-substitutedthiosemicarbazones) of 2,6-diacetylpyridine</b>		167
6.1	Introduction	167
6.2	Experimental	169
6.2.1	Materials	169
6.2.2	Syntheses of ligands	169

6.2.3	Synthesis of Zn(II) complexes	169
6.2.4	Synthesis of Cd(II) complexes	170
6.3	Physical measurements	171
6.3.1	X-Ray crystallography	172
6.4	Results and discussion	173
6.4.1	Crystal structure of $Zn_4(Ac_4Cy)_4 \cdot 4DMF$ ( <b>27a</b> )	176
6.4.2	Spectral characteristics of zinc complexes	183
6.4.2a	IR spectral studies	183
6.4.2b	Electronic spectral studies	187
6.4.2c	$^1H$ NMR spectral studies	188
6.4.3	Spectral characteristics of cadmium complexes	192
6.4.3a	IR spectral studies	192
6.4.3b	Electronic spectral studies	199
6.4.3c	$^1H$ NMR spectral studies	202
	Concluding remarks	211
	References	212
	<b>Summary and conclusion</b>	<b>215</b>

## **A prologue on the chemistry of bis(thiosemicarbazones)**

The first exploration of coordinated metal complexes dates back to the nineteenth century, during the days of Alfred Werner [1]. Thereafter, the inorganic chemistry witnessed a great outflow of coordination compounds, with unique structural characteristics and diverse applications. In the modern ages, the stereochemistry of most of the coordination compounds can be explored by accommodating the concepts of electronic energy levels and bonding, but however there are several instances where unusual structures and theoretical challenges are observed. The stereochemistry of coordination compounds is one of the major interests of the coordination chemist. Coordination complexes can assume a wide variety of structures depending on the metal ion, its coordination number and the denticity of the ligands used. The ligands also range from monodentate to polydentate based on the potential donor sites available in their structural skeleton. The diversity in structures exhibited by the coordination complexes of multidentate ligands have led to their usage as sensors, models for enzyme mimetic centers, medicines etc. The presence of more electronegative nitrogen, oxygen or sulfur atoms on the ligand structure is established to enhance the coordinating possibilities of ligands. Hence there has been a continuous quest over many years for nitrogen or sulfur donor ligands, which possess a variety of coordination possibilities.

In this aspect, thiosemicarbazones have been a subject of interest to researchers of different profiles. In view of the fact that these compounds form complexes with many metals are of diverse chemical, physical and

structural characteristics, they are of special interest to coordination chemists [2, 3]. Thiosemicarbazones of  $\alpha$ -(N)-heterocyclic aldehydes and ketones possess a broad spectrum of potentially useful chemotherapeutic activities such as antimalarial, antibacterial, antiviral activities [4, 5]. The transition metal complexes are far more biologically active than uncoordinated thiosemicarbazone and their enhanced biological activity has been an active area of investigation among medicinal researchers [6]. In general, thiosemicarbazones as chelating ligands with transition metal ions by binding through the thioketo sulfur and hydrazine nitrogen atoms and therefore this type of compounds can coordinate *in vivo* to metal ions. Thiosemicarbazones can coordinate to metal as neutral molecules or after deprotonation, as anionic ligands and can adopt a variety of different coordination modes. The possibility of their being able to transmit electronic effects between a reduce unit and a metal centre is suggested by the delocalization of the  $\pi$  bonds in the thiosemicarbazone chain [7]. Transition metal complexes with thiosemicarbazones exhibit a wide range of stereochemistry, biomimic activity and have potential application as sensors.

### **1.1. Importance of bis(thiosemicarbazones)**

Heterocyclic thiosemicarbazones capable of tridentate coordination have been studied extensively [7-10], and in recent years many reports involve crystal structures of these thiosemicarbazones and/or their metal complexes [11]. Also, the structures of bis(thiosemicarbazones) capable of tetradentate coordination and their complexes have been the subject of numerous recent reports [12-27]. Bis(thiosemicarbazones) are compounds derived from thiosemicarbazides as a result of condensation with a dialdehyde or diketone. Again, attaching groups with potential donor sites increases the denticity of

these bis(thiosemicarbazones). One such group is the  $-C=S$  group which also makes possible an electron delocalization. The presence of potential donor sites in the ketone or aldehyde chosen, gives a multidentate ligand. These resultant Schiff bases can function as chelating agents complexing with transition or main group metals producing complexes with versatile stereochemistries, applications and with enhanced bioactivity compared to the parental ligands. Bis(thiosemicarbazones) derived from dialdehydes and diketones are of considerable interest due to their biological activity [28-33]. This class of compounds contains two thiosemicarbazone moieties connected by their imine nitrogens to a two carbon skeleton, and it can act as tetradentate (SNNS donor) ligands (Figure 1) and in the presence of other donor atoms like nitrogen, it can act as pentadentate (SNNNS donor) ligands (Figure 2) [34].

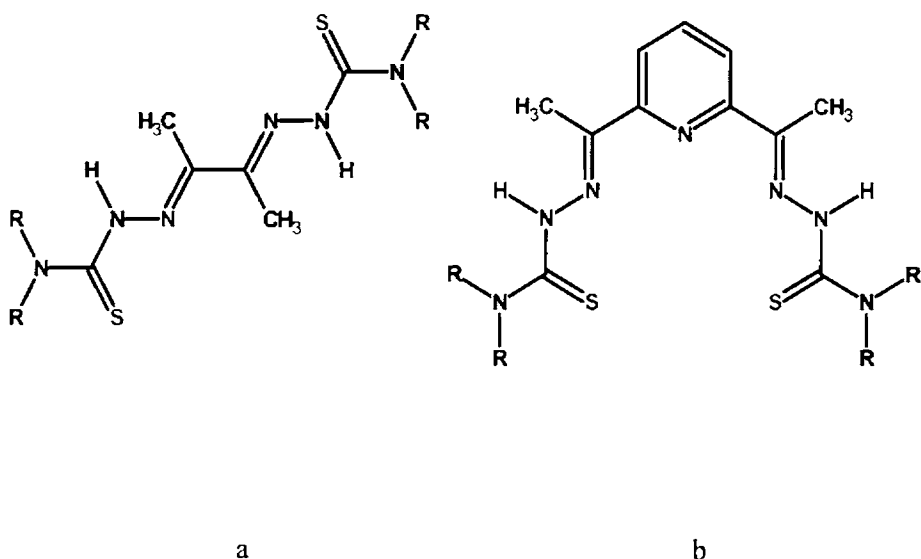


Figure 1

However, less attention has been given to heterocyclic bis(thiosemicarbazones) which are capable of higher denticity. This lack of

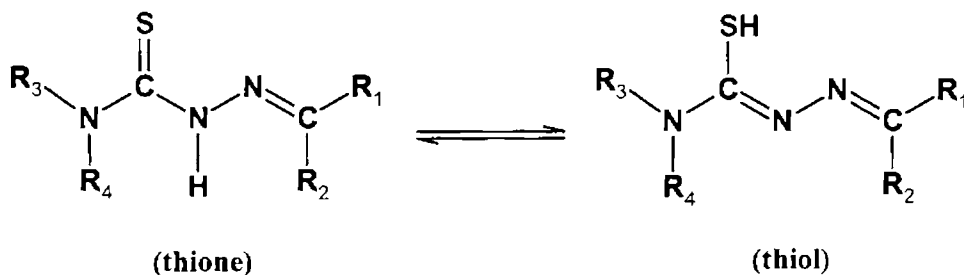


attention is particularly true for those heterocyclic bis(thiosemicarbazones) with substituents other than  $\text{NH}_2$  in the  $N^4$ -position of the thiosemicarbazone moiety. The coordinating ability of thiosemicarbazides to both transition and main group metallic cations is attributed to the extended delocalization of electron density over the thiosemicarbazone skeleton, which is enhanced by substitution at the  $N(4)$  position. Spectral and biological studies have been carried out on metal complexes of 2,6-diacetylpyridine bis{ $N(4)$ -substituted thiosemicarbazones}[35-37]. Structural information for a heterocyclic bis{ $N(4)$ -substituted thiosemicarbazone} has only recently been reported even though the  $N(4)$ -substituent(s) in other types of thiosemicarbazones, including bis(thiosemicarbazones), has been shown to significantly affect their biological activity [37]. The structural study of heterocyclic bis(thiosemicarbazones) and their metal complexes is the subject of this contribution, which is not exhaustive, but representative of this area of chemistry at this writing [38].

## 1.2. Bonding and stereochemistry

The stereochemistries adopted by thiosemicarbazones while interacting with transition metal ions, depend essentially upon the presence of an additional coordination centre in the ligand moiety and the charge on the ligand, which in turn is influenced by the thione $\leftrightarrow$ thiol equilibrium. It has been shown that the thiosemicarbazones, with the general formula  $\text{R}_1\text{R}_2\text{C}=\text{N}-\text{NH}-\text{CS}-\text{NR}_3\text{R}_4$  usually react as chelating ligands with transition metal ions by bonding through the sulfur and hydrazinic nitrogen atom. The group  $\text{N}-\text{C}=\text{S}$  is of considerable chemotherapeutic interest and is responsible for the pharmacological activity. Besides the denticity variation, consideration of the charge distribution is complicated in thiosemicarbazones due to the

existence of thione and thiol tautomers (Scheme 1.1). Although the thione form predominates in the solid state, solutions of thiosemicarbazone molecules show a mixture of both tautomers. As a result, depending upon the preparative conditions, the metal complex can be cationic neutral or anionic. Most of the earlier investigations of metal thiosemicarbazone complexes have involved ligands in the uncharged thione form, but a number of recent reports have featured complexes in which the  $^2\text{N}$ -hydrogen is lost, and thiosemicarbazones coordinate in the thiol form. Furthermore, it is possible to isolate complexes containing both the neutral and anionic forms of the ligand bonded to the same metal ion.



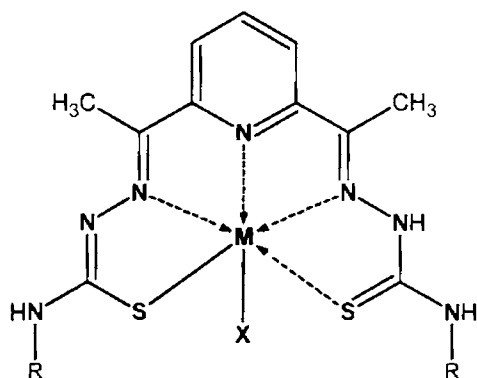
Scheme 1.1

The  $\text{R}_1$  and  $\text{R}_2$  groups may provide additional donor atoms and  $\text{R}_3$  and  $\text{R}_4$  are the  $\text{N}(4)$ -substituents.

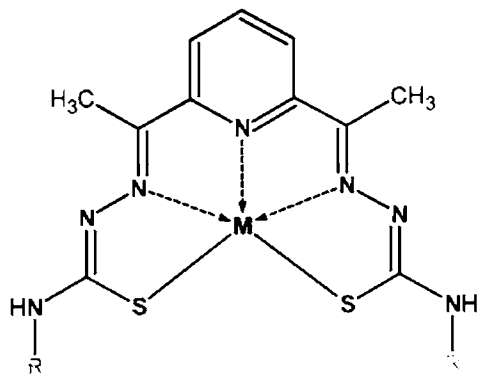
Depending on the reaction conditions and the stability of the metal complex formed, the bis(thiosemicarbazones) show a variety of coordination modes with transition metals. The number and type of the substituents influence the coordination mode. Bis(thiosemicarbazones) obtained by the condensation of a diketone like 2,6-diacetylpyridine with  $\text{N}^4$ -monosubstituted

thiosemicarbazides in 1:2 ratio will form a class of versatile SNNNS chelating ligands.

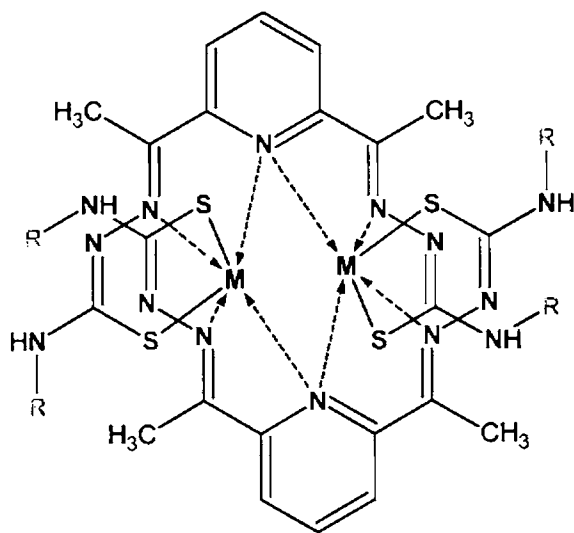
The presence of two thiosemicarbazone moieties and a donor atom like nitrogen in the carbon skeleton will provide three nitrogens and two sulfur atoms as donors in these ligands. A depiction of a six coordinate metal complex with the pentadentate ligand together with the anionic coligand 'X' is given in Structure I. It should be mentioned here that it is not necessary that the ligand should undergo mono-deprotonation and coordinate. Thus the ligand can also coordinate with the metal, in the dianionic and in the neutral form. The various possible coordination modes of the bis(thiosemicarbazone) ligand under study are shown below (Structures II-V).



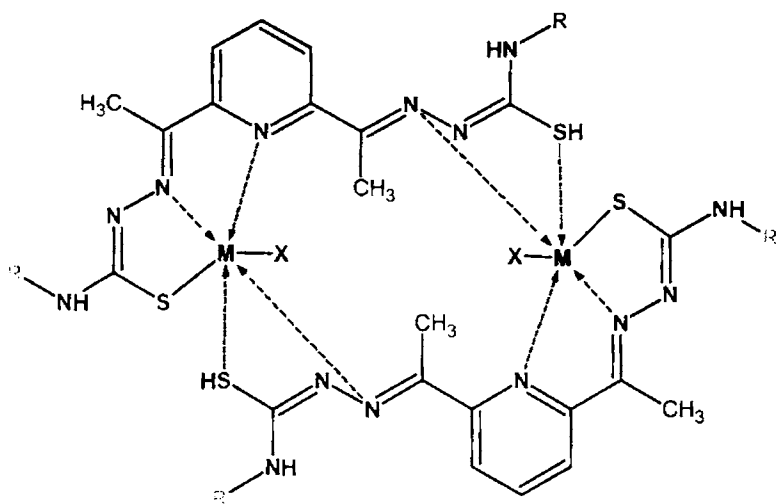
**Structure I**



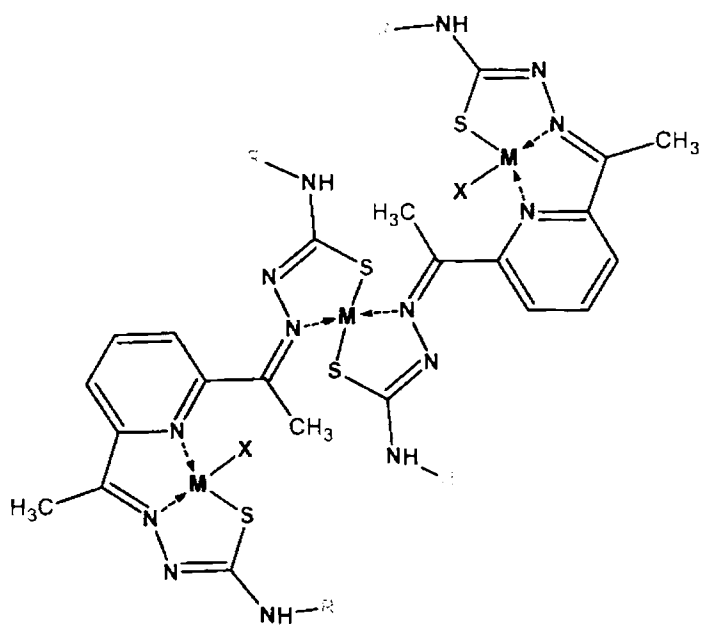
**Structure II**



**Structure III**



**Structure IV**



**Structure V**

There has been a large number of studies on metal complexes of tridentate thiosemicarbazones derived from N heterocyclic carboxaldehydes and ketones [39-43]. Metal complexes of tetradentate thiosemicarbazones derived from  $\alpha$ -ketoaldehydes and  $\alpha$ -diketones have also received considerable attention [44-47] because of their significant biological activities. Metal complexes of pentadentate thiosemicarbazones are less common. However, in recent years there have been several reports on complexes of the 2,6-diacetylpyridine bis(thiosemicarbazone) which has demonstrated its versatility as a chelating agent by forming different types of zinc(II) complexes depending on the reaction conditions and the types of zinc(II) salts used in the preparation of the complexes [48, 49].

The synthesis and characterization of metal complexes of tetradentate  $N_2S_2$  bis{N(3)-substituted thiosemicarbazone} ligands have been reported previously [49, 50]. Crystal structure determinations have shown that 1,2-bis(thiosemicarbazones) form planar  $N_2S_2$  tetradentate ligands with copper(II) and nickel(II), and that sulfurs of adjacent molecules coordinate weakly to the metal centre's axial positions [51, 52]. Because of the antitumor activity of  $\alpha$ -diketone and  $\alpha$ -ketoaldehyde bis(thiosemicarbazones) [53], as well as their metal complexes [54], and the considerable dependence of the biological activity on the nature of the N(3)-substituent attached to the thiosemicarbazone moiety in other series of thiosemicarbazones [54]. There are reports on a series of copper(II) and nickel(II) complexes of butane-2,3-dione [13], pyruvaldehyde and glyoxaldehyde [15] bis{N(3)-substituted thiosemicarbazones}.

### 1.3. Characterization techniques

#### 1.3.1. Elemental analyses

Elemental analyses of C, H and N were done on a Vario EL III CHN elemental analyzer at the SAIF, Cochin University of Science and Technology, Kochi 22, India.

#### 1.3.2. Magnetic susceptibility measurements

When a substance is placed in a magnetic field of strength  $H$ , the intensity of magnetic field in the substance is greater than  $H$ . If the field of the substance is greater than  $H$ , the substance is paramagnetic and if it is less than  $H$ , the substance is diamagnetic. Paramagnetism arises as a result of unpaired electron spins in the atom.

The mass magnetic susceptibility in  $\text{cm}^3 \cdot \text{g}^{-1}$  ( $\chi$  or  $\chi_g$ ) and the molar magnetic susceptibility ( $\chi_m$ ) in  $\text{cm}^3 \text{mol}^{-1}$  are defined as follows where  $\rho$  is the density in  $\text{g} \cdot \text{cm}^{-3}$  and  $M$  is molar mass in  $\text{g} \cdot \text{mol}^{-1}$ .

$$\chi_g = \chi_v / \rho$$

$$\chi_m = M\chi_g = M\chi_v / \rho$$

If  $\chi$  is positive, then  $(1+\chi) > 1$  and the material is called paramagnetic. In this case, the magnetic field is strengthened by the presence of the material. Alternatively, if  $\chi$  is negative, then  $(1+\chi) < 1$ , and the material is diamagnetic. As a result, the magnetic field is weakened in the presence of the material.

The magnetic susceptibility value calculated from magnetic measurements is the sum of paramagnetic and diamagnetic susceptibilities. To calculate the exact paramagnetic susceptibility ( $\mu_{eff}$ ), the value of diamagnetic susceptibility is subtracted from the susceptibility calculated from observed results [1]. When the structural formula of the complexes is correctly known, diamagnetic correction can be calculated from Pascal's constants.

$$\chi_M^{corr.} = \chi_M - (\text{Diamagnetic corrections})$$

From classical theory, the corrected paramagnetic molar susceptibility is related to the permanent paramagnetic moment of a molecule,  $\mu_{eff}$ , by :

$$\chi_M^{corr.} = \frac{N^2 \cdot \mu_{eff}^2}{3RT}$$

where, N is Avogadro's number, R is the ideal gas constant, T is the absolute temperature and  $\mu_{eff}$  is the effective magnetic moment and is expressed in Bohr Magnetons (B.M.). Solving the above expression, the effective magnetic moment is given by,

$$\mu_{eff} = \sqrt{\frac{3RT \cdot \chi_M^{corr.}}{N}} = 2.828 \sqrt{\chi_M^{corr.} \cdot T}$$

But, as the field strength (H) used for the present measurements is 5 k Oersted. Then,



$$\mu_{\text{eff}} = 2.828 \sqrt{\frac{\chi_{\text{M}}^{\text{corr. T}}}{5 \times 10^3}}$$

### ***1.3.3. IR spectroscopy***

Infrared spectroscopy (IR spectroscopy) is the subset of spectroscopy that deals with the Infrared part of the electromagnetic spectrum. As with all spectroscopic techniques, it can be used to identify and to investigate the geometry of a compound.

Infrared spectroscopy works because chemical bonds have specific frequencies at which they vibrate corresponding to energy levels. The resonant frequencies or vibrational frequencies are determined by the shape of the molecular potential energy surfaces, the masses of the atoms and, eventually by the associated vibronic coupling. In order for a vibrational mode in a molecule to be IR active, it must be associated with changes in the permanent dipole [55].

Sample preparation method is to grind a quantity of the sample with a specially purified salt (usually potassium bromide) finely (to remove scattering effects from large crystals). This powder mixture is then crushed in a mechanical die press to form a translucent pellet through which the beam of the spectrometer can pass.

### ***1.3.4. Electronic spectroscopy***

Electronic spectroscopy is an analytical technique to study the electronic structure and its dynamics in atoms and molecules. In general an

excitation source such as X-rays, electrons, or synchrotron radiation will eject an electron from an inner-shell orbital of an atom.

The Beer-Lambert law states that the absorbance of a solution is due to the solution's concentration. Thus UV/vis spectroscopy can be used to determine the concentration of a solution. It is necessary to know how quickly the absorbance changes with concentration.

The method is most often used in a quantitative way to determine concentrations of an absorbing species in solution, using the Beer-Lambert law:

$$A = -\log(I/I_0) = \epsilon \cdot c \cdot l$$

where  $A$  is the measured absorbance,  $I_0$  is the intensity of the incident light at a given wavelength,  $I$  is the transmitted intensity,  $l$  is the path length through the sample, and  $c$  is the concentration of the absorbing species.

Samples for UV/vis spectrophotometry are most often liquids, although the absorbance of gases and even of solids can also be measured. Samples are typically placed in a transparent cell, known as a cuvette. Cuvettes are typically rectangular in shape, commonly with an internal width of 1 cm. (This width becomes the path length,  $l$ , in the Beer-Lambert law). Test tubes can also be used as cuvettes in some instruments. The best cuvettes are made of high quality quartz, although glass or plastic cuvettes are common. (Glass and most plastics absorb in the UV, which limits their usefulness to visible wavelengths.)

An ultraviolet-visible spectrum is essentially a graph of light absorbance versus wavelength in a range of ultraviolet or visible regions.

Such a spectrum can often be produced by a more sophisticated spectrophotometer. Wavelength is often represented by the symbol  $\lambda$ . For the given substance, the wavelength at which maximum absorption in the spectrum occurs is called  $\lambda_{\text{max}}$ , pronounced "Lambda-max".

### *1.3.5. EPR spectroscopy*

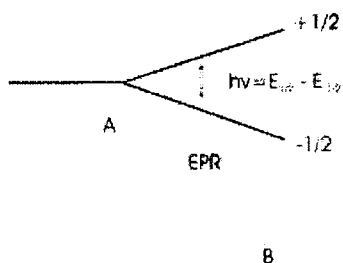
Electron Paramagnetic Resonance (EPR) is a spectroscopic technique which detects species that have unpaired electrons, generally meaning that the molecule in question is a free radical, if it is an organic molecule, or that it has transition metal ions if it is an inorganic complex. The basic physical concepts of the technique are analogous to those of NMR, but instead of the spins of the atom's nuclei, electron spins are excited. Because of the difference in mass between nuclei and electrons, weaker magnetic fields and higher frequencies are used.

An electron has a magnetic moment. When placed in an external magnetic field of strength  $B_0$ , this magnetic moment can align itself parallel or antiparallel to the external field. The former is at lower energy state than the latter (this is the Zeeman effect), and the energy separation between the two is  $\Delta E = g_e \mu_B B_0$ , where  $g_e$  is the gyromagnetic ratio of the electron, the ratio of its magnetic dipole moment to its angular momentum, and  $\mu_B$  is the Bohr magneton. To move between the two energy levels, the electron can absorb electromagnetic radiation of the correct energy:

$$\Delta E = h\nu = g_e \mu_B B_0$$

where  $h\nu$  is the microwave energy, and this is the fundamental equation of EPR spectroscopy. The paramagnetic centre is placed in a magnetic field and

the electron caused to resonate between the two states; the energy absorbed as it does so is monitored, and converted into the EPR spectrum.



EPR signals can be generated by resonant energy absorption measurements made at different electromagnetic radiation frequencies  $\nu$  in a constant external magnetic field. Measurements can be provided by changing the magnetic field  $B$  and using a constant frequency radiation. This means that an EPR spectrum is normally plotted with the magnetic field along the X-axis, with peaks at the field that cause resonance.

### 1.3.6. NMR spectroscopy

Nuclear Magnetic Resonance is a physical phenomenon based upon the magnetic properties of an atom's nucleus. All nuclei that contain odd numbers of nucleons and some that contain even numbers of nucleons have an intrinsic magnetic moment. The most commonly used nuclei are hydrogen-1 and carbon-13, although certain isotopes of many other elements nuclei can also be observed.

### ***1.3.7. X-ray crystallography***

Crystallography is the experimental science of determining the arrangement of atoms in solids. In order for an object to be seen, its size needs to be at least half the wavelength of the light being used to see it. Since visible light has a wavelength much longer than the distance between atoms, it is useless to see molecules. In order to see molecules it is necessary to use a form of electromagnetic radiation with a wavelength of the order of bond lengths, such as X-rays. When X-rays are beamed at the crystal, electrons diffract the X-rays, which cause a diffraction pattern. Using the mathematical Fourier transform, these patterns can convert into electron density maps. These maps show contour lines of electron density. Since electrons more or less surround atoms uniformly, it is possible to determine where atoms are located. Unfortunately since hydrogen has only one electron, it is difficult to map hydrogens. To get a three dimensional picture, the crystal is rotated while a computerized detector produces two dimensional electron density maps for each angle of rotation. The third dimension comes from comparing the rotation of the crystal with the series of images. Computer programs use this method to come up with three dimensional spatial coordinates.

Single crystal X-ray crystallographic analyses of the compounds were carried out using Siemens SMART CCD area-detector diffractometer at the Analytical Science Division, Bhavanagar, Gujarat, India. The structures were solved by direct methods and refined by least-square on  $F_0^2$  using the SHELXL software package [55].

#### **Objectives of the present work**

Coordination chemistry of pentadentate 2,6-diacetylpyridine bis(thiosemicarbazone) Schiff base ligands has been intensively studied due to

the versatility of the molecular chain in order to obtain very different geometries as well as their broad therapeutic activity. Metal complexes of thiosemicarbazone with aldehydes and ketones have been widely reported. But there have been fewer reports on potential pentadentate bis(thiosemicarbazones) formed from 2,6-diacetylpyridine. Keeping these in view, we have synthesized four bis(thiosemicarbazone) systems with 2,6-diacetylpyridine. In the present work, the chelating behavior of bis(thiosemicarbazones) are studied, with the aim of investigating the influence of coordination exerts on their conformation and or configuration, in connection with the nature of the metal and of the counter ion. The selection of the 2,6-diacetylpyridine as the ketonic part was based on its capability to form polynuclear complexes with different coordination number. The doubled armed bis(thiosemicarbazones) can coordinate to a metal centre as dianionic ligand by losing its amide protons or it can coordinate as monoanionic ligand by losing its amide proton from one of the thiosemicarbazone moiety or it can also be coordinate as neutral ligand. Hence it is interesting to explore the coordinating capabilities of these ligands whether in neutral form or anionic form and to study the structural variations occurring in the ligands during complexation such as change in conformation.

Transition metal ions were used for the synthesis of complexes. We have undertaken the work along the following lines:

- To synthesize the following  $N^4$ -monosubstituted SNNNS donor bis(thiosemicarbazones).
  - 2,6-diacetylpyridine bis( $N^4$ -phenylthiosemicarbaone) [ $H_2Ac_4Ph$ ]
  - 2,6-diacetylpyridine bis( $N^4$ -cyclohexylthiosemicarbaone) [ $H_2Ac_4Cy$ ]

- 2,6-diacetylpyridine bis(*N*<sup>4</sup>-methylthiosemicarbaone) [H<sub>2</sub>Ac4Me]
  - 2,6-diacetylpyridine bis(*N*<sup>4</sup>-ethylthiosemicarbaone) [H<sub>2</sub>Ac4Et]
- To characterize these ligands using elemental analyses, IR, electronic and <sup>1</sup>H NMR spectral studies.
  - To synthesize transition metal complexes and characterization of these complexes using elemental analyses, magnetic susceptibility measurements, IR, electronic, EPR and <sup>1</sup>H NMR spectral studies.
  - To isolate single crystals of the complexes and determine their structures using X-ray diffraction studies.

## References

1. J. E. Huheey, E. A. Keiter, R. L. Keiter, Inorganic Chemistry, Principles of Structure and Reactivity, 4<sup>th</sup> ed., Harper Collins College Publishers, New York, 1993.
2. M.J.M. Campbell, Coord. Chem. Rev. 15 (1975) 279.
3. S.B. Padhye, G.B. Kauffman, Coord. Chem. Rev. 63 (1985) 127.
4. D.L. Klayman, A.Lin, J.M. Hoch, J.P. Scovill, C. Lambross, A.S. Dobeck, J. Pharm. Sci. 73 (1984) 1763.
5. R.H. Dodd, C. Quannes, M. Robert Gero, P. Potier, J. Med. Chem. 32 (1989) 1272.
6. S.P. Mittal, S.K. Sharma, R.V. Singh, J.P. Tandon, Curr. Sci., 50 (1981) 483 and the references therein.

7. S.K. Jain, B.S. Garg, Y.K. Bhoon, *Trans. Met. Chem.* 11 (1986) 89.
8. M.A. Ali, S.E. Livingston, *Coord. Chem. Rev.* 13 (1974) 101.
9. D.X. West, S.B. Padhye, P.B. Sonawane, *Struct. Bonding*, 76 (1991) 1.
10. D.X. West, A.E. Liberta, S.B. Padhye, R.C. Chitake, P.B. Sonawane, A.S. Kumbhar, R.G. Yerande, *Coord. Chem. Rev.* 123 (1993) 49.
11. J.K. Swearingen, D.X. West, *Trans. Met. Chem.* 26 (2001) 252 and references therein.
12. D.X. West, J.S. Ives, G.A. Bain, A.E. Liberta, J. Valdés-Martínez, K.H. Ebert, S. Hernández-Ortega, *Polyhedron* 16 (1997) 1895.
13. H. Beraldo, D.X. West, *Trans. Met. Chem.* 22 (1997) 294.
14. H. Beraldo, J.S. Ives, S.B. Kaisner, J.D. Turner, I.S. Billeh, D.X. West, *Trans. Met. Chem.* 22 (1997) 459.
15. H. Beraldo, L.P. Boyd, D.X. West, *Trans. Met. Chem.* 23 (1998) 67.
16. A. Castiñeiras, E. Bermejo, D.X. West, A.K. El-Sawaf, J.K. Swearingen, *Polyhedron* 17 (1998) 2751.
17. A. Castiñeiras, E. Bermejo, L.J. Ackerman, H. Beraldo, D.X. West, *J. Mol. Struct.* 1 (1999) 477.
18. A. Castiñeiras, E. Bermejo, D.X. West, L.J. Ackerman, J. Valdés-Martínez, S. Hernández-Ortega, *Polyhedron* 18 (1999) 1463.
19. L.J. Ackerman, J.W. Webb, D.X. West, *Trans. Met. Chem.* 24 (1999) 562.



20. L.J. Ackerman, P.E. Fanwick, M.A. Green, E. John, W.E. Running, J.K. Swearingen, J.W. Webb, D.X. West, *Polyhedron* 18 (1999) 2759.
21. M.L. Durán, A. Sousa, J. Romero, A. Castiñeiras, E. Bermejo, D.X. West, *Inorg. Chim. Acta* 294 (1999) 79.
22. A. Castiñeiras, E. Bermejo, L.J. Ackerman, H. Beraldo, J. Valdés-Martínez, S. Hernández-Ortega, D.X. West, *J. Mol. Struct.* 510 (1999) 157.
23. M. Gil, E. Bermejo, A. Castiñeiras, H. Beraldo, D.X. West, *Z. Anorg. Allg. Chem.* 626 (2000) 2353.
24. H. Beraldo D.X. West, *Z. Naturforsch B*55 (2000) 863.
25. A. Castiñeiras, M. Gil, E. Bermejo, D.X. West, *Polyhedron* 20 (2001) 449.
26. A. Castiñeiras, M. Gil, E. Bermejo, D.X. West, *Z. Anorg. Allg. Chem.*, in press.
27. L.J. Ackerman, D.X. West, C.J Mathias, M.A. Green, *Nuclear Medicine and Biology* 26 (1999) 551.
28. K. Dey, D. Bandyopadhyay, *Trans. Met. Chem.* 16 (1991) 267.
29. V. M. Leovac, V. I. Cesljevic, G. Argay, A. KaËlmaËn, B. RibaËr, J. *Coord. Chem.* 34 (1995) 357.
30. M.R. Taylor, J. P. Glusker, E.J. Gabe, J.A. Minkin, *Bioinorg. Chem.* 3 (1974)189.

31. E. John, P.E. Fanwick, A.T. McKenzie, J.G. Stowell, M.A. Green, Nucl. Med. Biol. 16 (1989) 791.
32. H.G. Petering, H.H. Buskirk, G.E. Underwood, Cancer Res. 24 (1964) 367.
33. G.J. Van Giessen, J.A. Crim, D.H. Petering, H.G. Petering, J. Natl. Cancer Inst. 51 (1973)139.
34. J.K. Swearingen, D.X. West, Trans. Met. Chem. 25 (2000) 241.
35. M. Mohan, A. Agarawal, N.K. Jha, J. Inorg. Biochem. 34 (1998) 41.
36. M. Maji, S. Ghosh, S.K. Chattopadhyay, Trans. Met.Chem. 23 (1998) 81.
37. I.H. Hall, C.B. Lackey, T.D. Kistler, J.S. Ives, H. Beraldo, L.J. Ackerman, D.X. West, Arch. Pharm. Pharm. Med. Chem. 333 (2000) 217.
38. C.A. Brown, W. Kaminsky, K.A. Claborn, K.I. Gold-berg, D.X. West, J. Braz. Chem. Soc. 13 (2002) 10.
39. M.A. Ali, S.E. Livingstone, Coord. Chem. Rev. 13 (1974) 101.
40. M.J.M. Campbell, Coord. Chem. Rev. 15 (1975) 279.
41. D.X. West, S.B. Padhye, P.B. Sonawane, Struct. Bond. (Berlin) 76 (1991) 1.
42. J.S. Casas, M.S. García-Tasende, J. Sordo, Coord. Chem. Rev. 209 (2000) 197.

- 
43. H. Beraldo, S.B. Kaisner, J.D. Turner, I.S. Billeh, J.S. Ives, D.X. West, *Trans. Met. Chem.* 22 (1997) 459.
  44. A. Castineiras, M. Gil, E. Bermejo, D.X. West, *Polyhedron* 200 (2000) 449, and references therein.
  45. E. Bermejo, M. Gil, A. Castineiras, E. Labisbal, A. Sousa, H. Beraldo, D.X. West, *Z. Naturforsch. B55* (2000) 863.
  46. P.J. Blower, T.C. Castle, A.R. Cowley, J.R. Dilworth, P.S.E. Donnelly, E. Labisbal, F.E. Sowrey, S.J. Teat, M.J. Went, *Dalton Trans.* (2003) 4416.
  47. A. Bino, N. Cohen, *Inorg. Chim. Acta* 210 (1993) 11.
  48. A.I. Matesanz, I. Cuadrado, C. Pastor, P. Souza, *Z. Anorg. Allg. Chem.* 631 (2005) 780.
  49. K. Dey, D. Bandyopadhyay, *Trans. Met. Chem.* 16 (1991) 267.
  50. M.R. Taylor, J.P. Glusker, E.J. Gabe, J. Minkin, *Bioinorg. Chem.* 3 (1974) 189.
  51. E. John, P.E. Fanwick, A.T. McKenzie, J.G. Stowell, M.A. Green, *Nucl. Med. Biol.* 16 (1989) 791.
  52. H.G. Petering, H.H. Buskirk, G.E. Underwood, *Cancer Res.* 24 (1964) 367.
  53. G.J. Van Giessen, J.A. Crim, D.H. Petering, H.G. Petering, *J. Natl. Cancer Inst.* 51 (1973) 139.
  54. A.E. Liberta, D.X. West, *Biometals* 5 (1992) 121.
-

55. A. Bozkurt, A. Rosen, H. Rosen, B. Onaral, *Biomedical Engineering Online* 4 (2005) 29.

56. G.M. Sheldrick, *SHELXL-97 and SHELXS-97 Program for the solution of Crystal Structures*, University of Göttingen, Germany, 1997.

\*\*\*\*\*

# Synthesis and spectral characterization of bis(thiosemicarbazones)

## 2.1. Introduction

Heterocyclic thiosemicarbazones capable of tridentate coordination have been studied extensively [1–5], but heterocyclic bis(thiosemicarbazones), which are capable of higher denticity, have received less attention. This lack of attention is particularly true for those heterocyclic bis(thiosemicarbazones) with substituents other than  $\text{NH}_2$  in the  $N^4$ -position of the thiosemicarbazone moiety. The coordinating ability of thiosemicarbazides to both transition and main group metallic cations is attributed to the extended delocalization of electron density over the thiosemicarbazone skeleton, which is enhanced by substitution at the  $N^4$  position. Condensation of thiosemicarbazides with aromatic aldehydes or ketones extends the electron delocalization along the azomethine bond [6].

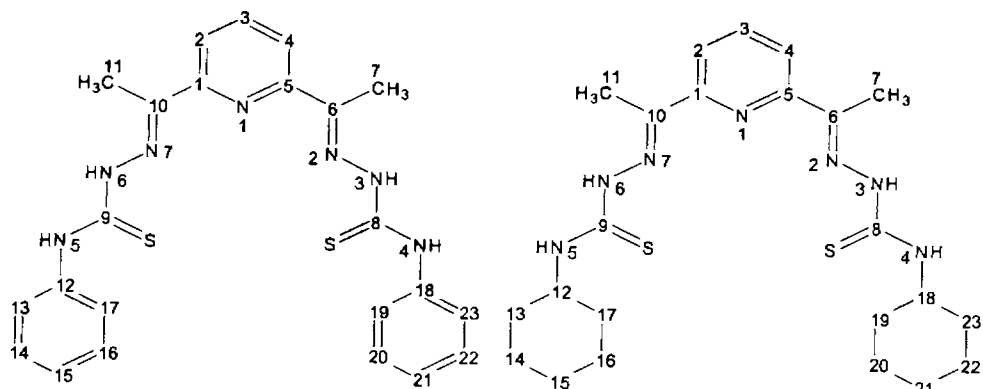
Transition metal complexes of bis(thiosemicarbazone) (btsc) ligands have been investigated as metallodrugs for a number of years. It has been reported that  $\alpha$ -diketone and  $\alpha$ -ketoaldehyde bis(thiosemicarbazones) and their metal complexes show antitumor activity [7, 8]. Since biological activity has been found to have a significant dependence on the thiosemicarbazone moiety's  $N^4$ -substituent [9], a series of bis(thiosemicarbazones) and their metal complexes were prepared and studied [10-13]. Spectral and biological studies have been carried out on metal complexes of 2,6-diacetylpyridine bis( $N^4$ -substituted thiosemicarbazones) [14, 15]. Recent studies of metal complexes of tetradentate bis(thiosemicarbazones) have included a number of structural [11-13, 16-17], as well as biological studies [18, 19]. However considerable

interest has been shown in 2,6-diacetylpyridine bis(thiosemicarbazone), and its metal complexes [14, 15].

Coordination chemistry of pentadentate 2,6-diacetylpyridine bis(thiosemicarbazone) Schiff base ligands has been intensively studied due to the versatility of the molecular chain in order to obtain very different geometries [20] as well as their broad therapeutic activity [21]. Metal complexes of thiosemicarbazones with aldehydes and ketones have been widely reported. But there have been fewer reports on potential pentadentate bis(thiosemicarbazones) formed from 2,6-diacetylpyridine [14, 15]. Keeping these in view, we have synthesized four bis(thiosemicarbazone) systems with 2,6-diacetylpyridine. The ligands synthesized are

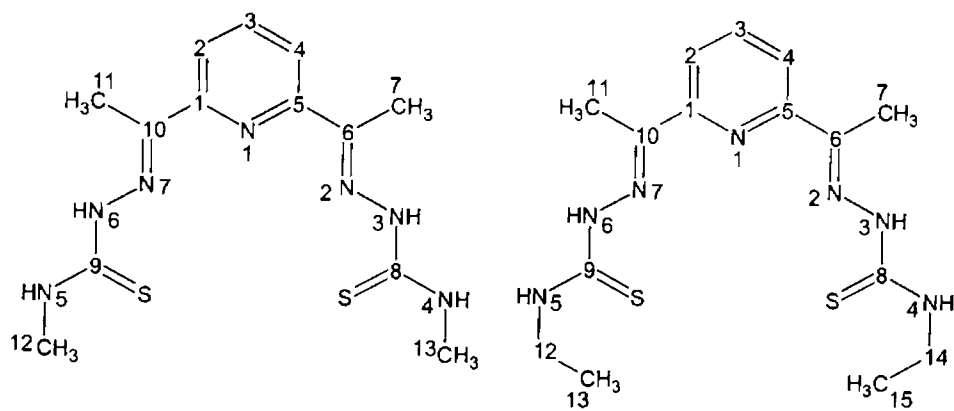
- 2,6-diacetylpyridine bis ( $N^4$ -phenylthiosemicarbazone) [ $H_2Ac_4Ph$ ]
- 2,6-diacetylpyridine bis ( $N^4$ -cyclohexylthiosemicarbazone) [ $H_2Ac_4Cy$ ]
- 2,6-diacetylpyridine bis ( $N^4$ -methylthiosemicarbazone) [ $H_2Ac_4Me$ ]
- 2,6-diacetylpyridine bis ( $N^4$ -ethylthiosemicarbazone) [ $H_2Ac_4Et$ ]

Thus the ligands are diprotic and coordinate with metal centre both in keto form as well as in enolate form under neutral conditions. All the four ligands in spite of two protons, sometimes remained in monoanionic form upon coordination. This chapter deals with the synthesis and spectral characterization of ligands. The general structure and the numbering of the two thiosemicarbazones are given in Figure 2.1. This numbering pattern is used throughout the entire work.



H<sub>2</sub>Ac4Ph

H<sub>2</sub>Ac4Cy



H<sub>2</sub>Ac4Me

H<sub>2</sub>Ac4Et

Figure 2.1. Structures and numbering schemes of bis(thiosemicarbazones)

## 2.2. Experimental

### 2.2.1. Materials

2,6-Diacetylpyridine (Aldrich), hydrazine hydrate, *N*<sup>4</sup>-phenyl isothiocyanate, *N*<sup>4</sup>-cyclohexyl isothiocyanate, *N*<sup>4</sup>-methylthiosemicarbazide, *N*<sup>4</sup>-ethylthiosemicarbazide.

Solvents used.

- (i) Ethanol: Commercially supplied ethanol, distilled and dried using standard methods and procedures.
- (ii) Methanol: Analar quality sample was used (Merck).
- (iii) Dimethylformamide: Analar quality was used.
- (iv) Chloroform: Analar quality was used.

### 2.2.2. Synthesis of Ligands

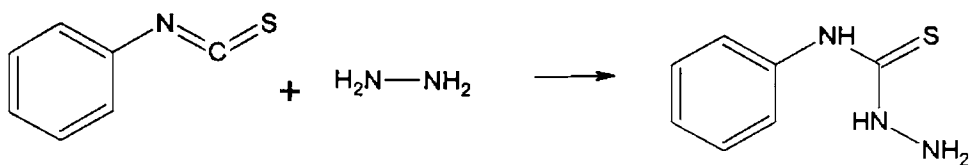
i) 2,6-Diacetylpyridine bis(*N*<sup>4</sup>-phenylthiosemicarbazone) [H<sub>2</sub>Ac4Ph]

Step-1:-

*Preparation of N<sup>4</sup>-phenylthiosemicarbazide:*

Phenyl isothiocyanate (100 mmol, 11.94 ml) in 25 ml ethanol and hydrazine hydrate (100 mmol, 4.86 ml) in 25 ml methanol were mixed with constant stirring. The resulting solution was kept in a stirred condition for ½ an hour. The white product, *N*<sup>4</sup>-phenylthiosemicarbazide formed was filtered, washed with ethanol and ether and dried *in vacuo* over P<sub>4</sub>O<sub>10</sub> (Scheme 2.1). m.p.=135 °C.



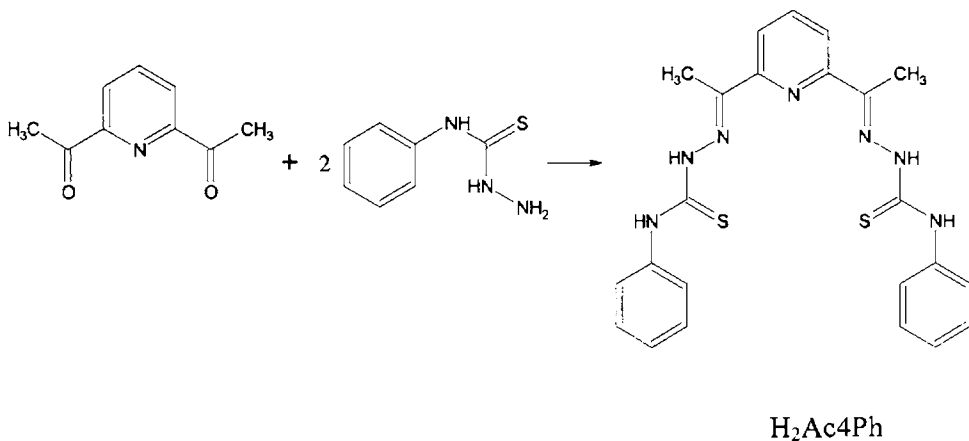


Scheme 2.1

Step-2:-

*Synthesis of 2,6-diacetylpyridine bis( $N^A$ -phenylthiosemicarbazone) [ $\text{H}_2\text{Ac4Ph}$ ]*

To a hot solution of 0.836 g (5 mmol) of phenylthiosemicarbazide in 25 ml of ethanol, added 0.407 g (2.5 mmol) of 2,6-diacetylpyridine in 25 ml of ethanol with constant stirring. The above mixture was slowly refluxed for 5 hrs. After cooling, the compound obtained as pale yellow solids, which was filtered, washed with ethanol and dried *in vacuo* over  $\text{P}_4\text{O}_{10}$  (Scheme 2.2).



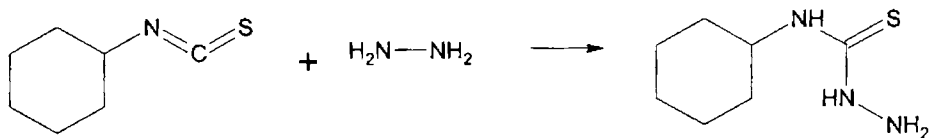
Scheme 2.2

ii) 2,6-diacetylpyridine bis(*N*<sup>4</sup>-cyclohexylthiosemicarbazone) [*H*<sub>2</sub>Ac4Cy]

Step-1:-

*Preparation of N*<sup>4</sup>-cyclohexylthiosemicarbazide

Cyclohexyl isothiocyanate (15 mmol, 2 ml) in 15 ml ethanol and hydrazine hydrate (90 mmol, 4.3 ml) in 15 ml ethanol were mixed with constant stirring. The resulting solution was kept in a stirred condition for ½ an hour. The white product, *N*<sup>4</sup>-cyclohexylthiosemicarbazide formed was filtered, washed with ethanol and dried *in vacuo* over P<sub>4</sub>O<sub>10</sub> (Scheme 2.3).  
m.p=140 °C.



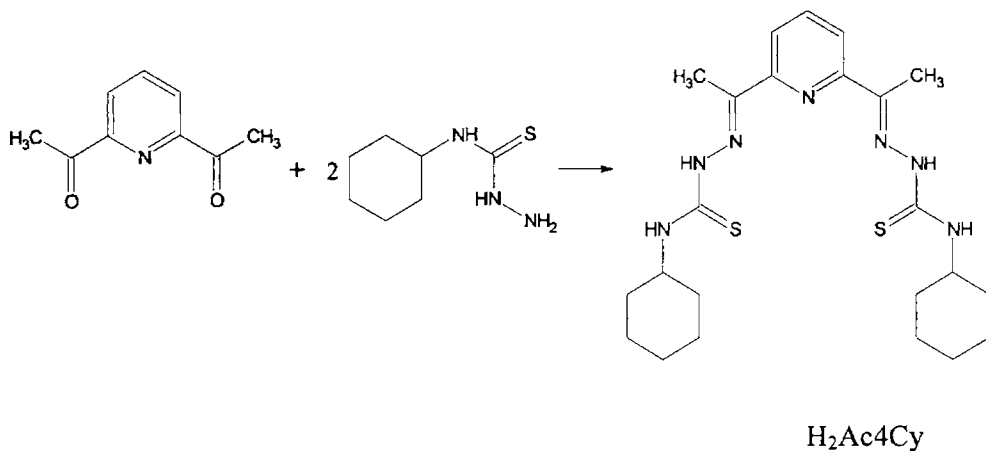
Scheme 2.3

Step-2:-

*Synthesis of 2,6-diacetylpyridine bis(N*<sup>4</sup>-cyclohexylthiosemicarbazone) [*H*<sub>2</sub>Ac4Cy]

To a hot solution of 0.886 g (5 mmol) of *N*<sup>4</sup>-cyclohexylthiosemicarbazide in 25 ml of ethanol, added 0.407 g (2.5 mmol) of 2,6-diacetylpyridine in 25 ml of ethanol with constant stirring. Two drops of glacial acetic acid was added to the above solution and the mixture was slowly refluxed for 5 hrs. After cooling, the compound was obtained as yellow

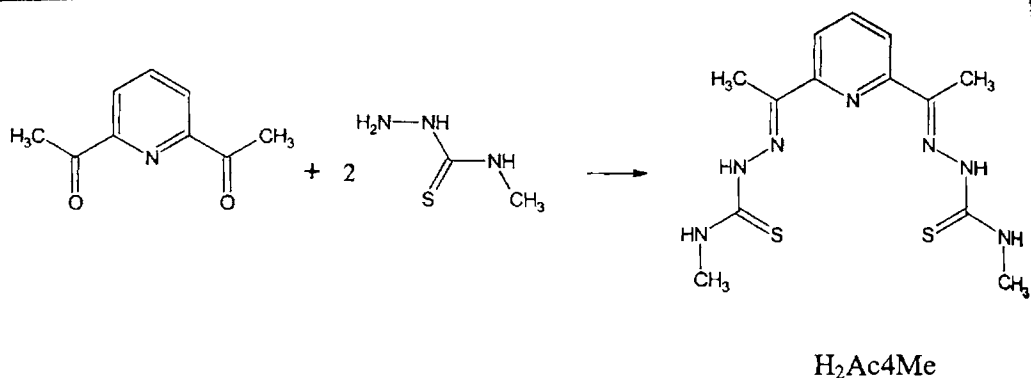
solids, which was filtered, washed with ethanol and ether and dried *in vacuo* over  $P_4O_{10}$  (Scheme 2.4).



Scheme 2.4

iii) 2,6-diacetylpyridine bis( $N^4$ -methylthiosemicarbazone) [ $H_2Ac4Me$ ]

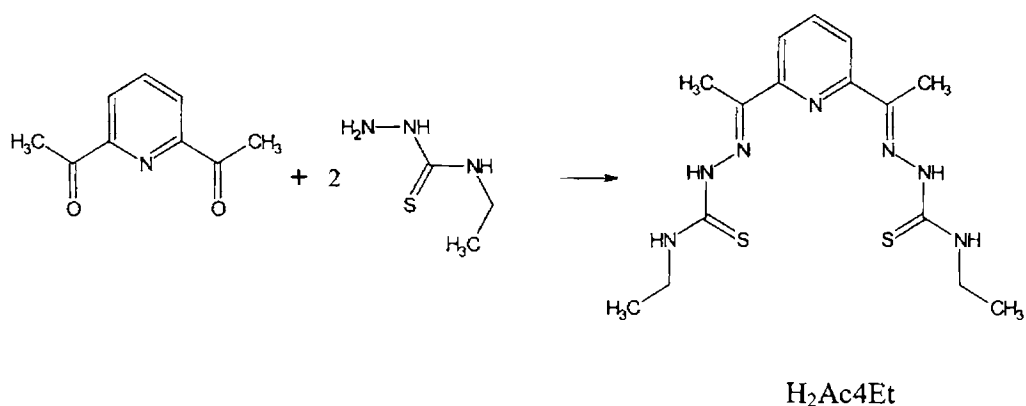
To a hot solution of 0.537 g (5 mmol) of  $N^4$ -methylthiosemicarbazide in 25 ml of ethanol, added 0.407 g (2.5 mmol) of 2,6-diacetylpyridine in 25 ml of ethanol with constant stirring. Two drops of glacial acetic acid was added to the above solution and the mixture was slowly refluxed for 5 hrs. After cooling, the compound was obtained as pale yellow solid, which was filtered, washed with ethanol and ether and dried *in vacuo* over  $P_4O_{10}$  (Scheme 2.5).



Scheme 2.5

iv) 2,6-diacetylpyridine bis(*N*<sup>4</sup>-ethylthiosemicarbazone) [H<sub>2</sub>Ac<sub>4</sub>Et]

To a hot solution of 0.595 g (5 mmol) of *N*<sup>4</sup>-ethylthiosemicarbazide in 25 ml of ethanol, added 0.407 g (2.5 mmol) of 2,6-diacetylpyridine in 25 ml of ethanol with constant stirring. Two drops of glacial acetic acid was added to the above solution and the mixture was slowly refluxed for 4 hrs. After cooling, the compound was obtained as yellow solid, which was filtered, washed with ethanol and ether and dried *in vacuo* over P<sub>4</sub>O<sub>10</sub> (Scheme 2.6).



Scheme 2.6

### 2.3. Physical measurements

Elemental analyses were carried out using a Vario EL III CHNS analyzer at SAIF, Kochi, India. Infrared spectral analyses were done using KBr pellets on Thermo Nicolet AVATAR 370 DTGS FT-IR spectrophotometer. Electronic spectra were recorded on a UVD-3500, UV-vis Double Beam Spectrophotometer from a solution in DMF.  $^1\text{H}$  NMR spectra were recorded using Bruker AMX 400 FT-NMR Spectrometer using TMS as the internal standard at the Sophisticated Instrumentation Facility, Indian Institute of Science, Bangalore.

### 2.4. Results and discussion

Condensation reaction of 2,6-diacetylpyridine and  $N^4$ -substituted thiosemicarbazides in a molar ratio of 1:2 resulted in ligand systems 2,6-diacetylpyridine bis( $N^4$ -substitutedthiosemicarbazones). The stoichiometries, colors and elemental analyses data are presented in Table 2.1.

Table 2.1. Stoichiometries and partial elemental analyses of bis(thiosemicarbazones)

Compound	Stoichiometry	Color	Composition (Found/Calcd) %		
			C	H	N
H <sub>2</sub> Ac4Ph	C <sub>23</sub> H <sub>23</sub> N <sub>7</sub> S <sub>2</sub>	yellow	59.44 (59.84)	4.75 (5.02)	21.87 (21.24)
H <sub>2</sub> Ac4Cy	C <sub>23</sub> H <sub>35</sub> N <sub>7</sub> S <sub>2</sub>	yellow	58.70 (58.32)	7.75 (7.45)	20.55 (20.70)
H <sub>2</sub> Ac4Me	C <sub>13</sub> H <sub>19</sub> N <sub>7</sub> S <sub>2</sub> ·H <sub>2</sub> O	yellow	44.16 (43.92)	5.46 (5.95)	26.97 (27.58)
H <sub>2</sub> Ac4Et	C <sub>15</sub> H <sub>22</sub> N <sub>7</sub> S <sub>2</sub>	yellow	49.05 (49.29)	6.93 (6.34)	26.64 (26.82)

### 2.4.1. IR spectral studies

The characteristic IR bands for the ligands ( $H_2Ac4Ph$ ,  $H_2Ac4Cy$ ,  $H_2Ac4Me$  and  $H_2Ac4Et$ ) recorded as KBr discs are listed in Table 2.2.

$H_2Ac4Ph$ : IR spectral analysis confirms the presence of characteristic groups present in the compound. Bands at  $3306$  and  $3220\text{ cm}^{-1}$  are assigned to  $\nu(^4N-H)$  and  $\nu(^2N-H)$ . The thiocarbonyl groups show stretching and bending vibrations at  $1322$  and  $808\text{ cm}^{-1}$ , while additional bands in the broad region of  $1500-700\text{ cm}^{-1}$  are due to vibrations involving interactions between C=S stretching and C-N stretching of the C=S groups attached to a nitrogen atoms [22]. Absence of any bands in the range  $2500-2800\text{ cm}^{-1}$  points towards the lack of -SH stretching absorptions in the molecule. It reveals the presence of only the thione tautomer in the solid state [23]. The azomethine stretching vibrations,  $C=N_{azo}$ , characteristic of a Schiff base is observed at  $1597\text{ cm}^{-1}$  [24-26]. Medium band observed at  $1028\text{ cm}^{-1}$ , assigned for hydrazinic (N-N) bonds. Aromatic and heteroaromatic compounds display strong out-of-plane C-H bending and ring bending absorption bands in the  $900-650\text{ cm}^{-1}$  region (Figure 2.2).

$H_2Ac4Cy$ : The bands at  $3296$  and  $3259\text{ cm}^{-1}$  are assigned to N-H stretching vibrations at N(4) and N(2) respectively. Thiocarbonyl vibrations are observed at  $1248$  and  $809\text{ cm}^{-1}$  and azomethine vibrations are at  $1596\text{ cm}^{-1}$ . The band at  $1102$  is assigned to (N-N) bonds. The -CH stretching vibrations of the cyclohexyl moiety are observed as two sharp bands at  $2930$  and  $2849\text{ cm}^{-1}$ . These bands confirm the existence of cyclohexyl ring in the molecular structure (Figure 2.3).

$H_2Ac4Me$ : In the IR spectrum of the ligand  $H_2Ac4Me$ , it is seen that the two N-H bands are very close to each other and give absorptions at  $3335$

and 3228  $\text{cm}^{-1}$ . Band assignable to  $\nu(\text{C}=\text{N}_{\text{azo}})$ , is observed at 1549  $\text{cm}^{-1}$ . Medium peak observed at 1045  $\text{cm}^{-1}$  corresponds to  $\nu(\text{N}-\text{N})$  band. The thiocarbonyl group shows stretching and bending vibrations at 1355 and 869  $\text{cm}^{-1}$ . Absence of any bands in the 2800–2550  $\text{cm}^{-1}$  region reveals the presence of only the thione tautomer in the solid state, as they imply the lack of  $-\text{SH}$  stretching absorptions in the molecule (Figure 2.4).

$\text{H}_2\text{Ac4Et}$ : IR spectrum of the ligand  $\text{H}_2\text{Ac4Et}$  shows bands at 3373 and 3328  $\text{cm}^{-1}$  corresponds to  $\nu(^4\text{N}-\text{H})$  and  $\nu(^2\text{N}-\text{H})$  respectively. The  $\nu(\text{CS})$  and  $\delta(\text{CS})$  vibrations are observed at 1307 and 857  $\text{cm}^{-1}$  and  $\nu(\text{C}=\text{N})$  vibration is observed at 1541  $\text{cm}^{-1}$ . A medium intensity band at 1050  $\text{cm}^{-1}$  assigned to  $\nu(\text{N}-\text{N})$  vibration. The absence of  $\nu(\text{S}-\text{H})$  band around 2600  $\text{cm}^{-1}$  suggests the existence of the bis(thiosemicarbazone) in the thione form (Figure 2.5). The 1600–1400  $\text{cm}^{-1}$  region of the spectra is complicated by the presence of thioamide bands and ring breathing vibrations of the pyridyl and phenyl rings. The band at 639  $\text{cm}^{-1}$  in the spectrum of ligand can be assigned as due to the in-plane ring deformation band of the pyridine ring [27].

Table 2.2. Infrared spectral assignments ( $\text{cm}^{-1}$ ) of bis(thiosemicarbazones)

Compound	$\nu(^4\text{N}-\text{H})$	$\nu(^2\text{N}-\text{H})$	$\nu(\text{C}=\text{N})$	$\nu(\text{N}-\text{N})$	$\nu/\delta(\text{C}-\text{S})$	py(ip)
$\text{H}_2\text{Ac4Ph}$	3306	3220	1597	1028	1322,808	628
$\text{H}_2\text{Ac4Cy}$	3296	3259	1596	1013	1307,857	601
$\text{H}_2\text{Ac4Me}$	3335	3325	1549	1043	1353,869	607
$\text{H}_2\text{Ac4Et}$	3373	3328	1541	1050	1307,857	639

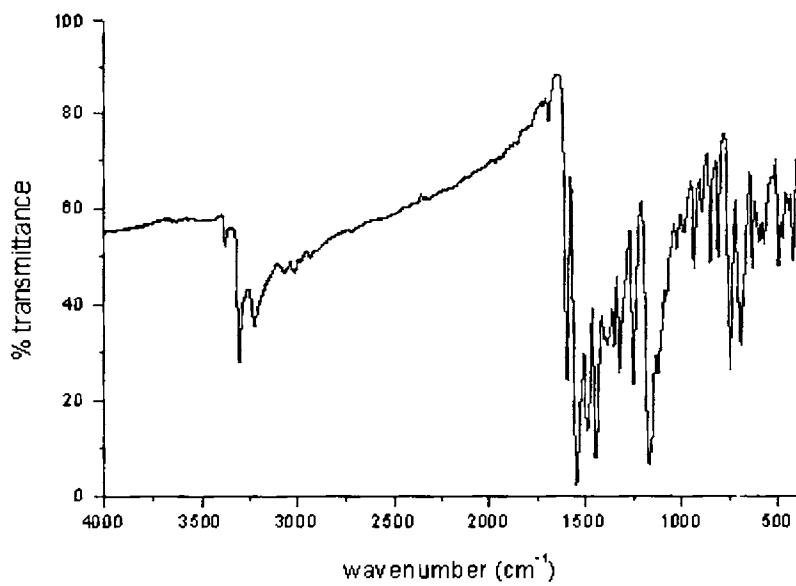


Figure 2.2. IR spectrum of H<sub>2</sub>Ac<sub>4</sub>Ph

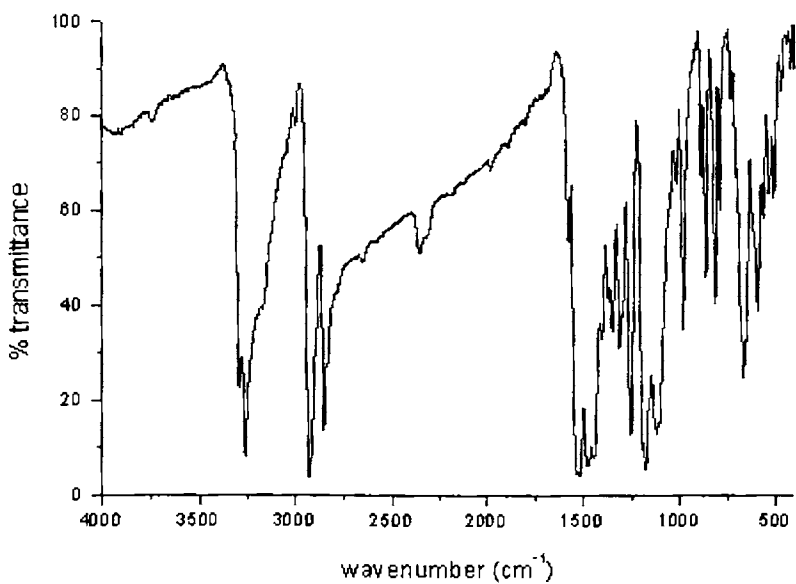


Figure 2.3. IR spectrum of H<sub>2</sub>Ac<sub>4</sub>Cy



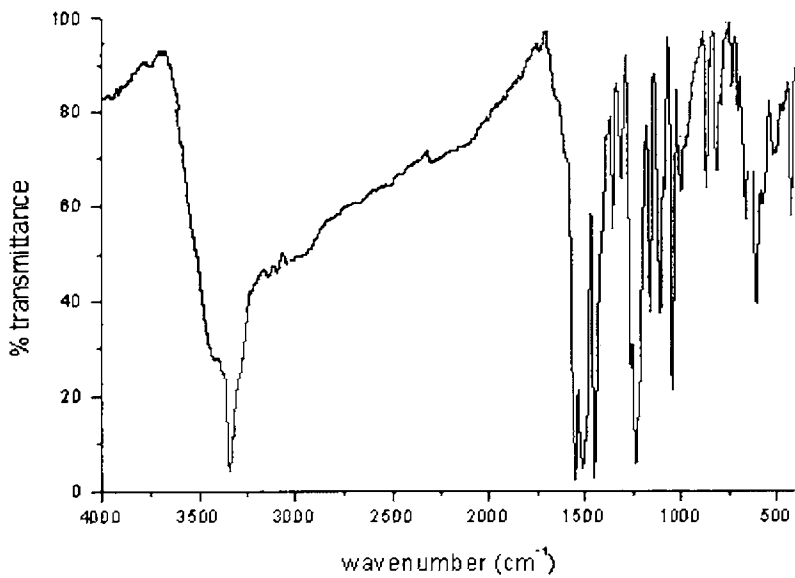


Figure 2.4. IR spectrum of H<sub>2</sub>Ac<sub>4</sub>Me

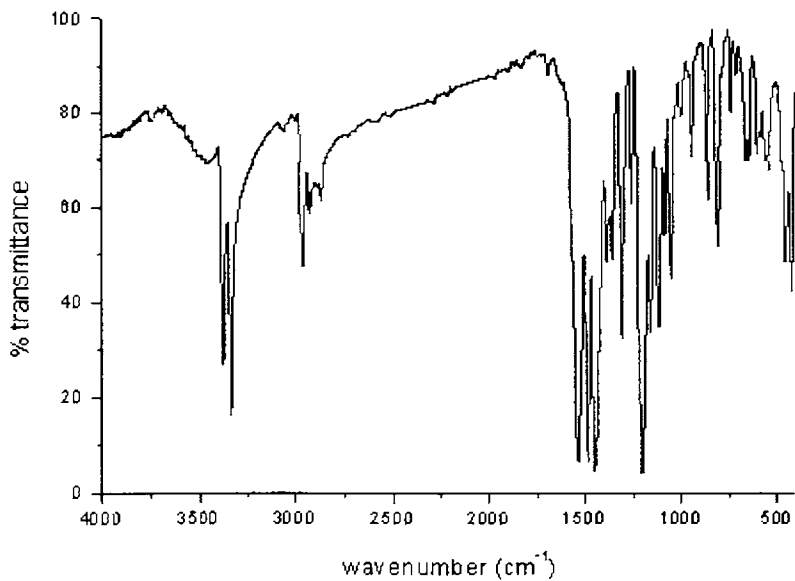


Figure 2.5. IR spectrum of H<sub>2</sub>Ac<sub>4</sub>Et

### 2.4.2. Electronic spectral studies

The UV-visible spectra of organic compounds are associated with the electronic transitions between energy levels, and at wavelengths above 200 nm, excitation of electrons from the  $\pi$ -orbitals usually occurs giving rise to informative spectra [28, 29]. The tentative assignments of the significant electronic spectral bands of ligands are presented in Table 2.3.

**H<sub>2</sub>Ac4Ph:** The electronic spectrum of the ligand (Figure 2.6) in DMF solution ( $10^{-4}$  M) shows a band at  $28,900\text{ cm}^{-1}$ , which corresponds to  $n \rightarrow \pi^*$  transition of the pyridyl ring and imine function of the thiosemicarbazone moiety. The  $\pi \rightarrow \pi^*$  transition observed as a band at  $32,250\text{ cm}^{-1}$  is assigned for the aromatic rings.

**H<sub>2</sub>Ac4Cy:** The  $n \rightarrow \pi^*$  and  $\pi \rightarrow \pi^*$  transitions are observed as a band and as a shoulder at  $29,210$  and  $32,450\text{ cm}^{-1}$  in the electronic spectrum of the ligand H<sub>2</sub>Ac4Cy (Figure 2.7) in DMF ( $10^{-4}$  M).

Table 2.3. Electronic spectral assignments ( $\text{cm}^{-1}$ ) of ligands

Compound	$n \rightarrow \pi^*$	$\pi \rightarrow \pi^*$
H <sub>2</sub> Ac4Ph	28,900	32,250
H <sub>2</sub> Ac4Cy	29,210	32,450
H <sub>2</sub> Ac4Me	29,620	32,050
H <sub>2</sub> Ac4Et	29,390	32,240

H<sub>2</sub>Ac4Me: The spectrum recorded for a 10<sup>-4</sup> M DMF solution of the ligand (Figure 2.8) consists of a shoulder at 29,620 cm<sup>-1</sup>, which corresponds to the *n* → *π*\* transition. The *π* → *π*\* transition was observed at 32,050 cm<sup>-1</sup>.

H<sub>2</sub>Ac4Et: The band corresponding to *n* → *π*\* transition is observed at 29,390 cm<sup>-1</sup> and the *π* → *π*\* transition is observed at 32,240 cm<sup>-1</sup> (Figure 2.9).

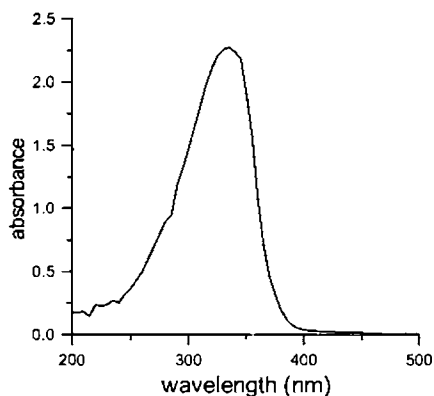


Figure 2.6. Electronic spectrum of H<sub>2</sub>Ac4Ph

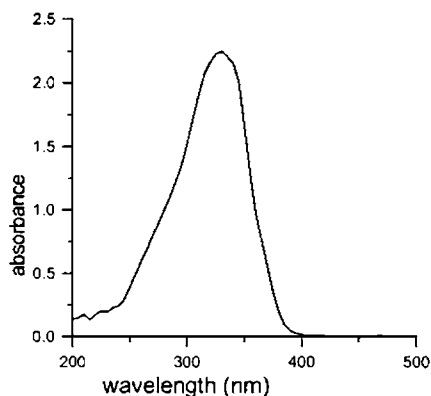


Figure 2.7. Electronic spectrum of H<sub>2</sub>Ac4Cy

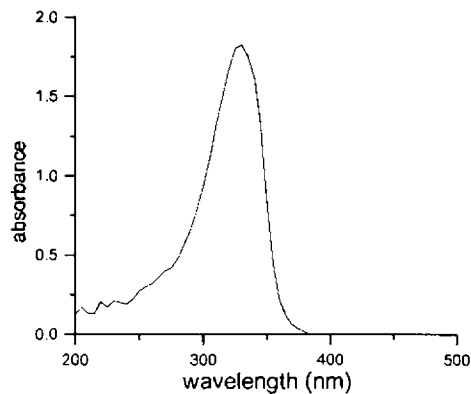


Figure 2.8. Electronic spectrum of H<sub>2</sub>Ac4Me

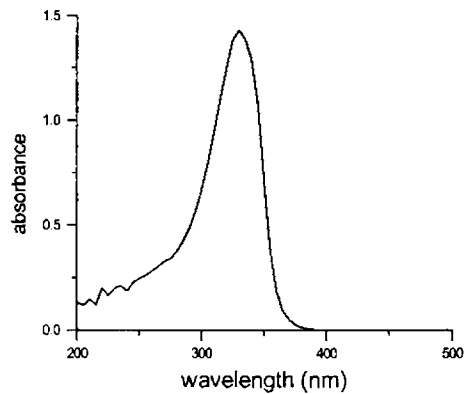


Figure 2.9. Electronic spectrum of H<sub>2</sub>Ac4Et

### 2.4.3. $^1\text{H}$ NMR spectral studies

Proton magnetic resonance spectroscopy is a helpful tool for the identification of organic compounds in conjunction with other spectrometric informations.

$\text{H}_2\text{Ac4Ph}$ : The  $^1\text{H}$  NMR spectrum of  $\text{H}_2\text{Ac4Ph}$  and the spectral assignments are given in Figure 2.10. Solution of the double-armed  $\text{H}_2\text{Ac4Ph}$  ligand in DMSO showed that N(3)H and N(6)H resonance, occur at  $\delta=10.21$ . The low field position of  $^{-4}\text{NH}$  and  $^{-5}\text{NH}$  ( $\delta=10.78$  ppm) could be attributable to the deshielding caused by the phenyl group. The presence of  $^{-3}\text{NH}$  and  $^{-6}\text{NH}$  proton signal suggests enolization of  $^{-3}\text{NH}-\text{C}=\text{C}$  and  $^{-6}\text{NH}-\text{C}=\text{C}$  groups to  $^{-3}\text{N}=\text{C}-\text{SH}$  and  $^{-6}\text{N}=\text{C}-\text{SH}$ , but  $\text{H}_2\text{Ac4Ph}$  does not show any peak attributable to  $-\text{SH}$  proton. A sharp singlet, which integrates as six hydrogen at  $\delta = 2.53$  ppm is assigned to the methyl protons attached to C(7) and C(11) which are chemically and magnetically equivalent. Aromatic protons appear as a multiplet at 7.20-8.62 ppm. A doublet at  $\delta=8.56$  is assigned to pyridyl ring protons at C(2) and C(4) and is more down field compared to the other proton C(3)H in the same ring,  $\delta=7.82$ , which appears as a triplet. Phenyl ring protons at C(13,17)H and C(19,23)H appear as a doublet at  $\delta=7.51$ . Two triplets ( $\delta=7.36$  and  $\delta=7.22$ ) are assigned to C(14,16)H, C(20,22)H and C(15,21)H respectively.

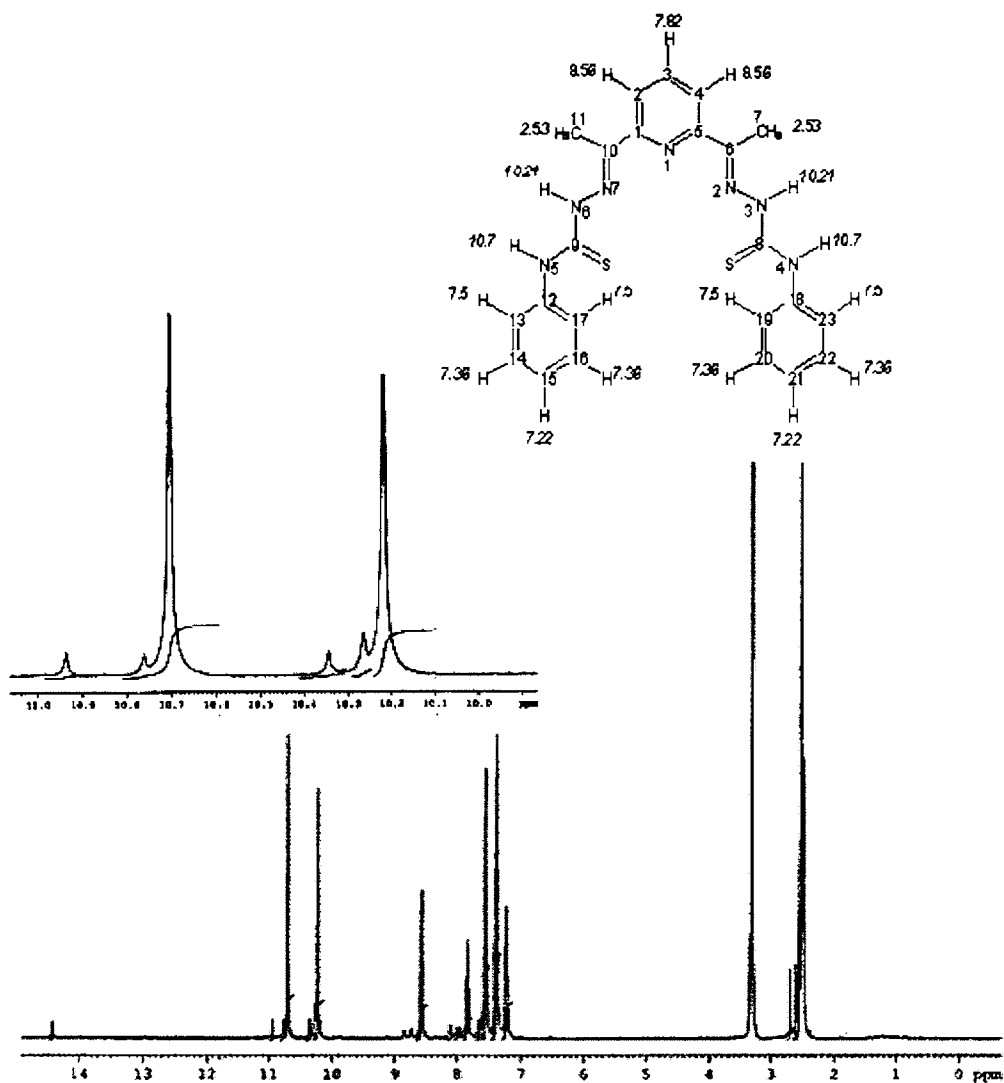


Figure 2.10.  $^1H$  NMR spectrum of  $H_2Ac_4Ph$

$H_2Ac_4Cy$ : The  $^1H$  NMR spectrum of  $H_2Ac_4Cy$  is represented in Figure 2.11. In this spectrum, the three protons of the pyridine ring appear at  $\delta$  values in the range 7.84 -8.20 ppm and signals for all the aliphatic protons of

methyl group and the cyclohexyl moiety have appeared at 1.24-3.37 ppm. N(4) and N(7) protons appear at  $\delta = 8.05$  ppm and a doublet, which integrates as two hydrogens at  $\delta = 8.09$  ppm is assigned to the protons attached to the pyridyl ring at C(2) and C(4). A one proton triplet at  $\delta = 7.26$  ppm is attributed to the C(3)H of the pyridyl ring. The absence of peaks corresponding to the S-H proton in the spectrum supports the fact that in solution, the predominant tautomer is in the thione form.

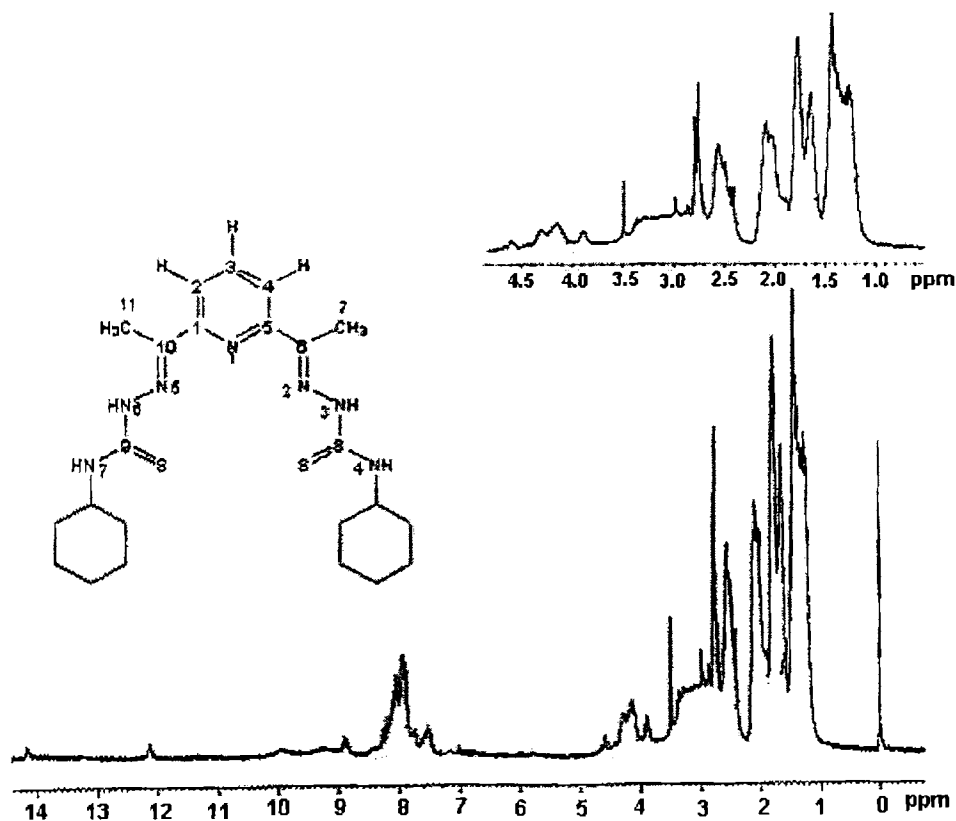


Figure 2.11.  $^1\text{H}$  NMR spectrum of  $\text{H}_2\text{Ac4Cy}$

**H<sub>2</sub>Ac<sub>4</sub>Me:** In the spectrum of H<sub>2</sub>Ac<sub>4</sub>Me (Figure 2.12), N(3)H and N(6)H protons at  $\delta = 10.372$  ppm which are more downfield, are easily distinguished from N(4)H and N(5)H protons ( $\delta = 8.66$ ), because the N(4,5)H appear as a doublet due to interaction with the methyl hydrogens of N(4,5)Me group. Absence of any coupling interactions by N(3)H and N(6)H protons due to the lack of availability of protons on neighbouring atoms render singlet peaks for the imine protons. A doublet, which integrates as two hydrogens at  $\delta = 8.41$  ppm is assigned to the protons attached to the pyridyl ring at C(2) and C(4) positions which are chemically and magnetically equivalent.

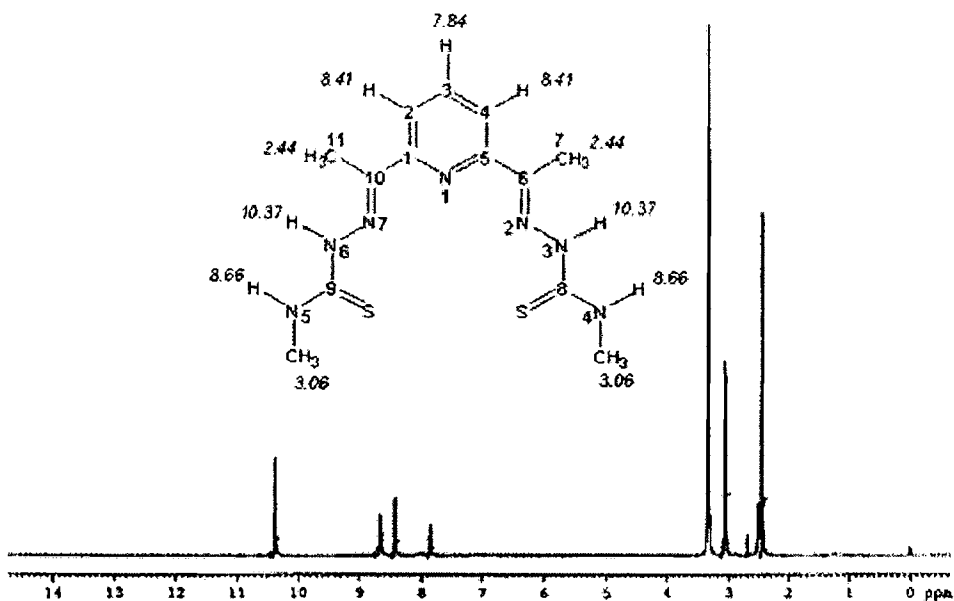


Figure 2.12. <sup>1</sup>H NMR spectrum of H<sub>2</sub>Ac<sub>4</sub>Me

A one proton triplet at  $\delta = 7.84$  ppm is attributed to the C(3)H of the pyridyl ring, which is unique in nature. It is observed that the protons of methyl groups attached to N(4) and N(5) are more deshielded than the protons attached to C(7) and C(11) ( $\delta = 2.44$ ).

$H_2Ac_4Et$ : In the spectrum of  $H_2Ac_4Et$  (Figure 2.13), N(3) and N(6) protons appear at  $\delta = 8.83$  ppm, which are shifted downfield because they are attached to heteroatoms and so are easily subjected to hydrogen bonding and are decoupled by the electrical quadrupole effects. These protons appear as a singlet as expected since the NH protons are decoupled from the nitrogen atoms and the protons from the adjacent atoms.

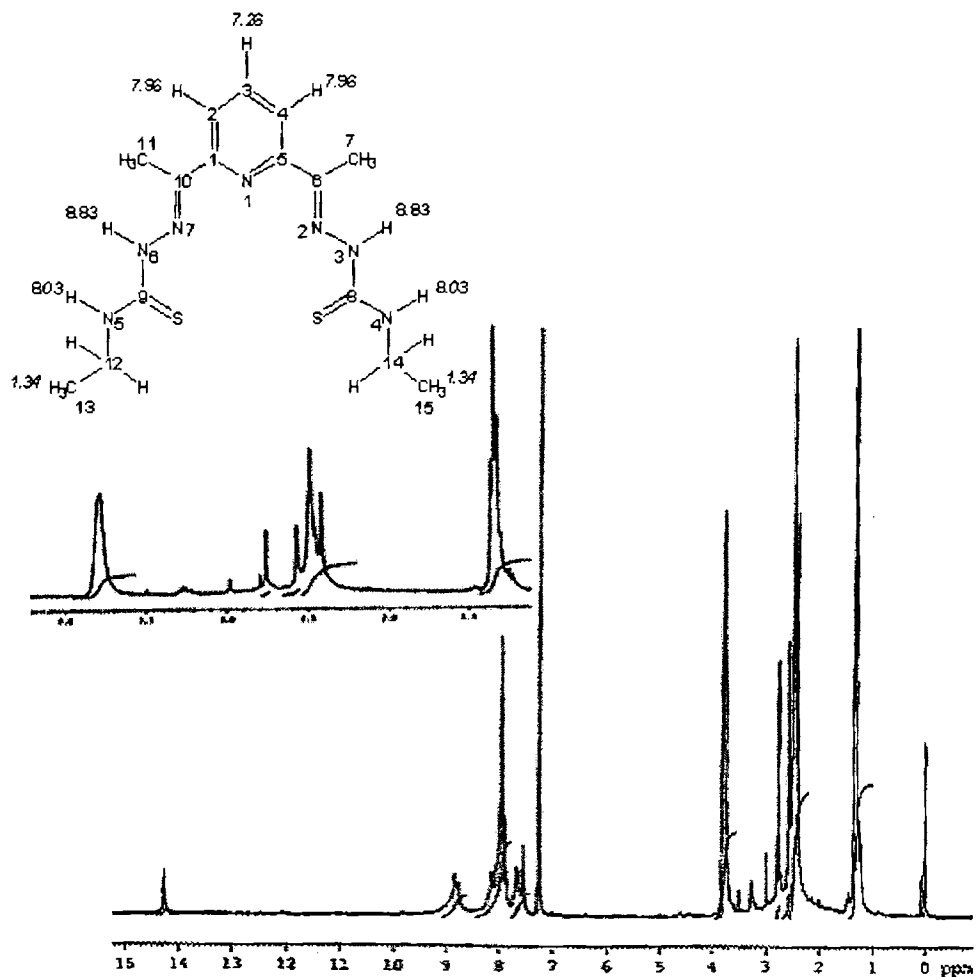


Figure 2.13.  $^1H$  NMR spectrum of  $H_2Ac_4Et$



The N(4)H and N(5)H protons ( $\delta=8.03$  ppm) appear as a triplet due to the interaction with the methylene hydrogens of the ethyl group. The three protons of the pyridine ring appear at  $\delta$  values 7.26 ppm for C(3)H and 7.96 ppm for C(2,4)H. A triplet at  $\delta=1.34$  ppm is assigned to the signal corresponding to the six protons of the methyl group attached to  $-\text{CH}_2$ . The remaining aliphatic protons of two  $-\text{CH}_3$  groups and two  $-\text{CH}_2$  groups are observed as a multiplet at about 2.41-3.13 ppm where the chemical shift values are very close and hence it is very difficult to be resolved. NMR assignments are in agreement with values already reported [30-33].

### Concluding remarks

This chapter presents the details regarding the syntheses of four ( $\text{H}_2\text{Ac4Ph}$ ,  $\text{H}_2\text{Ac4Cy}$ ,  $\text{H}_2\text{Ac4Me}$ ,  $\text{H}_2\text{Ac4Et}$ ), SNNNS donor ligands. The double armed bis(thiosemicarbazones) are pentadentate in nature with two thiosemicarbazone moieties in each system. Elemental analysis data is consistent with the empirical formulae of ligands. The compounds are further characterized by IR,  $^1\text{H}$  NMR and electronic spectral studies.

### References

1. M.A. Ali, S.E. Livingston, *Coord. Chem. Rev.* 13 (1974) 101.
2. M.J.M. Campbell, *Coord. Chem. Rev.* 15 (1975) 279.
3. S.B. Padhye, G.B. Kauffman, *Coord. Chem. Rev.* 63 (1985) 127.
4. D.X. West, S.B. Padhye, P.B. Sonawane, *Struct. Bonding* 76 (1991) 1.

5. D.X. West, A.E. Liberta, S.B. Padhye, R.C. Chitake, P.B. Sonawane, A.S. Kumbhar, R.G. Yerande, *Coord. Chem. Rev.* 123 (1993) 49.
6. J.S. Casas, M.S. García -Tasende, J. Sordo, *Coord. Chem. Rev.* 209 (2000) 197.
7. H.G. Petering, H.H. Buskirk, G.E. Underwood, *Cancer Res.* 24 (1964) 367.
8. G.H. Van Giessen, J.A. Crim, D.H. Petering, H.G. Petering, *J. Natl. Cancer Inst.* 51 (1973) 139.
9. A.E. Liberta, D.X. West, *Biometals* 5 (1992) 121.
10. H. Beraldo, S.B. Kaisner, J.D. Turner, I.S. Billeh, J.S. Ives, D.X. West, *Trans. Met. Chem.* 22 (1997) 459.
11. D.X. West, J.S. Ives, G.A. Bain, A.E. Liberta, J. Valdés- Martínez, K.H. Ebert, S. Hernández-Ortega, *Polyhedron* 16 (1997) 855.
12. H. Beraldo, D.X. West, *Trans. Met. Chem.* 22 (1997) 294.
13. H. Beraldo, L.P. Boyd, D.X. West, *Trans. Met. Chem.* 23 (1998) 67.
14. M. Mohan, P. Sharma, M. Kumar, N.K. Jha, *Inorg. Chim. Acta* 125 (1986) 9.
15. C.A. Brown, D.X. West, *Trans. Met. Chem.* 28 (2003) 154.
16. H. Beraldo, J.S. Ives, S.B. Kaisner, J.D. Turner, I.S. Billeh, D.X. West, *Trans. Met. Chem.* 22 (1997) 459.

17. A. Castineiras, E. Bermejo, D.X. West, A.K. El-Sawaf, J.K. Swearingen, *Polyhedron* 17 (1998) 2751.
18. L.J. Ackerman, D.X. West, C. J. Mathias, M.A. Green, *Nucl. Med. Biol.* 26 (1999) 551.
19. I.H. Hall, C.B. Lackey, T.D. Kistler, J.S. Ives, H. Beraldo, L.J. Ackerman, D.X. West, *Arch. Pharm. Med. Chem.* 333 (2000) 217.
20. S.N. Pandeya, D. Siram, G. Nath, E. DeClercq, *Eur. J. Pharm. Sci.* 9 (1999) 25.
21. M. Belicchi, F. Bisceglie, G. Gasparri, G. Pelosi, P. Tarasconi, R. Albertini, S. Pinelli, *J. Inorg. Biochem.* 89 (2002) 36.
22. D.X. West, A.M. Stark, G.A. Bain, A.E. Liberta, *Trans. Met. Chem.* 21 (1996) 289.
23. M.B. Ferrari, F. Bisceglie, G. Pelosi, M. Sassi, P. Tarasconi, M. Cornia, S. Capacchi, R. Albertini, S. Pinelli, *J. Inorg. Biochem.* 90 (2002) 113.
24. S.K. Jain, B.S. Garg, Y.K. Bhoon, D.L. Klayman, J.P. Scovill, *Spectrochim. Acta* 41A (1985) 407.
25. R.M. Silverstein, G.C. Bassler, T.C. Morrill, *Spectrometric Identification of Organic Compounds*, 4<sup>th</sup> ed. Wiley, New York, 1981.
26. D.X. West, Y.-H. Yang, T.L. Klein, K.I. Goldberg, A.E. Liberta, *Polyhedron* 14 (1995) 3051.
27. D.X. West, I.S. Billeh, J.P. Jesinski, J.M. Jesinski, R.J. Butcher, *Trans. Met. Chem.* 23 (1998) 209.

28. R.T. Morrison, R.N. Boyd, *Organic Chemistry*, 4<sup>th</sup> ed., Allyn and Bacon Inc., London, 1990.
29. D.H. Williams, I. Fleming, *Spectroscopic Methods in Organic Chemistry*, 4<sup>th</sup> ed., Mc. Graw-Hill, London, 1989.
30. R.P. John, A. Sreekanth, M.R.P. Kurup, A. Usman, A.R. Ibrahim, H.-K. Fun, *Spectrochim. Acta* 59A (2003) 1349.
31. P. Bindu, M.R.P. Kurup, T.R. Satyakeerthy, *Polyhedron* 18 (1999) 321.
32. S. Jayasree, K.K. Aravindakshan, *Trans. Met. Chem.* 18 (1993) 85.
33. M. Nazimuddin, M.A. Ali, F.E. Smith, *Polyhedron* 10 (1991) 1327.

\*\*\*\*\*

## Synthesis and spectral characterization of Cu(II) complexes of bis(*N*<sup>4</sup>-substitutedthiosemicarbazones) of 2,6-diacetylpyridine

### 3.1. Introduction

The most important contribution to copper chemistry must be the role that biological copper [1-4] has played in stimulating research in the inorganic chemistry of copper, not only in the chemistry of copper proteins, for which Cu(I), Cu(II) and Cu(III) species are relevant, but also in systems where more than one type of Cu is considered present. The copper(II) state is significantly more common and is extensively involved as an intermediate oxidation state in mechanistic studies especially those involving amino acid species. Electron paramagnetic resonance spectroscopy is one of the most suitable techniques for studying the changes in molecular structure of the paramagnetic complexes. Recently there has been considerable interest in the coordination chemistry of copper(II) complexes mainly due to their interesting physico-chemical and biological properties.

Copper bis(thiosemicarbazone) complexes [5, 6] have been the focus of investigation as metallodrugs for various medical applications for over thirty years. Several  $\alpha$ -diketone-bis(thiosemicarbazone) copper(II) complexes have validated biological activity. Kethoxal-bis(thiosemicarbazone)copper(II) (Cu-KTS), for example, has demonstrated carcinolytic and carcinostatic behavior against several established rat tumors [7, 8]. The biological function of these compounds is not clear, but presumably additional chemical insight into the nature of the compounds will contribute to the solution of the problem. Complexes where the donor atoms are nitrogen and sulfur may be

expected to possess unusual electronic structures, since complexes with sulfur donor atoms have exhibited a variety of oxidation states [9], and four-coordinated planar nitrogen complexes such as copper porphyrins and phthalocyanines are known to have highly delocalized electronic structures [10]. Except for the dithiosemicarbazones, there are only a very few other examples of coordination to copper where the donor atoms are sulfur and nitrogen [11].

## 3.2. Experimental

### 3.2.1. Materials

The synthesis of bis(thiosemicarbazone) ligands were discussed in Chapter 2 and solvents were purified by distillation.  $\text{Cu}(\text{OAc})_2 \cdot \text{H}_2\text{O}$  (Fluka),  $\text{CuCl}_2 \cdot 2\text{H}_2\text{O}$  (E-Merck), potassium thiocyanate (BDH, AR grade) and  $\text{Cu}(\text{NO}_3)_2 \cdot 3\text{H}_2\text{O}$  (S.D.fine-chemicals Ltd) were used as received.

### 3.2.2. Syntheses of complexes

**$[\text{Cu}_2(\text{HAc4Ph})_2(\text{OAc})_2] \cdot 2\text{H}_2\text{O}$  (1):** A solution of ligand  $\text{H}_2\text{Ac4Ph}$  (0.461 g, 1 mmol) in DMF-methanol mixture was treated solution of  $\text{Cu}(\text{OAc})_2 \cdot \text{H}_2\text{O}$  (0.199 g, 1 mmol) in methanol-water mixture. The above brown solution was refluxed for about 4 hrs and allowed to cool. The brown colored compound formed was filtered and washed with methanol and ether and dried *in vacuo* over  $\text{P}_4\text{O}_{10}$ .

**$[\text{Cu}(\text{HAc4Ph})\text{NO}_3] \cdot 2.5 \text{CH}_3\text{OH}$  (2):** A solution of ligand  $\text{H}_2\text{Ac4Ph}$  (0.461 g, 1 mmol) in DMF-methanol mixture was treated with a methanolic solution of  $\text{Cu}(\text{NO}_3)_2 \cdot 3\text{H}_2\text{O}$  (0.240 g, 1 mmol). The above brown solution was refluxed for about 4 hrs and allowed to cool. The brown compound formed

was filtered and washed with methanol and ether and dried *in vacuo* over  $P_4O_{10}$ .

**[Cu<sub>2</sub>(Ac4Ph)<sub>2</sub>·5H<sub>2</sub>O (3):** A solution of ligand H<sub>2</sub>Ac4Ph (0.461 g, 1 mmol) in DMF-methanol mixture was treated with a methanolic solution of CuCl<sub>2</sub>·2H<sub>2</sub>O (1 mmol, 0.168 g). The dark brown solution obtained was refluxed for about 4 hrs and allowed to cool. The brown compound formed was filtered and washed with methanol and ether and dried *in vacuo* over  $P_4O_{10}$ .

**[Cu(HAc4Cy)OAc]·2H<sub>2</sub>O (4):** A solution of ligand H<sub>2</sub>Ac4Cy (0.473 g, 1 mmol) in CHCl<sub>3</sub> was treated with solution of Cu(OAc)<sub>2</sub>·H<sub>2</sub>O (0.199 g, 1 mmol) in methanol-water mixture. The above green solution was refluxed for about 4 hrs and allowed to cool. The green colored compound formed was filtered and washed with methanol and ether and dried *in vacuo* over  $P_4O_{10}$ .

**[Cu(HAc4Cy)Cl]·C<sub>2</sub>H<sub>5</sub>OH (5):** A solution of ligand H<sub>2</sub>Ac4Cy (0.473 g, 1 mmol) in CHCl<sub>3</sub> was treated with a methanolic solution of CuCl<sub>2</sub>·2H<sub>2</sub>O (0.168 g, 1 mmol). The green solution obtained was refluxed for about 4 hrs and allowed to cool. The green compound formed was filtered and washed with methanol and ether and dried *in vacuo* over  $P_4O_{10}$ .

**[Cu(HAc4Cy)NCS]·3H<sub>2</sub>O·CH<sub>3</sub>OH (6):** A solution of ligand H<sub>2</sub>Ac4Cy (0.473 g, 1 mmol) in CHCl<sub>3</sub> was treated with a methanolic solution of Cu(OAc)<sub>2</sub>·H<sub>2</sub>O (0.199 g, 1 mmol). A solution of KCNS (1.5 mmol) in water was also added. The above dark green solution was refluxed for about 4 hrs and allowed to cool. The green compound formed was filtered and washed with methanol and ether and dried *in vacuo* over  $P_4O_{10}$ .

**[Cu<sub>2</sub>(Ac4Cy)<sub>2</sub>·8H<sub>2</sub>O (7):** A solution of ligand H<sub>2</sub>Ac4Cy (0.473 g, 1 mmol) in CHCl<sub>3</sub> was treated with a methanolic solution of Cu(NO<sub>3</sub>)<sub>2</sub>·3H<sub>2</sub>O (0.240 g, 1 mmol). The above green solution was refluxed for about 4 hrs and allowed to cool. The green compound formed was filtered and washed with methanol and ether and dried *in vacuo* over P<sub>4</sub>O<sub>10</sub>.

**[Cu<sub>2</sub>(HAc4Me)<sub>2</sub>(NO<sub>3</sub>)<sub>2</sub>·6H<sub>2</sub>O·CH<sub>3</sub>OH (8):** A solution of ligand H<sub>2</sub>Ac4Me (0.337 g, 1 mmol) in DMF-methanol mixture was treated with a methanolic solution of Cu(NO<sub>3</sub>)<sub>2</sub>·3H<sub>2</sub>O (0.240 g, 1 mmol). The above brown solution was refluxed for about 4 hrs and allowed to cool. The brown compound formed was filtered and washed with methanol and ether and dried *in vacuo* over P<sub>4</sub>O<sub>10</sub>.

**[Cu<sub>3</sub>(Ac4Et)<sub>2</sub>(NO<sub>3</sub>)<sub>2</sub>·3H<sub>2</sub>O (9):** A solution of ligand H<sub>2</sub>Ac4Et (0.365 g, 1 mmol) in CHCl<sub>3</sub> was treated with a methanolic solution of Cu(NO<sub>3</sub>)<sub>2</sub>·3H<sub>2</sub>O (0.240 g, 1 mmol). The above black solution was refluxed for about 4 hrs and allowed to cool. The black compound formed was filtered and washed with methanol and ether and dried *in vacuo* over P<sub>4</sub>O<sub>10</sub>.

### 3.3. Physical measurements

Elemental analyses of the ligand and the complexes were done on a Vario EL III CHNS analyzer at SAIF, Kochi, India. IR spectral analyses were done using KBr pellets on Thermo Nicolet AVATAR 370 DTGS FT-IR spectrophotometer in the 4000-400 cm<sup>-1</sup> region. The far IR spectra were recorded using polyethylene pellets in the 500-100 cm<sup>-1</sup> region on a Nicolet Magna 550 FT-IR instrument at Regional Sophisticated Instrument Facility, Indian Institute of Technology, Bombay. UVD-3500, UV-VIS Double Beam Spectrophotometer was used to record the electronic spectra from DMF



solutions in the range 200-900 nm. The magnetic susceptibility measurements were done in the polycrystalline state at room temperature on a Vibrating Sample Magnetometer at the Indian Institute of Technology, Roorkee, India. EPR spectral measurements were carried out on a Varian E-112 X-band spectrometer using TCNE as standard at the Sophisticated Analytical Instruments Facility, Indian Institute of Technology, Bombay, India. The molar conductivities of the complexes in dimethylformamide solutions ( $10^{-3}$  M) at room temperature were measured using a direct reading conductivity meter.

### 3.4. Results and discussion

All the complexes were prepared by reaction with equimolar ratios of corresponding ligands and metal salts in neutral condition. Colors, partial elemental analyses, molar conductivities and magnetic susceptibilities are listed in Table 3.1. Since all the four ligands are pentadentate, their metal complexes formed were having six coordination. The mode of coordination is different for all the four bis(thiosemicarbazone) ligands. They were able to coordinate as a dianionic ligand in complexes **3**, **7** and **9** when both of the thiosemicarbazone moieties have lost their thioamide protons and coordinate as a monoanionic ligand in complexes **1**, **2**, **4**, **5**, **6** and **8** when only one of the thiosemicarbazone moieties have lost an amide proton. In the Cu(II) complexes **3** and **7**, the ligands are coordinated to two metal centers to form binuclear complexes and in **9**, the ligand is coordinated to three metal centers to form trinuclear complex.

Table 3.1. Colors, partial elemental analyses, magnetic susceptibilities and molar conductivities of the complexes

Compound	Color	Composition % (Found/Calculated)			$\mu$ (B.M.)	$\Lambda_M$
		C	H	N		
$[\text{Cu}_2(\text{HAc4Ph})_2(\text{OAc})_2] \cdot 2\text{H}_2\text{O}$ (1)	brown	49.93(49.94)	4.31(4.53)	16.98(16.31)	1.20	13
$[\text{Cu}(\text{HAc4Ph})\text{NO}_3] \cdot 2.5 \text{CH}_3\text{OH}$ (2)	brown	45.77(45.97)	4.06(4.84)	16.30(16.82)	1.67	29
$[\text{Cu}_2(\text{Ac4Ph})_2] \cdot 5\text{H}_2\text{O}$ (3)	brown	48.49(48.62)	4.12(4.61)	17.24(17.26)	1.28	-
$[\text{Cu}(\text{HAc4Cy})\text{OAc}] \cdot 2\text{H}_2\text{O}$ (4)	green	47.72(47.56)	5.80(6.55)	15.13(15.53)	1.63	27
$[\text{Cu}(\text{HAc4Cy})\text{Cl}] \cdot \text{C}_2\text{H}_5\text{OH}$ (5)	green	48.78(48.61)	6.44(6.53)	16.04(15.87)	1.78	30
$[\text{Cu}(\text{HAc4Cy})\text{NCS}] \cdot 3\text{H}_2\text{O} \cdot \text{CH}_3\text{OH}$ (6)	green	44.08(44.13)	6.26(6.52)	15.82(16.47)	1.62	33
$[\text{Cu}_2(\text{Ac4Cy})_2] \cdot 8\text{H}_2\text{O}$ (7)	green	45.41(45.49)	6.56(6.80)	16.99(16.14)	1.06	-
$[\text{Cu}_2(\text{HAc4Me})_2(\text{NO}_3)_2] \cdot 6\text{H}_2\text{O} \cdot \text{CH}_3\text{OH}$ (8)	black	30.96(30.47)	4.63(4.93)	20.74(21.06)	1.64	52
$[\text{Cu}_3(\text{Ac4Et})_2(\text{NO}_3)_2] \cdot 3\text{H}_2\text{O}$ (9)	green	32.47(32.88)	3.88(4.42)	20.01(20.45)	1.10	18

Molar conductivity of  $10^{-3}$  M DMF solution, in  $\text{ohm}^{-1} \text{cm}^2 \text{mol}^{-1}$

It should be noted that no difference in the method of preparation of any of these complexes was undertaken and, yet, different stoichiometries have resulted with no apparent trends based on four ligands. The lack of significant solubility in even the most polar solvents, DMF and DMSO, has frustrated our attempts to grow crystals for structure determination of the complexes.

The green and brown colors are common to complexes involving thiosemicarbazone coordination due to the sulfur-metal charge-transfer bands, which dominate their visible spectra [12]. The molar conductivity values indicate that all the complexes are non-electrolytes, with values at high end of the non-electrolyte range [13] suggesting that the anion and the ligand are coordinated to the central copper(II). Magnetic moments of the complexes were calculated from magnetic susceptibility measurements using diamagnetic corrections. Mononuclear Cu(II) complexes exhibit magnetic moments in the range 1.5-1.9 B.M., which are close to the spin only value [14]. The magnetic moments of the binuclear Cu(II) complexes were found to be in the range 1.15-1.40 B.M. This low magnetic moment may be attributed to the presence of a strong antiferromagnetic spin-spin interaction.

### ***3.4.1. IR spectral studies***

The infrared spectral data of the complexes 1-9 are presented in Table 3.2 with their tentative assignments. The high frequency bands of the uncomplexed ligand H<sub>2</sub>Ac4Ph centered at 3297, 3220 cm<sup>-1</sup> and H<sub>2</sub>Ac4Cy at 3290, 3259 cm<sup>-1</sup> and H<sub>2</sub>Ac4Me at 3380, 3328 cm<sup>-1</sup> and H<sub>2</sub>Ac4Et at 3363, 3328 cm<sup>-1</sup>, are attributed to  $\nu(\text{N-H})$  stretching vibrations. The absence of large systematic shifts of the first value in all the complexes indicate that this absorption is best assigned to the *N*<sup>4</sup>-substituted  $\nu(\text{N-H})$  vibration. In most of the complexes it is difficult to observe the disappearance of  $\nu(\text{N-H})$  bands

due to the partial deprotonation of the ligand, as found for similar complexes where the ligand was not completely deprotonated [15]. The  $\nu(^2\text{N-H})$  bands of the free ligands got disappeared in the spectra of complexes **3** (Figure 3.1), **7** (Figure 3.5) and **9** (Figure 3.6) providing a strong evidence for the ligand coordination around copper(II) ion in the deprotonated thiol form.

Significant changes in the ligand bands upon complexation include variations in the  $\nu(\text{C=N}, \text{C=C})$  vibration energies and systematic shifts of the  $\nu(\text{C-S})$  absorption bands to lower frequencies. These data indicate coordination through two azomethine nitrogen, the pyridyl nitrogen and two sulfur atoms [16]. The azomethine  $\text{C=N}$  band for the bis(thiosemicarbazones) is similar in energy to the heterocyclic thiosemicarbazones [17-21] with the band appearing in the  $1540\text{-}1600\text{ cm}^{-1}$  region and shifting to lower energy upon coordination. In the past, evidence of coordination of thiosemicarbazones and dithiocarbazate ligands to metal ions via the azomethine nitrogen atom was based on the shifting of the azomethine  $\text{C=N}$  band of the free ligand from higher to lower wavenumbers [22]. However shifting of the  $\nu(\text{C=N})$  band to both higher [23, 24] and lower [25] wavenumbers has been reported. Since the azomethine  $\text{C=N}$  band is expected to couple with other bands, its shifting will also be dependent on how much it is in combination with other bands [26]. In all the complexes, a second band {*ie.*,  $\nu[\text{C=N}(2)]$ } is found near  $1600\text{ cm}^{-1}$  due to the formation of a double bond upon loss of the  $\text{N}(2)\text{H}$  and coordination of the deprotonized sulfur atom [27]. The pyridine nitrogen appears to be involved in coordination based on the in-plane and out-of-plane ring deformation bands shifting towards higher energies. Pyridine nitrogen coordination is further proved by strong bands observed in the region  $262\text{-}313\text{ cm}^{-1}$  assignable to  $\nu(\text{Cu-N}_{\text{py}})$  as suggested by Clark and Williams [28]. The coordination of the azomethine nitrogen to

copper(II) in the spectra of all the complexes is confirmed due to the presence of a band in the range 423-470  $\text{cm}^{-1}$  [29]. Strong bands found at 1033-1102  $\text{cm}^{-1}$  in the ligands are assigned to the  $\nu(\text{N-N})$  band of the bis(thiosemicarbazone). The increase in frequency of this band in the spectra of complexes is due to the increase in bond strength, again confirming the coordination *via* the azomethine nitrogen [30, 31].

The bands appearing in the range 857-869  $\text{cm}^{-1}$  (thioamide IV band) in the spectra of ligands have been shifted to lower frequencies (795-801) in complexes 3, 7 and 9 indicating coordination of the thione/thiolato sulphur [32] due to formation of a greater single C-S bond character and loss of the N(2)H hydrogen coordination which is found to be consistent with earlier reports [33]. The presence of bands in the range 323-350  $\text{cm}^{-1}$  in all complexes is assignable to  $\nu(\text{Cu-S})$  is another indication of sulphur coordination. Since one thiosemicarbazone moiety is anionic and the other is neutral in complexes 1, 2, 4, 5, 6 and 8, both  $\nu(\text{C=S})$  and  $\nu(^2\text{N-H})$  bands are present.

For the acetate complex 1, the bands at 1593 and 1412  $\text{cm}^{-1}$  and in complex 4 (Figure 3.2) at 1574 and 1436  $\text{cm}^{-1}$  correspond to symmetric and asymmetric stretching vibrations of the acetate group are in consistent with the presence of a monodentate acetate group in both cases [34]. In the chloro complex 5 (Figure 3.3), a strong band observed at 226.6  $\text{cm}^{-1}$  has been assigned to the  $\nu(\text{Cu-Cl})$  band which is similar to its assignment for terminal chloro ligands in other thiosemicarbazone complexes [35].

Table 3.2. Infrared spectral assignments ( $\text{cm}^{-1}$ ) of ligands and their Cu(II) complexes

Compound	$\nu(\text{C}=\text{N})$	$\nu(\text{N}=\text{C})$	$\nu(\delta(\text{C}-\text{S}))$	$\nu(\text{Cu}-\text{N})$	$\nu(\text{N}-\text{N})$
$\text{H}_2\text{Ac4Ph}$	1597	-	1322, 808	-	1028
$[\text{Cu}_2(\text{HAc4Ph})_2(\text{OAc})_2] \cdot 2\text{H}_2\text{O}$ (1)	1593	1660	1312, 795	477	1150
$[\text{Cu}(\text{HAc4Ph})\text{NO}_3] \cdot 2.5 \text{CH}_3\text{OH}$ (2)	1545	1600	1317, 802	430	1157
$[\text{Cu}_2(\text{Ac4Ph})_2] \cdot 5\text{H}_2\text{O}$ (3)	1535	1602	1220, 702	450	1150
$\text{H}_2\text{Ac4Cy}$	1596	-	1307, 857	-	1013
$[\text{Cu}(\text{HAc4Cy})\text{OAc}] \cdot 2\text{H}_2\text{O}$ (4)	1571	1646	1294, 802	460	1081
$[\text{Cu}(\text{HAc4Cy})\text{Cl}] \cdot \text{C}_2\text{H}_5\text{OH}$ (5)	1538	1611	1290, 802	426	1081
$[\text{Cu}(\text{HAc4Cy})\text{NCS}] \cdot 3\text{H}_2\text{O} \cdot \text{CH}_3\text{OH}$ (6)	1534	1600	1281, 800	424	1088
$[\text{Cu}_2(\text{Ac4Cy})_2] \cdot 8\text{H}_2\text{O}$ (7)	1589	1617	1201, 765	426	1074
$\text{H}_2\text{Ac4Me}$	1549	-	1353, 869	-	1043
$[\text{Cu}_2(\text{HAc4Me})_2(\text{NO}_3)_2] \cdot 6\text{H}_2\text{O} \cdot \text{CH}_3\text{OH}$ (8)	1544	1586	1308, 842	420	1126
$\text{H}_2\text{Ac4Et}$	1541	-	1307, 857	-	1050
$[\text{Cu}_3(\text{Ac4Et})_2(\text{NO}_3)_2] \cdot 3\text{H}_2\text{O}$ (9)	1534	1593	1238, 755	450	1088

Thiocyanato complex **6** (Figure 3.4) exhibits a strong and sharp band at  $2081\text{ cm}^{-1}$  [36], a weak band at  $761\text{ cm}^{-1}$  and another weak band at  $480\text{ cm}^{-1}$  which can be attributed to  $\nu(\text{CN})$ ,  $\nu(\text{CS})$  and  $\delta(\text{NCS})$  respectively. These values are typical for N-bonded thiocyanato complexes [37]. The presence of a medium band at  $325\text{ cm}^{-1}$  corresponds to  $\nu(\text{Cu}-\text{N}_{\text{thiocyanato}})$  vibrations is in agreement with earlier reported values [38].

According to Gatehouse et al, for nitrate complexes, the unidentate and bidentate  $\text{NO}_3$  groups exhibit three NO stretching bands. The separation of two highest frequency bands is  $115\text{ cm}^{-1}$  for unidentate complex whereas it is  $186\text{ cm}^{-1}$  for bidentate complex. Here in the nitrate complexes, the three bands observed at  $1434$ ,  $1317$  and  $1023\text{ cm}^{-1}$  for complex **2**,  $1494$ ,  $1381$  and  $1043\text{ cm}^{-1}$  for complex **8** and  $1429$ ,  $1307$  and  $1049\text{ cm}^{-1}$  for complex **9** (Figure 3.6) indicate the bands of the nitrate group. The fact that the nitrate group is terminally bonded in these cases is understood from the separation of  $117\text{ cm}^{-1}$  in **2**,  $113\text{ cm}^{-1}$  in **8** and  $122$  in **9** between the two highest frequency bands just mentioned above and these are unidentate in nature. Besides in the far IR spectrum (Figure 3.7) of the complexes, the bands observed at  $247.3$  can be assigned to  $\nu(\text{Cu}-\text{ONO}_2)$  consistence with the bands at  $253-280\text{ cm}^{-1}$  reported earlier for  $\text{Cu}-\text{ONO}_2$  in metal complexes [39]. A broad band at  $3455\text{ cm}^{-1}$  is assigned to lattice water in compound **3**, and at  $3446\text{ cm}^{-1}$  in compound **9**.

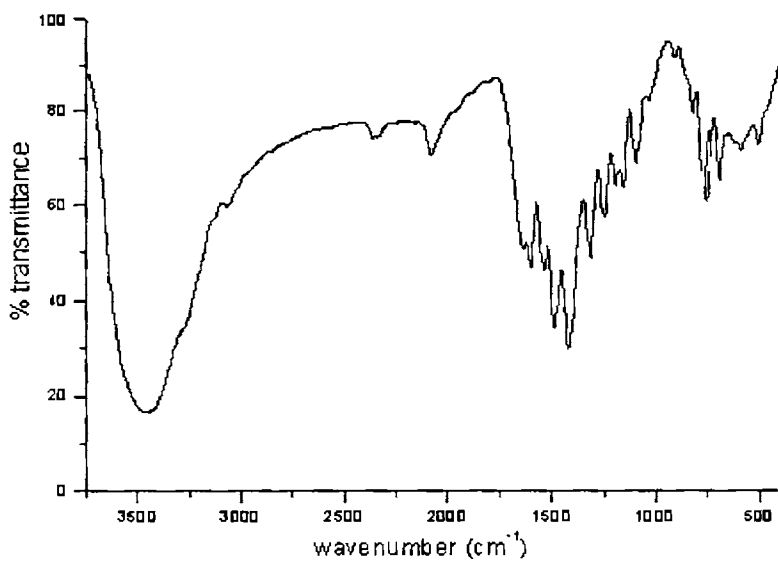


Figure 3.1. IR spectrum of compound  $[\text{Cu}_2(\text{Ac4Ph})_2] \cdot 5\text{H}_2\text{O}$  (3)

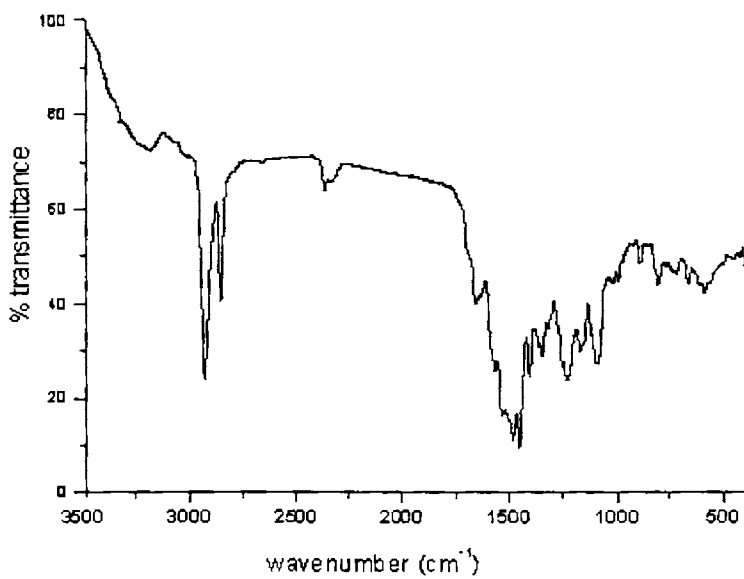


Figure 3.2. IR spectrum of compound  $[\text{Cu}(\text{HAc4Cy})\text{OAc}] \cdot 2\text{H}_2\text{O}$  (4)



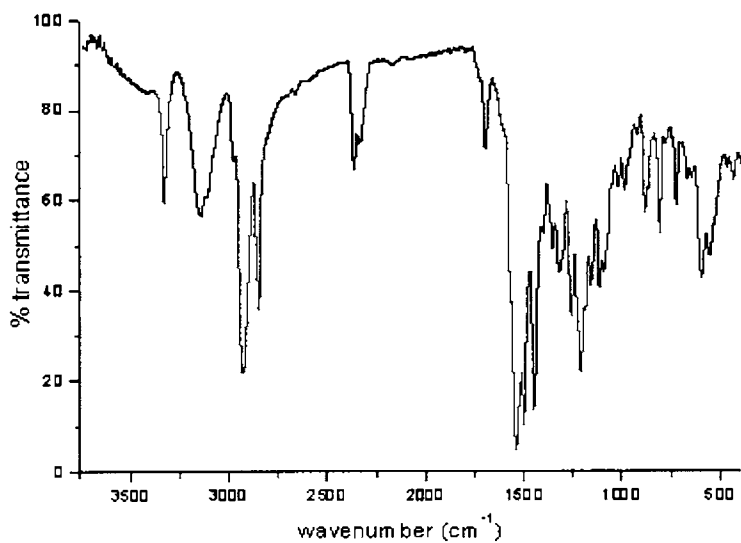


Figure 3.3. IR spectrum of compound  $[\text{Cu}(\text{HAc4Cy})\text{Cl}] \cdot \text{C}_2\text{H}_5\text{OH}$  (5)

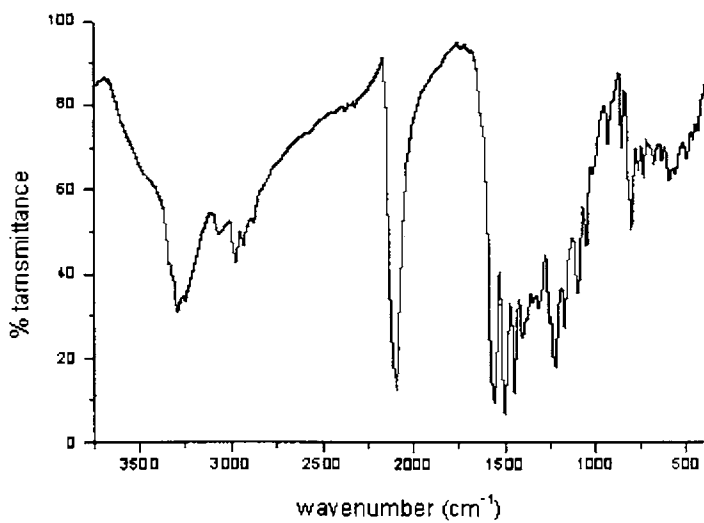


Figure 3.4. IR spectrum of compound  $[\text{Cu}(\text{HAc4Cy})\text{NCS}] \cdot 3\text{H}_2\text{O} \cdot \text{CH}_3\text{OH}$  (6)

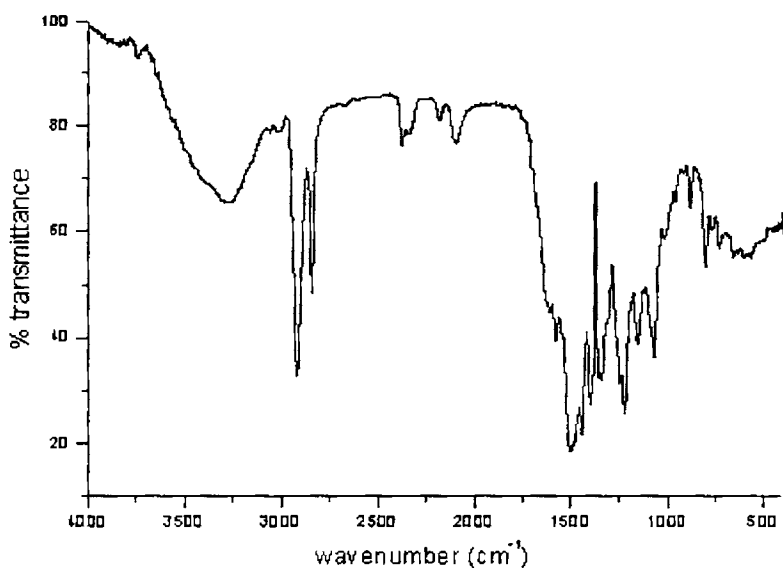


Figure 3.5. IR spectrum of compound  $[\text{Cu}_2(\text{Ac4Cy})_2] \cdot 8\text{H}_2\text{O}$  (7)

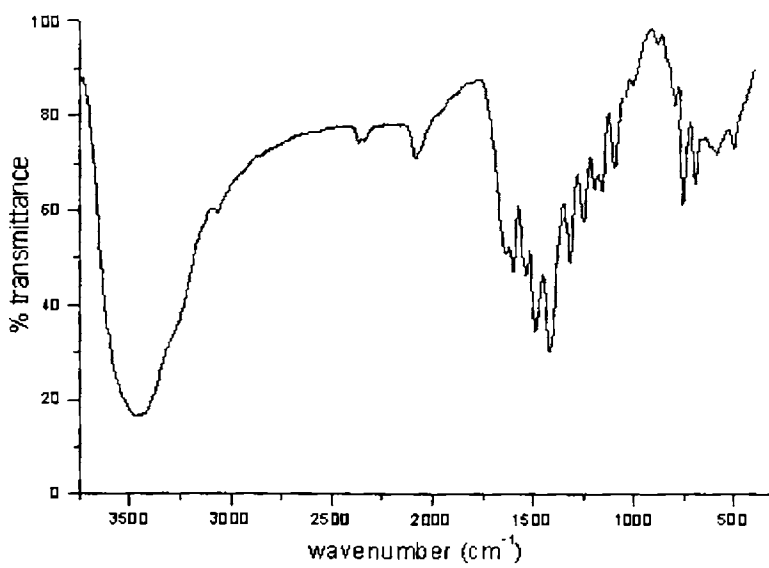


Figure 3.6. IR spectrum of compound  $[\text{Cu}_3(\text{Ac4Et})_2(\text{NO}_3)_2] \cdot 3\text{H}_2\text{O}$  (9)

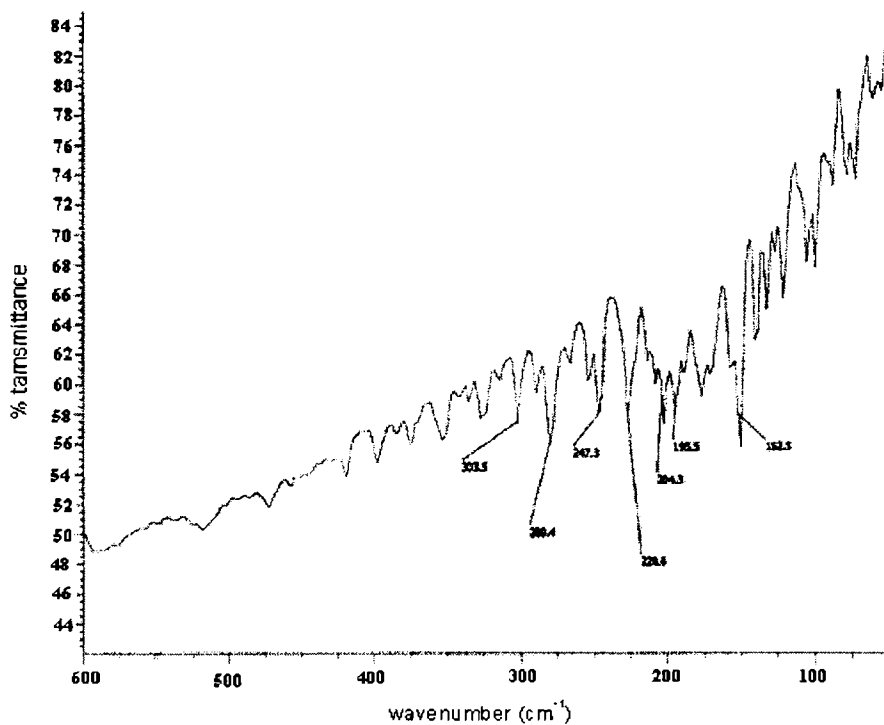


Figure 3.7. Far IR spectrum of  $[\text{Cu}(\text{HAc4Ph})\text{NO}_3] \cdot 2.5 \text{CH}_3\text{OH}$  (2)

### 3.4.2. Electronic spectral studies

The electronic spectra of copper(II) complexes is probably the most easily determined electronic property to measure but equally the most difficult from which to obtain useful structural information, due to flexible stereochemistry of the copper(II) ions. The electronic states of several transition metal complexes have been extensively studied in the last two decades and detailed knowledge has been accumulated for octahedral complexes.

There is extraordinary amount of spectroscopic interaction available in the literature because of the general ease with which copper(II) complexes can

be made. By far the bulk of this consists of complexes with a single broad poorly resolved asymmetric band in the visible region. The copper(II) complexes of lower coordination numbers are also appear to exist in a wide range of stereochemistries making it difficult to use electronic spectroscopy alone as a definitive tool for identifying structures [40].

The unique feature of first row transition metals is their ability to form transition metal complexes in which tetrahedral, octahedral, square coplanar and their stereochemistries predominate. The copper(II) ion is a typical transition metal ion which forms coordination complexes of different stereochemistries, but it is reluctant to take up regular octahedral or tetrahedral stereochemistry. Due to large distortion in bond lengths, the splitting of electronic energy levels in copper(II) ions tend to be larger than other first row transition metals. Thus the electronic properties of transitions of copper(II) complexes are relatively sensitive to stereochemistry. The magnetic and EPR properties are mainly determined by electronic configuration of copper(II) ion in the ground state.

The variety of colors among transition metal complexes arises from the electronic transition between energy levels whose spacing corresponds to the wavelengths available in visible light. In complexes, these transitions are frequently referred to as *d-d* transitions because they involve the molecular orbitals that are mainly metal *d* in character [41]. Since this spacing depends on factors such as the geometry of the complex, the nature of the ligands present, and the oxidation state of the central metal atom, the electronic spectra of complexes can provide valuable information relating to bonding and structure [42]. The Cu(II) complexes are characterized generally by intense blue or green colors.

These colors are probably caused by a strong absorption in the ultraviolet region arising from the charge transfer transitions. Charge transfer transitions are transitions in which an electron is transferred from one atom or group in the molecule to another atom or group. Such transitions are of high intensity and usually occur at the ultraviolet or the near ultraviolet i.e. at the high-energy end of the visible spectrum. Since a charge transfer transition originates from the redox character of the metal ion and the ligand, it is of two distinct types, namely ligand to metal and metal to ligand.

The electronic spectra of complexes in DMF solution are presented in Table 3.3. Each bis(thiosemicarbazone) and its Cu(II) complexes have a higher energy ring  $\pi$ - $\pi^*$  bands in the range 32,450-31,900  $\text{cm}^{-1}$  which are not significantly altered on complex formation. The  $n \rightarrow \pi^*$  transitions associated with azomethine and thioamide functions of the free thiosemicarbazones are found in the range 29,620-28,090  $\text{cm}^{-1}$ . Representative spectra of the complexes are presented in Figures 3.8a, 3.8b and 3.8c.

The six coordinated complex  $[\text{Cu}_2(\text{HAc4Ph})_2(\text{OAc})_2] \cdot 2\text{H}_2\text{O}$  (1), exhibits the  $d-d$  band at 16,450  $\text{cm}^{-1}$ . Due to the broadness of the band only one transition could be distinguished. The band at 24,470  $\text{cm}^{-1}$  corresponds to the  $\text{S} \rightarrow \text{Cu(II)}$  charge transfer transition [4,14]. The  $n \rightarrow \pi^*$  and  $\pi \rightarrow \pi^*$  transitions due to the ligand are obtained at 28,090 and 32,150  $\text{cm}^{-1}$  respectively.

Compound  $[\text{Cu}(\text{HAc4Ph})\text{NO}_3] \cdot 2.5 \text{CH}_3\text{OH}$  (2) exhibited a broad band at 16,230  $\text{cm}^{-1}$  characteristic of  $\text{Cu}^{2+}$  complex with a  ${}^2\text{B}_1$  ground state [36]. Due to broadness of the band, other two  $d-d$  transitions could not be assigned. The intense charge transfer band occurs at 23,800  $\text{cm}^{-1}$ . The complex has a shoulder at 28,210  $\text{cm}^{-1}$  corresponding to  $n \rightarrow \pi^*$  transition. The  $\pi \rightarrow \pi^*$

transition is observed at  $32,120\text{ cm}^{-1}$ .

The *d-d* transition for  $[\text{Cu}_2(\text{Ac4Ph})_2]\cdot 5\text{H}_2\text{O}$  (3) is observed as a broad band at  $14,430\text{ cm}^{-1}$ . The charge transfer band was assigned at  $25,790\text{ cm}^{-1}$  and the ligand transitions at  $28,150$  and  $32,100\text{ cm}^{-1}$ . In compound  $[\text{Cu}(\text{HAc4Cy})\text{OAc}]\cdot 2\text{H}_2\text{O}$  (4), *d-d* transitions are observed as weak shoulders at  $16,470\text{ cm}^{-1}$ . Ligand to metal charge transfer band appeared at  $24,030\text{ cm}^{-1}$  and the ligand transitions at  $29,200$  and  $32,140\text{ cm}^{-1}$ .

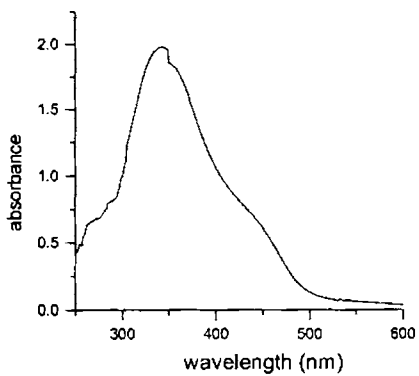
For compound  $[\text{Cu}(\text{HAc4Cy})\text{Cl}]\cdot \text{C}_2\text{H}_5\text{OH}$  (5), the *d-d* transition as a broad band is observed at  $15,810\text{ cm}^{-1}$ . Due to the broadness of the band, the other expected transitions in this range could not be assigned. The band at  $23,370\text{ cm}^{-1}$  corresponds to the charge transfer transition. The  $n \rightarrow \pi^*$  and  $\pi \rightarrow \pi^*$  transitions due to the ligand are obtained at  $28,160$  (sh) and  $32,250\text{ cm}^{-1}$  respectively. The *d-d* electronic transition for the single electron in  $\text{Cu}^{2+}$  in compound  $[\text{Cu}(\text{HAc4Cy})\text{NCS}]\cdot 3\text{H}_2\text{O}\cdot \text{CH}_3\text{OH}$  (6) was observed as a broad band at  $16,530\text{ cm}^{-1}$ . The  $\text{S} \rightarrow \text{Cu}(\text{II})$  charge transfer band consisted of a high intense peak at  $23,500\text{ cm}^{-1}$  [17, 18]. The ligand transitions are obtained at  $28,560$  (sh) and  $32,260\text{ cm}^{-1}$ .

For compound  $[\text{Cu}_2(\text{Ac4Cy})_2]\cdot 8\text{H}_2\text{O}$  (7), the *d-d* band is observed at  $15,920\text{ cm}^{-1}$ . The band at  $23,810\text{ cm}^{-1}$  corresponds to the charge transfer transition. The  $n \rightarrow \pi^*$  and  $\pi \rightarrow \pi^*$  transitions due to the ligand are obtained at  $28,290$  and  $32,290\text{ cm}^{-1}$  respectively. The *d-d* transition for  $[\text{Cu}_2(\text{HAc4Me})_2(\text{NO}_3)_2]\cdot 6\text{H}_2\text{O}\cdot \text{CH}_3\text{OH}$  (8) is observed as a broad band at  $15,360\text{ cm}^{-1}$ . The charge transfer band was assigned at  $25,030\text{ cm}^{-1}$  and the ligand transitions at  $29,600$  and  $32,000\text{ cm}^{-1}$ . In compound  $[\text{Cu}_3(\text{Ac4Et})_2(\text{NO}_3)_2]\cdot 3\text{H}_2\text{O}$  (9), *d-d* transitions are observed as weak shoulders at  $16,350\text{ cm}^{-1}$ . Ligand to metal charge transfer band appeared at  $23,070\text{ cm}^{-1}$ .

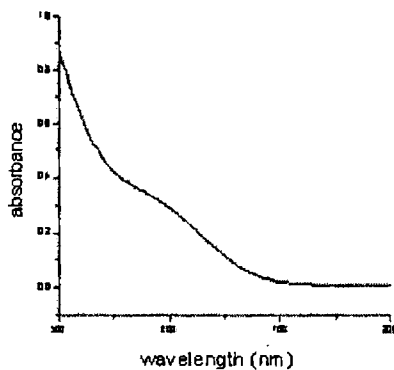
and the ligand transitions at 28,650 and 32,010  $\text{cm}^{-1}$ .

Table 3.3. Electronic spectral assignments ( $\text{cm}^{-1}$ ) for the ligands and their Cu(II) complexes

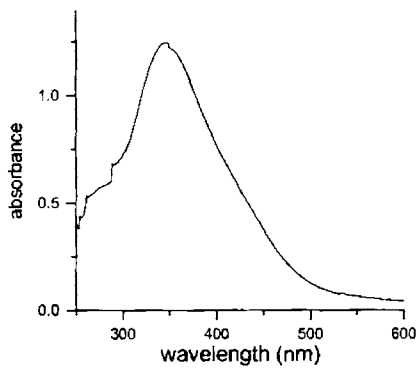
Compound	$\pi-\pi^*$	$n-\pi^*$	LMCT	$d-d$
$\text{H}_2\text{Ac4Ph}$	32,250	28,900	-	-
$[\text{Cu}_2(\text{HAc4Ph})_2(\text{OAc})_2] \cdot 2\text{H}_2\text{O}$ (1)	32,150	28,090	24,470	16,450
$[\text{Cu}(\text{HAc4Ph})\text{NO}_3] \cdot 2.5 \text{CH}_3\text{OH}$ (2)	32,120	28,210	23,800	16,230
$[(\text{CuAc4Ph})_2] \cdot 5\text{H}_2\text{O}$ (3)	32,100	28,150	25,790	14,430
$\text{H}_2\text{Ac4Cy}$	32,450	29,210	-	-
$[\text{Cu}(\text{HAc4Cy})\text{OAc}] \cdot 2\text{H}_2\text{O}$ (4)	32,140	29,200	24,030	16,470
$[\text{Cu}(\text{HAc4Cy})\text{Cl}] \cdot \text{C}_2\text{H}_5\text{OH}$ (5)	32,250	28,160	23,370	15,810
$[\text{Cu}(\text{HAc4Cy})\text{NCS}] \cdot 3\text{H}_2\text{O} \cdot \text{CH}_3\text{OH}$ (6)	32,260	28,560	23,500	16,530
$[\text{Cu}_2(\text{Ac4Cy})_2] \cdot 8\text{H}_2\text{O}$ (7)	32,290	28,290	23,810	15,920
$\text{H}_2\text{Ac4Me}$	32,050	29,620	-	-
$[\text{Cu}_2(\text{HAc4Me})_2(\text{NO}_3)_2] \cdot 6\text{H}_2\text{O} \cdot \text{CH}_3\text{OH}$ (8)	32,000	29,600	25,030	15,360
$\text{H}_2\text{Ac4Et}$	32,240	29,390	-	-
$[\text{Cu}_3(\text{Ac4Et})_2(\text{NO}_3)_2] \cdot 3\text{H}_2\text{O}$ (9)	32,010	28,650	23,070	16,350



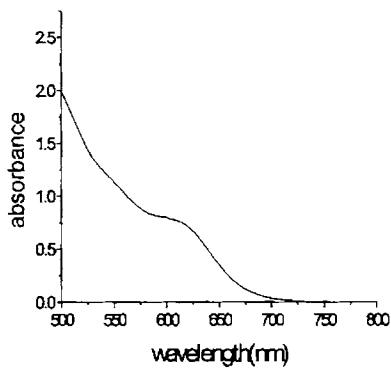
$[\text{Cu}_2(\text{HAc4Ph})_2(\text{OAc})_2] \cdot 2\text{H}_2\text{O}$  (1)



$[\text{Cu}_2(\text{HAc4Ph})_2(\text{OAc})_2] \cdot 2\text{H}_2\text{O}$  (1)



$[\text{Cu}(\text{HAc4Ph})\text{NO}_3] \cdot 2.5 \text{CH}_3\text{OH}$  (2)



$[\text{Cu}(\text{HAc4Ph})\text{NO}_3] \cdot 2.5 \text{CH}_3\text{OH}$  (2)

Figure 3.8a. Electronic spectra of the compounds 1 and 2



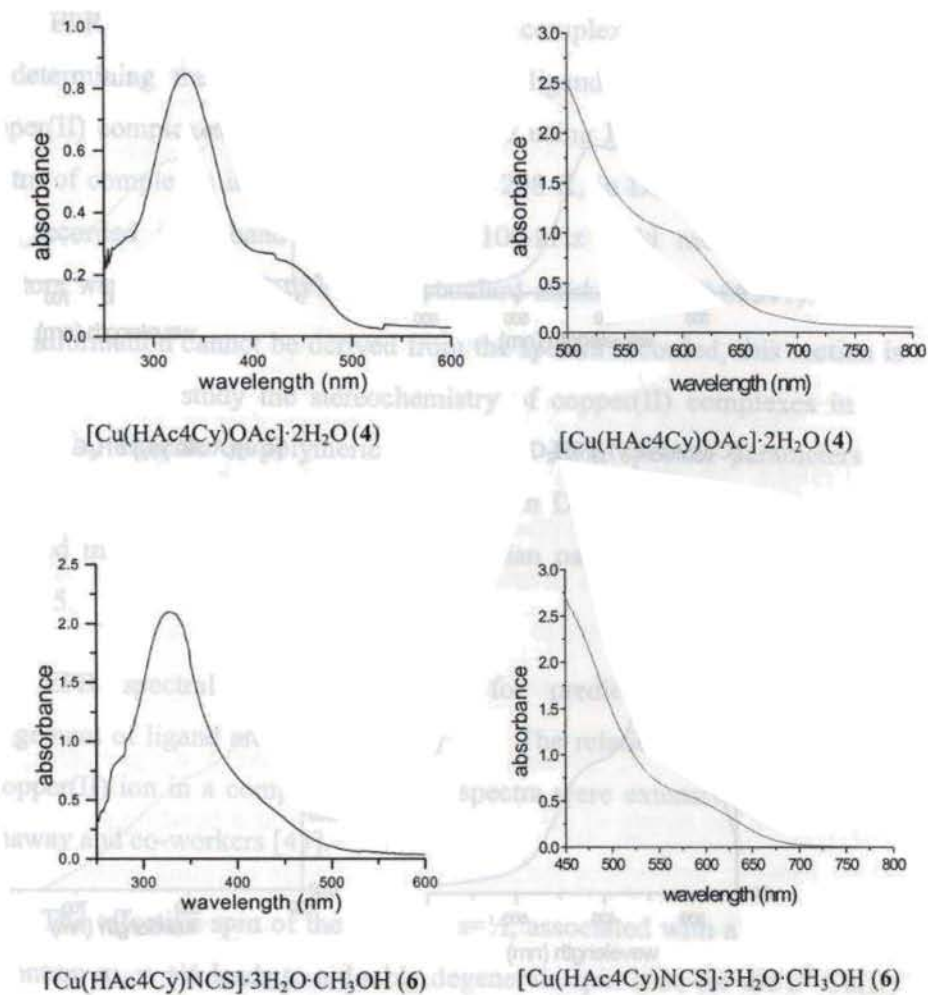


Figure 3.8b. Electronic spectra of the compounds 4 and 6

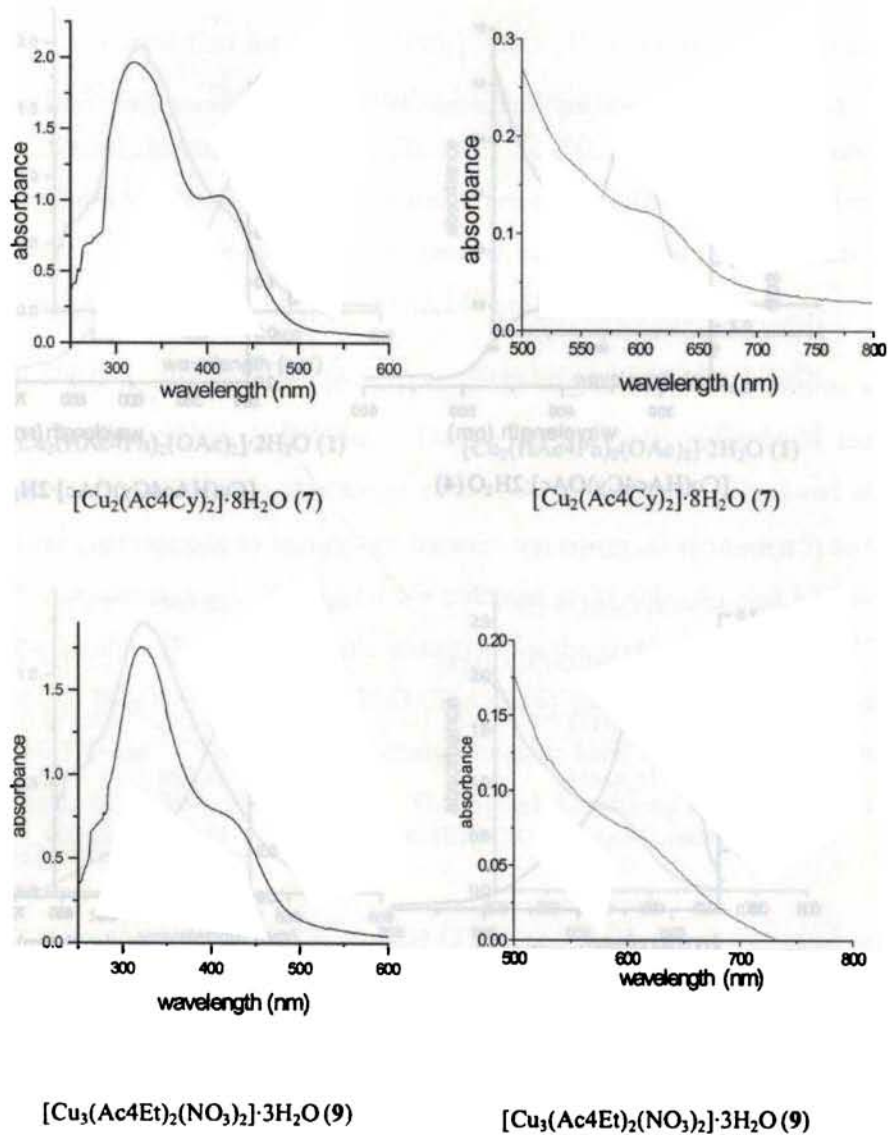


Figure 3.8c. Electronic spectra of the compounds 7 and 9

### 3.4.3. EPR Spectral studies

EPR spectral studies on paramagnetic complexes are an effective tool for determining the stereochemistry of the ligand around the metal ion. Copper(II) complexes are extensively studied using EPR spectroscopy. The spectra of complexes in the powder state at 298 K, in DMF solution at 77 K were recorded in X-band spectra with 100-kHz field modulation. The  $g$  factors were quoted relative to the standard marker ( $g = 2.00277$ ). Since much information cannot be derived from the spectra recorded, this section is only an effort to study the stereochemistry of copper(II) complexes in the monomeric, dimeric or polymeric state. The EPR spectral parameters of complexes in the powder state at 298 K and in DMF solution at 77 K were presented in Table 3.4. The spin Hamiltonian parameters are presented in Table 3.5.

EPR spectral studies are used for predicting the geometrical arrangement of ligand around copper(II) ion. The relation between geometry of copper(II) ion in a complex and EPR spectra were extensively studied by Hathaway and co-workers [43].

The effective spin of the electron  $s = 1/2$ , associated with a spin angular momentum  $m_s = +1/2$  leads to a doubly degenerate spin state for the  $d^9$  Cu(II) ion, in the absence of magnetic field. In the presence of a magnetic field, this degeneracy is lifted resulting in an energy difference between these two states given as

$$\Delta E = h\nu = g\beta H$$

where  $h$  is Planck's constant,  $\nu$  is the frequency,  $g$  is the Lande splitting factor,  $\beta$  is the electron Bohr magneton and  $H$  is the magnetic field. For a

copper(II) ion, the appropriate Spin Hamiltonian assuming a  $B_{1g}$  ground state is given by [44],

$$\hat{H} = \beta[g_{\parallel}H_zS_z + g_{\perp}(H_xS_x + H_yS_y)] + A_{\parallel}I_zS_z + A_{\perp}(I_xS_x + I_yS_y)$$

The factors that determine the type of ESR spectrum are:

- a) the nature of the electronic ground state.
- b) the symmetry of the effective ligand-field about the copper(II) ion.
- c) the mutual orientations of the local molecular axes of the separate copper(II) chromophores in the unit cell.

The factors a and b deal with the mode of splitting of the five-fold degenerate 3d-orbitals by crystal fields of octahedral and tetrahedral symmetries which are inverse of each other. The orbital sequences of the various stereochemistries determine their ground states. The vast majority of Cu(II) complexes give rise to orbitally non-degenerate ground states involving a static form of distortion and a  $d_{x^2-y^2}$  ground state; a substantial number of complexes have a  $d_{z^2}$  ground state and a few have a  $d_{xy}$  ground state. It depends on the nature of the ligands regarding their  $\pi$  bonding potential. The third factor c, determines the amount of exchange coupling present, which is the major factor in reducing the amount of stereochemical information available from the EPR spectra [31].

The EPR spectra of the compounds **1-9** were recorded in the X-band frequency. Compound  $[\text{Cu}_2(\text{HAc}4\text{Ph})_2(\text{OAc})_2] \cdot 2\text{H}_2\text{O}$  (**1**) in polycrystalline state at 298 K (Figure 3.9) displayed an axial spectrum with  $g_{\parallel}$  2.132 and  $g_{\perp}$  2.054. However, the frozen solution EPR spectrum (Figure 3.9a) of the compound in DMF at 77 K revealed a dimeric structure. At 77 K, the signal appears more resolved with  $g_{\parallel} = 2.175$  and  $g_{\perp} = 2.058$ , corresponding to the

pattern of Cu(II) ion in an elongated geometry,  $g_{\parallel} > g_{\perp} > 2.0$  with the  $d_{x^2-y^2}$  ground state. For Cu(II) complexes, the  $g$  values may display evidence for copper nuclear hyperfine splitting,  $2I+1$ , for  $^{63}\text{Cu}$ ,  $I = 3/2$  and each  $g$  value is split into four lines, separated by the nuclear hyperfine splitting constant  $A$  [45,46].  $A_{\parallel}$  value of the present compound is found to be  $190 \times 10^{-4} \text{ cm}^{-1}$ .

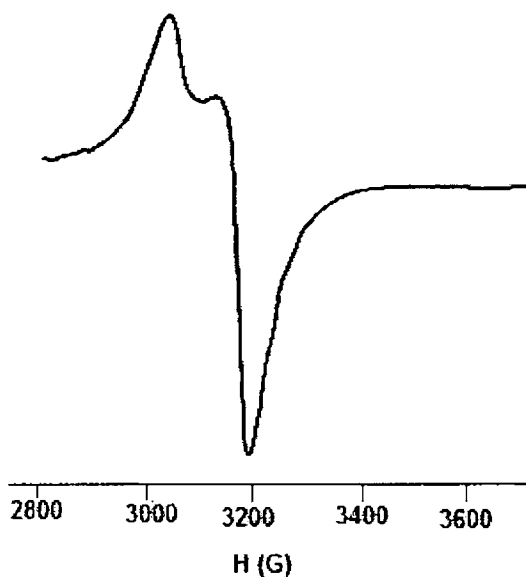


Figure 3.9. EPR spectrum of compound  $[\text{Cu}_2(\text{HAc4Ph})_2(\text{OAc})_2] \cdot 2\text{H}_2\text{O}$  (1) in polycrystalline state at 298 K

In polynuclear copper(II) complexes, due to Cu–Cu dipolar interaction, the zero field splitting parameter,  $D$  gives rise to transitions corresponding to  $\Delta M_s = \pm 2$ . In the X-band spectra,  $\Delta M_s = \pm 1$  transitions are associated with fields of *ca.* 3000 Gauss, while the  $\Delta M_s = \pm 2$  transition generate an absorption at the half field value of *ca.* 1500 gauss and the presence of this half field band is a useful criterion for dipolar interaction from the presence of some dinuclear (or polynuclear) complex formation. The solution EPR

spectrum of compound  $[\text{Cu}_2(\text{HAc4Ph})_2(\text{OAc})_2] \cdot 2\text{H}_2\text{O}$  (1) at 77 K, exhibited a half field signal at approximately 1520 G, which indicates that indeed a weak interaction between two Cu(II) ions within this compound is present (Figure 3.9a). Moreover, the broad signal in the low field region indicates that spin exchange interactions exist between the Cu(II) ions [30, 47, 48].

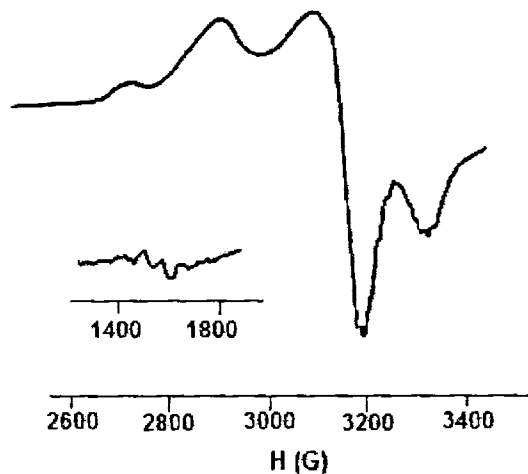


Figure 3.9a. EPR spectrum of compound  $[\text{Cu}_2(\text{HAc4Ph})_2(\text{OAc})_2] \cdot 2\text{H}_2\text{O}$  (1) in DMF at 77 K

The geometric parameter  $G$ , which is a measure of exchange interaction between copper centers in the polycrystalline compound, is calculated using the equation

$$G = (g_{\parallel} - 2.00277) / (g_{\perp} - 2.00277)$$

If  $G > 4$ , exchange interaction is negligible and if it is less than 4, considerable exchange interaction is indicated in the solid complex. The geometric parameter  $G$  for the complexes is found to be in the range 2.1-3.8 indicating that the exchange interactions are considerable in the complexes.

For all complexes with  $g_{\parallel} > g_{\perp} > 2$  and  $G$  value fall within this range, is consistent with a  $d_{x^2-y^2}$  ground state.

The EPR spectrum of compound  $[\text{Cu}(\text{HAc4Ph})\text{NO}_3] \cdot 2.5\text{CH}_3\text{OH}$  (**2**) in the polycrystalline state at 298 K (Figure 3.10) shows only one broad signal at  $g = 2.062$ . Such isotropic spectra, consisting of a broad signal, and hence only one  $g$  value, arise from extensive exchange coupling through misalignment of the local molecular axes between different molecules in the unit cell (dipolar broadening) and enhanced spin lattice relaxation. This type of spectra unfortunately gives no information on the electronic ground state of Cu(II) ion present in the complexes.

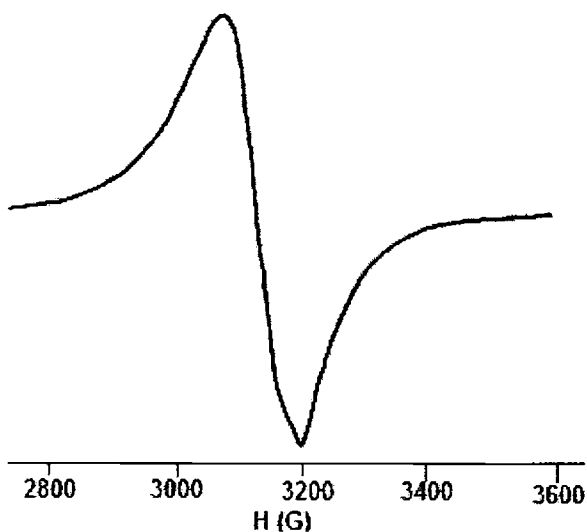


Figure 3.10. EPR spectrum of compound  $[\text{Cu}(\text{HAc4Ph})\text{NO}_3] \cdot 2.5 \text{CH}_3\text{OH}$  (**2**) in polycrystalline state at 298 K

The solution EPR spectrum of the compound in DMF at 77 K (Figure 3.10a), displayed axial features with  $g_{\parallel} = 2.154$  and  $g_{\perp} = 2.052$ .

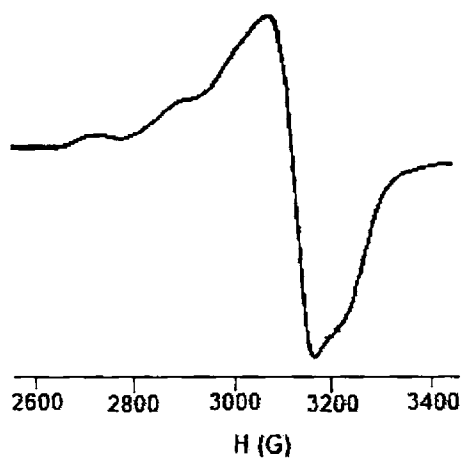


Figure 3.10a. EPR spectrum of compound  $[\text{Cu}(\text{HAc4Ph})\text{NO}_3] \cdot 2.5 \text{CH}_3\text{OH}$  (2) in DMF at 77 K

The distorted octahedral compound  $[\text{Cu}_2(\text{Ac4Ph})_2] \cdot 5\text{H}_2\text{O}$  (3) exhibited an isotropic spectrum with  $g = 2.143$  in polycrystalline state at 298 K (Figure 3.11).

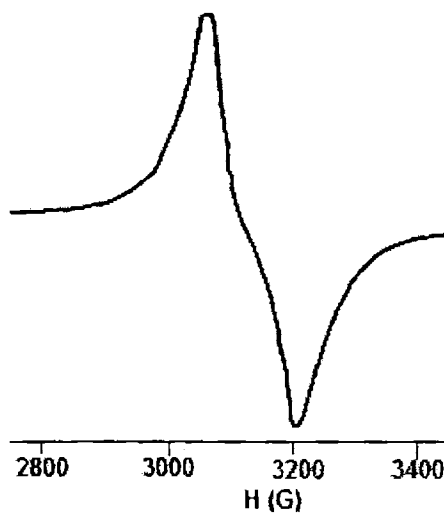


Figure 3.11. EPR spectrum of compound  $[\text{Cu}_2(\text{Ac4Ph})_2] \cdot 5\text{H}_2\text{O}$  (3) in polycrystalline state at 298 K



The solution EPR spectrum of the compound in DMF at 77 K revealed a dimeric structure (Figure 3.11a) with axial features  $g_{\parallel} = 2.172$  and  $g_{\perp} = 2.065$ .

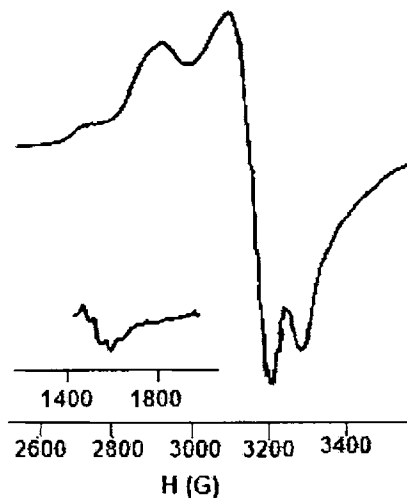


Figure 3.11a. EPR spectrum of compound  $[\text{Cu}_2(\text{Ac4Ph})_2] \cdot 5\text{H}_2\text{O}$  (3) in DMF at 77 K

It exhibits a half field signal at approximately 1590 G ( $g = 4.343$ ), which indicate that indeed a weak interaction between two Cu(II) ions within this compound is present. The presence of this half field band is a useful criterion for dipolar interaction from the presence of some binuclear complex formation.

The EPR spectra of the compound  $[\text{Cu}(\text{HAc4Cy})\text{OAc}] \cdot 2\text{H}_2\text{O}$  (4) recorded in solid at 298 K (Figure 3.12) and in solution in DMF at 77 K (Figure 3.12a) exhibited axial features. The variation in the  $g_{\parallel}$  and  $g_{\perp}$  values indicate that the geometry of the compounds in the solid state is affected by the nature of the coordinating gegenions.

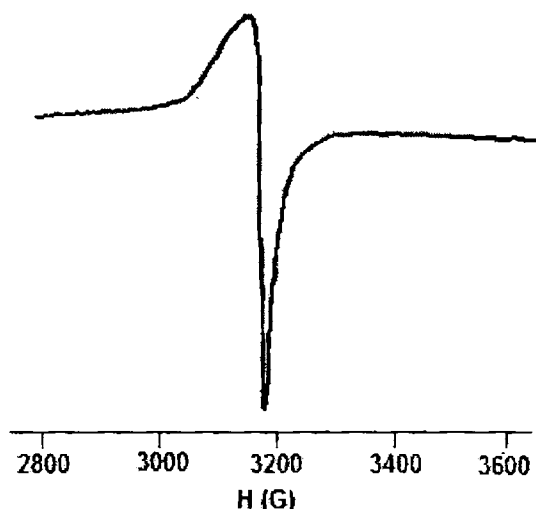


Figure 3.12. EPR spectrum of compound  $[\text{Cu}(\text{HAc}_4\text{Cy})\text{OAc}] \cdot 2\text{H}_2\text{O}$  (4) in polycrystalline state at 298 K

The well resolved  $g_{\parallel}$  feature at 2.140, indicating considerable covalency to the metal to ligand bonding, a consequence of two sulfur donor atoms in the coordination sphere. The absence of hyperfine interactions at room temperature, can be attributed to strong dipolar and exchange interactions between the Cu(II) ions in the unit cell. However, the hyperfine splittings were well resolved in the frozen solution state. The superhyperfine splitting in the high field component consists of more than nine lines which are expected from the splitting by the three coordinated nitrogens [51].

Calculation of orbital reduction factors,  $K_{\parallel} = 0.5841$  and  $K_{\perp} = 0.6246$ , indicate considerable  $\pi$ -bonding, and that in-plane and out-of-plane contributions are nearly same [15]. The exchange interaction parameter  $G$  [ $G = (g_{\parallel} - 2)/(g_{\perp} - 2)$ ] is found to be less than 4.0, suggesting considerable exchange coupling interactions [49, 50] in the octahedral dimeric complex.

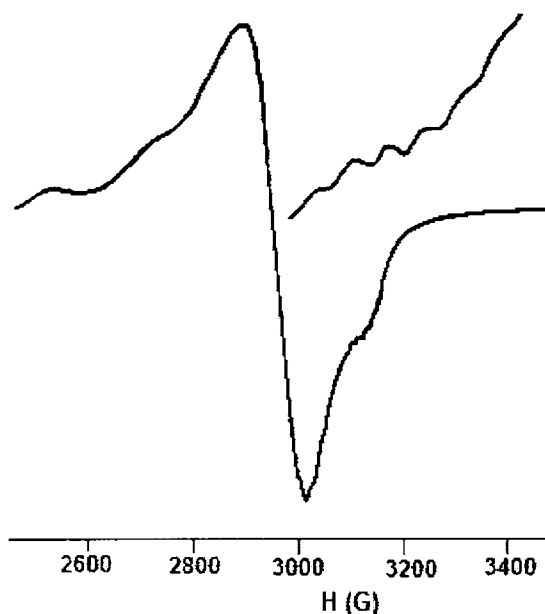


Figure 3.12a. EPR spectrum of compound  $[\text{Cu}(\text{HAc4Cy})\text{OAc}] \cdot 2\text{H}_2\text{O}$  (4) in DMF at 77 K

The EPR spectrum of the compound  $[\text{Cu}(\text{HAc4Cy})\text{Cl}] \cdot \text{C}_2\text{H}_5\text{OH}$  (5) recorded in solid at 298 K (Figure 3.13) exhibited an isotropic spectrum with  $g$  value 2.063. The solution EPR spectrum of the compound in DMF at 77 K (Figure 3.13a) displayed axial features with  $g_{\parallel} = 2.157$  and  $g_{\perp} = 2.045$ . The lack of observable nitrogen hyperfine coupling in the spectrum of the complex is probably due to the additional coupling of the of the pyridine nitrogen which broadens the superhyperfine lines of both types of nitrogen.

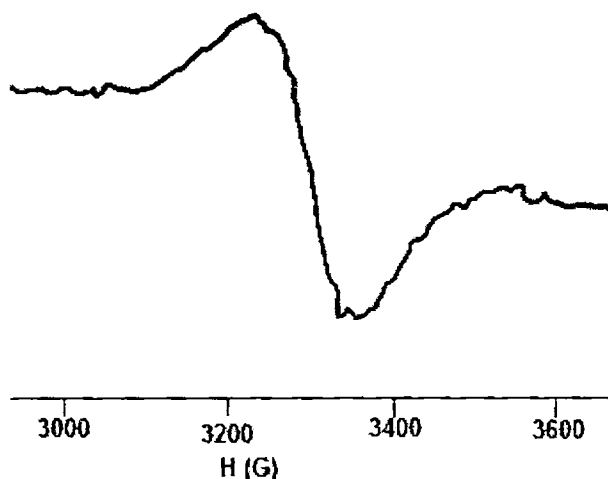


Figure 3.13. EPR spectrum of compound  $[\text{Cu}(\text{HAc4Cy})\text{Cl}] \cdot \text{C}_2\text{H}_5\text{OH}$  (5) in polycrystalline state at 298 K

The EPR spectrum of the complex in DMF solution at 77 K consists of three of the four hyperfine lines. The fourth copper hyperfine line ( $m_l = 3/2$ ) is expected to overlap with the high field component ( $g_{\perp}$ ).

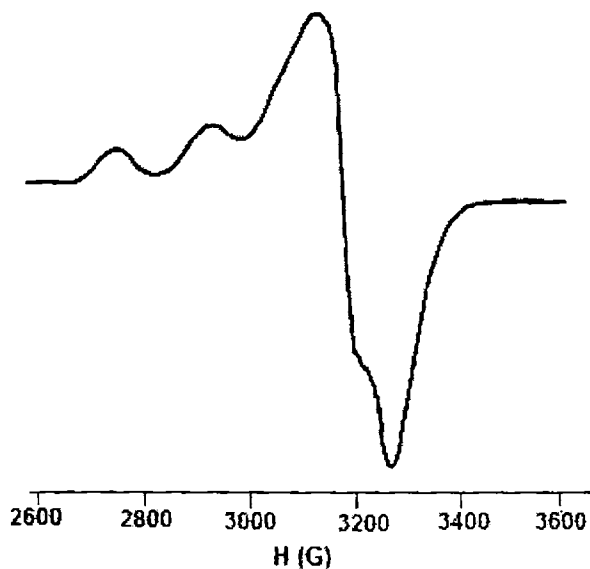


Figure 3.13a. EPR spectrum of compound  $[\text{Cu}(\text{HAc4Cy})\text{Cl}] \cdot \text{C}_2\text{H}_5\text{OH}$  (5) in DMF at 77 K

The EPR spectrum of the compound  $[\text{Cu}(\text{HAc4Cy})\text{NCS}] \cdot 3\text{H}_2\text{O} \cdot \text{CH}_3\text{OH}$  (**6**) recorded in solid at 298 K (Figure 3.14) and in solution in DMF at 77 K (Figure 3.14a) exhibited axial features.

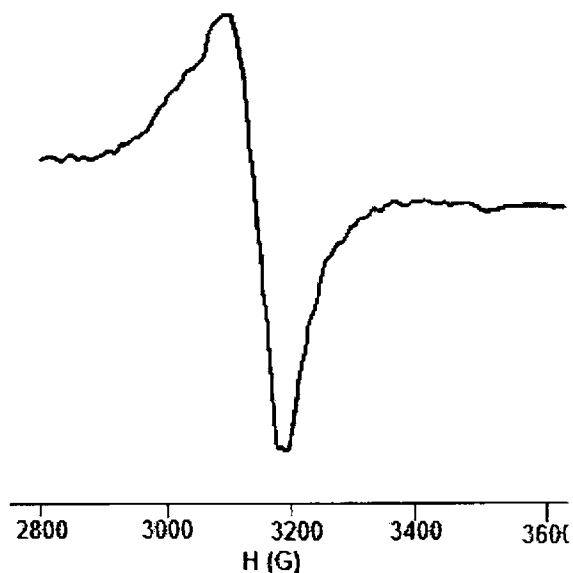


Figure 3.14. EPR spectrum of compound  $[\text{Cu}(\text{HAc4Cy})\text{NCS}] \cdot 3\text{H}_2\text{O} \cdot \text{CH}_3\text{OH}$  (**6**) in polycrystalline state at 298 K

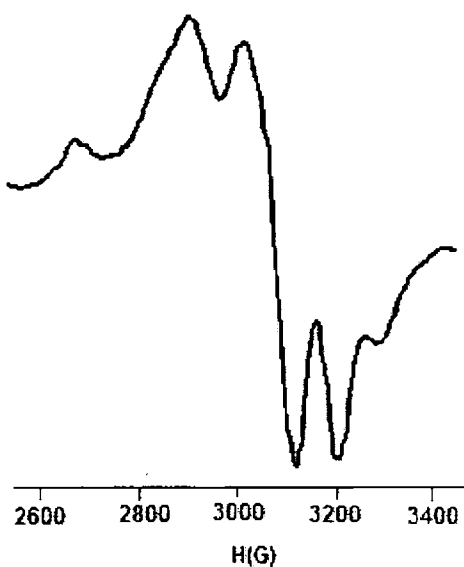


Figure 3.14a. EPR spectrum of compound  $[\text{Cu}(\text{HAc4Cy})\text{NCS}] \cdot 3\text{H}_2\text{O} \cdot \text{CH}_3\text{OH}$  in DMF at 77 K

The EPR spectrum of the compound  $[\text{Cu}_2(\text{Ac}_4\text{Cy})_2] \cdot 8\text{H}_2\text{O}$  (**7**) recorded in solid at 298 K (Figure 3.15) exhibited an isotropic spectrum with  $g$  value 2.110.

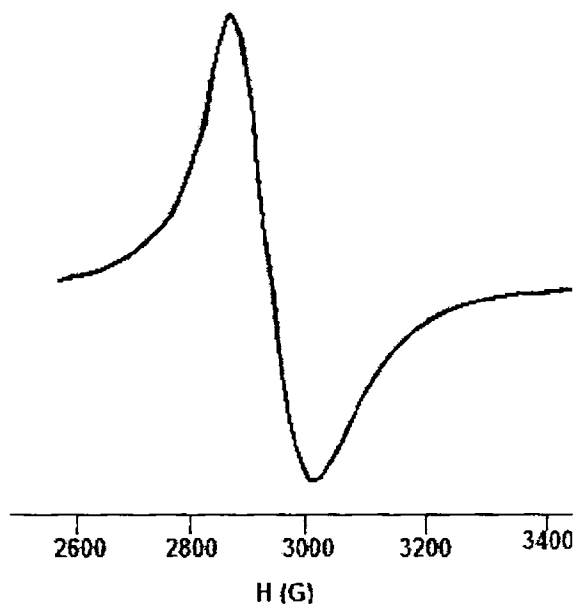


Figure 3.15. EPR spectrum of compound  $[\text{Cu}_2(\text{Ac}_4\text{Cy})_2] \cdot 8\text{H}_2\text{O}$  (**7**) in polycrystalline state at 298 K

The solution EPR spectrum of the compound **7** in DMF at 77 K (Figure 3.15a) displayed axial features with  $g_{\parallel} = 2.152$  and  $g_{\perp} = 2.055$ . The nitrogen superhyperfine splittings by aromatic nitrogen donors are commonly observed at 77 K, and in the EPR spectrum of **7** the seven hyperfine splittings characteristic of the bimetallic Cu(II) complex are well resolved, which can be attributed to a distorted structure. At room temperature, the EPR spectrum shows relatively lesser  $g$ -tensor anisotropy presumably due to larger spin-lattice relaxation time and smaller spin-orbit coupling interactions.

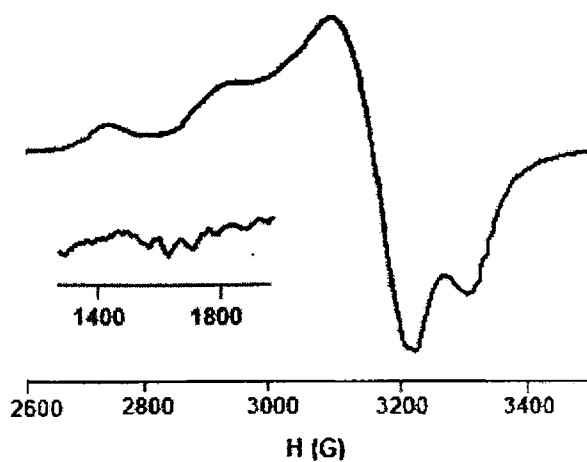


Figure 3.15a. EPR spectrum of compound  $[\text{Cu}_2(\text{Ac}_4\text{Cy})_2] \cdot 8\text{H}_2\text{O}$  (7) in DMF at 77 K

The solution EPR spectrum of the compound 7 in DMF at 298 K (Figure. 3.15b) exhibited an isotropic spectrum with  $g$  value 2.148.

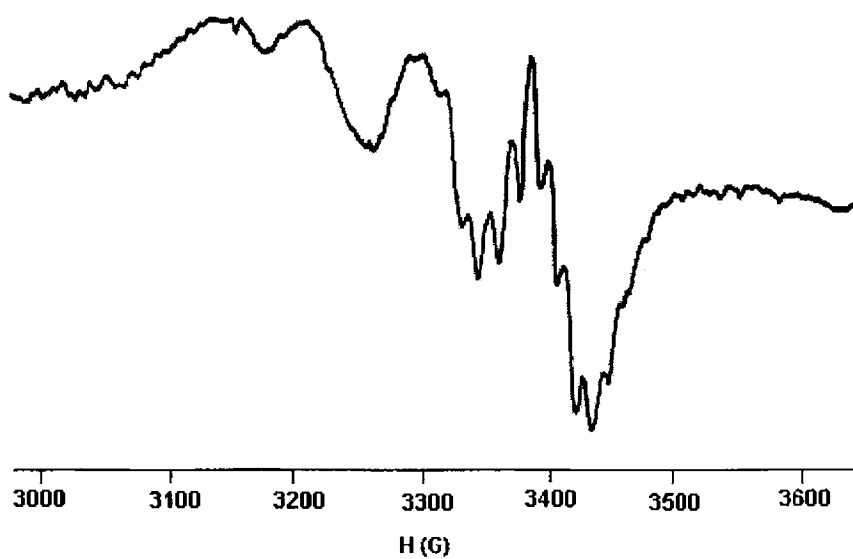


Figure 3.15b. EPR spectrum of compound  $[\text{Cu}_2(\text{Ac}_4\text{Cy})_2] \cdot 8\text{H}_2\text{O}$  (7) in DMF at 298 K

The present spectrum clearly show four well resolved hyperfine lines ( $^{63}\text{Cu}$ ,  $I=3/2$ ) corresponding to  $-3/2$ ,  $-1/2$ ,  $+1/2$ ,  $+3/2$  transitions. The signal corresponding  $M_I = +3/2$  splits clearly in to nine peaks with a superhyperfine (shf) or ligand hyperfine coupling constant  $A^N \approx 28.33 \text{ G}$  which arises from the coupling of the electron spin with the nuclear spin of the two coordinating non-equivalent nitrogen atoms. In this compound the nitrogen superhyperfine splitting is observed on the high field component of the hyperfine lines due to the varying relaxation times of the transitions caused by the different  $M_I$  values. The presence of nine superhyperfine lines indicate that there are two non equivalent nitrogen atoms around the  $\text{Cu(II)}$  ion and that the covalence in the metal ligand bond is strong due to the effective delocalization of the unpaired electron of the metal ion to the ligand atom orbitals. The isotropic hyperfine splitting constant,  $A_{\text{iso}}$  ( $190 \text{ G}$ ) is measured from the mean of the splittings.

Compound  $[\text{Cu}_2(\text{HAc4Me})_2(\text{NO}_3)_2] \cdot 6\text{H}_2\text{O} \cdot \text{CH}_3\text{OH}$  (**8**), was much less informative in interpreting the geometry as the broad spectra revealed isotropic features at  $298 \text{ K}$  (powder),  $g_{\text{iso}} 2.066$  (Figure 3.16) but it revealed axial features at  $77 \text{ K}$  (DMF),  $g_{\parallel} = 2.174$  and  $g_{\perp} = 2.052$  (Figure 3.16a).



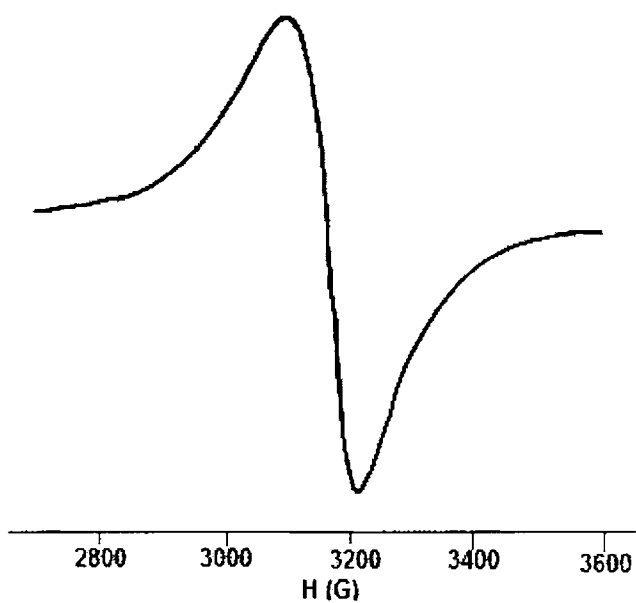


Figure 3.16. EPR spectrum of compound  $[\text{Cu}_2(\text{HAc4Me})_2(\text{NO}_3)_2] \cdot 6\text{H}_2\text{O} \cdot \text{CH}_3\text{OH}$  (**8**) in polycrystalline state at 298 K

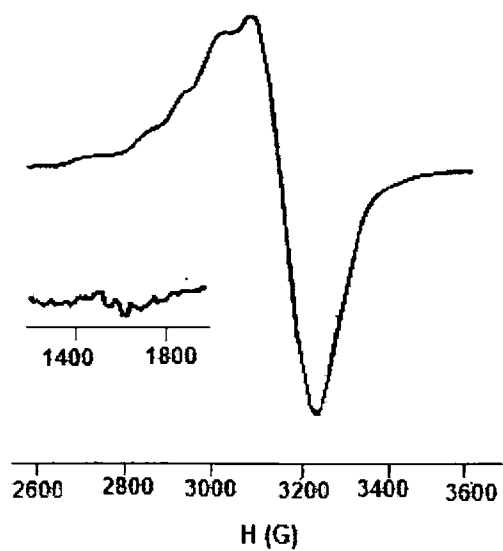


Figure 3.16a. EPR spectrum of compound  $[\text{Cu}_2(\text{HAc4Me})_2(\text{NO}_3)_2] \cdot 6\text{H}_2\text{O} \cdot \text{CH}_3\text{OH}$  (**8**) in DMF at 77 K

Table 3.4. EPR spectral assignments for Cu(II) complexes in polycrystalline state at 298 K and in DMF solution at 77 K

Compound	Polycrystalline state (298 K)				in DMF solution (77 K)				
	$g_{\parallel}$	$g_{\perp}$	$g_{av}$	$A_{\perp}$	$g_{\parallel}$	$g_{\perp}$	$g_{av}$	$A_{\parallel}$	$A_{\perp}$
$[\text{Cu}_2(\text{HAc4Ph})_2(\text{OAc})_2] \cdot 2\text{H}_2\text{O}$ (1)		2.132/2.054 ( $g_{\parallel}/g_{\perp}$ )			2.175	2.058	2.097	190	-
$[\text{Cu}(\text{HAc4Ph})\text{NO}_3] \cdot 2.5 \text{CH}_3\text{OH}$ (2)		2.062 ( $g_{iso}$ )			2.154	2.052	2.736	176.6	-
$[\text{Cu}_2(\text{Ac4Ph})_2] \cdot 5\text{H}_2\text{O}$ (3)		2.143 ( $g_{iso}$ )			2.172	2.065	2.100	183.3	16.6
$[\text{Cu}(\text{HAc4Cy})\text{OAc}] \cdot 2\text{H}_2\text{O}$ (4)		2.102/2.045 ( $g_{\parallel}/g_{\perp}$ )			2.140	2.042	2.074	186.6	-
$[\text{Cu}(\text{HAc4Cy})\text{Cl}] \cdot \text{C}_2\text{H}_5\text{OH}$ (5)		2.063 ( $g_{iso}$ )			2.157	2.045	2.082	176.6	-
$[\text{Cu}(\text{HAc4Cy})\text{NCS}] \cdot 3\text{H}_2\text{O} \cdot \text{CH}_3\text{OH}$ (6)		2.127/2.062 ( $g_{\parallel}/g_{\perp}$ )			2.175	2.051	2.092	178	-
$[\text{Cu}_2(\text{Ac4Cy})_2] \cdot 8\text{H}_2\text{O}$ (7)		2.110 ( $g_{iso}$ )			2.152	2.055	2.087	190	-
$[\text{Cu}_2(\text{HAc4Me})_2(\text{NO}_3)_2] \cdot 6\text{H}_2\text{O} \cdot \text{CH}_3\text{OH}$ (8)		2.066 ( $g_{iso}$ )			2.174	2.052	2.092	166.6	-
$[\text{Cu}_2(\text{Ac4Et})_2(\text{NO}_3)_2] \cdot 3\text{H}_2\text{O}$ (9)		2.053 ( $g_{iso}$ )			2.167	2.054	2.091	186.6	-

Table 3.5. EPR bonding parameters for Cu(II) complexes

Compound	G (298 K)	DMF solution (77 K)					
		$\alpha^2$	$\beta^2$	$\gamma^2$	$K_{\parallel}$	$K_{\perp}$	$f$
[Cu <sub>2</sub> (HAc4Ph) <sub>2</sub> (OAc) <sub>2</sub> ]·2H <sub>2</sub> O (1)	2.69	0.7692	0.8501	0.9628	0.6539	0.7406	113.28
[Cu(HAc4Ph)NO <sub>3</sub> ]·2.5 CH <sub>3</sub> OH (2)	-	0.7011	0.8682	0.9907	0.6087	0.6946	121.69
[Cu <sub>2</sub> (Ac4Ph) <sub>2</sub> ]·5H <sub>2</sub> O (3)	-	0.7483	0.8113	0.9839	0.6071	0.7363	117.40
[Cu(HAc4Cy)OAc]·2H <sub>2</sub> O (4)	2.61	0.7106	0.8219	0.8789	0.5841	0.6246	115.05
[Cu(HAc4Cy)Cl]·C <sub>2</sub> H <sub>5</sub> OH (5)	-	0.7038	0.8620	0.9021	0.6067	0.6349	121.86
[Cu(HAc4Cy)NCS]·3H <sub>2</sub> O·CH <sub>3</sub> OH (6)	2.04	0.7604	0.8620	0.9124	0.6555	0.6938	120.83
[Cu <sub>2</sub> (Ac4Cy) <sub>2</sub> ]·8H <sub>2</sub> O (7)	-	0.7392	0.8100	0.9586	0.5988	0.7086	113.26
[Cu <sub>2</sub> (HAc4Me) <sub>2</sub> (NO <sub>3</sub> ) <sub>2</sub> ]·6H <sub>2</sub> O·CH <sub>3</sub> OH (8)	-	0.7298	0.8633	0.9258	0.6301	0.6757	128.63
[Cu <sub>3</sub> (Ac4Et) <sub>2</sub> (NO <sub>3</sub> ) <sub>2</sub> ]·3H <sub>2</sub> O (9)	-	0.7776	0.8186	0.9144	0.6366	0.7111	115.26

The EPR spectra of the compound **9**  $[\text{Cu}_3(\text{Ac4Et})_2(\text{NO}_3)_2] \cdot 3\text{H}_2\text{O}$  recorded in solid at 298 K (Figure 3.17) exhibited an isotropic spectrum with  $g$  value 2.053.

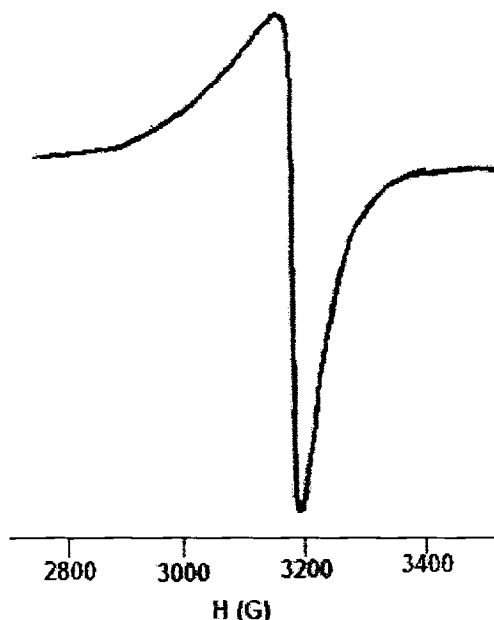


Figure 3.17. EPR spectrum of compound  $[\text{Cu}_3(\text{Ac4Et})_2(\text{NO}_3)_2] \cdot 3\text{H}_2\text{O}$  (**9**) in polycrystalline state at 298 K.

The EPR spectra of the compound **9**  $[\text{Cu}_3(\text{Ac4Et})_2(\text{NO}_3)_2] \cdot 3\text{H}_2\text{O}$  in DMF at 77 K has a normal axial spectrum consistent with a  $d_{x^2-y^2}$  ground state and based on similar EPR spectra for  $\text{CuN}_2\text{SCl}$  centers [54], suggests that the coordination involves considerable axial interaction (Figure 3.17a). It exhibits a half field signal at approximately 1650 G ( $g = 4.356$ ). The low lying magnetic susceptibility value also indicates considerable interaction between copper(II) centers. Therefore, we suggest that two of the copper(II) centers involve the pyridyl nitrogen, the imine nitrogen and the thiolato sulphur of one thiosemicarbazone moiety of a bis(thiosemicarbazone) along with a nitrate

ligand and substantial interaction with one or two solvent molecules. The third copper(II) center is likely to be coordinated  $\text{CuN}_2\text{S}_2$  by the remaining thiosemicarbazone functions and may involve solvent molecule interaction. The similarity of  $\text{CuN}_2\text{SNO}_3$  and  $\text{CuN}_2\text{S}_2$  centers provide a composite EPR spectrum suggesting a single type of copper(II) center for  $[\text{Cu}_3(\text{Ac4Et})_2(\text{NO}_3)_2] \cdot 3\text{H}_2\text{O}$ . A similar complex is also reported [23].

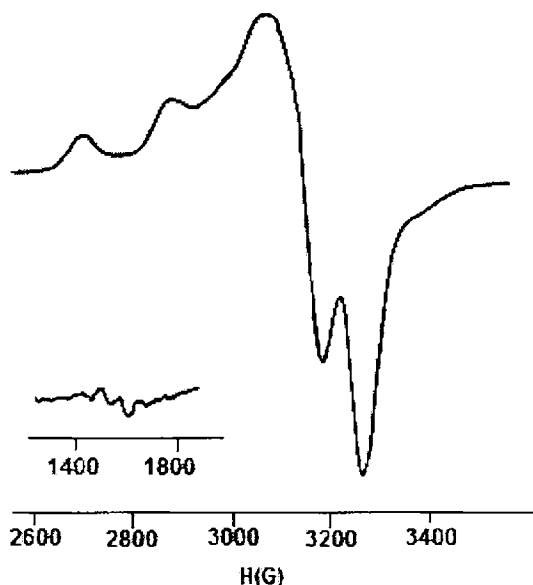


Figure 3.17a. EPR spectrum of compound  $[\text{Cu}_3(\text{Ac4Et})_2(\text{NO}_3)_2] \cdot 3\text{H}_2\text{O}$  (9) in DMF at 77 K

Hexacoordinated  $\text{Cu}(\text{II})$  complexes due to Jahn Teller effect exhibits a tetragonal distortion which reduces its symmetry from  $O_h$  to  $D_{4h}$  [51, 52]. This results in an anisotropy of the  $g$ -tensor. As the coordinated groups are not equivalent, only static distortion can occur [47, 53]. As  $g_{\parallel} > g_{\perp}$ , a tetragonal distortion is suggested, corresponding to an elongation along the

four-fold symmetry Z-axis. The unpaired electron still remains in  $d_{x^2-y^2}$  orbital; in the distorted octahedral structure because the Jahn Teller induced distortion generally favours  $d_{x^2-y^2}$  while  $d_{z^2}$  configuration are rare. As the  $g$  values are less than 2.3 and the calculated  $\alpha^2$ ,  $\beta^2$  and  $\gamma^2$  values are less than 1.0, it means that considerable covalent character is imparted to the metal-ligand bonds.

The EPR spectrum of the compound **9** in DMF solution at 298 K (Figure. 3.17b) revealed an isotropic spectrum with  $g$  value 2.094.

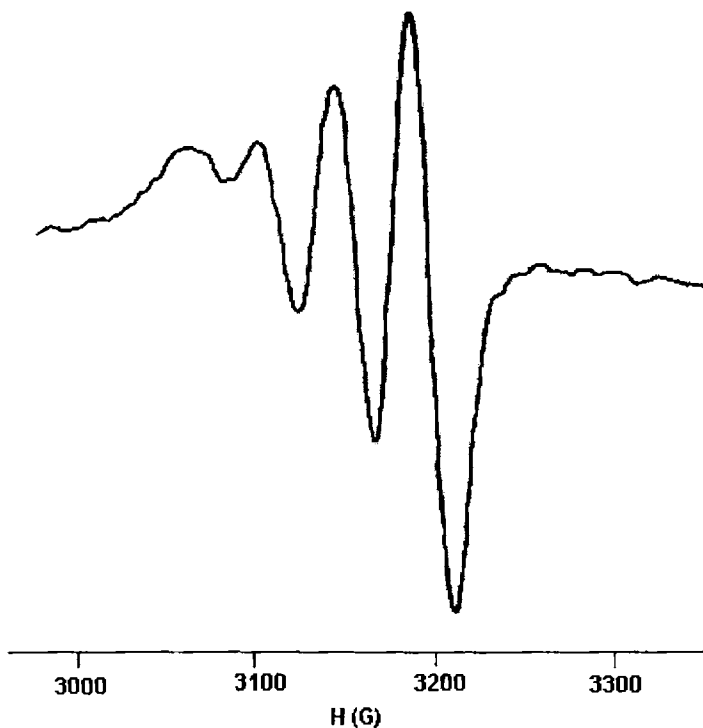


Figure 3.17b. EPR spectrum of compound  $[\text{Cu}_3(\text{Ac}_4\text{Et})_2(\text{NO}_3)_2] \cdot 3\text{H}_2\text{O}$  (**9**) in DMF at 298 K

It is assumed to be due to tumbling motion of the molecules in dimethylformamide solution. The spectral features of this complex clearly show four fairly resolved hyperfine lines ( $^{63}\text{Cu}$ ,  $I = 3/2$ ). The small variation in the  $g_{\text{iso}}$  value of the complex in DMF solution from the  $g_{\text{iso}}$  value calculated for polycrystalline spectrum can be attributed to the variation in the geometric environment of the compounds upon dissolution. The isotropic  $g$  value,  $g_{\text{iso}}$  is calculated at the centre of the spectrum of the four lines. The isotropic hyperfine splitting constant,  $A_{\text{iso}}$  (86.6 G) is measured from the mean of the splittings.

The values of magnetic parameters and the energies of the electronic  $d-d$  transitions have been used for estimating the nature of the chemical bonding between the copper and donor atoms of the ligand. The fraction of unpaired electron density located on the copper ion i.e. the value of in-plane sigma bonding parameter  $\alpha^2$  was estimated from the expression [49, 50].

$$\alpha^2 = -\frac{A_{\parallel}}{0.036} + (g_{\parallel} - 2.0023) + \frac{3(g_{\perp} - 2.0023)}{7} + 0.04$$

where  $A_{\parallel}$  is the parallel coupling constant. The value of  $\alpha^2$  indicates that the copper(II) complex is fairly covalent. The orbital reduction factors  $K_{\parallel}$  and  $K_{\perp}$  are calculated using expressions:

$$K_{\parallel}^2 = (g_{\parallel} - 2.0023) \frac{\Delta E(d_{xy} \rightarrow d_{x^2-y^2})}{8\lambda_0}$$

$$K_{\perp}^2 = (g_{\perp} - 2.0023) \frac{\Delta E(d_{xz}, d_{yz} \rightarrow d_{x^2-y^2})}{2\lambda_0}$$

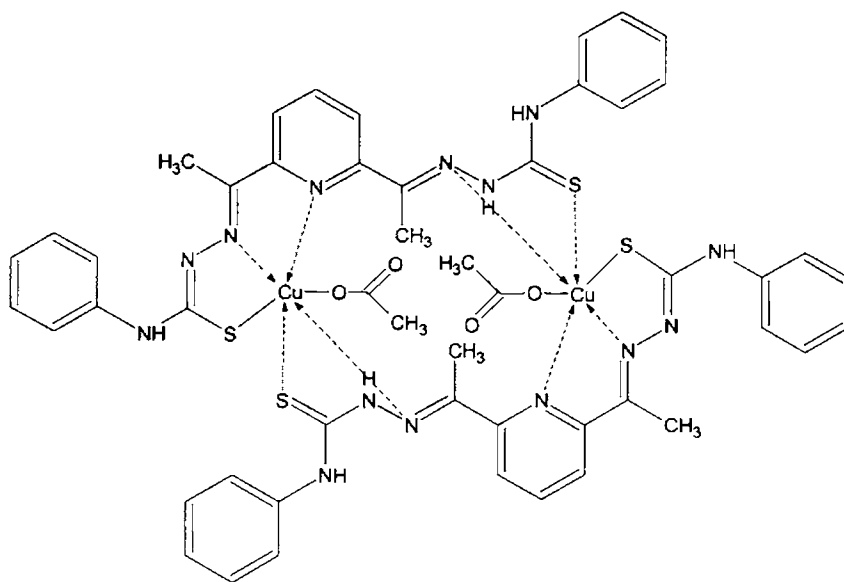
$$K_{\parallel} = \alpha^2 \beta^2$$

$$K_{\perp} = \alpha^2 \gamma^2$$

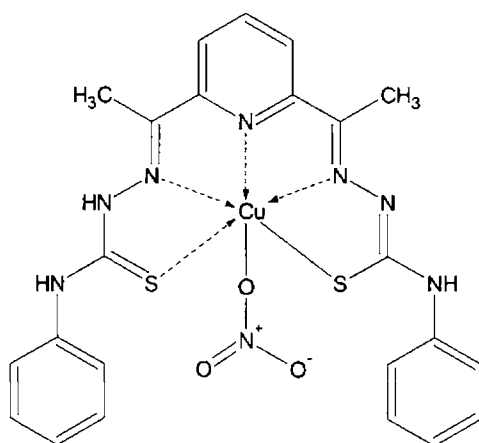
where  $\lambda_0$  is the spin-orbit coupling constant and has a value  $-828 \text{ cm}^{-1}$  for Cu(II)  $d^9$  system,  $\alpha^2$  is the in-plane  $\sigma$ -bonding,  $\beta^2$  the in-plane  $\pi$ -bonding and  $\gamma^2$ , the out-of-plane  $\pi$ -bonding. The value of  $\alpha^2$  indicates the extent of covalent nature, where the value of 1.0 corresponds to a purely ionic nature. The covalency of the metal-ligand bond points toward a  $\alpha^2$  value less than 1.0. Hathaway proposed that, for pure  $\sigma$  bonding,  $K_{\parallel} \sim K_{\perp} \sim 0.77$ ; for in-plane  $\pi$ -bonding,  $K_{\parallel} < K_{\perp}$  and for out-of-plane  $\pi$ -bonding,  $K_{\perp} < K_{\parallel}$ . The fact that the  $K_{\parallel}$  and  $K_{\perp}$  values calculated for our copper complexes showed the trend  $K_{\parallel} < K_{\perp}$  suggesting stronger in-plane  $\pi$ -bonding.

Based on the elemental analyses and spectral investigations, following tentative structures were assigned for the complexes for which, single crystals suitable for crystallographic studies could not be isolated.

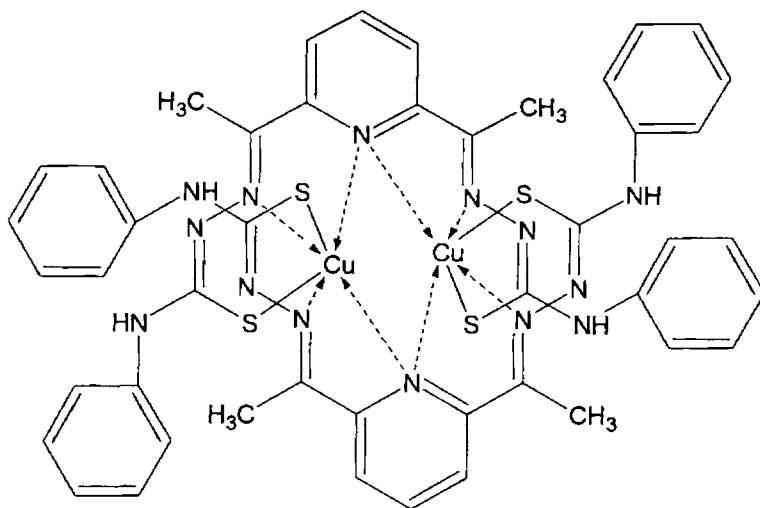




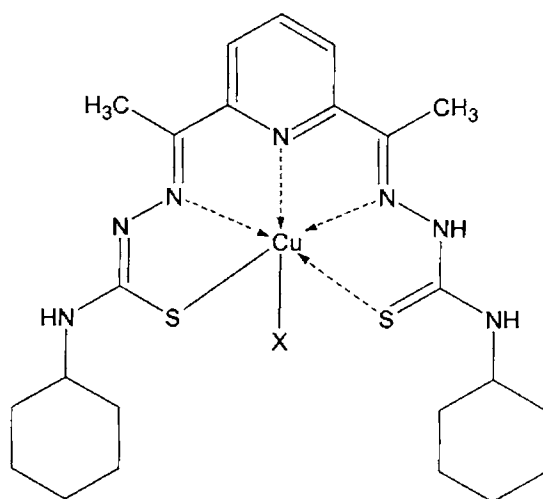
$[\text{Cu}_2(\text{HAc4Ph})_2(\text{OAc})_2] \cdot 2\text{H}_2\text{O}$  (1)



$[\text{Cu}(\text{HAc4Ph})\text{NO}_3] \cdot 2.5 \text{CH}_3\text{OH}$  (2)

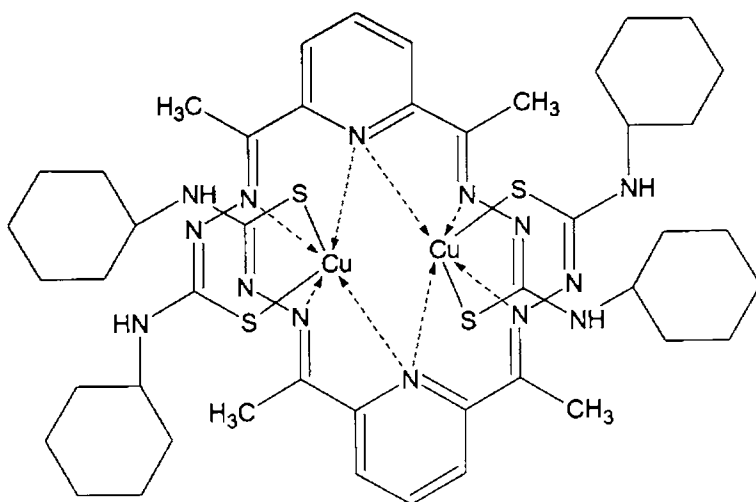


$[\text{Cu}_2(\text{Ac4Ph})_2] \cdot 5\text{H}_2\text{O}$  (3)

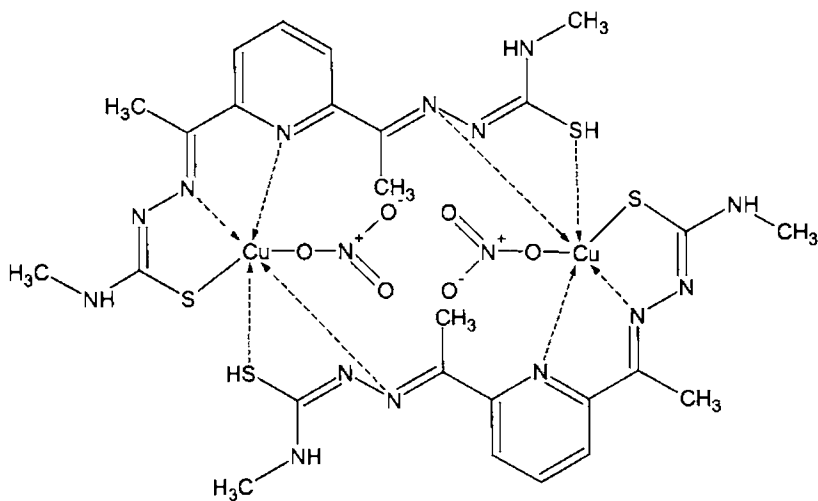


$[\text{Cu}(\text{HAc4Cy})\text{X}]$

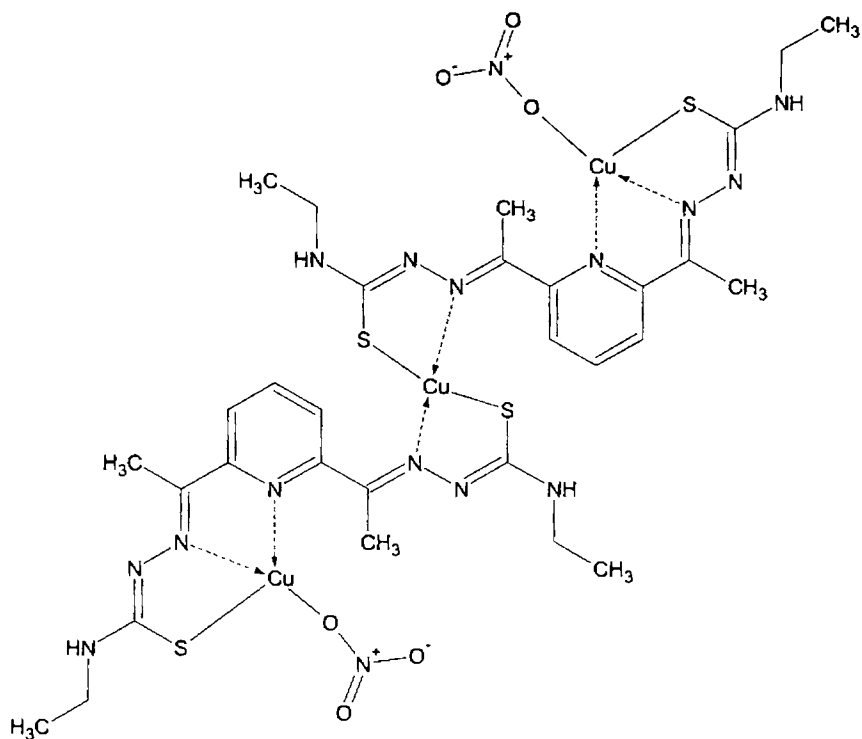
$\text{X} = \text{OAc}, \text{Cl}, \text{NCS}$



$[\text{Cu}_2(\text{Ac4Cy})_2] \cdot 8\text{H}_2\text{O}$  (7)



$[\text{Cu}_2(\text{HAc4Me})_2(\text{NO}_3)_2] \cdot 6\text{H}_2\text{O} \cdot \text{CH}_3\text{OH}$  (8)



[Cu<sub>3</sub>(Ac4Et)<sub>2</sub>(NO<sub>3</sub>)<sub>2</sub>]·3H<sub>2</sub>O (9)

### Concluding remarks

This chapter describes the synthesis and characterization of nine copper(II) complexes of four ligands *viz.* 2,6-diacetylpyridine bis(*N*<sup>4</sup>-phenylthiosemicarbazone) H<sub>2</sub>Ac4Ph, 2,6-diacetylpyridine bis(*N*<sup>4</sup>-cyclohexylthiosemicarbazone) H<sub>2</sub>Ac4Cy, 2,6-diacetylpyridine bis(*N*<sup>4</sup>-methylthiosemicarbazone) H<sub>2</sub>Ac4Me, 2,6-diacetylpyridine bis(*N*<sup>4</sup>-ethylthiosemicarbazone) H<sub>2</sub>Ac4Et. The physico-chemical methods of characterization include partial elemental analyses, conductivity and room temperature magnetic susceptibility measurements and IR, electronic and EPR spectral studies. The structures

proposed in this study are tentative because of the lack of X-ray crystal structure data, the complicated I.R. spectra and the masking of the *d-d* bands. Unfortunately instead of repeated attempts to grow X-ray quality crystals for structural studies of these metal complexes have failed.

## References

1. R. Osterberg, *Coord. Chem. Rev.* 12 (1974) 309.
2. J.A. Fee, *Struct. Bonding* 23 (1975) 1.
3. H. Beinert, *Coord. Chem. Rev.* 23 (1977) 119.
4. E.L. Ulrich, J.L. Markey, *Coord. Chem. Rev.* 27 (1978) 109.
5. G. Bahr, *Z. Anorg. Allg. Chem.* 268 (1952) 351.
  - a) G. Bahr, *Z. Anorg. Allg. Chem.* 273 (1953) 325.
  - b) G. Bahr, E. Schleitzer, *Z. Anorg. Allg. Chem.* 278 (1955) 136.
6. C.J. Jones, J.A. McCleverty, *J. Chem. Soc.* (1970) 2829.
7. NDEA Title IV Fellow, 1969-1970.
8. H.G. Petering and G.J. Van Giessen in "The Biochemistry of Copper," J. Peisach, P. Aisen, W.E. Blumberg, Ed., Academic Press, New York, S. Y. (1966) 197.
9. S.I. Shupack, E. Billig, R.J.H. Clark, R. Williams, H.B. Gray, *J. Amer. Chem. Soc.* 86 (1964) 4594.
10. Chen, M. Abkowitz, J. H. Sharp, *J. Chem. Phys.* 50 (1969) 2.

11. L.E. Warren, S.M. Horner, W.E. Hatfield, *J. Amer. Chem. Soc.* 94 (1972) 181.
12. D.X. West, J.S. Ives, G.A. Bain, A.E. Liberta, J. Valdés-Martínez, K.H. Ebert, S. Hernández-Ortega, *Polyhedron* 16 (1997) 1895.
13. W.J. Geary, *Coord. Chem. Rev.* 7 (1971) 81.
14. P.R. Athappan, G. Rajagopal, *Polyhedron* 15 (1996) 527.
15. L.J. Ackerman, J.W. Webb, D.X. West, *Trans. Met. Chem.* 24 (1999) 558.
16. G.F. de Sousa, V.M. Deflon, E. Niquet, A. Abras, *J. Braz. Chem. Soc.* 12 (2001) 493.
17. D.X. West, I.S. Billeh, G.A. Bain, J. Valdez-Martínez, K.H. Ebert, S. Hernández-Ortega, *Trans. Met. Chem.* 21 (1996) 572.
18. D.X. West, G.A. Bain, R.J. Butcher, J.P. Jasinski, Y. Li, R.Y. Pozdniakiv, J. Valdés-Martínez, R.A. Toscano, S. Hernández-Ortega, *Polyhedron* 15 (1996) 665.
19. D.X. West, C.S. Carlson, A.E. Liberia, J.N. Albert and C.R. Daniel, *Trans. Met. Chem.* 15, 341 (1990);
  - a) D.X. West, C.S. Carlson, K.J. Bouck, A.E. Liberta. *Trans. Met. Chem.* 16 (1991) 271.
20. J.K. Swearingen, D.X. West, *Trans. Met. Chem.* 26 (2001) 252.
21. D.X. West, J.K. Swearingen, A.K. El-Sawaf, *Trans. Met. Chem.* 25 (2000) 87.

22. M. Mohanan, P. Sharma, *Inorg. Chim. Acta* 106 (1985) 197.
23. D.X. West, A.K. El-Sawaf, G.A. Bain, *Trans. Met. Chem.* 23 (1998) 1.
24. A. Monaci, F. Trali, *J. Chem. Soc. Dalton Trans.* 417 (1977).
25. M.A. Ali, D.J. Philips, S.E. Livingstone, *Inorg. Chim Acta* 5 (1971) 119.
26. M.A. Ali, A.H. Mirza, C.W. Voo, A.L. Tan, P.V. Bernhardt, *Polyhedron* 22 (2003) 3433.
27. L.J. Ackerman, J.W. Webb, D.X. West, *Trans. Met. Chem.* 24 (1999) 562.
28. R.J.H. Clark, C.S. Williams, *Inorg. Chem.* 4 (1965) 350.
29. C.A. Brown, D.X. West, *Trans. Met. Chem.* 28 (2003) 154.
30. D.X. West, H. Gebremedhin, T.J. Romack, A.E. Liberta, *Trans. Met. Chem.* 19 (1994) 426.
31. M. Joseph, V. Suni, M.R.P. Kurup, M. Nethaji, A. Kishore, S.G. Bhat, *Polyhedron* 23 (2004) 3069.
32. R.P. John, A. Sreekanth, M.R.P. Kurup, S.M. Mobin, *Polyhedron* 21 (2002) 2515.
33. K.H. Reddy, M.R. Reddy, K.M. Raju. *Ind. J. Chem* 38A (1999) 299.
34. B.S. Garg, M.R.P. Kurup, S.K. Jain, Y.K. Bhoon, *Trans. Met. Chem.* 13 (1988) 309.

35. M.B. Ferrari, G.G. Fava, M. Lanfranchi, C. Pelizzi, M. Tarasconi, *Inorg. Chim. Acta* 181 (1991) 253.
36. E.W. Ainscough, A.M. Brodie, J.D. Ranford, J.M. Waters, *Dalton Trans.* 23 (1991) 2125.
37. K. Nakamoto, *Infrared spectra of Inorganic and coordination compounds*, 4<sup>th</sup> edn, Wiley-Interscience, New York (1997) 256.
38. E.W. Ainscough, A.M. Brodie, J.D. Ranford, J.M. Waters, *Dalton Trans.* 23 (1991) 2125.
39. S.K. Jain, B.S. Garg, Y.K. Bhoon, *Spectrochim. Acta* 42 A (1986) 959.
40. B. Singh, B.P. Yadav, R.C. Aggarwal, *Ind. J. Chem.* 23A (1984) 441.
41. J.E. Huheey, E.A. Keiter, R.L. Keiter, *Inorganic Chemistry*, 4<sup>th</sup> ed., Addison-Wesley Publishing Company, India, 1993.
42. R.S. Drago, *Physical Methods in Inorganic Chemistry*, Reinhold Publishing Corporation, New York.
43. B.J. Hathaway, D.E. Billing, *Coord. Chem. Rev.* 5 (1970) 143.
44. M.A. Ali, M.T.H. Tarafder, *J. Inorg. Nucl. Chem.*, 39 (1977) 1785.
45. P.S. Zacharias, J.M. Elizabathe, A. Ramachandraiah, *Indian J. Chem.* A23A (1984) 26.
46. B. Swamy, J.R. Swamy, *Trans. Met. Chem.* 16 (1991) 35.
47. J.C. Einstein, *J. Chem. Phys.* 28 (1958) 323.



48. M. Maajan, K.N. Saxena, C.P. Saxena, J. Inorg. Nucl. Chem. 43 (1981) 2148.
49. D. Kivelson, R. Neiman, J. Chem. Phys. 35 (1961) 149.
50. A.H. Maki, B.R. McGarvey, J. Chem. Phys. 29 (1958) 35.
51. A. Hudson, J. Mol. Phys. 10 (1966) 575.
52. I.B. Bersuker, Coord. Chem. Rev. 14 (1975) 357.
53. K.K. Sharma, S. Chandra, Trans. Met. Chem. 9 (1984) 401.
54. D.X. West, J.K. Swearingen, T.J. Romack, I.S. Billeh, J.P. Jasinski, Y.Li, R.J. Staples, J. Mol. Struct. 570 (2001) 129.

\*\*\*\*\*

# Synthesis and spectral characterization of Mn(II) complexes of bis(*N*<sup>4</sup>-substitutedthiosemicarbazones) of 2,6-diacetylpyridine

## 4.1. Introduction

Manganese coordination chemistry with a diverse range of ligands has much relevance in biological systems with a number of model manganese complexes. Manganese coordination compounds are also of growing importance as homogeneous catalysts in oxidation reactions [1-4]. The manganese porphyrins are very efficient catalysts for fractionalization of hydrocarbons in processes that involve high valent intermediates [5-7]. It is an essential trace element, forming the active sites of a number of metalloproteins. In these metalloproteins, manganese can exist in any of the five oxidation states or in mixed valence states. For inorganic chemists, metalloproteins with two or even more manganese atoms per sub unit are particularly interesting. The most important natural role of manganese is in the oxidation of water in green plant photosynthesis where its presence in photosystem II is essential [8].

The most well known of manganese enzyme is the tetranuclear system which is active in oxygen evolution step [9]. This tetranuclear manganese(IV) complex has led to a spurt in research in this field and as a consequence, different oxygen evolving models were synthesized and their importance was investigated. In such studies manganese complexes in different oxidation states were obtained and studied their magnetic and spectral properties in depth. Their spectral and magnetic properties were an active domain of research. Manganese exhibits a wide variety of oxidation states ranging from

-3 to +7 which is very common in biochemical systems. High spin Mn(II) complexes are characterized by the absence of ligand field stabilization energy and this has two main consequences such that the possibility to obtain various coordination geometries and a lower stability of Mn(II) complexes compared with those of other divalent 3d metals.

The syntheses and study of coordination complexes with unusual geometry and coordination number is a challenging task for the practical chemist. The most important factor in this objective is probably the design of ligands with an appropriate structural backbone that can coerce the metal ion into the desired coordination geometry. Such pentacoordinating ligands with mixed N-S donor points at strategic positions of the donor-framework are seldom encountered in coordination chemistry. The chelating properties of 2,6-diacetylpyridine bis(thiosemicarbazone), have been investigated and several different coordination modes have been found [10-13]. There are reports on heptacoordinated bis(thiosemicarbazones) of 2,6-diacetylpyridine [14]. This type of coordination is commonly found in metals like Sn(IV) [15], Mn(II) [16] and In(III) [17]. As previous research [18, 19] show, these ligands tend to originate pentagonal bipyramidal complexes in which the ligand forms a pentacoordinated chelate and the two arms (thiosemicarbazide groups) of the ligand have remained protonated [20].

## **4.2. Experimental**

### ***4.2.1. Materials***

The reagents used for the synthesis of the ligands are discussed in Chapter 2. Solvents were purified by standard methods. Manganese(II) chloride tetrahydrate and manganese(II) acetate tetrahydrate were used as

supplied for the preparation of complexes. Solvents used were methanol, DMF and chloroform.

#### 4.2.2. Synthesis of complexes

**[Mn(H<sub>2</sub>Ac4Ph)Cl<sub>2</sub>] (10)**: A solution of ligand H<sub>2</sub>Ac4Ph (0.461 g, 1 mmol) in DMF was treated with a methanolic solution of MnCl<sub>2</sub>·4H<sub>2</sub>O (0.197 g, 1 mmol). The above yellow solution was refluxed for about 4 hrs and allowed to cool. The yellow compound formed was filtered and washed with methanol and ether and dried *in vacuo* over P<sub>4</sub>O<sub>10</sub>.

**[Mn(Ac4Ph)H<sub>2</sub>O] (11)**: A solution of ligand H<sub>2</sub>Ac4Ph (0.461 g, 1 mmol) in DMF was treated with a methanolic solution of Mn(OAc)<sub>2</sub>·4H<sub>2</sub>O (0.245 g, 1 mmol). The above yellow solution was refluxed for about 4 hrs and allowed to cool. The yellow compound formed was filtered and washed with methanol and ether and dried *in vacuo* over P<sub>4</sub>O<sub>10</sub>.

**[Mn(H<sub>2</sub>Ac4Cy)Cl<sub>2</sub>]·H<sub>2</sub>O (12)**: A solution of ligand H<sub>2</sub>Ac4Cy (0.473 g, 1 mmol) in chloroform was treated with a methanolic solution of MnCl<sub>2</sub>·4H<sub>2</sub>O (0.197 g, 1 mmol). The above yellow solution was refluxed for about 4 hrs and allowed to cool. The yellow compound formed was filtered and washed with methanol and ether and dried *in vacuo* over P<sub>4</sub>O<sub>10</sub>.

**[Mn(H<sub>2</sub>Ac4Et)Cl<sub>2</sub>]·3H<sub>2</sub>O (13)**: A solution of ligand H<sub>2</sub>Ac4Et (0.365 g, 1 mmol) in chloroform was treated with a methanolic solution of MnCl<sub>2</sub>·4H<sub>2</sub>O (0.197 g, 1 mmol). The above yellow solution was refluxed for about 4 hrs and allowed to cool. The yellow compound formed was filtered and washed with methanol and ether and dried *in vacuo* over P<sub>4</sub>O<sub>10</sub>.

**[Mn(H<sub>2</sub>Ac4Et)(OAc)<sub>2</sub>·3H<sub>2</sub>O (14):** A solution of ligand H<sub>2</sub>Ac4Et (0.365 g, 1 mmol) in chloroform was treated with a methanolic solution of Mn(OAc)<sub>2</sub>·4H<sub>2</sub>O (0.245 g, 1 mmol). The above yellow solution was refluxed for about 4 hrs and allowed to cool. The yellow compound formed was filtered and washed with methanol and ether and dried *in vacuo* over P<sub>4</sub>O<sub>10</sub>.

### 4.3. Physical measurements

Elemental analyses of the ligand and the complexes were done on a Vario EL III CHNS analyzer at SAIF, Kochi, India. IR spectral analyses were done using KBr pellets on Thermo Nicolet AVATAR 370 DTGS FT-IR spectrophotometer in the 4000-400 cm<sup>-1</sup> region. The far IR spectra were recorded using polyethylene pellets in the 500-100 cm<sup>-1</sup> region on a Nicolet Magna 550 FTIR instrument at the SAIF, Indian Institute of Technology, Bombay. UVD-3500, UV-VIS Double Beam Spectrophotometer was used to record the electronic spectra in DMF solution in the range 200-900 nm. The magnetic susceptibility measurements were done in the polycrystalline state at room temperature on a Vibrating Sample Magnetometer at the Indian Institute of Technology, Roorkee, India. EPR spectral measurements were carried out on a Varian E-112 X-band spectrometer using TCNE as standard at the Sophisticated Analytical Instruments Facility, Indian Institute of Technology, Bombay, India. The molar conductivities of the complexes in dimethylformamide solutions (10<sup>-3</sup> M) at room temperature were measured using a direct reading conductivity meter.

#### 4.4. Results and discussion

All the five Mn(II) complexes were prepared by the reaction of corresponding ligands with metal salts in 1:1 ratio. In all the complexes except **11**, the ligands act as pentadentate neutral molecules and coordinate to Mn(II) ion through two thione sulfur atoms, two azomethine nitrogens and the pyridine nitrogen, suggesting a heptacoordination. While in compound **11**, the dianionic ligand is coordinated to the metal by losing its amide protons from the two thiosemicarbazone moieties, suggesting six coordination in this case. Unfortunately, attempts to date to grow crystals for structural studies of these metal complexes have failed. However the bonding to the metal ion is expected to be similar to that found for a Mn(II) complex of bis(thiosemicarbazone) [21] in all the cases except **11**.

Colors, partial elemental analyses, molar conductivities and magnetic susceptibilities are listed in Table 4.1. Conductivity measurements were done in  $10^{-3}$  DMF solutions and these values, although indicate extensive dissociation of these complexes in DMF, are much lower than that observed for 1:1 electrolytes in this solvent. They can, therefore, be considered as non-electrolytes in this solvent. This is a strong evidence that the anions are coordinated to the Mn(II) ion and that the ligand is coordinated as a neutral chelating agent. Because of the additional stability of the half filled *d* shell, Mn(II) generally forms high spin complexes with an orbitally degenerate  ${}^6S$  ground state term and the spin only magnetic moment of 5.92 B.M., which will be independent of the temperature and stereochemistry, is expected [22].

Table 4.1. Colors, partial elemental analyses, magnetic susceptibilities and molar conductivities of the Mn(II) complexes

Compound	Color	Composition % (Found/Calculated)			$\mu$ (B.M.)	$\Lambda_M$
		C	H	N		
[Mn(H <sub>2</sub> Ac4Ph)Cl <sub>2</sub> ] (10)	pale yellow	46.87(47.02)	4.08 (3.95)	16.61(16.69)	5.91	33
[Mn(Ac4Ph)H <sub>2</sub> O] (11)	yellow	52.94(52.77)	4.17(4.24)	18.84(18.73)	5.83	29
[Mn(H <sub>2</sub> Ac4Cy)Cl <sub>2</sub> ]·H <sub>2</sub> O (12)	pale yellow	45.39(44.73)	5.81(6.04)	15.99(15.88)	5.84	14
[Mn(H <sub>2</sub> Ac4Et)Cl <sub>2</sub> ]·3H <sub>2</sub> O (13)	yellow	33.54(33.03)	5.59(5.36)	18.21(17.98)	5.78	10
[Mn(H <sub>2</sub> Ac4Et)(OAc) <sub>2</sub> ]·3H <sub>2</sub> O (14)	yellow	39.07(38.51)	6.14(5.95)	17.03(16.55)	6.08	20

\*Molar conductivity of 10<sup>-3</sup> M DMF solution, in ohm<sup>-1</sup>cm<sup>2</sup>mol<sup>-1</sup>

The magnetic moments of the five Mn(II) complexes are calculated from the magnetic susceptibility measurements are found in the range 5.78-6.08 B.M., indicating the presence of five unpaired electrons and hence these are high spin complexes [23].

#### 4.4.1. IR spectral studies

The shifts in bands assigned in spectra of ligands because of coordination are illustrated in Table 4.2. The IR spectrum of the ligand in its uncoordinated form shows bands in the 3300-3000  $\text{cm}^{-1}$  region, attributable to stretching modes of NH groups. The hydrate nature of most of complexes makes it difficult to observe the  $\nu(\text{NH})$  bands due to the presence of neutral ligand, as found for similar complexes where the ligand was not completely deprotonated [24]. The bands corresponding to  $\nu(\text{C}=\text{N})$  and  $\nu(\text{C}-\text{N})$  modes appear slightly shifted in all complexes and overlapped with  $\nu(\text{C}=\text{C})$  absorptions which is indicative of coordination of the metal to the pyridine and imine nitrogen atoms. The pyridine nitrogen coordination is again evidenced by the shift of pyridine ring deformation mode from a higher to lower frequency region in all the complexes. The  $\nu(\text{C}=\text{N})$  bands of thiosemicarbazones are found to be shifted to lower wavenumbers in the spectra of all complexes suggesting the coordination of the azomethine nitrogen to the metal. The involvement of this nitrogen in bonding is also supported by a shift in  $\nu(\text{N}-\text{N})$  band to higher frequencies. Coordination of azomethine nitrogen is again confirmed with the presence of new band in the range 450-470  $\text{cm}^{-1}$ , assignable to  $\nu(\text{Mn}-\text{N}_{\text{azo}})$  for these complexes [25-27].

Compound  $[\text{Mn}(\text{H}_2\text{Ac4Ph})\text{Cl}_2]$  (**10**) (Figure 4.1) consisting of chloro ligand, shows two bands at 3050 and 3220  $\text{cm}^{-1}$  corresponds to the  $\nu(\text{N}-\text{H})$



vibrations of the neutral ligand. Since the ligand is coordinated in the neutral form, there is no considerable negative shift in the case of  $\nu(\text{C}=\text{S})$  band. The azomethine band is shifted to  $1562\text{ cm}^{-1}$  due to binding with the metal ion. Bands at  $1047$  and  $486\text{ cm}^{-1}$  are assigned to  $\nu(\text{N}-\text{N})$  and  $\nu(\text{Mn}-\text{N})$  respectively.

The IR spectrum of the compound  $[\text{Mn}(\text{Ac}4\text{Ph})\text{H}_2\text{O}]$  (11), (Figure 4.2) exhibits a band at  $3197\text{ cm}^{-1}$  indicating the presence of coordinated water in the molecule. The band at  $1606\text{ cm}^{-1}$  is assigned to the  $-\text{C}=\text{N}-\text{N}=\text{C}-$  moiety, newly formed as a result of deprotonation of the ligand for coordination. The azomethine band suffered a negative shift and is observed at  $1560\text{ cm}^{-1}$ . The  $\nu(\text{C}=\text{S})$  band shifts to lower wavenumber and that may be due to the formation of strong metal-sulfur bonds [26]. Absence of any band in the region  $2600-2800\text{ cm}^{-1}$  suggests the coordination through thiolato sulfur. The aromatic ring vibrations occur at  $1482$  and  $1438\text{ cm}^{-1}$ .

Table 4.2. Infrared spectral assignments ( $\text{cm}^{-1}$ ) of ligands and their Mn(II) complexes

Compound	$\nu(\text{C}=\text{N})$	$\nu/\delta(\text{C}-\text{S})$	$\nu(\text{Mn}-\text{N})$	$\nu(\text{N}-\text{N})$	py(ip)
$\text{H}_2\text{Ac}4\text{Ph}$	1597	1322,808	-	1028	628
$[\text{Mn}(\text{H}_2\text{Ac}4\text{Ph})\text{Cl}_2]$ (10)	1562	1320, 802	486	1047	663
$[\text{Mn}(\text{Ac}4\text{Ph})\text{H}_2\text{O}]$ (11)	1560	1205, 710	434	1095	676
$\text{H}_2\text{Ac}4\text{Cy}$	1596	1307, 857	-	1013	601
$[\text{Mn}(\text{H}_2\text{Ac}4\text{Cy})\text{Cl}_2]\cdot\text{H}_2\text{O}$ (12)	1555	1208, 802	460	1068	680
$\text{H}_2\text{Ac}4\text{Et}$	1541	1305, 857	-	1050	639
$[\text{Mn}(\text{H}_2\text{Ac}4\text{Et})\text{Cl}_2]\cdot 3\text{H}_2\text{O}$ (13)	1527	1289, 726	427	1068	652
$[\text{Mn}(\text{H}_2\text{Ac}4\text{Et})(\text{OAc})_2]\cdot 3\text{H}_2\text{O}$ (14)	1526	1293, 806	489	1086	663

The IR spectrum of compound  $[\text{Mn}(\text{H}_2\text{Ac}4\text{Cy})\text{Cl}_2]\cdot\text{H}_2\text{O}$  (**12**) (Figure 4.3) reveals a broad band with low intensity around  $3420\text{ cm}^{-1}$ , which can be attributed to the presence of non-hydrogen bonded lattice water content in the sample.  $\nu(\text{NH})$  vibrations are observed *ca*  $3030\text{ cm}^{-1}$ . A band observed at  $247\text{ cm}^{-1}$  (Figure 4.3a) in the far IR spectrum have been assigned to terminal  $\nu(\text{Mn}-\text{Cl})$  band. A shift towards lower frequency of  $\nu(\text{C}-\text{N})$  at  $1555\text{ cm}^{-1}$  suggests bonding through azomethine nitrogen. The cyclohexyl stretching vibrations typical of the ligand moiety appear at  $2926$  and  $2852\text{ cm}^{-1}$ .

IR spectrum of compound  $[\text{Mn}(\text{H}_2\text{Ac}4\text{Et})\text{Cl}_2]\cdot 3\text{H}_2\text{O}$  (**13**) (Figure 4.4) shows bands around  $3278\text{ cm}^{-1}$  corresponds to  $\nu(\text{N}-\text{H})$ . A band at  $3441\text{ cm}^{-1}$  is assigned for lattice water. A negative shift of  $\nu(\text{C}-\text{N})$  band at  $1527\text{ cm}^{-1}$  suggests the coordination through azomethine nitrogen.

In the IR spectrum of compound  $[\text{Mn}(\text{H}_2\text{Ac}4\text{Et})(\text{OAc})_2]\cdot 3\text{H}_2\text{O}$  (**14**) (Figure 4.5), a broad band observed at  $3431\text{ cm}^{-1}$  indicates the presence of lattice water in the molecule. It is difficult to identify the  $\nu(\text{N}-\text{H})$  band at  $3200\text{ cm}^{-1}$  supporting the protonated form of the ligand during coordination. This spectrum supports the coordination of ligand to metal through azomethine nitrogen atom by shifting the  $\nu(\text{C}-\text{N})$  band to lower frequency. Band at  $1086\text{ cm}^{-1}$  is assigned to  $\nu(\text{N}-\text{N})$ . Bands at  $1526$  and  $1484\text{ cm}^{-1}$  correspond to symmetric and asymmetric stretching vibrations of the acetate group, consistent with the presence of a monodentate acetate group in this complex [28].

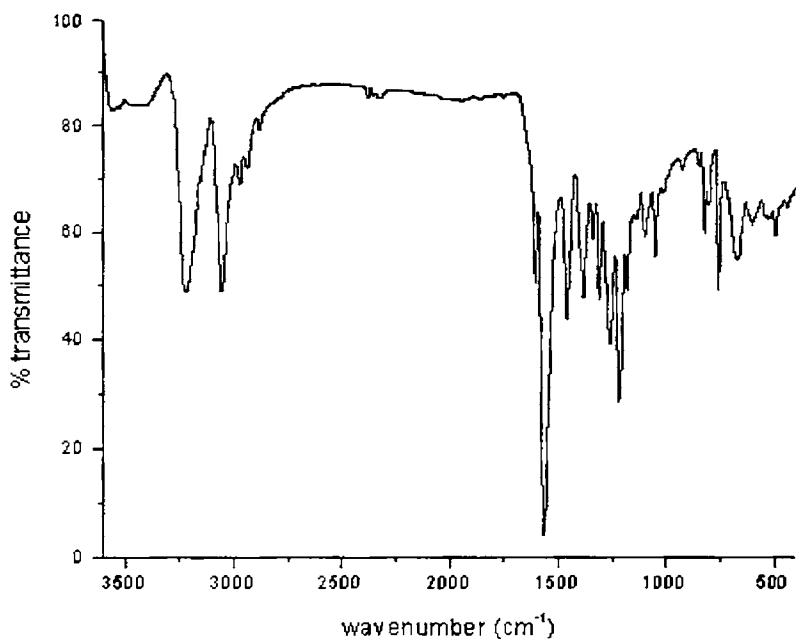


Figure 4.1. IR spectrum of compound  $[\text{Mn}(\text{H}_2\text{Ac4Ph})\text{Cl}_2]$  (10)

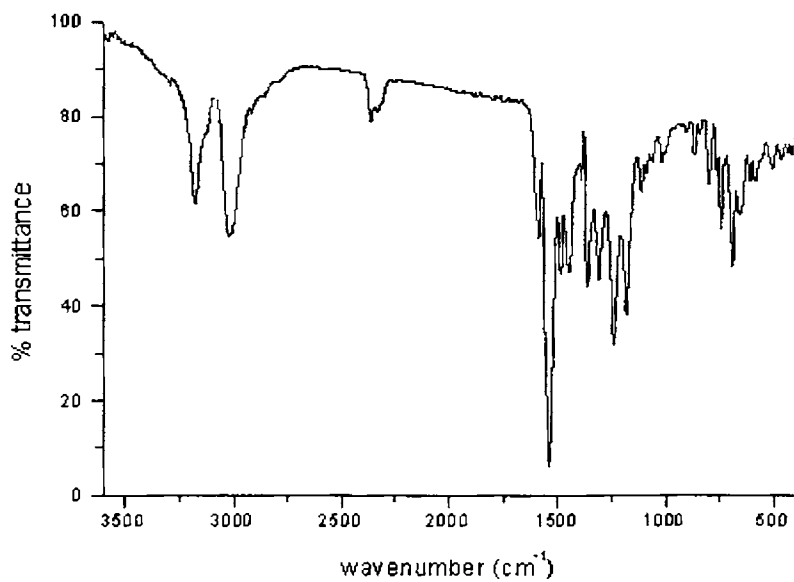


Figure 4.2. IR spectrum of compound  $[\text{Mn}(\text{Ac4Ph})\text{H}_2\text{O}]$  (11)

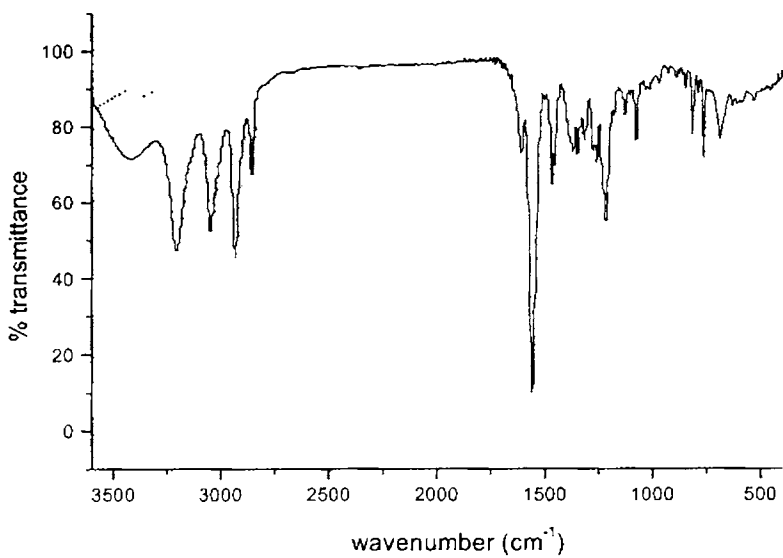


Figure 4.3. IR spectrum of compound  $[\text{Mn}(\text{H}_2\text{Ac4Cy})\text{Cl}_2]\cdot\text{H}_2\text{O}$  (**12**)

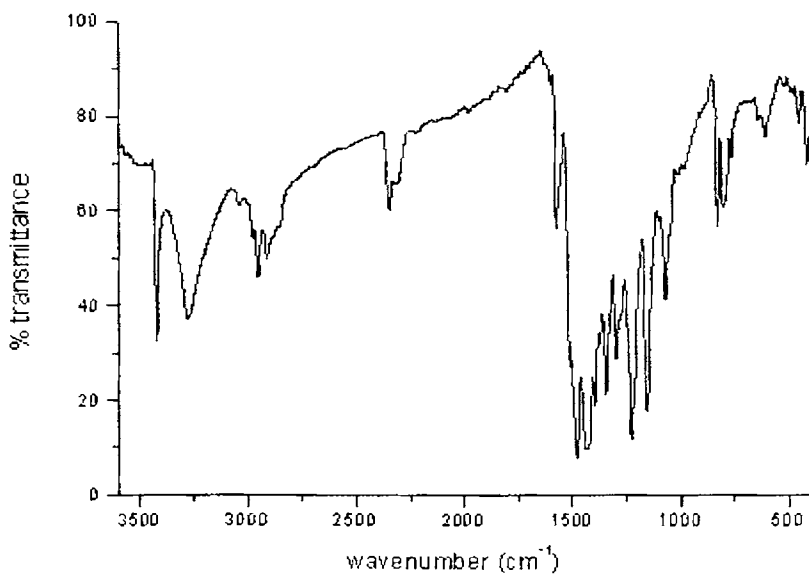


Figure 4.4. IR spectrum of compound  $[\text{Mn}(\text{H}_2\text{Ac4Et})\text{Cl}_2]\cdot 3\text{H}_2\text{O}$  (**13**)

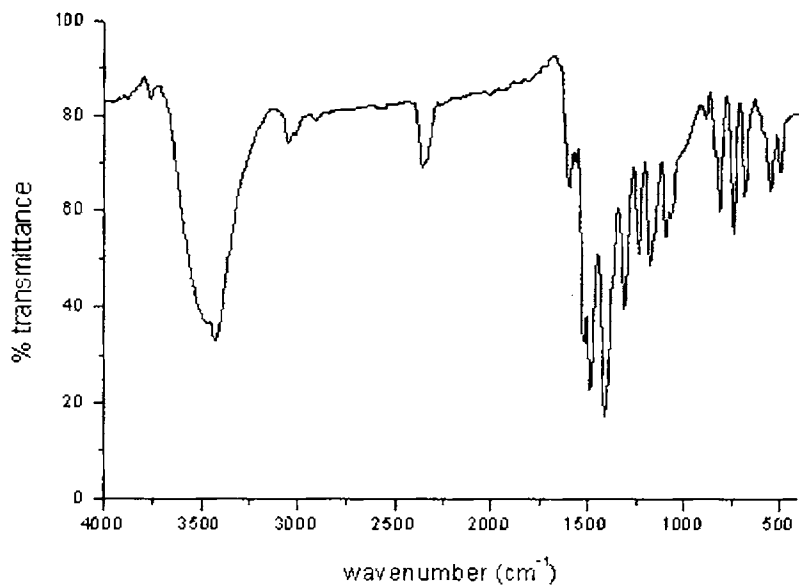


Figure 4.5. IR spectrum of compound  $[\text{Mn}(\text{H}_2\text{Ac}_4\text{Et})(\text{OAc})_2] \cdot 3\text{H}_2\text{O}$  (14)

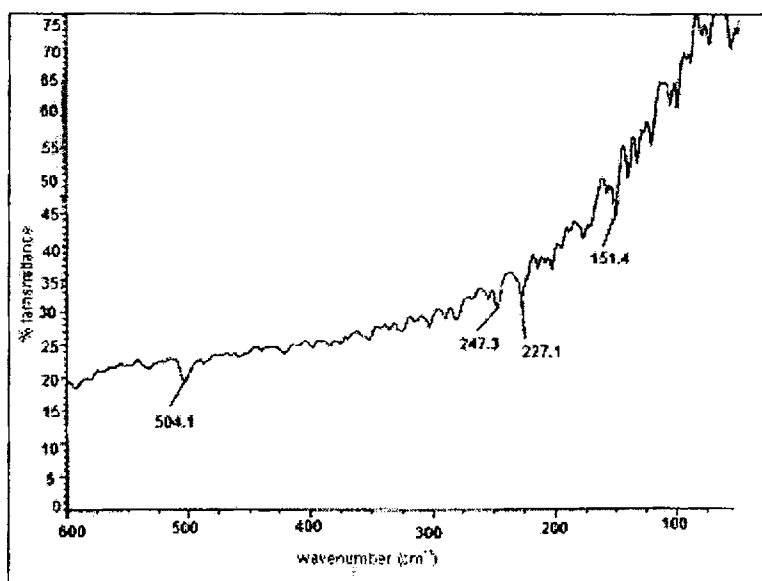


Figure 4.3a. Far IR spectrum of compound  $[\text{Mn}(\text{H}_2\text{Ac}_4\text{Cy})\text{Cl}_2] \cdot \text{H}_2\text{O}$  (12)

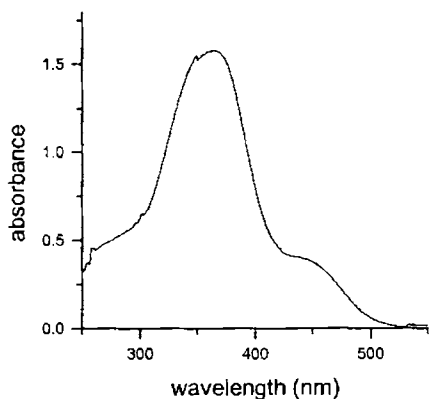
#### 4.4.2. Electronic spectral studies

The high spin  $d^5$  configuration of Mn(II) with five unpaired electrons reveals the  ${}^6A_{1g}$  ground state, which is an orbital singlet with no possible spin-sextet excited states. Thus, for a  $d^5$  complex, all transitions are not only Laporte-forbidden but also spin-forbidden. Absorptions associated with doubly forbidden transitions are extremely weak, with extinction coefficients several hundred times smaller than those for singly forbidden transitions. However, out of the eleven possible excited states, four of them involve spin quartets, namely  ${}^4G$ ,  ${}^4F$ ,  ${}^4D$  and  ${}^4P$ . The transitions from  ${}^6S$  to these four involve only one reversal of spin. These four states split in several very weak absorption bands and the interpretation of these types of weak absorptions where the spin multiplicity of the excited state is lower than the ground state; Tanabe- Sugano diagram is used. It shows that the four possible transitions from the high-spin  $d^5$  configurations are  ${}^4A_{1g}(G), {}^4E_g(G) \leftarrow {}^6A_{1g}$ ,  ${}^4E_g(D) \leftarrow {}^6A_{1g}$ ,  ${}^4T_{1g} \leftarrow {}^6A_{1g}$  and  ${}^4T_2(G) \leftarrow {}^6A_{1g}$ .

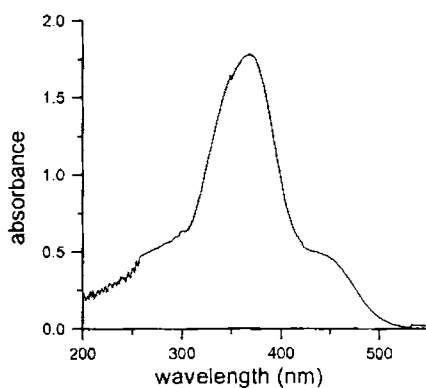
The  $d-d$  transitions in the manganese(II) systems are doubly forbidden hence they don't register any characteristic bands in the visible region. In the present compounds,  $d-d$  bands could not be identified due to their low intensity (Figure 4.6). All the compounds possessed high intense bands in the region *ca*  $27,300\text{ cm}^{-1}$ . The absorption bands found for the complexes under study are listed in Table 4.3.

Table 4.3. Electronic spectral assignments ( $\text{cm}^{-1}$ ) for the ligands and their Mn(II) complexes

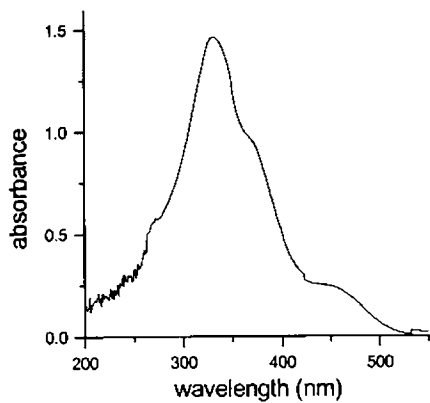
Compound	$\pi \rightarrow \pi^*$	$n \rightarrow \pi^*$	LMCT
$\text{H}_2\text{Ac4Ph}$	32,250	28,900	-
$[\text{Mn}(\text{H}_2\text{Ac4Ph})\text{Cl}_2]$ (10)	32,200	28,250	25,180
$[\text{Mn}(\text{Ac4Ph})\text{H}_2\text{O}]$ (11)	32,110	28,500	24,690
$\text{H}_2\text{Ac4Cy}$	32,450	29,210	-
$[\text{Mn}(\text{H}_2\text{Ac4Cy})\text{Cl}_2] \cdot \text{H}_2\text{O}$ (12)	32,220	28,990	25,830
$\text{H}_2\text{Ac4Et}$	32,240	29,390	-
$[\text{Mn}(\text{H}_2\text{Ac4Et})\text{Cl}_2] \cdot 3\text{H}_2\text{O}$ (13)	32,150	29,120	24,870
$[\text{Mn}(\text{H}_2\text{Ac4Et})(\text{OAc})_2] \cdot 3\text{H}_2\text{O}$ (14)	32,210	28,900	24,720



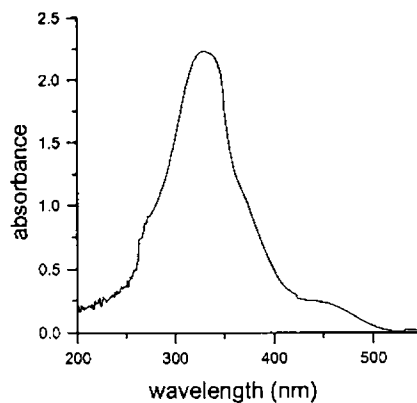
$[\text{Mn}(\text{H}_2\text{Ac4Ph})\text{Cl}_2]$  (10)



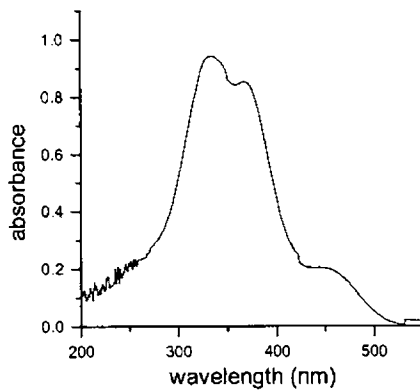
$[\text{Mn}(\text{Ac4Ph})\text{H}_2\text{O}]$  (11)



$[\text{Mn}(\text{H}_2\text{Ac4Cy})\text{Cl}_2] \cdot \text{H}_2\text{O}$  (12)



$[\text{Mn}(\text{H}_2\text{Ac4Et})\text{Cl}_2] \cdot 3\text{H}_2\text{O}$  (13)



$[\text{Mn}(\text{H}_2\text{Ac4Et})(\text{OAc})_2] \cdot 3\text{H}_2\text{O}$  (14)

Figure 4.6. Electronic spectra of Mn(II) complexes



#### 4.4.3. EPR spectral studies

Manganese complexes show a wide variety of bonding geometries and EPR spectroscopy has been used successfully to probe the structures of these compounds [29, 30]. The spin Hamiltonian for Mn(II) may be described as

$$\hat{H} = g\beta H_s + D[S_z^2 - S(S+1)/3] + E(S_x^2 - S_y^2) \quad (4.1)$$

where  $H$  is the magnetic field vector,  $D$  is the axial zero field splitting term,  $E$  is the rhombic zero field splitting parameter. If  $D$  and  $E$  are very small compared to  $g\beta H_s$ , five EPR transitions corresponding to  $\Delta m_s = \pm 1$  are expected with a  $g$  value of 2.0. However, for the case where  $D$  or  $E$  is very large, the lowest doublet has effective  $g$  values of  $g_{\parallel} = 2$ ,  $g_{\perp} = 6$  for  $D \neq 0$  and  $E = 0$  but for  $D = 0$  and  $E \neq 0$ , the middle Kramer's doublet has an isotropic  $g$  value of 4.29 [28, 31].

The EPR spectrum of compound  $[\text{Mn}(\text{H}_2\text{Ac}4\text{Ph})\text{Cl}_2]$  (**10**) at 298 K (Figure 4.7), in polycrystalline state exhibited a broad signal with a  $g$  value at 2.027 with no hyperfine splittings. However, the solution spectrum in DMF at 77 K (Figure 4.7a), displayed a hyperfine sextet with  $g_{iso}$  2.012 (Figure 4.7). High spin  $\text{Mn}^{2+}$  ions with five unpaired electrons ( $S=5/2$ ) have an orbitally non-degenerate  ${}^6A_{1g}$  ground state. Hence the spin-orbit coupling is expected to be unimportant and the zero field splitting should be rather small. This is usually observed with complexes of weak field ligands, which give only one 'g' value close to 2.0023, the free electron 'g' value. However, in the present complex, Mn(II) is present in a sufficiently strong ligand field of two thiosemicarbazone moieties, only one resonance corresponding to  $\Delta M_s = \pm 1$  is

observed. This may mean that the manganese in compound **10** exists in a nearly cubic field. The  $A_{iso}$  value calculated for the hyperfine sextet is 92 G.

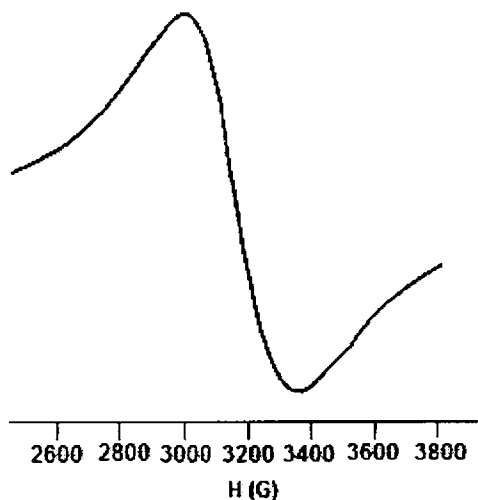


Figure 4.7. EPR spectrum of compound  $[\text{MnH}_2\text{Ac}_4\text{PhCl}_2]$  (**10**) in polycrystalline state at 298 K

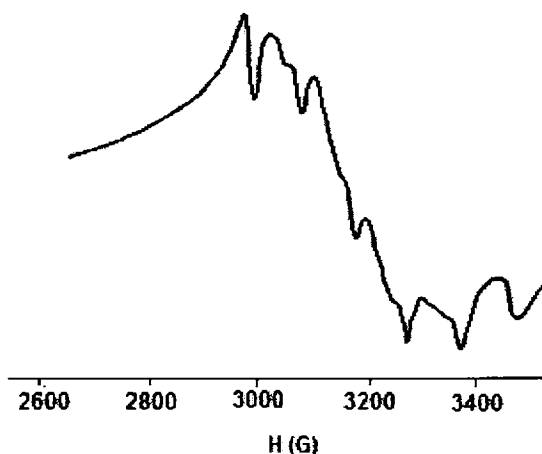


Figure 4.7a. EPR spectrum of compound  $[\text{MnH}_2\text{Ac}_4\text{PhCl}_2]$  (**10**) in DMF at 77 K

In the case of  $\text{Mn}^{2+}$  ions with five unpaired electrons,  $S=5/2$  has  $M_s = \pm 5/2, \pm 3/2, \pm 1/2$  indicate the presence of doubly degenerate spin states known as Kramer's degeneracy and no  $M_s = 0$  state, leads to a special case of zero field splitting. These doublet sets will be slightly different in energy from

each other due to the zero field already present. On the application of a magnetic field, each of the doubly degenerate sets will further split, and hence a series of lines will appear in the spectrum (Figure 4.8). Since the manganese nucleus has a nuclear spin  $I = 5/2$ , each spectral lines due to a particular  $M_s$  level undergoes hyperfine splitting into six fine lines. Hence we get a spectrum with five sets of lines corresponding to five transitions with different energy, appear at different positions, each with six hyperfine splittings (Figure 4.9). Such a spectrum is obtained in the case of compound  $[\text{Mn}(\text{Ac}4\text{Ph})\text{H}_2\text{O}]$  (11) in DMF with five  $g$  values of 5.69, 3.22, 2.65, 2.23 and 1.82 (Figure 4.10a). This compound exhibited a broad signal centered on  $g_{\text{iso}}=2.005$  in polycrystalline state at 298 K (Figure 4.10) which is due to dipolar interactions and enhanced spin lattice relaxation [28].

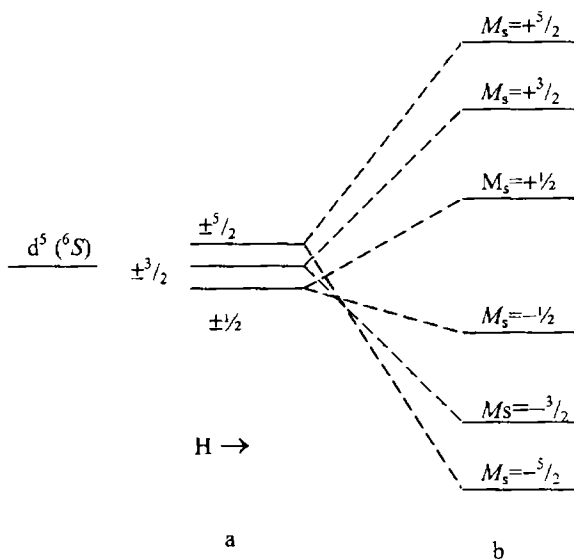


Figure 4.8. Kramer's degeneracy a) zero field splitting of high-spin  $d^5 \text{Mn(II)}$  b) splitting of  $M_s$  levels on application of magnetic field

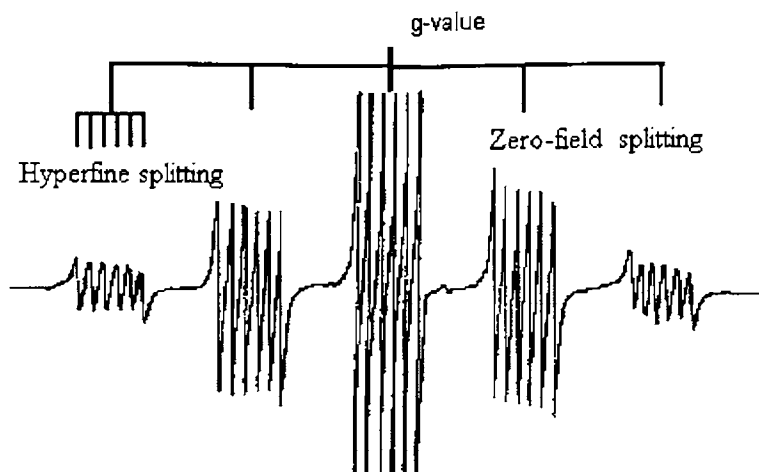


Figure 4.9. Spectrum showing hyperfine splitting and zero-field splitting on the application of a magnetic field

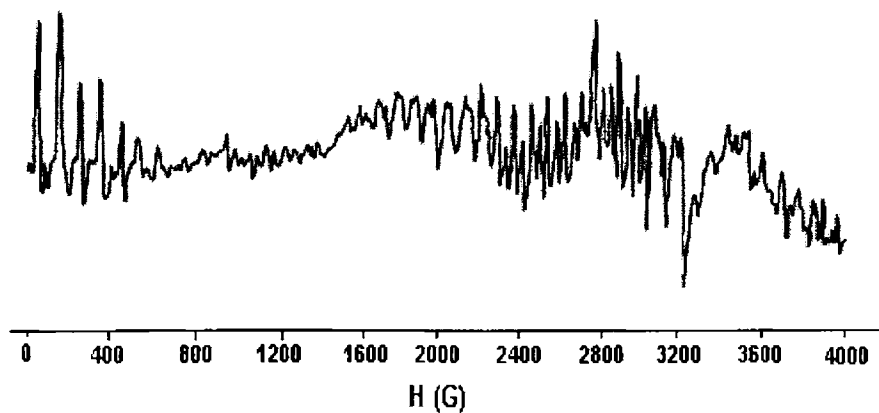


Figure 4.10a. EPR spectrum of compound  $[\text{Mn}(\text{Ac}_4\text{Ph})\text{H}_2\text{O}]$  (11) in DMF at 77 K

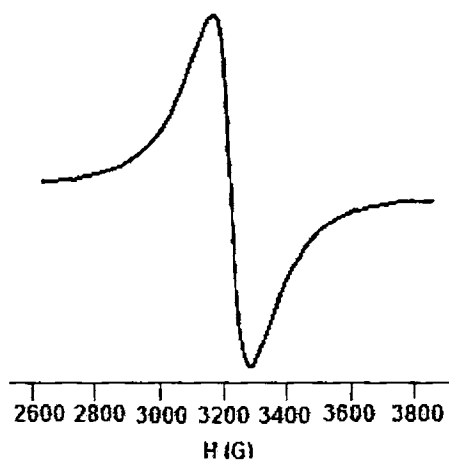


Figure 4.10. EPR spectrum of compound  $[\text{Mn}(\text{Ac4Ph})\text{H}_2\text{O}]$  (**11**) in polycrystalline state at 298 K

A broad isotropic signal with  $g=2.050$  was found for the compound  $[\text{Mn}(\text{H}_2\text{Ac4Cy})\text{Cl}_2]\cdot\text{H}_2\text{O}$  (**12**) in polycrystalline state at 298 K (Figure 4.11).

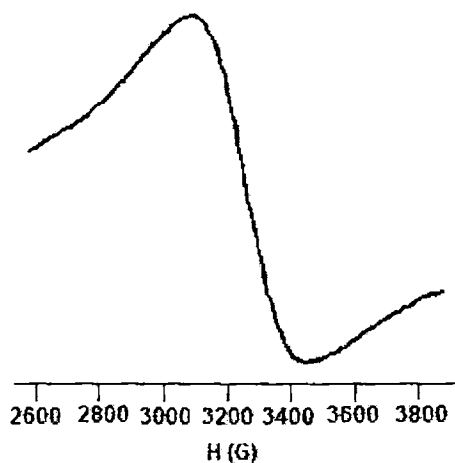


Figure 4.11. EPR spectrum of compound  $[\text{Mn}(\text{H}_2\text{Ac4Cy})\text{Cl}_2]\cdot\text{H}_2\text{O}$  (**12**) in polycrystalline state at 298 K.

The solution spectrum in DMF at 77 K (Figure 4.11a), displayed a hyperfine sextet with  $g_{iso}$  value of 1.996.

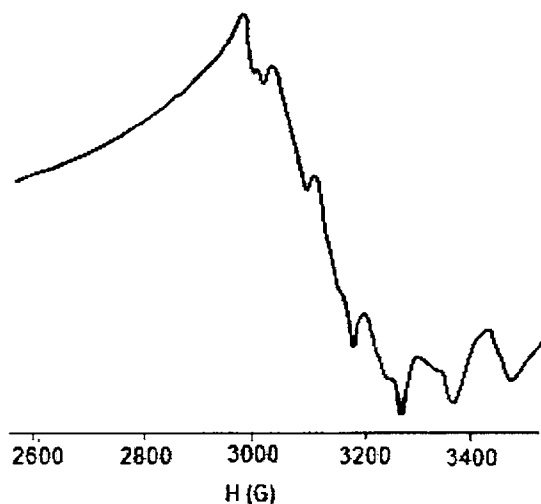


Figure 4.11a. EPR spectrum of compound  $[\text{Mn}(\text{H}_2\text{Ac}_4\text{Cy})\text{Cl}_2]\cdot\text{H}_2\text{O}$  (**12**) in DMF at 77 K.

The observance of hyperfine sextet is as expected due to the interaction of the unpaired electron with the Mn(II) nucleus of spin  $I=5/2$ , resulting in  $2nI+1$  lines. Thus the six lines observed corresponds to  $M_s = +5/2, +1/2, \dots -5/2$  with  $\Delta M_I = 0$ . The hyperfine coupling constant is found to be 96 G. Additional lines present in between each of the two main hyperfine lines can be explained as follows. It is possible that in ESR spectra, involving interaction with nuclei with quadrupole moments (nuclear spin  $I>1$ ), a violation of the selection rules occurs. Thus in addition to the transition due to  $\Delta M_s = \pm 1, \Delta M_I = 0$ , transitions associated with  $\Delta M_I = \pm 1$  also occur. This effect is seen as weak lines midway between the principal hyperfine lines. The forbidden transitions are further split into doublets by spin-spin interaction of the sextuplet states and this causes variations in the hyperfine splitting separation of the forbidden transitions.

The EPR spectrum of compound  $[\text{Mn}(\text{H}_2\text{Ac}_4\text{Et})\text{Cl}_2]\cdot 3\text{H}_2\text{O}$  (13) at 298 K in polycrystalline state (Figure 4.12) exhibited a broad signal with a  $g$  value at 2.040.

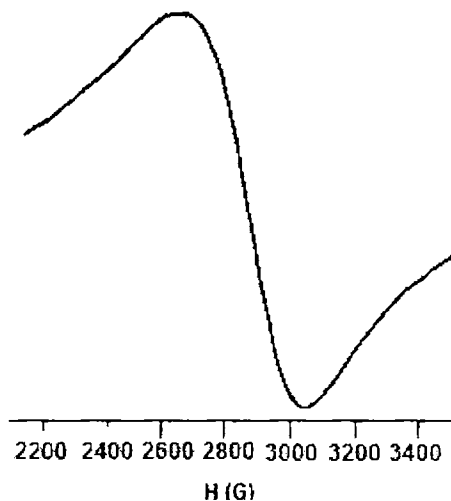


Figure 4.12. EPR spectrum of compound  $[\text{Mn}(\text{H}_2\text{Ac}_4\text{Et})\text{Cl}_2]\cdot 3\text{H}_2\text{O}$  (13) in polycrystalline state at 298 K

The frozen solution spectrum (Figure 4.12a) of the compound in DMF, displayed one  $g$  value 1.992 with a central hyperfine sextet. A pair of low intensity forbidden lines lying between each of the two main hyperfine lines is observed. The forbidden lines in the spectrum arise due to the mixing of the nuclear hyperfine levels by the zero-field splitting factor of the Hamiltonian [32, 33]. The coupling constant  $A_{iso}$ , for the central sextet hyperfine lines is found to be 96 G.

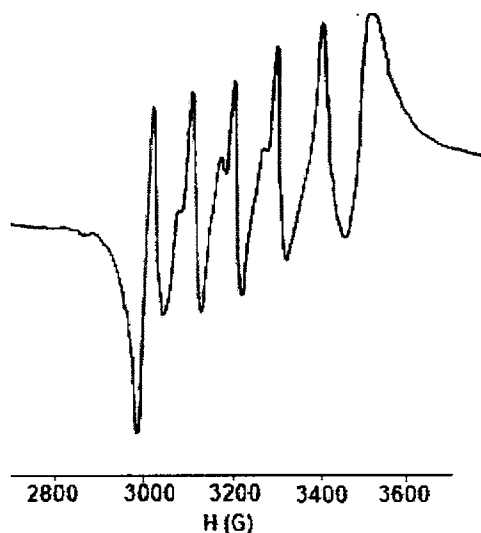


Figure 4.12a. EPR spectrum of compound  $[\text{Mn}(\text{H}_2\text{Ac}_4\text{Et})\text{Cl}_2]\cdot 3\text{H}_2\text{O}$  (13) in DMF at 77K

In the case of compound  $[\text{Mn}(\text{H}_2\text{Ac}_4\text{Et})(\text{OAc})_2]\cdot 3\text{H}_2\text{O}$  (14), the EPR spectrum at 298 K in polycrystalline state (Figure 4.13) exhibited a broad signal with a  $g$  value at 2.070.

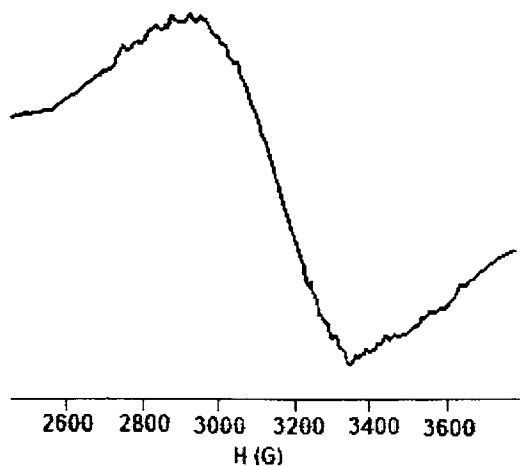


Figure 4.13. EPR spectrum of compound  $[\text{Mn}(\text{H}_2\text{Ac}_4\text{Et})(\text{OAc})_2]\cdot 3\text{H}_2\text{O}$  (14) in polycrystalline state at 298 K



In DMF at 77 K the compound **14** reveals one  $g$  value at 2.021 (Figure 4.13a). A six line manganese hyperfine sextet with a hyperfine coupling constant 92 G is also observed.

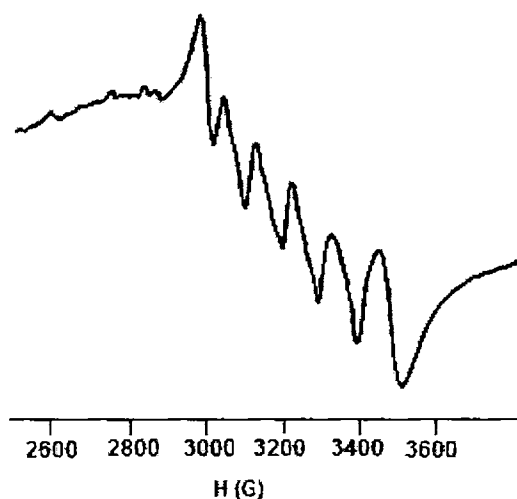
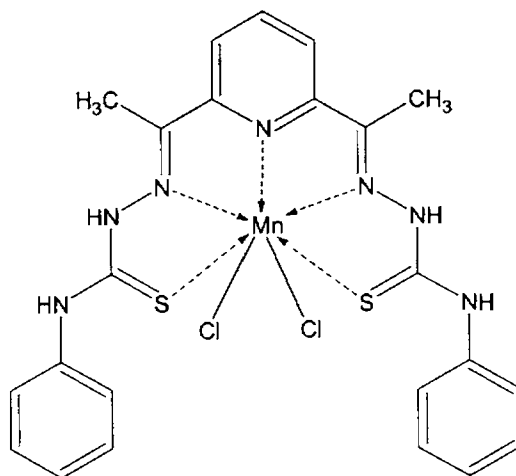


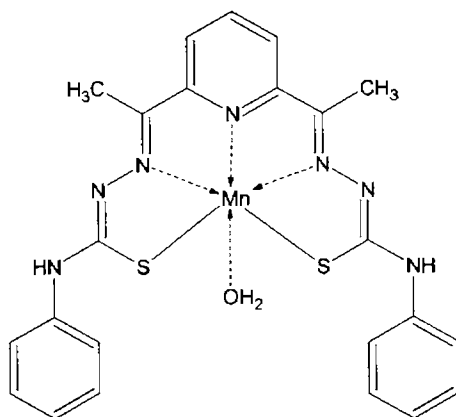
Figure 4.13a. EPR spectrum of compound  $[\text{Mn}(\text{H}_2\text{Ac}_4\text{Et})(\text{OAc})_2] \cdot 3\text{H}_2\text{O}$  (**14**) in DMF at 77K

In all the EPR spectra of  $\text{Mn}^{2+}$  complexes under study, it is observed that the separation between adjacent lines in the hyperfine multiplet differ slightly, and this can be attributed to the inequivalent spacing of the  $2nI+1$  nuclear levels.  $\text{Mn}(\text{II})$  nuclei with  $S=5/2$  has an appreciable quadrupole moment and the electric field gradient from the surrounding ligand ions compete with the magnetic hyperfine interaction in determining the orientation of the nuclear spin, due to which the degeneracy of the nuclear levels is lost resulting in difference in the separation between adjacent lines in the hyperfine splittings.

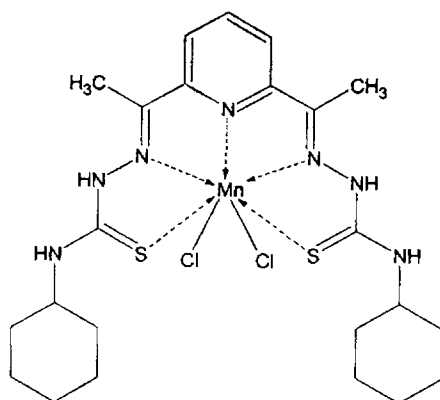
Based on the elemental analyses and spectral studies following tentative structures were assigned for the complexes. Water molecules are not included in structures for clarity.



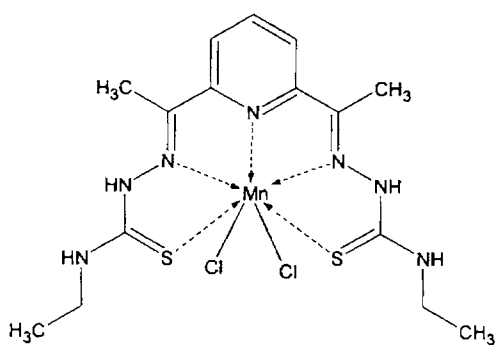
**[Mn(H<sub>2</sub>Ac<sub>4</sub>Ph)Cl<sub>2</sub>] (10)**



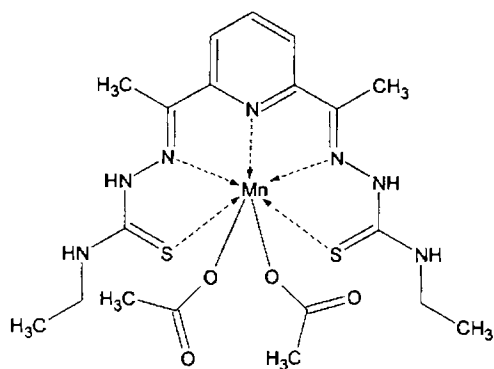
**[Mn(Ac<sub>4</sub>Ph)H<sub>2</sub>O] (11)**



**[Mn(H<sub>2</sub>Ac4Cy)Cl<sub>2</sub>]·H<sub>2</sub>O (12)**



**[Mn(H<sub>2</sub>Ac4Et)Cl<sub>2</sub>]·3H<sub>2</sub>O (13)**



**[Mn(H<sub>2</sub>Ac4Et)(OAc)<sub>2</sub>]·3H<sub>2</sub>O (14)**

## Concluding remarks

This chapter deals with the synthesis and spectral characterization of five manganese(II) complexes of four ligands viz. 2,6-diacetylpyridine bis(*N*<sup>4</sup>-phenylthiosemicarbazone) [H<sub>2</sub>Ac4Ph], 2,6-diacetylpyridinebis(*N*<sup>4</sup>-cyclohexylthiosemicarbazone) [H<sub>2</sub>Ac4Cy], 2,6-diacetylpyridine bis(*N*<sup>4</sup>-methylthiosemicarbazone) [H<sub>2</sub>Ac4Me], 2,6-diacetylpyridine bis(*N*<sup>4</sup>-ethylthiosemicarbazone) [H<sub>2</sub>Ac4Et]. The complexes were characterized by partial elemental analyses, molar conductivity and room temperature magnetic susceptibility measurements and IR, electronic and EPR spectral studies. All the complexes except **11** were assigned a pentagonal bipyramidal geometry based on analytical spectral data. Compound **11** is assigned an octahedral geometry. The structures proposed in this study are tentative because of the lack of X-ray crystal structure data.

## References

1. R. Hage, Recl. Trav. Chim. Pays-Bas 115 (1996) 385.
2. W. Zhang, J.L. Loebach, S.R. Wilson, E.N. Jacobsen, J. Am. Chem. Soc. 112 (1990) 2801.
3. J. Brinksma, R. Hage, J. Kerschner, B.L. Feringa, Chem. Commun. (2000) 537.
4. K.B. Jensen, E. Johansen, F.B. Larsen, C.J. McKenzie, Inorg. Chem. 43 (2004) 3801.

- 
5. J. Bendix, H.B. Gray, G. Golubkov, Z. Gross, *Soc. Chem. Commun.* (2000) 1957.
  6. B. Meunier, in *Metalloporphyrin Catalysed Oxidations*, ed. F. Montanari, L. Casella, Kluwer Academic Publishers, Dordrecht, (1994) 4.
  7. J.T. Groves, in *Cytochrome P450: Structure, Mechanism and Biochemistry*, Ed. P. R. Ortiz de Montellano, 2<sup>nd</sup> ed., Plenum Press, New York, 1995.
  8. K. Wieghardt, *Angew. Chem. Int. Ed. Engl.* 28 (1989) 1153.
  9. D. Evans, K.S. Hallwood, C.H. Cashin, H. Jackson, *J. Med. Chem.* 10 (1967) 428.
  10. G.F. De Sousa, C.A.L. Filgueiras, A. Abras, S.S. Al-Juaid, P.B. Hitchcock, J. F. Nixon, *Inorg. Chim. Acta* 218 (1994) 139.
  11. P.C. Moreno, R.H.P. Francisco, M.T.P. Gambardella, G. F. de Sousa, A. Abras, *Acta Cryst. C*53 (1997) 1411.
  12. D.X. West, G.A. Bain, R.J. Butcher, J.P. Jasinski, Y. Li, R.Y. Pozdniakiv, J. Valdés-Martínez, R.A. Toscano, S. Hernández-Ortega, *Polyhedron* 15 (1996) 665.
  13. A. Bino, N. Cohen; *Inorg. Chim. Acta* 210 (1993) 11.
  14. M. Maji, S. Ghosh, S.K. Chattopadhyay, *Trans. Met. Chem.* 23 (1998) 81.

15. S. Casas, A. Castineiras, A. Sanches, J. Sordo, A. Vasquez-Lopes, M.C. Arguelles, U. Russo, *Inorg. Chim. Acta* 221 (1994) 61.
16. A.H. Othman, K.-L. Lee, H.-K. Fun, B.-C. Yip, *Acta Cryst. C* 52 (1996) 602.
17. S. Abram, C. Maichle-Mossmer, U. Abram, *Polyhedron* 17 (1998) 131.
18. C. Carini, G. Pelizzi, P. Tarasconi, C. Pelizzi, K.C. Molloy, P.C. Waterfield, *J. Chem. Soc. Dalton Trans.* 2 (1989) 289.
19. J.S. Casas, A. Castiñeiras, A. Sánchez, J. Sordo, A. Vázquez- López, M.C. Rodríguez-Argüelles, U. Russo, *Inorg. Chim. Acta* 221 (1994) 61.
20. G.F. de Sousa, J Valdes-Martinez, G.E. Perez, R.A. Toscano, A. Abrasc, C.A.Filgueiras *J. Braz. Chem. Soc.* 13 (2002) 559.
21. R. Pedrio, M.R. Bermejo, M.J. Romeo, M. Vázquez, A.M. González-Noya, M. Maneiro, M. Jesús Rodriguez, M.I. Fernandez *Dalton Trans.* (2005) 572.
22. B.N. Figgis, *Introduction to Ligand fields*, Wiley Eastern Limited, New Delhi, 1976.
23. B.N. Figgis, J. Lewis, *Prog. Inorg. Chem.* 6 (1964) 37.
24. M.C. Rodriguez-Arguelles, M.B. Ferrari, F. Bisceglie, C. Pelizzi, G. Pelosi, S. Pinelli, M. Sassi, *J. Inorg. Biochem.* 98 (2004) 313.

25. V.B. Rana, J.N. Gurthu, M.P. Teotia, *J. Inorg. Nucl. Chem* 42 (1980) 331.
26. R.P. John, A. Sreekanth, M.R.P. Kurup, H.-K. Fun, *Polyhedron* 24 (2005) 601.
27. D.K. Demertzi, U. Gangadharmath, M.A. Demertzis, Y. Sanakis, *Inorg. Chem. Commun.* 8 (2005) 616.
28. B.S. Garg, M.R.P. Kurup, S.K. Jain, Y.K. Bhoon, *Trans. Met. Chem.* 13 (1988) 309.
29. R. Luck, R. Stosser, O.G. Poluektov, O. Ya. Grinberg, Ya.S. Lebedev, G.M. Woltermann, J.R. Wasson, *Inorg. Chem.* 12 (1973).
30. E. Meirovitch, R. Poupko, *J. Phys. Chem.* 82 (1978) 1920.
31. K.B. Pandeya, R. Singh, P.K. Mathur, R.P. Singh, *Trans. Met. Chem.* 11 (1986) 347.
32. B. Bleaney, R.S. Rubins, *Proc. Phys. Soc. London* 77 (1961) 103.
33. W. Linert, F. Renz, R. Boca, M. Valko, R. Klement, M. Mazur, *J. Coord. Chem.* 40 (1996) 293.

\*\*\*\*\*

# Synthesis and spectral characterization of Ni(II) and Pd(II) complexes of bis(*N*<sup>4</sup>-substitutedthiosemicarbazones) of 2,6-diacetylpyridine

## 5.1. Introduction

Thiosemicarbazones comprise an intriguing class of chelating molecules, which possess a wide range of beneficial medicinal properties [1]. In the last few years, nickel(II) complexes containing sulfur donors have received considerable attention due to the identification of a sulfur rich coordination environment in biological nickel centers such as the active sites of certain ureases, methyl-S-coenzyme reductase, hydrogenases and dehydrogenases and may play a role in the supposed mutagenicity of nickel compounds. Several aspects of the chemistry of these biological nickel ions are unusual in the context of the known coordination chemistry of nickel: three of the four enzymes are known to contain redox active nickel centers that can cycle between the 3, 2, and/or 1 oxidation states, in thiolate rich or tetrapyrrole ligand environments that were not previously thought to favor metal centered redox processes in the nickel complexes [2-5].

The chemistry of divalent and trivalent nickel complexes with nitrogen-sulfur donor ligands has received much attention [6-16] particularly since the discovery [15-17] that a number of dehydrogenases contain nickel at their active sites, surrounded by more than one thiolate ligand, as well as one or two nitrogen donors. Nickel(II) is also used as a spectroscopic probe in metal replacement studies of other metalloenzyme systems [18-22]. Although a variety of nitrogen sulfur donors have been investigated, thiosemicarbazides and thiosemicarbazones have received inadequate attention. Biological



activities of metal complexes differ from those of either ligands or the metal ions and increased and/or decreased biological activities are reported for several transition metal complexes, such as nickel(II) and zinc(II) [23, 24]. Thiosemicarbazone containing a pyridine ring give rise to NNS tridentate systems, which have been extensively investigated [23-25]. Kasuga et al. reported that antimicrobial activities of nickel(II) complexes were significantly influenced by the molecular structure [23]. There are reports on nickel(II) complexes of butane-2,3-dione [26], pyruvaldehyde [27] and glyoxaldehyde [28] bis{N(3)-substitutedthiosemicarbazones}.

## 5.2. Experimental

### 5.2.1. Materials

The reagents used for the synthesis of the ligands are discussed in Chapter 2. Solvents were purified by standard methods. Nickel salts and palladium salts used were of Analar grade and used as supplied for the preparation of complexes. Solvents used were methanol, ethanol, DMF and chloroform.

### 5.2.2. Syntheses of ligands

Ligands  $H_2Ac4Ph$ ,  $H_2Ac4Cy$ ,  $H_2Ac4Me$  and  $H_2Ac4Et$  were synthesized as described previously in Chapter 2.

### 5.2.3. Synthesis of Ni(II) complexes

**[Ni(Ac4Ph)H<sub>2</sub>O]·CH<sub>3</sub>OH (15):** To a solution of ligand  $H_2Ac4Ph$  (0.461 g, 1 mmol) in DMF was added  $NiSO_4 \cdot 7H_2O$  (0.280 g, 1 mmol) in methanol and heated under reflux for 3 hours and kept at room temperature.

The complex formed was filtered, washed thoroughly with methanol and ether and dried *in vacuo* over P<sub>4</sub>O<sub>10</sub>.

**[Ni(HAc4Cy)OAc]·C<sub>2</sub>H<sub>5</sub>OH (16):** To a solution of ligand H<sub>2</sub>Ac4Cy (0.473 g, 1 mmol) in CHCl<sub>3</sub> was added Ni(OAc)<sub>2</sub>·4H<sub>2</sub>O (0.248 g, 1 mmol) in ethanol and heated under reflux for 2 hours and kept at room temperature. The complex formed was filtered, washed thoroughly with methanol and ether and dried *in vacuo* over P<sub>4</sub>O<sub>10</sub>.

**[Ni(Ac4Cy)H<sub>2</sub>O] (17):** To a solution of ligand H<sub>2</sub>Ac4Cy (0.473 g, 1 mmol) in CHCl<sub>3</sub> was added Ni(NO<sub>3</sub>)<sub>2</sub>·6H<sub>2</sub>O (0.228 g, 1 mmol) in methanol and heated under reflux for 3 hours and kept at room temperature. The complex formed was filtered, washed thoroughly with methanol and ether and dried *in vacuo* over P<sub>4</sub>O<sub>10</sub>.

**[Ni<sub>3</sub>(Ac4Cy)<sub>2</sub>(OAc)<sub>2</sub>]·H<sub>2</sub>O (18):** To a solution of ligand H<sub>2</sub>Ac4Cy (0.473 g, 1 mmol) in CHCl<sub>3</sub> was added Ni(OAc)<sub>2</sub>·4H<sub>2</sub>O (0.248 g, 1 mmol) in methanol and heated under reflux for 4 hours and kept at room temperature. The complex formed was filtered, washed thoroughly with methanol and ether and dried *in vacuo* over P<sub>4</sub>O<sub>10</sub>.

**[Ni(H<sub>2</sub>Ac4Me)H<sub>2</sub>O]SO<sub>4</sub> (19):** To a solution of ligand H<sub>2</sub>Ac4Me (0.337 g, 1 mmol) in DMF was added NiSO<sub>4</sub>·7H<sub>2</sub>O (0.280 g, 1 mmol) in methanol and heated under reflux for 2 hours and kept at room temperature. The complex formed was filtered, washed thoroughly with methanol and ether and dried *in vacuo* over P<sub>4</sub>O<sub>10</sub>.

**[Ni<sub>3</sub>(Ac4Me)<sub>2</sub>(OAc)<sub>2</sub>]·2H<sub>2</sub>O (20):** To a solution of ligand H<sub>2</sub>Ac4Me (0.337 g, 1 mmol) in DMF was added Ni(OAc)<sub>2</sub>·4H<sub>2</sub>O (0.248 g, 1 mmol) in methanol and heated under reflux for 4 hours and kept at room temperature.

The complex formed was filtered, washed thoroughly with methanol and ether and dried *in vacuo* over P<sub>4</sub>O<sub>10</sub>.

**[Ni(HAc4Et)OAc]·CH<sub>3</sub>OH (21):** To a solution of ligand H<sub>2</sub>Ac4Et (0.365 g, 1 mmol) in CHCl<sub>3</sub> was added Ni(OAc)<sub>2</sub>·4H<sub>2</sub>O (0.248 g, 1 mmol) in methanol and heated under reflux for 3 hours and kept at room temperature. The complex formed was filtered, washed thoroughly with methanol and ether and dried *in vacuo* over P<sub>4</sub>O<sub>10</sub>.

**[Ni(H<sub>2</sub>Ac4Et)H<sub>2</sub>O]SO<sub>4</sub> (22):** To a solution of ligand H<sub>2</sub>Ac4Et (0.365 g, 1 mmol) in CHCl<sub>3</sub> was added NiSO<sub>4</sub>·7H<sub>2</sub>O (0.280 g, 1 mmol) in methanol and heated under reflux for 3 hours and kept at room temperature. The complex formed was filtered, washed thoroughly with methanol and ether and dried *in vacuo* over P<sub>4</sub>O<sub>10</sub>.

#### 5.2.4. Synthesis of Pd(II) complexes

**[Pd(Ac4Ph)H<sub>2</sub>O] (23):** To a solution of ligand H<sub>2</sub>Ac4Ph (0.461 g, 1 mmol) in DMF was added PdCl<sub>2</sub> (0.177 g, 1 mmol) in methanol and heated under reflux for 3 hours and kept at room temperature. The complex formed was filtered, washed thoroughly with methanol and ether and dried *in vacuo* over P<sub>4</sub>O<sub>10</sub>.

**[Pd(HAc4Me)Cl]·2H<sub>2</sub>O (24):** To a solution of ligand H<sub>2</sub>Ac4Me (0.337 g, 1 mmol) in DMF was added PdCl<sub>2</sub> (0.177 g, 1 mmol) in methanol and heated under reflux for 2 hours and kept at room temperature. The complex formed was filtered, washed thoroughly with methanol and ether and dried *in vacuo* over P<sub>4</sub>O<sub>10</sub>.

**[Pd(HAc4Et)Cl]·2H<sub>2</sub>O (25):** To a solution of ligand H<sub>2</sub>Ac4Et (0.365 g, 1 mmol) in CHCl<sub>3</sub> was added PdCl<sub>2</sub> (0.177 g, 1 mmol) in methanol and heated under reflux for 2 hours and kept at room temperature. The complex formed was filtered, washed thoroughly with methanol and ether and dried *in vacuo* over P<sub>4</sub>O<sub>10</sub>.

### 5.3. Physical measurements

Elemental analyses of the ligand and the complexes were done on a Vario EL III CHNS analyzer at the SAIF, Kochi, India. IR spectral analyses were done using KBr pellets on Thermo Nicolet AVATAR 370 DTGS FT-IR spectrophotometer in the 4000-400 cm<sup>-1</sup> region. The far IR spectra were recorded using polyethylene pellets in the 500-100 cm<sup>-1</sup> region on a Nicolet Magna 550 FTIR instrument at the SAIF, Indian Institute of Technology, Bombay. UVD-3500, UV-VIS Double Beam Spectrophotometer was used to record the electronic spectra from DMF solution in the range 200-900 nm. The magnetic susceptibility measurements were done in the polycrystalline state at room temperature on a Vibrating Sample Magnetometer at the Indian Institute of Technology, Roorkee, India. The molar conductivities of the complexes in dimethylformamide solutions (10<sup>-3</sup> M) at room temperature were measured using a direct reading conductivity meter.

### 5.4. Results and discussion

Reaction of equimolar ratios of the ligand and the metal salt yielded compounds of different stoichiometry for nickel and a stoichiometry of [M(HL)Cl]·2H<sub>2</sub>O for compounds **24** (L is Ac4Me) and **25** (L is Ac4Et) and a stoichiometry of [MLH<sub>2</sub>O] for compound **23** (L is Ac4Ph) of palladium. Since all the four ligands are pentadentate, their metal complexes formed were

**having six coordination.** The mode of coordination is different for all the four bis(thiosemicarbazone) ligands. In compounds **15**, **17**, **18** and **20** it coordinate as a dianionic ligand. It is very interesting to note that in compounds **16** and **21**, the ligands coordinate both as thiol form via deprotonation of the S-H group and as thione form. By elemental analyses, it is found that all the Pd(II) complexes suggest a six coordination. Pd(II) complexes generally have square planar geometry around the palladium atom, and six-coordinate complexes of Pd(II) are very rare, but has been reported with crystal structure evidences [29, 30].

Colors, partial elemental analyses, molar conductivities and magnetic susceptibilities of the Ni(II) complexes are listed in Table 5.1. Magnetic moments of the complexes were calculated from magnetic susceptibility measurements was found to be in the range 2.8-3.1 B.M. for compounds **15**, **16**, **17**, **19**, **21** and **22** which are quite normal for octahedral Ni(II) complexes. Considerable planarity for the nickel(II) centers is suggested in the case of compounds **18** and **20** by their magnetic moments and it propose a polymeric structure as indicated by the formulas. Such types of complexes are already reported [31]. Though square planar Ni(II) complexes are diamagnetic, there are reports [32] on weakly paramagnetic Ni(II) complexes with low spin. To explain this phenomenon equilibrium between spin free and spin paired configuration is suggested. The molar conductance of all the Ni(II) complexes except **19** and **22** in DMF indicate that they are essentially non-electrolytes in this solvent. The complexes containing sulfate as counter ions show conductance value is in the range that exhibited by 1:1 electrolytes in this solvent.

Table 5.1. Colors, partial elemental analyses, magnetic susceptibilities and molar conductivities of the Ni(II) complexes

Compound	Color	Composition % (Found/Calculated)			$\mu$ (B.M.)	$\chi_M$
		C	H	N		
[Ni(Ac4Ph)H <sub>2</sub> O]·CH <sub>3</sub> OH (15)	black	50.39(50.72)	4.46(4.79)	16.99(17.25)	2.8	30
[Ni(HAc4Cy)(OAc)]·C <sub>2</sub> H <sub>5</sub> OH (16)	brown	51.40(50.95)	6.47(6.81)	15.31(15.40)	3.0	27
[Ni(Ac4Cy)H <sub>2</sub> O] (17)	brown	49.98(50.37)	6.44(6.43)	18.08(17.88)	3.2	10
[Ni <sub>3</sub> (Ac4Cy) <sub>2</sub> (OAc) <sub>2</sub> ]·H <sub>2</sub> O (18)	black	47.57(47.83)	6.00(5.94)	15.51(15.62)	1.5	25
[Ni(H <sub>2</sub> Ac4Me)H <sub>2</sub> O]SO <sub>4</sub> (19)	brown	30.92(30.60)	4.40(4.15)	18.79(19.22)	2.9	77
[Ni <sub>3</sub> (Ac4Me) <sub>2</sub> (OAc) <sub>2</sub> ]·2H <sub>2</sub> O (20)	brown	35.53(35.99)	3.91(4.43)	19.65(19.59)	1.4	15
[Ni(HAc4Et)(OAc)]·CH <sub>3</sub> OH (21)	brown	42.33(42.04)	6.18(5.68)	19.42(19.06)	3.1	23
[Ni(H <sub>2</sub> Ac4Et)H <sub>2</sub> O]SO <sub>4</sub> (22)	black	33.91(33.47)	4.88(4.68)	17.74(18.21)	3.1	80

\*Molar conductivity of 10<sup>-3</sup> M DMF solution, in ohm<sup>-1</sup>cm<sup>2</sup>mol<sup>-1</sup>

Molar conductance of all the Pd(II) complexes in DMF are much lower than that observed for 1:1 electrolytes, indicate that they are essentially non-electrolytes in this solvent. Colors, partial elemental analyses, molar conductivities and of the Pd(II) complexes are listed in Table 5.2.

Table 5.2. Colors, partial elemental analyses and molar conductivities of the Pd(II) complexes

Compound	Color	Composition % (Found/Calculated)			$\Lambda_M$
		C	H	N	
[Pd(Ac4Ph)H <sub>2</sub> O] (23)	red	47.80(47.30)	3.75(3.97)	17.22(16.79)	12
[Pd(HAc4Me)Cl]·2H <sub>2</sub> O(24)	red	30.24(30.36)	4.14(4.31)	18.93(19.06)	16
[Pd(HAc4Et)Cl]·2H <sub>2</sub> O(25)	red	32.80(33.21)	4.90(4.83)	17.88(18.08)	03

\*Molar conductivity of 10<sup>-3</sup> M DMF solution, in ohm<sup>-1</sup>cm<sup>2</sup>mol<sup>-1</sup>

#### 5.4.1. Spectral characteristics of nickel complexes

##### 5.4.1a. IR spectral studies

The significant bands obtained in the vibrational spectra of the four ligands and their Ni(II) complexes and their tentative assignments are presented in Table 5.3. Coordination of the azomethine nitrogen has been proposed for the majority of thiosemicarbazone ligands with the evidence for this coordination based on a shifting of the  $\nu(\text{C}=\text{N})$  band expected for both the neutral and anionic ligands. This shifting has been reported both to higher [33, 34] and to lower energies [35, 36]. It appears that both types of shifts can occur due to the differences in energies of the bands with which  $\nu(\text{C}=\text{N})$  band is in combination [37]. The coordination of azomethine nitrogen to nickel can be confirmed by assigning the  $\nu(\text{Ni}-\text{N}_{\text{azo}})$  band at *ca.* 465 cm<sup>-1</sup> in the far IR

spectra of the complexes [38]. Coordination of pyridine nitrogen to the metal in the complexes is indicated by an increase in energy of the out-of-plane modes of the pyridine ring. The strong bands observed in the far IR spectra of the Ni(II) complexes at *ca.* 280  $\text{cm}^{-1}$  can be assigned to  $\nu(\text{Ni}-\text{N}_{\text{py}})$  of the pyridine ring [39]. The increase in  $\nu(\text{N}-\text{N})$  in the spectra of complexes is due to enhanced double bond character through chelation, thus offsetting the loss of electron density *via* donation to the metal ion, and is supportive of azomethine coordination.

In the IR spectrum of compound  $[\text{Ni}(\text{Ac}4\text{Ph})\text{H}_2\text{O}]\cdot\text{CH}_3\text{OH}$  (15) (Figure 5.1), a band at 3282  $\text{cm}^{-1}$  is assigned to coordinated water in the molecule. A medium band at *ca.* 3220  $\text{cm}^{-1}$  in the free ligand due to the  $\nu(^2\text{N}-\text{H})$  vibration disappeared in the spectrum providing strong evidence for ligand coordination around the Ni(II) ion in its deprotonated form. The azomethine band suffered a negative shift and is observed at 1580  $\text{cm}^{-1}$ . A new band at 1657  $\text{cm}^{-1}$  is assigned to  $-\text{C}=\text{N}-\text{N}=\text{C}-$  moiety. Absence of any band in the region 2600-2800  $\text{cm}^{-1}$  suggests the coordination through thiolato sulfur.

IR spectrum of compound  $[\text{Ni}(\text{HAc}4\text{Cy})\text{OAc}]\cdot\text{C}_2\text{H}_5\text{OH}$  (16) (Figure 5.2), shows bands in at *ca.* 3300  $\text{cm}^{-1}$  corresponding to  $\nu(\text{N}-\text{H})$ . The azomethine band is shifted to 1560  $\text{cm}^{-1}$  due to binding with the metal ion. Bands at 1044 and 486  $\text{cm}^{-1}$  are assigned to  $\nu(\text{N}-\text{N})$  and  $\nu(\text{Ni}-\text{N})$  respectively. The cyclohexyl stretching vibrations typical of the ligand moiety appear at 2962 and 2850  $\text{cm}^{-1}$ . Bands at 1533 and 1485  $\text{cm}^{-1}$  correspond to symmetric and asymmetric stretching vibrations of the acetate group, consistent with the presence of a monodentate acetate group in this complex [40].



---

The IR spectrum of the compound  $[\text{Ni}(\text{Ac4Cy})\text{H}_2\text{O}]$  (17), (Figure 5.3) exhibits a band at  $3220\text{ cm}^{-1}$  indicating the presence of coordinated water in the molecule. The cyclohexyl ring vibrations are seen at  $2927$  and  $2843\text{ cm}^{-1}$ . A band at  $1562\text{ cm}^{-1}$  is assigned to  $\nu(\text{C}=\text{N})$ .

In the IR spectrum of compound  $[\text{Ni}_3(\text{Ac4Cy})_2(\text{OAc})_2]\cdot\text{H}_2\text{O}$  (18) (Figure 5.4), a broad band observed at  $3403\text{ cm}^{-1}$  indicates the presence of lattice water in the molecule. A negative shift of  $\nu(\text{C}=\text{N})$  band at  $1564\text{ cm}^{-1}$  suggests the coordination through azomethine nitrogen. Bands at  $1520$  and  $1450\text{ cm}^{-1}$  indicate the presence of a monodentate acetate group in this complex.

The IR spectrum of compound  $[\text{Ni}(\text{H}_2\text{Ac4Me})\text{H}_2\text{O}]\text{SO}_4$  (19) (Figure 5.5), shows a very broad band in the range  $3000\text{-}3500\text{ cm}^{-1}$ . It is difficult to identify the  $\nu(\text{N-H})$  band at *ca*  $3200\text{ cm}^{-1}$  supporting the neutral form of the ligand during coordination. Water molecules are present in the sample by elemental analysis. This spectrum supports the coordination of ligand to metal through azomethine nitrogen atom by shifting the  $\nu(\text{C}=\text{N})$  band to lower frequency.

The IR spectrum of compound  $[\text{Ni}_3(\text{Ac4Me})_2(\text{OAc})_2]\cdot 2\text{H}_2\text{O}$  (20), reveals a broad band with low intensity around  $3470\text{ cm}^{-1}$ , which can be attributed to the presence of non-hydrogen bonded lattice water content in the sample. Bands at  $1513$  and  $1450\text{ cm}^{-1}$  correspond to symmetric and asymmetric stretching vibrations of the acetate group, consistent with the presence of a monodentate acetate group in this complex.

Table 5.3. Infrared spectral assignments ( $\text{cm}^{-1}$ ) of ligands and their Ni(II) complexes

Compound	$\nu(\text{C}=\text{N})$	$\nu/\delta(\text{C}-\text{S})$	$\nu(\text{M}-\text{N})$	$\nu(\text{N}-\text{N})$	py(ip)
$\text{H}_2\text{Ac4Ph}$	1597	1322, 808	-	1028	628
$[\text{Ni}(\text{Ac4Ph})\text{H}_2\text{O}]\cdot\text{CH}_3\text{OH}$ ( <b>15</b> )	1580	1217, 718	470	1093	693
$\text{H}_2\text{Ac4Cy}$	1596	1307, 857	-	1013	601
$[\text{Ni}(\text{HAc4Cy})(\text{OAc})]\cdot\text{C}_2\text{H}_5\text{OH}$ ( <b>16</b> )	1560	1294, 827	475	1044	630
$[\text{Ni}(\text{Ac4Cy})\text{H}_2\text{O}]$ ( <b>17</b> )	1562	1202, 721	450	1016	638
$[\text{Ni}_3(\text{Ac4Cy})_2(\text{OAc})_2]\cdot\text{H}_2\text{O}$ ( <b>18</b> )	1564	1209, 738	470	1017	635
$\text{H}_2\text{Ac4Me}$	1549	1357, 869		1045	607
$[\text{Ni}(\text{H}_2\text{Ac4Me})\text{H}_2\text{O}]\text{SO}_4$ ( <b>19</b> )	1543	1317, 820	465	1055	617
$[\text{Ni}_3(\text{Ac4Me})_2(\text{OAc})_2]\cdot 2\text{H}_2\text{O}$ ( <b>20</b> )	1540	1240, 756	450	1079	638
$\text{H}_2\text{Ac4Et}$	1541	1307, 857	-	1050	639
$[\text{Ni}(\text{HAc4Et})(\text{OAc})]\cdot\text{CH}_3\text{OH}$ ( <b>21</b> )	1538	1284, 820	470	1061	652
$[\text{Ni}(\text{H}_2\text{Ac4Et})\text{H}_2\text{O}]\text{SO}_4$ ( <b>22</b> )	1537	1297, 840	475	1086	665

Compound  $[\text{Ni}(\text{HAc}4\text{Et})\text{OAc}] \cdot \text{CH}_3\text{OH}$  (**21**) (Figure 5.6) consisting of acetate ligand, shows bands at *ca.*  $3249 \text{ cm}^{-1}$  corresponds to the  $\nu(\text{N-H})$  vibrations of the monoanionic ligand. Bands at  $1520$  and  $1450 \text{ cm}^{-1}$  indicate the presence of a monodentate acetate group in this complex

The IR spectrum of compound  $[\text{Ni}(\text{H}_2\text{Ac}4\text{Et})\text{H}_2\text{O}]\text{SO}_4$  (**22**), reveals a broad band with low intensity around  $3471 \text{ cm}^{-1}$ , which can be attributed to the presence of non-hydrogen bonded water content in the sample. A shift towards lower frequency of  $\nu(\text{C=N})$  at  $1537 \text{ cm}^{-1}$  suggests bonding through azomethine nitrogen. Since the ligand is coordinated in the neutral form, there is no considerable negative shift in the case of  $\nu(\text{C=S})$  band.



Figure 5.1. IR spectrum of compound  $[\text{Ni}(\text{Ac}4\text{Ph})\text{H}_2\text{O}] \cdot \text{CH}_3\text{OH}$  (**15**)

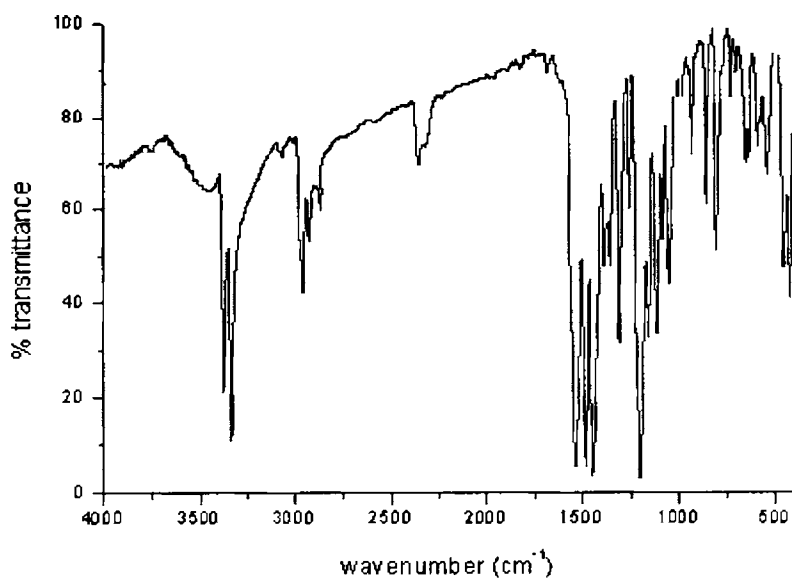


Figure 5.2. IR spectrum of compound  $[\text{Ni}(\text{HAc4Cy})\text{OAc}] \cdot \text{C}_2\text{H}_5\text{OH}$  (16)

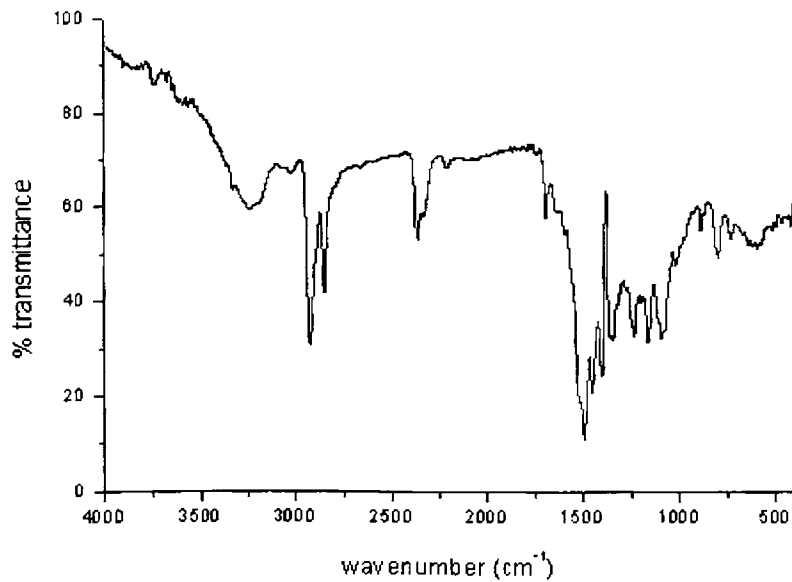


Figure 5.3. IR spectrum of compound  $[\text{Ni}(\text{Ac4Cy})\text{H}_2\text{O}]$  (17)

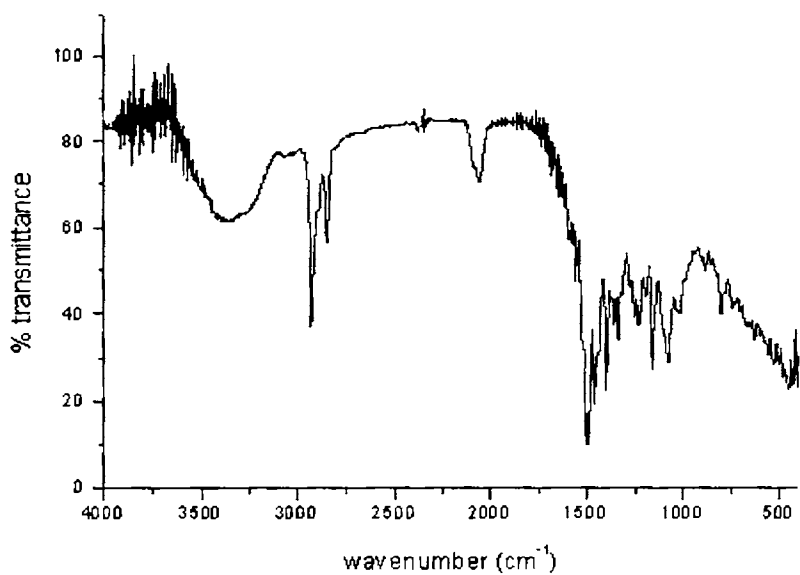


Figure 5.4. IR spectrum of compound  $[\text{Ni}_3(\text{Ac4Cy})_2(\text{OAc})_2] \cdot \text{H}_2\text{O}$  (18)

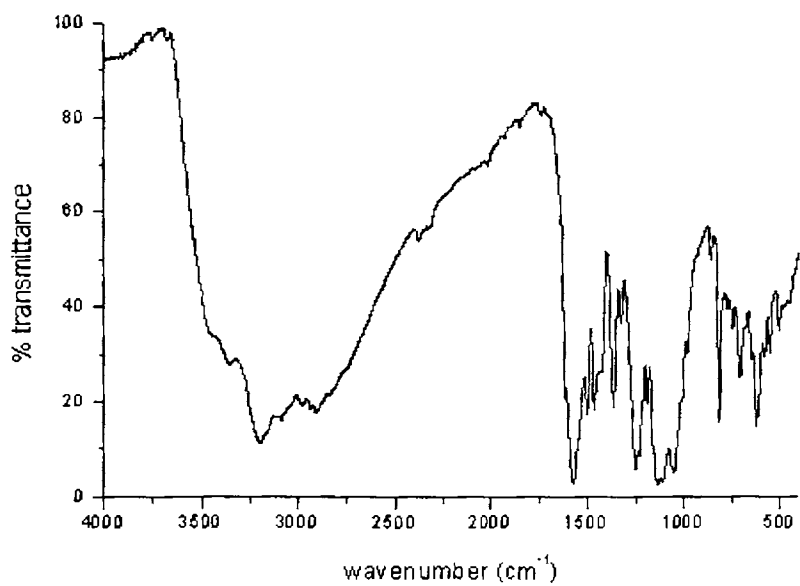


Figure 5.5. IR spectrum of compound  $[\text{Ni}(\text{H}_2\text{Ac4Me})\text{H}_2\text{O}]\text{SO}_4$  (19)

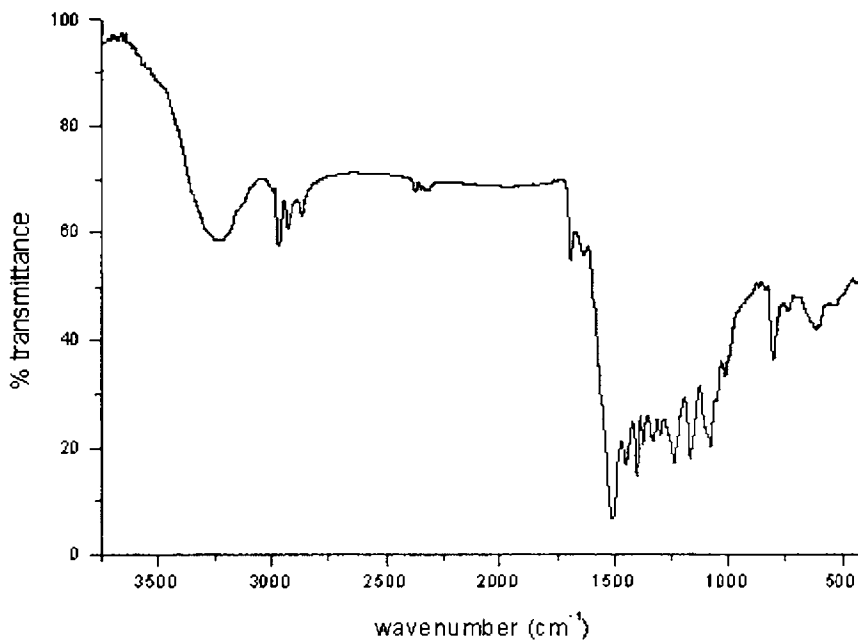


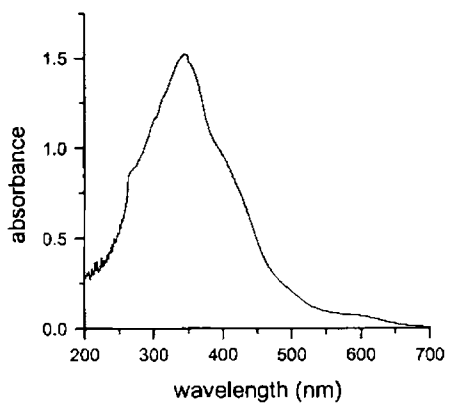
Figure 5.6. IR spectrum of compound  $[\text{Ni}(\text{HAc4Et})\text{OAc}] \cdot \text{CH}_3\text{OH}$  (**21**)

#### 5.4.1b. Electronic spectral studies

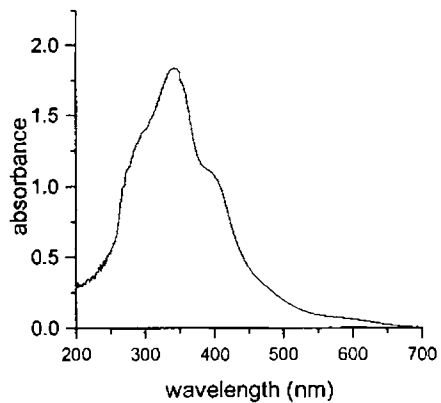
For an octahedral nickel(II) complex, three absorptions are expected *viz.*  $\nu_1$  ( $8000 - 13000 \text{ cm}^{-1}$ ) for  ${}^3\text{A}_{2g} \rightarrow {}^3\text{T}_{2g}$ ,  $\nu_2$  ( $15000 - 19000 \text{ cm}^{-1}$ ) corresponding to  ${}^3\text{A}_{2g} \rightarrow {}^3\text{T}_{1g}(\text{F})$  and  $\nu_3$  ( $25000 - 30000 \text{ cm}^{-1}$ ) assigned to  ${}^3\text{A}_{2g} \rightarrow {}^3\text{T}_{1g}(\text{P})$ . In the spectra of all the complexes the broad band appearing at *ca.*  $15,000 \text{ cm}^{-1}$  can be assigned to  ${}^3\text{A}_{2g} \rightarrow {}^3\text{T}_{1g}(\text{F})$ . This band and the charge transfer band observed at *ca.*  $25,000 \text{ cm}^{-1}$  may have masked the other two *d-d* bands (Figure 5.7). The ligand-based transitions ( $n \rightarrow \pi^*$ ,  $\pi \rightarrow \pi^*$ ) were shifted upon complexation. They were observed as a shoulder and as a sharp peak at *ca.*  $29,000$  and  $32,000 \text{ cm}^{-1}$  respectively. The absorption bands found for the complexes under study are listed in Table 5.4.

Table 5.4. Electronic spectral assignments ( $\text{cm}^{-1}$ ) for the ligands and their Ni(II) complexes

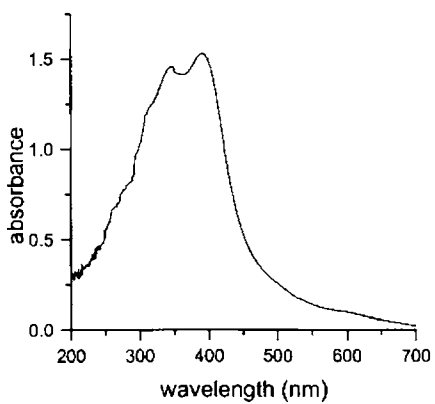
Compound	$\pi \rightarrow \pi^*$	$n \rightarrow \pi^*$	LMCT	$d-d$
$\text{H}_2\text{Ac4Ph}$	32,250	28,900	-	-
$[\text{Ni}(\text{Ac4Ph})_2(\text{H}_2\text{O}) \cdot \text{CH}_3\text{OH}]$ (15)	32,150	28,560	25,840	16,030
$\text{H}_2\text{Ac4Cy}$	32,450	29,210	-	-
$[\text{Ni}(\text{HAc4Cy})(\text{OAc})] \cdot \text{C}_2\text{H}_5\text{OH}$ (16)	32,250	29,150	24,810	16,470
$[\text{Ni}(\text{Ac4Cy})_2(\text{H}_2\text{O})]$ (17)	32,040	29,160	24,630	16,100
$[\text{Ni}_3(\text{Ac4Cy})_2(\text{OAc})_2] \cdot \text{H}_2\text{O}$ (18)	32,150	29,150	25,320	14,660
$\text{H}_2\text{Ac4Me}$	32,050	29,620	-	-
$[\text{Ni}(\text{H}_2\text{Ac4Me})_2(\text{H}_2\text{O})\text{SO}_4]$ (19)	32,000	29,330	24,120	15,970
$[\text{Ni}_3(\text{Ac4Me})_2(\text{OAc})_2] \cdot 2\text{H}_2\text{O}$ (20)	32,010	29,270	24,630	15,120
$\text{H}_2\text{Ac4Et}$	32,240	29,390	-	-
$[\text{Ni}(\text{HAc4Et})(\text{OAc})] \cdot \text{CH}_3\text{OH}$ (21)	32,120	28,740	24,900	14,160
$[\text{Ni}(\text{H}_2\text{Ac4Et})_2(\text{H}_2\text{O})\text{SO}_4]$ (22)	31,900	28,180	24,450	15,050



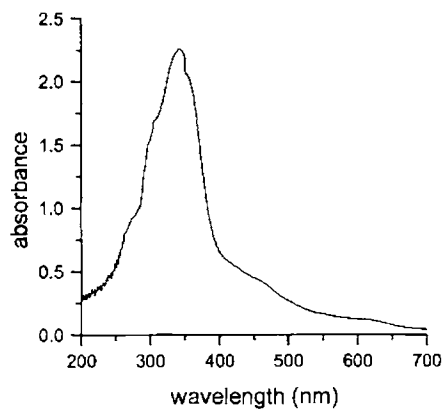
$[\text{Ni}(\text{HAc4Cy})\text{OAc}] \cdot \text{C}_2\text{H}_5\text{OH}$  (**16**)



$[\text{Ni}(\text{Ac4Cy})\text{H}_2\text{O}]$  (**17**)



$[\text{Ni}_3(\text{Ac4Cy})_2(\text{OAc})_2] \cdot \text{H}_2\text{O}$  (**18**)



$[\text{Ni}(\text{H}_2\text{Ac4Me})\text{H}_2\text{O}] \text{SO}_4$  (**19**)



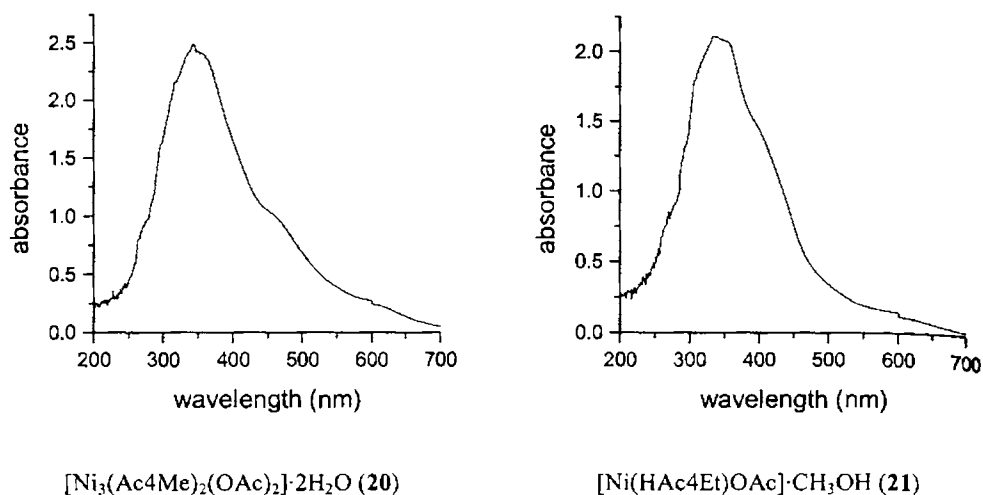


Figure 5.7. Electronic spectra of Ni(II) complexes

## 5.4.2. Spectral characteristics of palladium complexes

### 5.4.2a. IR spectral studies

The significant bands obtained in the vibrational spectra of the four ligands and their Pd(II) complexes and their tentative assignments are presented in Table 5.5.

The IR spectrum of the compound  $[\text{Pd}(\text{Ac4Ph})\text{H}_2\text{O}]$  (23) (Figure 5.8) exhibits a band at  $3284\text{ cm}^{-1}$  indicating the presence of coordinated water in the molecule. The aromatic ring vibrations occur at  $1482$  and  $1438\text{ cm}^{-1}$ .  $\nu(\text{N-H})$  vibrations are observed *ca*  $3030\text{ cm}^{-1}$ . A shift towards lower

frequency of  $\nu(\text{C}=\text{N})$  at  $1555\text{ cm}^{-1}$  suggests bonding through azomethine nitrogen.

Compound  $[\text{Pd}(\text{HAc4Me})\text{Cl}]\cdot 2\text{H}_2\text{O}$  (**24**) (Figure 5.9) consisting of chloro ligand, shows bands at *ca.*  $3333\text{ cm}^{-1}$  corresponds to the  $\nu(\text{N}-\text{H})$  vibrations of the protonated ligand. In this chloro complex (Figure 5.9a), a strong band observed at  $225\text{ cm}^{-1}$  has been assigned to the  $\nu(\text{Pd}-\text{Cl})$  band which is similar to its assignment for terminal chloro ligands in other thiosemicarbazone complexes. Broad band observed at  $3423\text{ cm}^{-1}$  corresponds to lattice water.

In the IR spectrum of compound  $[\text{Pd}(\text{HAc4Et})\text{Cl}]\cdot 2\text{H}_2\text{O}$  (**25**) (Figure 5.10), a broad band observed at  $3325\text{ cm}^{-1}$  indicates the presence of lattice water in the molecule. Band at *ca.*  $3165\text{ cm}^{-1}$  is assigned to  $\nu(\text{N}-\text{H})$  vibration. A shift towards lower frequency of  $\nu(\text{C}=\text{N})$  at  $1540\text{ cm}^{-1}$  suggests bonding through azomethine nitrogen.

Table 5.5. Infrared spectral assignments ( $\text{cm}^{-1}$ ) of ligands and their Pd(II) complexes

Compound	$\nu(\text{C}=\text{N})$	$\nu/\delta(\text{C}-\text{S})$	$\nu(\text{M}-\text{N})$	$\nu(\text{N}-\text{N})$	py(ip)
$\text{H}_2\text{Ac4Ph}$	1597	1322,808	-	1028	628
$[\text{Pd}(\text{Ac4Ph})\text{H}_2\text{O}]$ ( <b>23</b> )	1545	1210,725	480	1064	638
$\text{H}_2\text{Ac4Me}$	1549	1357,869		1045	607
$[\text{Pd}(\text{HAc4Me})\text{Cl}]\cdot 2\text{H}_2\text{O}$ ( <b>24</b> )	1541	1317,820	475	1051	617
$\text{H}_2\text{Ac4Et}$	1541	1307, 857	-	1050	639
$[\text{Pd}(\text{HAc4Et})\text{Cl}]\cdot 2\text{H}_2\text{O}$ ( <b>25</b> )	1540	1282,826	480	1071	645

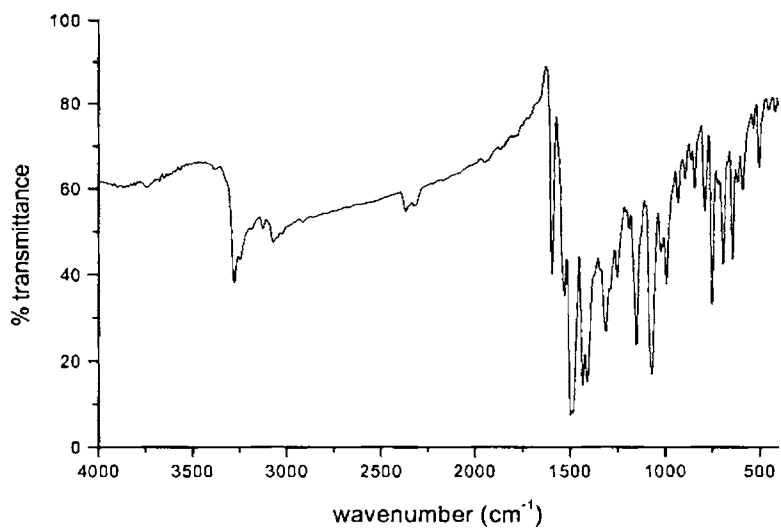


Figure 5.8. IR spectrum of compound  $[\text{Pd}(\text{Ac4Ph})\text{H}_2\text{O}]$  (**23**)

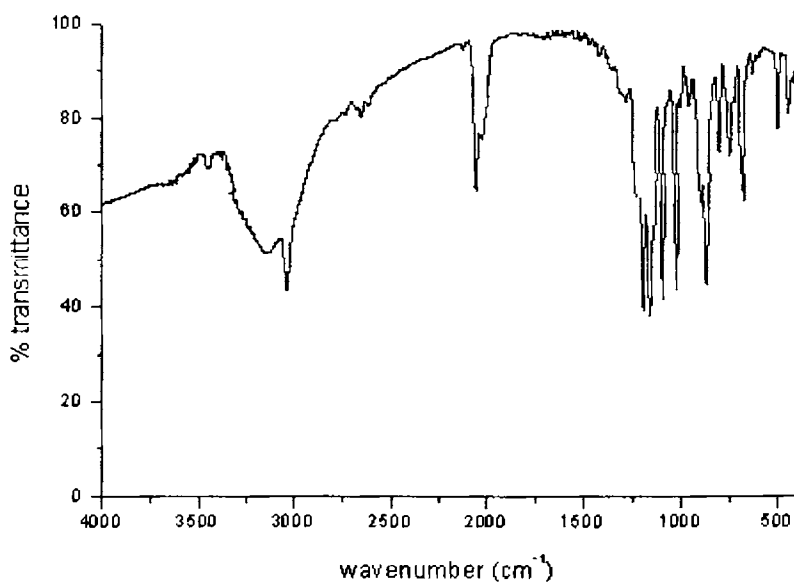


Figure 5.9. IR spectrum of compound  $[\text{Pd}(\text{HAc4Me})\text{Cl}] \cdot 2\text{H}_2\text{O}$  (**24**)

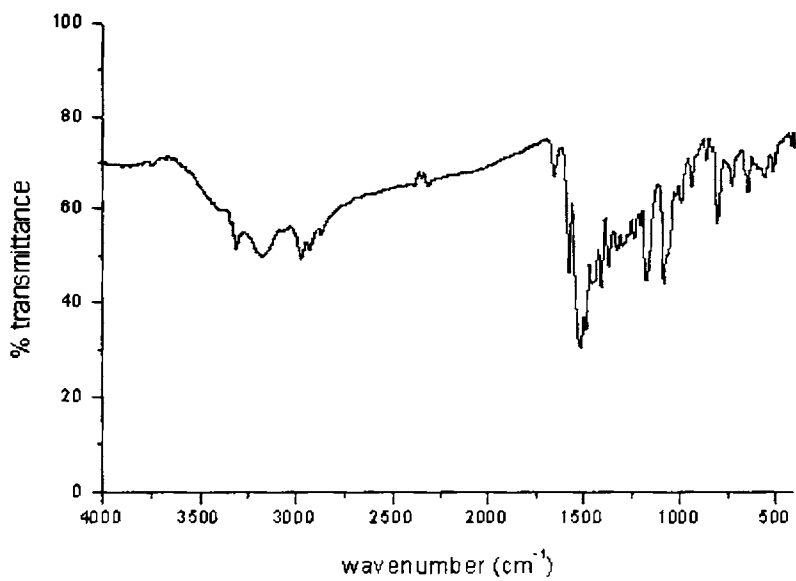


Figure 5.10. IR spectrum of compound  $[\text{Pd}(\text{HAc4Et})\text{Cl}] \cdot 2\text{H}_2\text{O}$  (25)

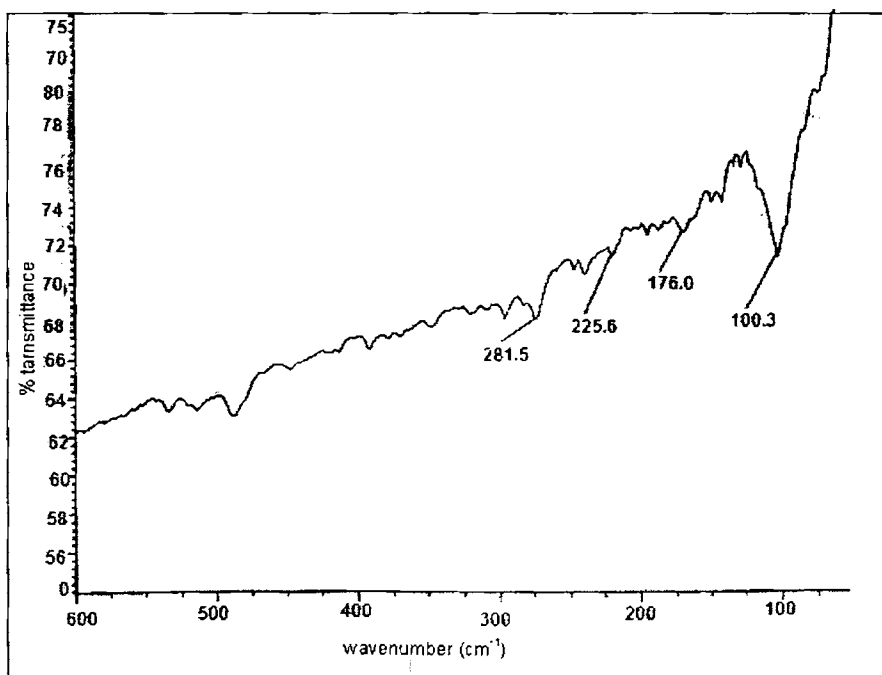


Figure 5.9a. Far IR spectrum of  $[\text{Pd}(\text{HAc4Me})\text{Cl}] \cdot 2\text{H}_2\text{O}$  (24)

### 5.4.2b. Electronic spectral studies

The electronic spectra of the bis(thiosemicarbazones) have absorption bands at *ca.* 29,000  $\text{cm}^{-1}$  due to the  $n \rightarrow \pi^*$  transition of the thiosemicarbazone moiety and at *ca.* 32,000  $\text{cm}^{-1}$  due to  $\pi \rightarrow \pi^*$  transitions. These bands suffer marginal shifts on complexation. The electronic spectra of the palladium compounds were recorded in DMF solution. The  $d-d$  bands observed were considerably weak (Figure 5.11). The electronic spectral assignments of the complexes are listed in Table 5.6.

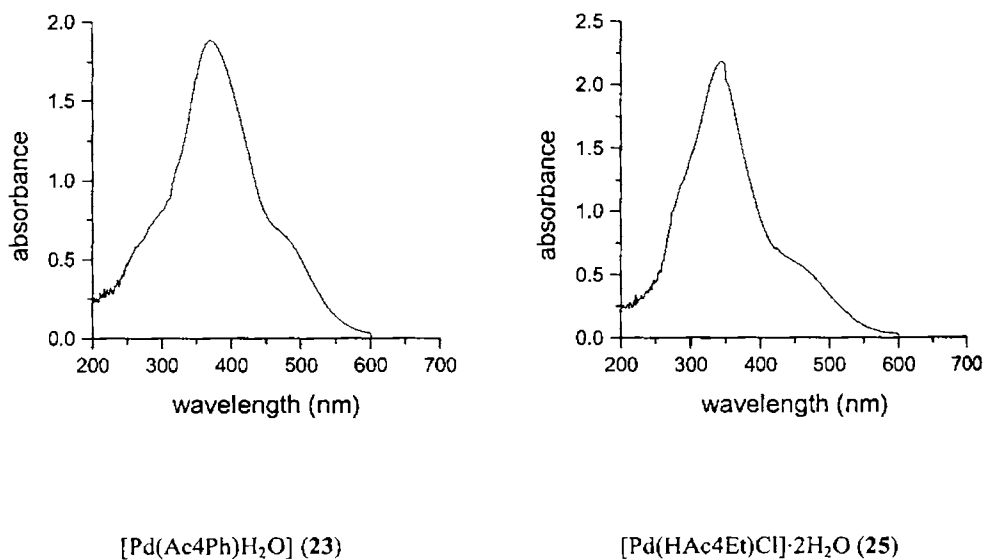


Figure 5.11. Electronic spectra of Pd(II) complexes

Table 5.6. Electronic spectral assignments ( $\text{cm}^{-1}$ ) for the ligands and their Pd(II) complexes

Compound	$\pi \rightarrow \pi^*$	$n \rightarrow \pi^*$	LMCT	$d-d$
$\text{H}_2\text{Ac4Ph}$	32,250	28,900	-	-
[Pd(Ac4Ph) $\text{H}_2\text{O}$ ] ( <b>23</b> )	32,100	28,500	20,530	15,000
$\text{H}_2\text{Ac4Me}$	32,050	29,620	-	-
[Pd(HAc4Me)Cl] $\cdot 2\text{H}_2\text{O}$ ( <b>24</b> )	32,020	29,420	22,130	14,120
$\text{H}_2\text{Ac4Et}$	32,240	29,390	-	-
[Pd(HAc4Et)Cl] $\cdot 2\text{H}_2\text{O}$ ( <b>25</b> )	32,060	29,154	21,830	16,600

#### 5.4.2c. $^1\text{H}$ NMR spectral studies

In compound **23** (Figure 5.12), the anionic coordination of the ligand is evidenced by the disappearance of a signal at 10.21 corresponding to N(3) and N(6) H. Two signals at 10.72 and 10.02 corresponds to N(4)H and N(5)H which are having different environment on coordination. A sharp singlet, which integrates as six hydrogen at  $\delta=2.53$  ppm is assigned to methyl protons attached to C(7) and C(11) which are chemically and magnetically equivalent. Aromatic protons appear at 7.21-8.60 ppm. Two doublets observed at  $\delta=7.69$  and  $\delta=7.60$  are assigned to phenyl protons C(14,16)H and C(20,22)H. Proton at C(15) and C(21) appear as doublet of a doublet at  $\delta=7.36$  ppm. There is downfield shifting of the signals for the pyridyl ring protons in the spectra of complexes compared to the uncomplexed bis(thiosemicarbazone).

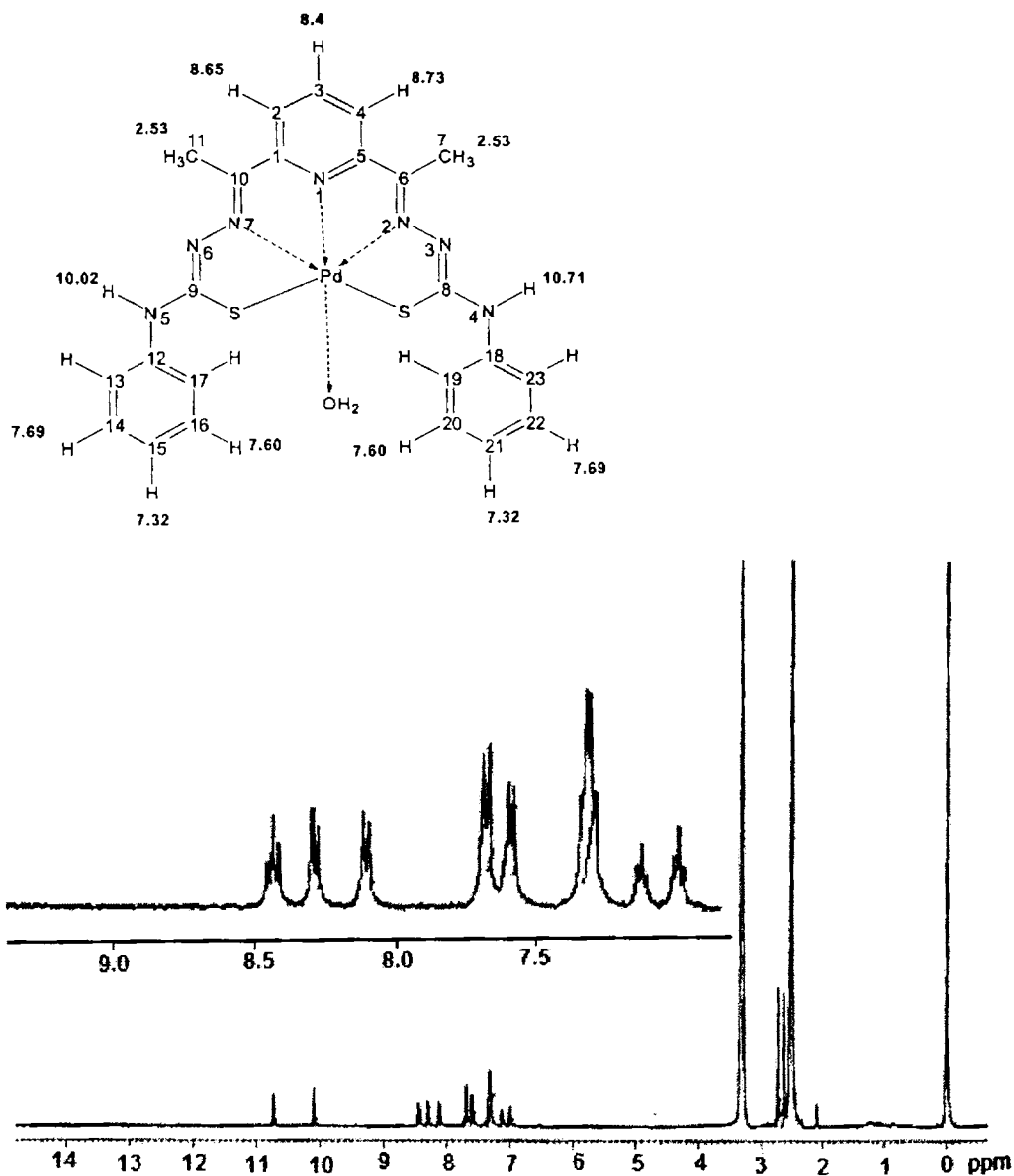


Figure 5.12. <sup>1</sup>H NMR spectrum of compound [Pd(Ac<sub>4</sub>Ph)H<sub>2</sub>O] (23)

This may be due to the loss of electron density *via* coordination of the ligand to metal centre. Two doublets observed at  $\delta=8.63$  and  $\delta=8.74$  are assigned to

C(2)H and C(4)H which are more deshielded than C(3)H which appears as a triplet at  $\delta=8.42$  ppm.

Elemental analysis of the compound **24** (Figure 5.13) suggested a partial deprotonated ligand, implying the coordination of one arm of the ligand in enolate form.

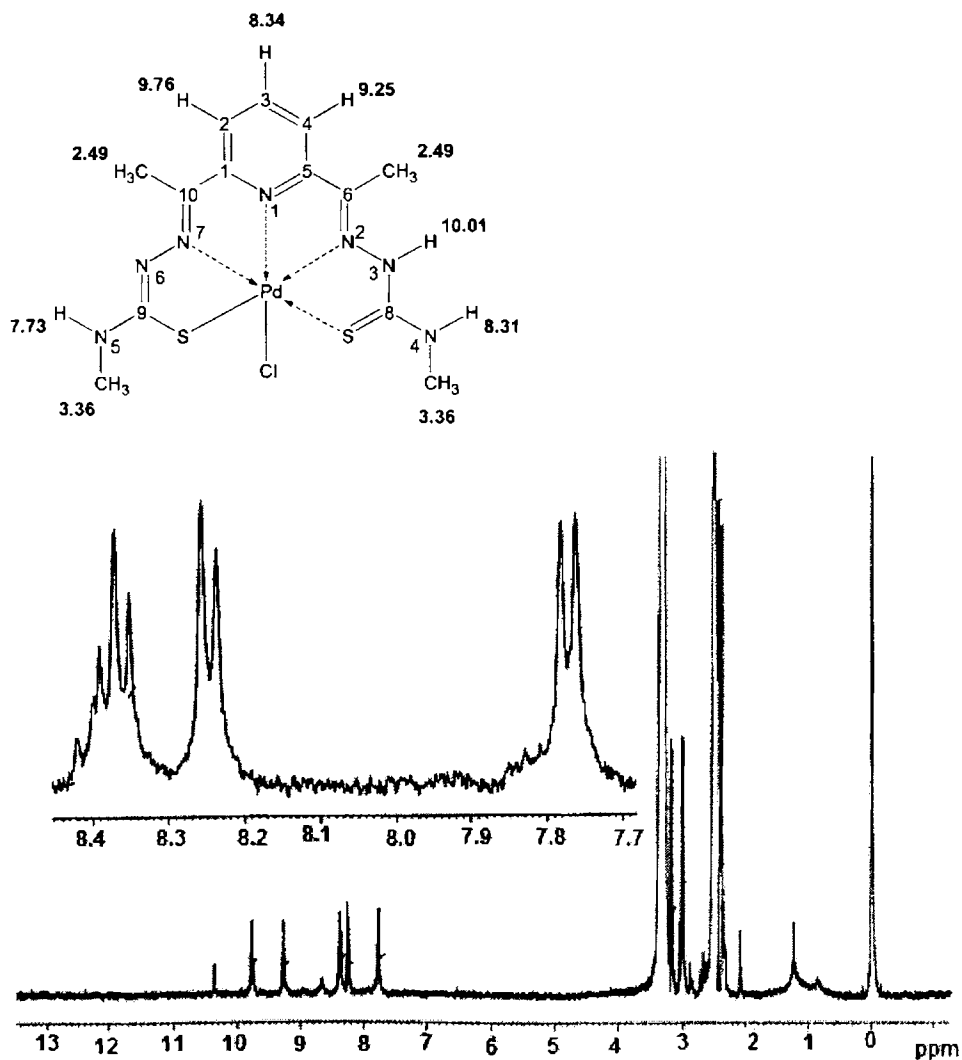


Figure 5.13. <sup>1</sup>H NMR spectrum of compound [Pd(HAc4Me)Cl]·2H<sub>2</sub>O (**24**)



A signal at  $\delta=10.01$  ppm is assigned to the proton at either N(3) or N(6). Two doublets observed at  $\delta=8.31$  and  $\delta=7.73$  are assigned to N(4) H and N(5) H. A comparison with ligand spectrum, it is observed that all the pyridyl ring protons are shifted to downfield suggesting the involvement of pyridyl nitrogen in coordination.

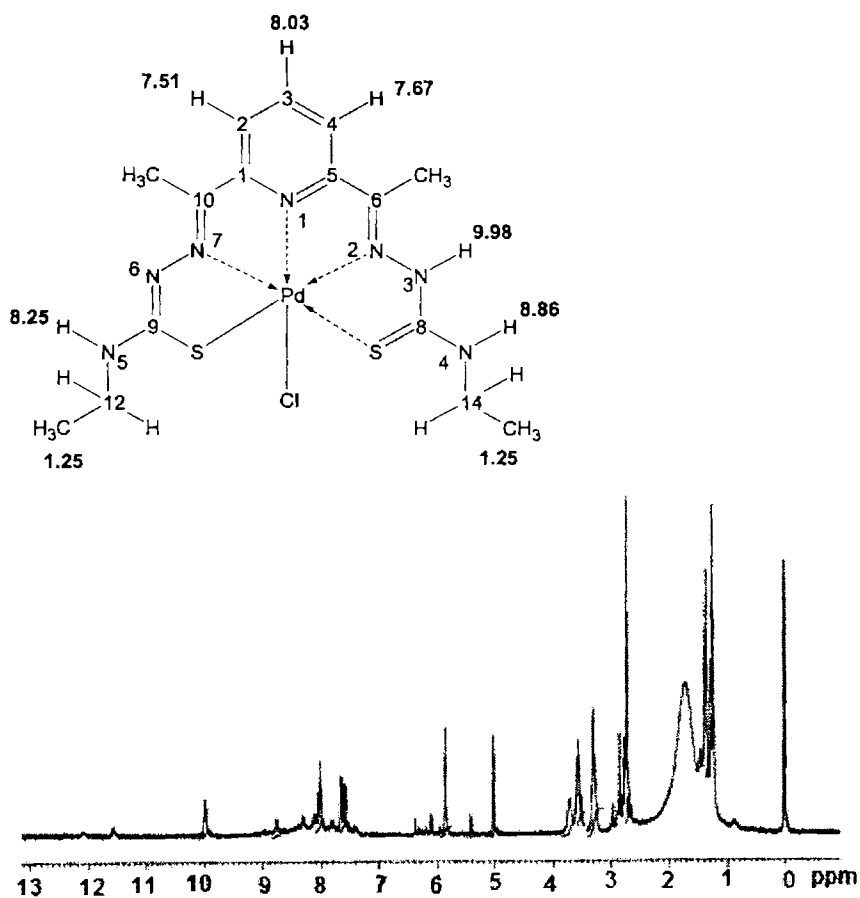


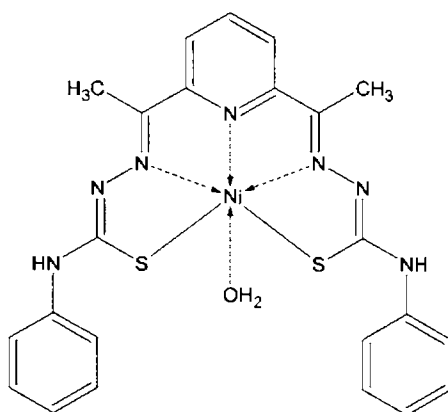
Figure 5.14. <sup>1</sup>H NMR spectrum of compound [Pd(HAc4Et)Cl]·2H<sub>2</sub>O (25)

Protons at C(2) and C(4) appear as doublets at  $\delta=9.73$  and  $\delta=9.25$ , while proton at C(3) appears as a doublet of a doublet at 8.33 ppm. A sharp singlet

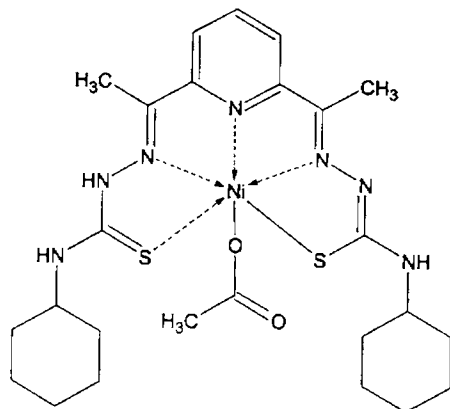
at  $\delta=2.49$  ppm is assigned to methyl protons at C(7) and C(11). Signal at  $\delta=3.36$  is assigned to methyl protons attached to N(4) and N(5).

In the spectrum of compound **25** (Figure 5.14), N(4) and N(5) protons appear at  $\delta=8.83$  and  $\delta=8.26$  ppm as triplets. Here also by elemental analysis it is observed that the ligand is coordinated by partial deprotonation, this can be proved by the appearance of a single signal at  $\delta=9.98$  ppm which corresponds to the proton attached to either N(6) or N(3). The three protons of the pyridine ring appear at  $\delta$  values 8.03 ppm for C(3)H and 7.54 ppm and 7.65 ppm for C(2)H and C(4)H. A triplet at  $\delta=1.23$  ppm is assigned to the signal corresponding to the six protons of the methyl group attached to  $-\text{CH}_2$ . The remaining aliphatic protons of two  $-\text{CH}_3$  groups and two  $-\text{CH}_2$  groups are observed as a multiplet at about 2.46-3.59 ppm where the chemical shift values are very close and hence it is very difficult to be resolved.

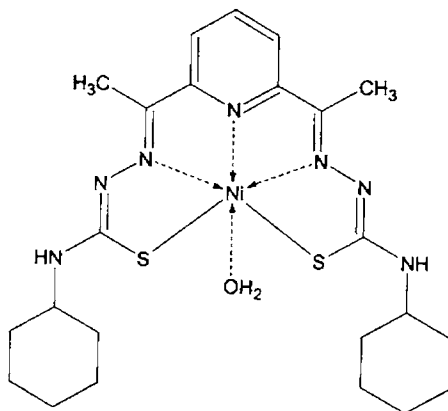
Based on the elemental analyses and spectral studies following tentative structures were assigned for the complexes. Non-coordinated solvent molecules are not included in structures for clarity.



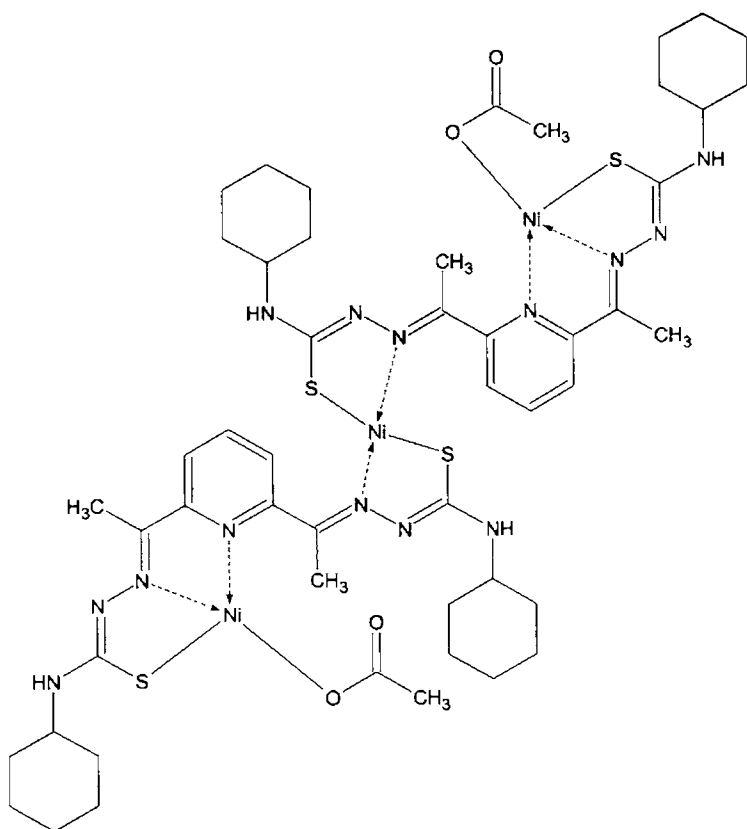
[Ni(Ac4Ph)H<sub>2</sub>O]·CH<sub>3</sub>OH (15)



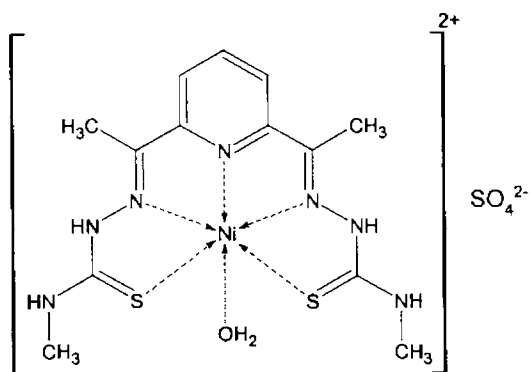
**[Ni(HAc4Cy)OAc]·C<sub>2</sub>H<sub>5</sub>OH (16)**



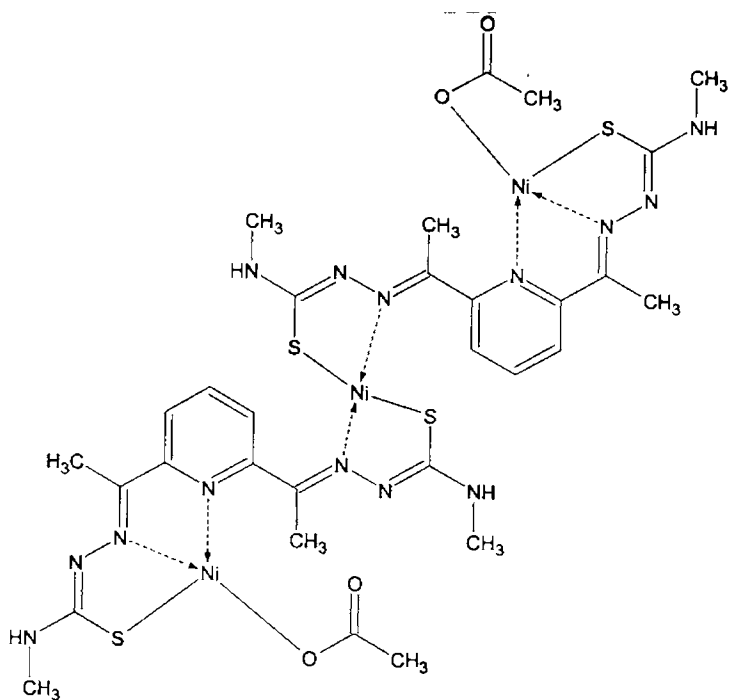
**[Ni(Ac4Cy)H<sub>2</sub>O] (17)**



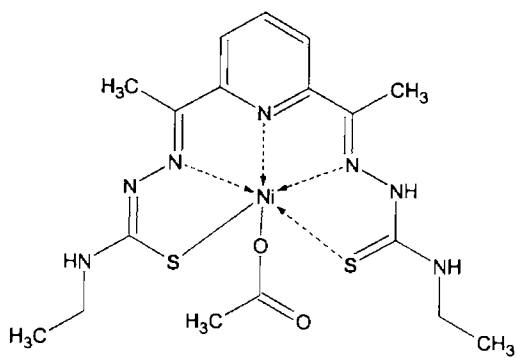
$[\text{Ni}_3(\text{Ac4Cy})_2(\text{OAc})_2] \cdot \text{H}_2\text{O}$  (18)



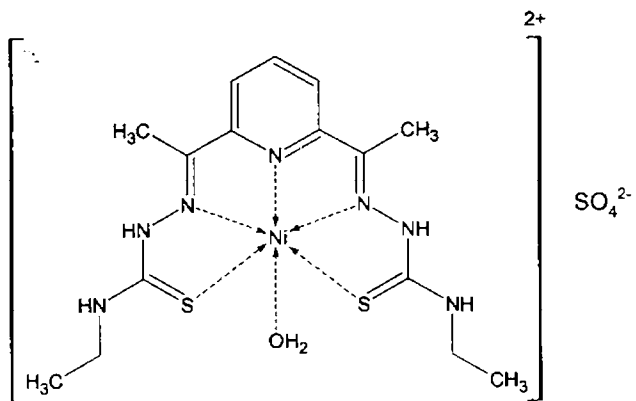
$[\text{Ni}(\text{H}_2\text{Ac4Me})\text{H}_2\text{O}]\text{SO}_4$  (19)



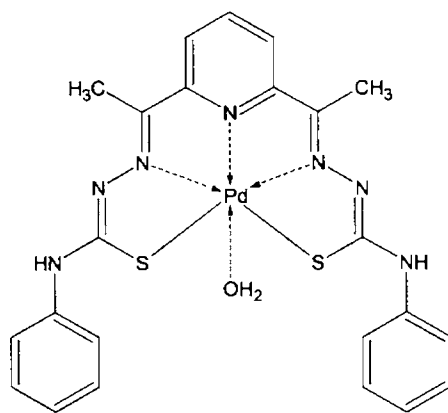
$[\text{Ni}_3(\text{Ac4Me})_2(\text{OAc})_2] \cdot 2\text{H}_2\text{O}$  (20)



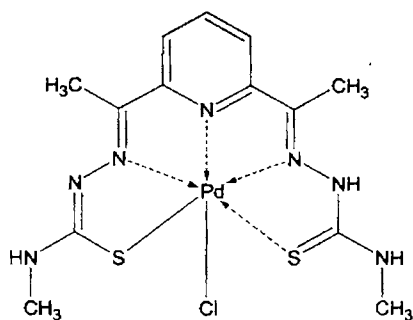
$[\text{Ni}(\text{HAc4Et})\text{OAc}] \cdot \text{CH}_3\text{OH}$  (21)



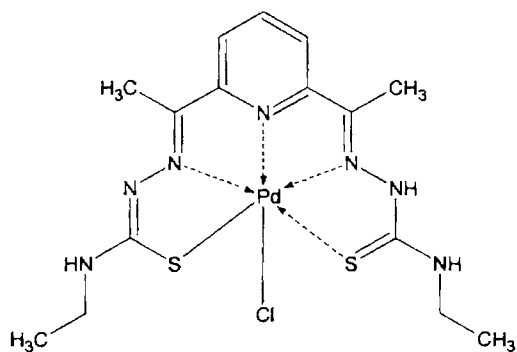
**[Ni(H<sub>2</sub>Ac<sub>4</sub>Et)H<sub>2</sub>O]SO<sub>4</sub> (22)**



**[Pd(Ac<sub>4</sub>Ph)H<sub>2</sub>O] (23)**



[Pd(HAc4Me)Cl]·2H<sub>2</sub>O (24)



[Pd(HAc4Et)Cl]·2H<sub>2</sub>O (25)

### Concluding remarks

This chapter deals with the synthesis and spectral characterization of eight nickel(II) complexes and three palladium(II) complexes of four ligands viz. 2,6-diacetylpyridine bis(*N*<sup>4</sup>-phenylthiosemicarbazone) H<sub>2</sub>Ac4Ph, 2,6-diacetylpyridine bis(*N*<sup>4</sup>-cyclohexylthiosemicarbazone) H<sub>2</sub>Ac4Cy, 2,6-diacetyl-

pyridine bis(*N*<sup>4</sup>-methylthiosemicarbazone) H<sub>2</sub>Ac4Me, 2,6-diacetylpyridine bis(*N*<sup>4</sup>-ethylthiosemicarbazone) H<sub>2</sub>Ac4Et. The nickel complexes were characterized by partial elemental analyses, molar conductivity and room temperature magnetic susceptibility measurements and IR, electronic spectral studies while the palladium complexes were characterized by partial elemental analyses, molar conductivity and IR, electronic studies and NMR studies. All the complexes are assigned a distorted octahedral geometry based on analytical data. The structures proposed in this study are tentative because of the lack of X-ray crystal structure data.

## References

1. M.J.M. Campbell, *Coord. Chem. Rev.* 15 (1975) 279.
2. V.V. Pavlishchuk, S.V. Kolotilov, A.W. Addison, R.J. Butcher, E. Sinn, *J. Chem. Soc., Dalton Trans.* (2000) 355.
3. W.P. Schammel, L. Lawrence, D.H. Busch, *Inorg. Chem.* 19 (1980) 3159.
4. M.A. Halcrow, G. Christou, *Chem. Rev.* 94 (1994) 2421.
5. W. Levason, C.A. McAuliffe, *Coord. Chem. Rev.* 12 (1974) 151.
6. H.J. Kruger, R.H. Holm, *Inorg. Chem.* 28 (1989) 1148.
7. H.J. Kruger, R.H. Holm, *Inorg. Chem.* 26 (1987) 3645.
8. M. Kumar, R.O. Day, G.J. Colpas, M.J. Maroney, *J. Am. Chem. Soc.* 111 (1989) 5974.



9. G.J. Colpas, M. Kumar, R.O. Day, M.J. Maroney, *Inorg. Chem.* 29 (1990) 4779.
10. M.A. Turner, W.L. Driessen, J. Reedijk, *Inorg. Chem.* 29 (1990) 3331.
11. S.G. Rosenfield, M.L.Y. Wong, D.W. Stephen, P.K. Mascharak, S. K. Chattopadhyay et al. *Inorg. Chem.* 26 (1987) 4119.
12. S.G. Rosenfield, W.H. Armstrong, P.K. Mascharak, *Inorg. Chem.* 26 (1986) 3014.
13. N. Baidya, M.M. Olmstead, P.K. Mascharak, *J. Am. Chem. Soc.* 114 (1992) 9666.
14. S.B. Choudhury, D. Ray, A. Chakravorty, *Inorg. Chem.* 29 (1990) 4603.
15. Z. Lu, C. White, A.L. Rheingold, R.H. Crabtree, *Inorg. Chem.* 32 (1993) 3991.
16. S. Mandal, P.K. Bharadraj, Z. Zhose, T.C.W. Mak, *Polyhedron* 14 (1995) 919.
17. J.R. Lancaster, Jr., (ed.), *The Bioinorganic Chemistry-Nickel*. VCH Publishers, New York, 1988.
18. R. Cammack, D.S. Patil, E.C. Hatchikian, V.M. Fernande, *Biochem. Biophys. Acta* 98 (1987) 912.
19. D.L. Tennent, R.D. McMillin, *J. Am. Chem. Soc.* 101 (1979) 2307.
20. V. Lum, H.B. Gray, *Isr. J. Chem.* 21 (1981) 23.

21. H.R. Engeseth, D.R. McMillin, E.L. Ulrich, *Inorg. Chim. Acta* 67 (1982) 145.
22. J.A. Blaszk, E.L. Ulrich, J.L. Markley, D.R. McMillin, *Biochemistry* 21 (1981) 6253.
23. N.C. Kasuga, K. Sekino, C. Koumo, N. Shimada, M. Ishikawa, K. Nomiya, *J. Inorg. Biochem.* 84 (2001) 55.
24. N.C. Kasuga, K. Sekino, M. Ishikawa, A. Honda, M. Yokoyama, S. Nakano, N. Shimada, C. Loumo, K. Nomiya, *J. Inorg. Biochem.* 96 (2003) 298.
25. D.X. West, S.B. Padhye, P.B. Sonawane, *Struct. Bond.* 76 (1991) 1.
26. D.X. West, J.S. Ives, G.A. Bain, A.E. Liberta, J. ValdeÂ s-MartõÂ nez, K. H. Ebert, S. HernaÂ ndez-Ortega, *Polyhedron* 16 (1997) 855.
27. H. Beraldo, D.X. West, *Trans. Met. Chem.* 22 (1997) 249.
28. H. Beraldo, L.P. Boyd, D.X. West, *Trans. Met. Chem.* 23 (1998) 67.
29. N. Takeda, D. Shimizu, N. Tokitoh, *Inorg. Chem.* 44 (2005) 8561.
30. A.L. Hector, W. Levason, M. Webster, *Inorg. Chim. Acta* 343 (2003) 90.
31. C.A. Brown, D.X. West, *Trans. Met. Chem.* 28 (2003) 154.
32. M. Mathew, G.J. Palenik, G.R. Clark, *J. Inorg. Chem.* 12 (1973) 446.
33. R. Raina, T.S. Srivastava, *Inorg. Chim. Acta* 67 (1982) 83.

34. S. Chandra, B.B. Kaul, K.B. Pandeya, R.P. Singh, *J. Inorg. Nucl. Chem.* 39 (1977) 2079.
35. M. Mohan, Manmohan, *Synth. React. Inorg. Met-Org. Chem.* 12 (1982) 761.
36. B.B. Mahapatra, S.K. Pujari, *Ind. J. Chem.* 12 (1982) 761.
37. D.X. West, J.P. Scovill, J.V. Silverton, A. Bavoso, *Trans. Met. Chem* 11 (1986) 123.
38. N.C. Mishra, B.B. Mohapatra, S. Guru, *J. Inorg. Nucl. Chem.* 41 (1979) 418.
39. V. Philip, V. Suni, M.R.P. Kurup, M. Nethaji, *Polyhedron* 23 (2004) 1225.
40. B.S. Garg, M.R.P. Kurup, S.K. Jain, Y.K. Bhoon, *Trans. Met. Chem.* 13 (1988) 309.

\*\*\*\*\*

# **Synthesis and spectral characterization of Zn(II) and Cd(II) complexes of bis(*N*<sup>4</sup>-substitutedthiosemicarbazones) of 2,6-diacetylpyridine**

## **6.1. Introduction**

Zinc with atomic number 30, atomic weight 65.39 and oxidation state +2 is an essential element in all living systems and play a structural role in many proteins and enzymes. Many proteins have been found to have a zinc-containing motif that serves to bind DNA embedded in their structure. It has an important role in several enzymes, both as metallo-enzyme and enzyme-activator, as well as filling a structural role [1]. Zinc(II)- sulfur interactions are of great interest in biochemical systems, due to the presence of sulfur at the active sites of several enzymes, vitamins and proteins [2]. Biologically it is the second most important transition metal. Its most vital function may be concerned with the synthesis of DNA and RNA. Zinc deficiency leads to impaired DNA synthesis, delayed wound healing and decrease in collagen synthesis [2, 3]. Surprisingly, zinc was found to have important physiological and pharmaceutical functions involving insulin-mimetic activity. Although Zn(II) ion has been revealed to have an insulin-mimetic activity, zinc complexes have never been examined. Glucose normalizing effects of zinc complexes are reported [4, 5].

Cadmium is an extremely toxic element that is naturally present in the environment and also as a result of human activities. Analysis of biosystems with cadmium ion becomes a problem of particular importance in view of the established toxic influence of this metal, associated with Hg and Pb to the

group of the most toxic environmental pollutants [6-8]. Its toxicity derives from the fact that it is rapidly localized intracellularly, mainly in the liver and then bound to metallothionein forming a complex that is slowly transferred to the blood stream to be deposited in the kidneys. This metal competes with Zn and blocks active sites of metal-enzymes and as a relatively soft acid it can dislodge Zn(II) in cysteine-coordinated zinc compounds or Ca(II) ions in bone cells. The development of chelating agents is essential for the treatment of cadmium intoxication. The ability to coordinate *via* sulphur is enhanced for cadmium (compared to zinc), whose toxic properties could be related to strong cadmium(II)-sulfur bond [9]. Moreover, chelating sulfur donors are actually under study as antidotes in cadmium(II) poisoning [10, 11]. The enhancement of antitumor activity in presence of Cd(II) [12] ions has been reported.

In view of the stability of the filled *d* sublevel ( $d^{10}$ ), the element shows few of the characteristics of transition metals despite its position in the d-block of the periodic table. It resembles other transition metals in the formation of stable complexes with O, N and S-donor ligands and with ions like cyanide, halide etc. Since the  $d^{10}$  configuration affords no crystal field stabilization, the stereochemistry of a particular compound depends on the size and polarizing power of the M(II) cation and the steric requirement of the ligands. The  $M^{2+}$  ion with its  $d^{10}$  configuration shows no stereochemical preferences arising from ligand field stabilization effects. Therefore they display a variety of coordination numbers ranging from two to six, and geometries based on the interplay of electrostatic forces, covalence and the size factor. Both Zn(II) and Cd(II) favour 4-coordinate tetrahedral complexes though Cd(II), being the larger one, forms 6-coordinate octahedral complexes more readily than does Zn(II). Coordination numbers 4, 5 and 6 are the common ones for both elements.

## 6.2. Experimental

### 6.2.1. Materials

The reagents used for the synthesis of the ligands are discussed in Chapter 2. Solvents were purified by standard methods. Zinc salts and cadmium salts used were Analar grade and used as supplied for the preparation of complexes. Solvents used were methanol, ethanol, DMF and chloroform.

### 6.2.2. Syntheses of ligands

Ligands  $\text{H}_2\text{Ac4Ph}$ ,  $\text{H}_2\text{Ac4Cy}$ ,  $\text{H}_2\text{Ac4Me}$  and  $\text{H}_2\text{Ac4Et}$  were synthesized as described previously in Chapter 2.

### 6.2.3. Synthesis of Zn(II) complexes

**$[\text{Zn}_2(\text{Ac4Ph})_2] \cdot 2\text{H}_2\text{O}$  (26):** To a solution of the ligand  $\text{H}_2\text{Ac4Ph}$  (0.461 g, 1 mmol) in DMF, zinc acetate (0.218 g, 1 mmol) in methanol was added and refluxed for 3 hours. The complex formed was filtered, washed with methanol, followed by ether and dried over  $\text{P}_4\text{O}_{10}$  *in vacuo*.

**$[\text{Zn}_2(\text{Ac4Cy})_2] \cdot \text{H}_2\text{O}$  (27):** To a solution of the ligand  $\text{H}_2\text{Ac4Cy}$  (0.473 g, 1 mmol) in  $\text{CHCl}_3$ , zinc acetate (0.218 g, 1 mmol) in methanol was added and refluxed for 4 hours. The complex formed was filtered, washed with methanol, followed by ether and dried over  $\text{P}_4\text{O}_{10}$  *in vacuo*.

**$[\text{Zn}_2(\text{Ac4Me})_2] \cdot \text{H}_2\text{O}$  (28):** To a solution of the ligand  $\text{H}_2\text{Ac4Me}$  (0.337 g, 1 mmol) in DMF, zinc acetate (0.218 g, 1 mmol) in methanol was added and refluxed for 3 hours. The complex formed was filtered, washed with methanol, followed by ether and dried over  $\text{P}_4\text{O}_{10}$  *in vacuo*.

---

**[Zn<sub>2</sub>(Ac4Et)<sub>2</sub>·H<sub>2</sub>O (29):** To a solution of the ligand H<sub>2</sub>Ac4Et (0.365 g, 1 mmol) in CHCl<sub>3</sub>, zinc acetate (0.218 g, 1 mmol) in methanol was added and refluxed for 3 hours. The complex formed was filtered, washed with methanol, followed by ether and dried over P<sub>4</sub>O<sub>10</sub> *in vacuo*.

#### 6.2.4. Synthesis of Cd(II) complexes

**[Cd(HAc4Ph)Cl]·H<sub>2</sub>O (30):** To a solution of the ligand H<sub>2</sub>Ac4Ph (0.461 g, 1 mmol) in DMF, CdCl<sub>2</sub>·2.5H<sub>2</sub>O (0.228 g, 1 mmol) in methanol was added and refluxed for 2 hours. The complex formed was filtered, washed with methanol, followed by ether and dried over P<sub>4</sub>O<sub>10</sub> *in vacuo*.

**[Cd<sub>2</sub>(Ac4Ph)<sub>2</sub>]·2H<sub>2</sub>O (31):** To a solution of the ligand H<sub>2</sub>Ac4Ph (0.461 g, 1 mmol) in DMF, Cd(CH<sub>3</sub>COO)<sub>2</sub>·2H<sub>2</sub>O (0.266 g, 0.5 mmol) in methanol was added and stirred for 3 hours. The complex formed was filtered, washed with methanol, followed by ether and dried over P<sub>4</sub>O<sub>10</sub> *in vacuo*.

**[Cd(H<sub>2</sub>Ac4Cy)Cl]Cl·H<sub>2</sub>O (32):** To a solution of the ligand H<sub>2</sub>Ac4Cy (0.473 g, 1 mmol) in CHCl<sub>3</sub>, CdCl<sub>2</sub>·2.5H<sub>2</sub>O (0.228 g, 1 mmol) in methanol was added and refluxed for 2 hours. The complex formed was filtered, washed with methanol, followed by ether and dried over P<sub>4</sub>O<sub>10</sub> *in vacuo*.

**[Cd<sub>2</sub>(Ac4Cy)<sub>2</sub>]·H<sub>2</sub>O (33):** To a solution of the ligand H<sub>2</sub>Ac4Cy (0.473 g, 1 mmol) in CHCl<sub>3</sub>, Cd(CH<sub>3</sub>COO)<sub>2</sub>·2H<sub>2</sub>O (0.266 g, 0.5 mmol) in methanol was added and stirred for 2 hours. The complex formed was filtered, washed with methanol, followed by ether and dried over P<sub>4</sub>O<sub>10</sub> *in vacuo*.

**[Cd(H<sub>2</sub>Ac4Cy)NO<sub>3</sub>]NO<sub>3</sub>·H<sub>2</sub>O (34):** To a solution of the ligand H<sub>2</sub>Ac4Cy (0.473 g, 1 mmol) in CHCl<sub>3</sub>, Cd(NO<sub>3</sub>)<sub>2</sub>·4H<sub>2</sub>O (0.310 g, 1 mmol) in

methanol was added and refluxed for 3 hours. The complex formed was filtered, washed with methanol, followed by ether and dried over  $P_4O_{10}$  *in vacuo*.

**[Cd<sub>2</sub>(Ac4Me)<sub>2</sub>]·2H<sub>2</sub>O (35):** To a solution of the ligand H<sub>2</sub>Ac4Me (0.337 g, 1 mmol) in DMF, Cd(CH<sub>3</sub>COO)<sub>2</sub>·2H<sub>2</sub>O (0.266 g, 0.5 mmol) in methanol was added and stirred for 2 hours. The complex formed was filtered, washed with methanol, followed by ether and dried over  $P_4O_{10}$  *in vacuo*.

**[Cd<sub>2</sub>(Ac4Et)<sub>2</sub>]·H<sub>2</sub>O (36):** To a solution of the ligand H<sub>2</sub>Ac4Et (0.365 g, 1 mmol) in CHCl<sub>3</sub>, Cd(CH<sub>3</sub>COO)<sub>2</sub>·2H<sub>2</sub>O (0.266 g, 0.5 mmol) in methanol was added and stirred for 3 hours. The complex formed was filtered, washed with methanol, followed by ether and dried over  $P_4O_{10}$  *in vacuo*.

**[Cd(H<sub>2</sub>Ac4Et)Br]Br (37):** To a solution of the ligand H<sub>2</sub>Ac4Et (0.365 g, 1 mmol) in CHCl<sub>3</sub>, CdBr<sub>2</sub>·4H<sub>2</sub>O (0.344 g, 1 mmol) in methanol was added and refluxed for 2 hours. The complex formed was filtered, washed with methanol, followed by ether and dried over  $P_4O_{10}$  *in vacuo*.

**[Cd(HAc4Et)Cl]·4H<sub>2</sub>O (38):** To a solution of the ligand H<sub>2</sub>Ac4Et (0.365 g, 1 mmol) in CHCl<sub>3</sub>, CdCl<sub>2</sub>·2.5H<sub>2</sub>O (0.228 g, 1 mmol) in methanol was added and refluxed for 3 hours. The complex formed was filtered, washed with methanol, followed by ether and dried over  $P_4O_{10}$  *in vacuo*.

### 6.3. Physical measurements

Elemental analyses of the ligand and the complexes were done on a Vario EL III CHNS analyzer at SAIF, Kochi, India. IR spectral analyses



were done using KBr pellets on Thermo Nicolet AVATAR 370 DTGS FT-IR spectrophotometer in the 4000-400  $\text{cm}^{-1}$  region. The far IR spectra were recorded using polyethylene pellets in the 500-100  $\text{cm}^{-1}$  region on a Nicolet Magna 550 FTIR instrument at SAIF, Indian Institute of Technology, Bombay. UVD-3500, UV-VIS Double Beam Spectrophotometer was used to record the electronic spectra in DMF solution in the range 200-900 nm. NMR spectra were recorded using Bruker AMX 400 FT-NMR Spectrometer using TMS as the internal standard at Sophisticated Instruments Facility, Indian Institute of Science, Bangalore, India. The molar conductivities of the complexes in dimethylformamide solutions ( $10^{-3}$  M) at room temperature were measured using a direct reading conductivity meter.

### 6.3.1. X-ray crystallography

X-ray quality single crystals of the complex **27a** were obtained from its solution in DMF and dichloromethane in 1:1 ratio by slow evaporation over a period of 5 days. Yellow crystal of the compound **27a** having approximate dimensions of 0.22 x 0.13 x 0.02  $\text{mm}^3$  was selected and performed on a Bruker Smart Apex CCD diffractometer equipped with fine-focused sealed tube at the Analytical Sciences Division, Central Salt & Marine Chemicals Research Institute, Gujarat. The unit cell parameters were determined and the data collections were performed using a graphite-monochromated Mo  $K\alpha$  ( $\lambda = 0.71073 \text{ \AA}$ ) radiation. The trial structure was obtained by direct methods [13] using SHELXS-97, which revealed the position of all non-hydrogen atoms and refined by full-matrix least squares on  $F^2$  (SHELXL-97) [14] and hydrogen atoms were geometrically fixed at calculated positions. The graphics tools used include MERCURY, ORTEP and PLATON [15]. The crystallographic data and structure refinement parameters for the complex **27a** are given in Table 6.1.

Table 6.1. Crystal data and experimental parameters of compound 27a

Empirical formula	C <sub>116</sub> H <sub>188</sub> N <sub>36</sub> O <sub>8</sub> S <sub>8</sub> Zn <sub>4</sub>
Formula weight	2733.126
Temperature	293(2) K
Wavelength	0.71073 Å
Crystal system	Monoclinic
Space group	C2/c
Unit cell dimensions	a = 21.493(2) b = 21.850(2) Å c = 29.190(3) Å α = 93.652(2)° β = 93.652(2)° γ = 90.00°
Volume	13680(2) Å <sup>3</sup>
Z	4
Density (calculated)	1.3079(2)g/cm <sup>3</sup>
Absorption coefficient	0.880 mm <sup>-1</sup>
F(000)	5648
Crystal size	0.22 x 0.13 x 0.02 mm <sup>3</sup>
θ range for data collection	1.33 to 28.37 °
Index ranges	-27 ≤ h ≤ 28, -18 ≤ k ≤ 28, -38 ≤ l ≤ 35
Reflections collected	15655
Refinement method	Full-matrix on F <sub>o</sub> <sup>2</sup>
Data / restraints/parameters	1.108 -
Goodness-of-fit on F <sup>2</sup>	
Final R indices	1.107
[I > 2σ(I)]	R1 = 0.1702, wR2 = 0.2503
R indices (all data)	R1 = 0.1141, wR2 = 0.2253

#### 6.4. Results and discussion

Reaction of equimolar ratios of the ligand 2,6-diacetylpyridine bis(thiosemicarbazone) and the metal salt yielded metal complexes. The

related bis(thiosemicarbazone) ligands have been found to react with metal salts forming complexes containing both protonated and deprotonated forms [16-18] of the ligand. Its reaction with cadmium(II) salts has been shown to be very interesting in that, three different types of complexes were obtained, independent of the nature of cadmium(II) salts. In compounds **30** and **38**, the ligand acts as a monoanionic one by losing one of its amide protons while in compounds **32**, **34** and **37**, the ligands coordinate in the neutral form. But in the case of the remaining four Cd(II) complexes **31**, **33**, **35** and **36**, ligands act as dianionic one and are coordinated in enolate forms and probably suggest a dimeric structure having a six coordinate geometry since five coordination is less common in the case of Cd(II) complexes. Colors, partial elemental analyses and molar conductivities of the Zn(II) and Cd(II) complexes are listed in Tables 6.2 and 6.3.

Table 6.2. Colors and partial elemental analyses of the Zn(II) complexes

Compound	Color	Composition % (Found/Calculated)		
		C	H	N
$[\text{Zn}_2(\text{Ac4Ph})_2] \cdot 2\text{H}_2\text{O}$ ( <b>26</b> )	yellow	50.95(50.87)	4.55(4.27)	18.84(18.06)
$[\text{Zn}_2(\text{Ac4Cy})_2] \cdot \text{H}_2\text{O}$ ( <b>27</b> )	yellow	50.78(50.59)	6.57(6.28)	17.90(17.95)
$[\text{Zn}_2(\text{Ac4Me})_2] \cdot \text{H}_2\text{O}$ ( <b>28</b> )	yellow	37.74(38.10)	4.46(4.43)	23.90(23.92)
$[\text{Zn}_2(\text{Ac4Et})_2] \cdot \text{H}_2\text{O}$ ( <b>29</b> )	yellow	41.05(41.14)	5.24(5.06)	22.39(22.39)

Table 6.3. Colors, partial elemental analyses and molar conductivities of the Cd(II) complexes

Compound	Color	Composition % (Found/Calculated)			* $\Lambda_M$
		C	H	N	
[Cd(HAc4Ph)Cl]·H <sub>2</sub> O (30)	yellow	44.44(44.10)	3.74(3.86)	16.06(15.65)	22
[Cd <sub>2</sub> (Ac4Ph) <sub>2</sub> ]·2H <sub>2</sub> O (31)	yellow	44.95(45.43)	4.26(4.14)	16.17(16.13)	-
[Cd(H <sub>2</sub> Ac4Cy)Cl]Cl·H <sub>2</sub> O (32)	colorless	41.01(40.92)	5.27(5.52)	14.38(14.52)	75
[Cd <sub>2</sub> (Ac4Cy) <sub>2</sub> ]·H <sub>2</sub> O (33)	yellow	46.29(46.58)	5.97(5.78)	16.35(16.53)	-
[Cd(H <sub>2</sub> Ac4Cy)NO <sub>3</sub> ]NO <sub>3</sub> ·H <sub>2</sub> O (34)	yellow	37.77(37.94)	5.69(5.12)	17.90(17.31)	86
[Cd <sub>2</sub> (Ac4Me) <sub>2</sub> ]·2H <sub>2</sub> O (35)	yellow	32.64(32.88)	3.88(4.24)	20.46(20.65)	-
[Cd <sub>2</sub> (Ac4Et) <sub>2</sub> ]·H <sub>2</sub> O (36)	yellow	37.05(37.15)	4.54(4.57)	19.97(20.22)	-
[Cd(H <sub>2</sub> Ac4Et)Br]Br (37)	colorless	27.91(28.25)	3.71(3.64)	15.18(15.37)	73
[Cd(HAc4Et)Cl]·4H <sub>2</sub> O (38)	colorless	30.89(30.83)	5.50(5.17)	17.02(16.78)	29

\*Molar conductivity of 10<sup>-3</sup> M DMF solution, in ohm<sup>-1</sup>cm<sup>2</sup>mol<sup>-1</sup>

In the solid state, the Schiff base ligand remains in the thioketo tautomeric form but, in solution and in the presence of zinc(II) ion, it is quickly converted to the thiol form with the concomitant formation of a novel dimeric zinc(II) complex in the case of compound **27**, containing the deprotonated thiolate form of the ligand. In all the other cases also the ligand is coordinated in its deprotonated form suggesting a dimeric structure. All the Zn(II) complexes and the Cd(II) complexes except **32**, **37** and **38** were found to be colored yellow. The other three Cd(II) complexes were found to be colorless. The compounds are less soluble in organic solvents such as ethanol, methanol and chloroform, but more soluble in solvents like DMSO and DMF. The molar conductivity values indicate that all the complexes except **32**, **34** and **37** are non-electrolytes, with values at high end of the non-electrolyte range [19]. All the complexes are found to be diamagnetic as expected due to the  $d^{10}$  configuration of the metal ion.

#### 6.4.1. Crystal structure of $Zn_4(Ac4Cy)_4 \cdot 4DMF$ (**27a**)

The yellow colored crystals suitable for single crystal X-ray analysis was obtained from a solution of the compound in dichloromethane and DMF (1:1 v/v) mixture. The crystal is monoclinic in nature with  $C2/c$  symmetry and having a stoichiometry of  $Zn_4(Ac4Cy)_4 \cdot 4DMF$  (Figure 6.1). A summary of the key crystallographic information is given in Table 6.1. Selected bond lengths and bond angles are listed in Table 6.4.

The compound crystallizes in a monoclinic lattice with space group  $C2/c$ . Two dimers are present in one asymmetric unit and one unit cell contains 4 molecules. Each Zn atom in the dinuclear complex is coordinated to two sulfur and two nitrogen atoms from two different, fully deprotonated, ligand molecules.

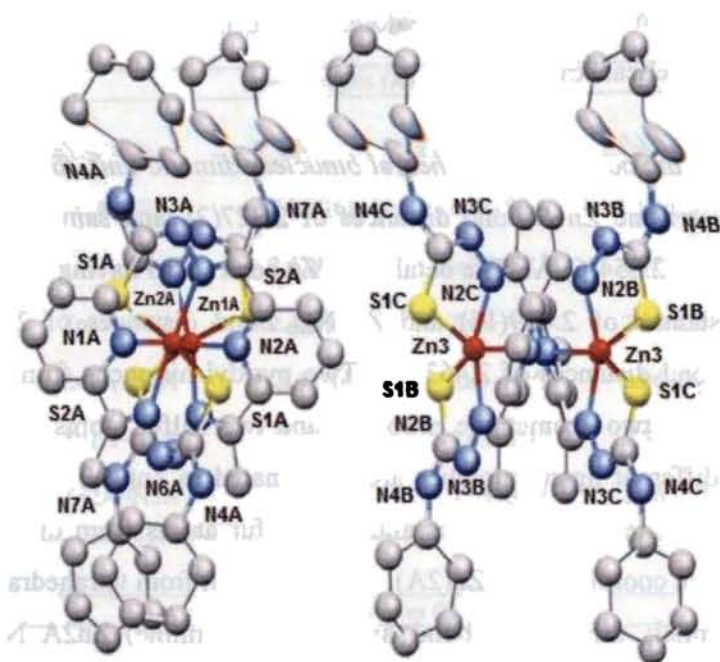


Figure 6.1. Molecular structure of  $Zn_4(Ac_4Cy)_4 \cdot 4DMF$  Hydrogen atoms and solvent molecules are omitted for clarity

Two dimers are entirely different and in each unit one of the Zn atoms Zn(1A) is coordinated to two sulfur and four nitrogen atoms in a distorted octahedron and Zn(2A) is coordinated to two sulfur and two nitrogens in a tetrahedral geometry while in other unit both of the Zn atoms are coordinated in similar way. This structure shows both zinc atoms adopting five-coordinate square pyramid geometry with a [SNNNS] donor environment, *via* the pyridine nitrogen atom, both imine nitrogen atoms and both thiolato sulphur atoms. Each ligand thread uses one imine nitrogen atom and one thiolato sulphur atom to bind each zinc centre. A rotation around the C–C bond adjacent to the pyridine ring allows the pyridine nitrogen atom of one bis(thiosemicarbazone) unit to be coordinated to a different zinc atom. A further rotation around the

symmetrical adjacent C–C bond leads to the chelation of the remaining imine nitrogen and thiolato sulphur atoms to a second metal centre, giving rise to a double helical structure.

In the octahedral-tetrahedral binuclear dimeric unit, the tetrahedral Zn center has same Zn–S bond distances of 2.327(2), and same Zn–N<sub>azo</sub> bond distances of 2.054(6) Å. The octahedral Zn centre also having the same Zn–S bond distances of 2.429(18) and Zn–N<sub>azo</sub> bond distances of 2.104(6) and Zn–N<sub>py</sub> bond distances of 2.453(6). Two pyridyl nitrogens from two ligand moieties and two azomethine nitrogens and two sulfur atoms from one arm each of different ligand moieties are coordinated to Zn(1A). The remaining two azomethine nitrogen atoms and two sulfur atoms from different ligand moieties are coordinated to Zn(2A). The distortion from tetrahedral symmetry is substantial; the largest bond angle is N5A(imine)–Zn2A–N5A(imine), 140.9(3), the S2A–Zn2A–S2A angle with the two largest donor atoms is 117.90(11), and the smallest is a chelating S2A–Zn2A–N5A(imine), 84.08(17). The smallness of the latter angle is due to the requirements of the chelating thiosemicarbazonato moiety. The chelating S–Zn–N(imine) angles are essentially the same, but the other two angles show significant differences. Differences are not surprising since in this complex the two arms are from different bis(thiosemicarbazone) ligands. The distorted octahedral geometry around the metal center is well evident from the departure of bond angles from the ideal octahedral values. The angles around the octahedral zinc center are as follows: S1A–Zn1A–S1A {108.59(10)}, S1A–Zn1A–N1A {151.06(13)}, S1A–Zn1A–N2A {81.15(17)}, N1A–Zn1A–N2A {71.10(2)} and N1A–Zn1A–N1A {90.8(3)}.

Table 6.4. Selected bond lengths (Å) and bond angles (°) for Zn<sub>4</sub>(Ac<sub>4</sub>Cy)<sub>4</sub>·4DMF (**27a**)

Bond lengths (Å)			
Zn1A–N2A	2.104(6)	Zn2A–N5A	2.054(6)
Zn1A–N2A	2.104(6)	Zn2A–S2A	2.327(2)
Zn1A–S1A	2.429(18)	Zn2A–S2A	2.327(2)
Zn1A–S1A	2.429(18)	Zn3–N2B	2.066(7)
Zn1A–N1A	2.453(6)	Zn3–N2C	2.066(6)
Zn1A–N1A	2.453(6)	Zn3–S1C	2.353(2)
Zn2A–N5A	2.054(6)	Zn3–S1B	2.360(2)
Bond angles (°)			
N2A–Zn1A–N2A	170.61(3)	N1A–Zn1A–N1A	90.8(3)
N2A–Zn1A–S1A	04.42(17)	N5A–Zn2A–N5A	140.9(3)
N2A–Zn1A–S1A	81.15(17)	N5A–Zn2A–S2A	84.08(17)
N2A–Zn1A–S1A	81.15(17)	N5A–Zn2A–S2A	116.62(17)
N2A–Zn1A–S1A	104.42(17)	N5A–Zn2A–S2A	116.62(17)
S1A–Zn1A–S1A	108.59(10)	N5A–Zn2A–S2A	84.08(17)
N2A–Zn1A–N1A	71.10(2)	S2A–Zn2A–S2A	117.90(11)
N2A–Zn1A–N1A	102.0(2)	N2B–Zn3–N2C	158.41(3)
S1A–Zn1A–N1A	86.80(14)	N2B–Zn3–S1C	08.23(19)
S1A–Zn1A–N1A	151.06(13)	N2C–Zn3–S1C	83.52(18)
N2A–Zn1A–N1A	102.00(2)	N2B–Zn3–S1B	83.38(19)
N2A–Zn1A–N1A	71.10(2)	S1C–Zn3–S1B	114.27(8)
S1A–Zn1A–N1A	86.80(14)		



In the next binuclear dimeric unit, it is observed that both the Zn centers are of similar geometry. This pentacoordinated Zn(3) has Zn–S bond distance of 2.353(2) (Zn3–S1C) and 2.360(2) (Zn3–S1B) and same Zn–N<sub>azo</sub> bond distance of 2.066(7) (Zn3–N2B and Zn3–N2C) for both centers. Two sulfur atoms and two nitrogen atoms from one arm each of different ligand moieties are coordinated to Zn(3). The fifth coordination position is occupied by the pyridyl nitrogen of one ligand and it is bridging between the two Zn atoms at a distance of 2.554 while the other pyridyl nitrogen is not coordinated to any metal. The zinc atom in this dimer has an approximately square pyramidal geometry at both centers with S1B of the one ligand moiety at the apical site. The pyridyl nitrogen N1C, the imino nitrogen N2C and the thiolato sulfur S1C from one arm of the ligand together with imino nitrogen N2B from the other arm, constitute the basal plane. In a five-coordinated system, the angular structural parameter ( $\tau$ ) is used to propose an index of trigonality. The  $\tau$  is defined by  $\tau=(\alpha-\beta)/60$ , (Where  $\tau=0$  for a square pyramidal geometry and 1 for trigonal bipyramidal geometry), and  $\alpha$  and  $\beta$  are the trans angles [17]. The value of  $\tau$  for this compound is 0.095, indicates that the coordination geometry around Zn(II) is best described as square pyramid with a basal plane containing the four donor atoms N1C, N2C, S1C and N2B and the apical position is occupied by thiolato sulfur S1B.

The packing diagram of the compound is given in Figure 6.2. The basic unit consisted of four molecules, two sets with each consisting of two dimers in the asymmetric unit. Each set of two molecules was arranged on an off-set fashion, and this whole unit of four molecules is repeated one dimensionally in the lattice. The assemblage of molecules in the respective manner within the unit cell is resulted by the diverse  $\pi$ - $\pi$  stacking, C–H $\cdots$  $\pi$  and hydrogen bonding interactions depicted in Table 6.5. The centroid Cg(5) is involved in  $\pi$ - $\pi$  interactions with pyridyl ring of the one ligand unit at a

distance of 3.7119 Å. However, some C–H $\cdots$  $\pi$  interactions, which are rather short are observed. They are C(32S)–H(32S) $\cdots$ Cg(5)<sup>i</sup> [Cg(5): Zn2A,S(2A), C(16A), N(6A), N(5A);  $d_{\text{C(32S)}\cdots\text{Cg}}=2.83$  Å;  $i = x, y, z$ ] and C(32S)–H(32S) $\cdots$ Cg(6)<sup>i</sup> [Cg(6): Zn(2A), S(2A), C(16A), N(6A<sub>a</sub>), N(5A<sub>a</sub>);  $d_{\text{C(32S)}\cdots\text{Cg}} = 2.83$  Å;  $i = 1-x, y, \frac{1}{2}-z$ ]. The presence of the water molecule and the DMF molecule leads to an extensive packing interconnecting the adjacent layers. The intramolecular and intermolecular hydrogen bonding interactions found are listed in Table 6.5.

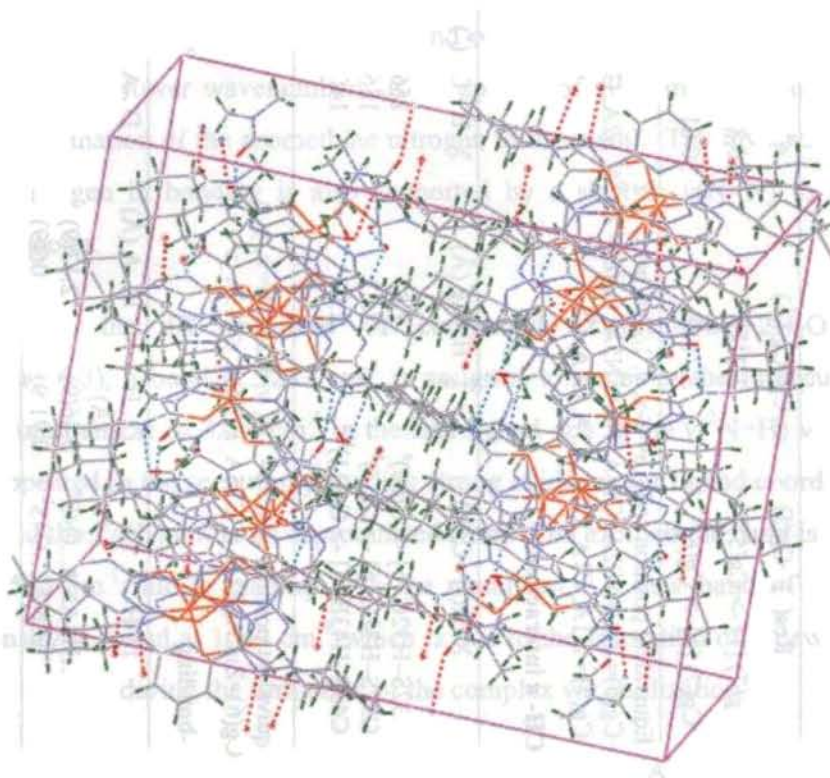


Figure 6.2. Packing diagram of  $\text{Zn}_4(\text{Ac}_4\text{Cy})_4 \cdot 4\text{DMF}$

Table 6.5. Interaction parameters of the compound 27a

$\pi$ - $\pi$  interactions

Cg(I)-Res(1)···Cg(J)	Cg-Cg (Å)	$\alpha^\circ$	$\beta^\circ$
Cg(7) [1] -> Cg(5) <sup>a</sup>	3.7119	30.81	20.00
Cg(7) [1] -> Cg(6) <sup>b</sup>	3.7119	30.81	20.00

Equivalent position code: a= 1-x, y, 1/2-z; b= x, y, z

Cg(5)= Zn2A, S2A, C16A, N6A, N5A; Cg(6)= Zn2A, S2A, C16A, N6A, N5A\_a;  
Cg(7)= N1A, C1A, C2A, C3A, C4A, C5A

CH- $\pi$  interactions

X-H(I)···Cg(J)	H···Cg (Å)	X-H···Cg (°)	X···Cg (Å)
C32S-H32C [6] -> Cg(6) <sup>a</sup>	2.83	156	3.7255
C32S-H32C [6] -> Cg(5) <sup>b</sup>	2.83	156	3.7255
C43S-H43B [5] -> Cg(11) <sup>b</sup>	2.97	140	3.7585

Equivalent position code: a= 1-x, y, 1/2-z; b= x, y, z

Cg(6)= Zn2A, S2A, C16A\_a, N6A\_a, N5A\_a

H-bonding

D-H...A	D...H (Å)	H...A (Å)	D...A (Å)	D-H...A (°)
N4A...H4ANA...O4S <sup>a</sup>	0.86(9)	2.13(9)	2.933(8)	155(8)
N7A...H7NA...O1S <sup>b</sup>	0.91(9)	2.06(9)	2.912(11)	157(7)

D= donor, A= acceptor,  $\alpha$  = Dihedral angle between planes I and J (°)

$\beta$  = Angle Cg(I)->Cg(J) or Cg(I)->Me vector and normal to plane I (°)

Equivalent position code: a= 1/2+x, -y+1/2, z; b= 1-x, y, 1/2-z

## 6.4.2. Spectral characteristics of zinc complexes

### 6.4.2a. IR spectral studies

The significant bands obtained in the vibrational spectra of the four ligands and their Zn(II) complexes and their tentative assignments are presented in Table 6.6. The IR spectrum of the ligand in its uncoordinated form shows bands in the 3300-3000  $\text{cm}^{-1}$  region, attributable to stretching modes of NH groups. The  $\nu(\text{C}=\text{N})$  band of thiosemicarbazones are found to be shifted to lower wavenumbers in the spectra of all complexes suggesting the coordination of the azomethine nitrogen to the metal. The involvement of this nitrogen in bonding is also supported by a shift in  $\nu(\text{N}-\text{N})$  to higher frequencies.

In the IR spectrum of compound  $[\text{Zn}_2(\text{Ac4Ph})_2]\cdot 2\text{H}_2\text{O}$  (26) (Figure 6.3), a band at 3282  $\text{cm}^{-1}$  is assigned to water in the molecule. A medium band at *ca* 3220  $\text{cm}^{-1}$  in the free ligand due to the  $\nu(^2\text{N}-\text{H})$  vibration disappeared in the spectrum providing strong evidence for ligand coordination around the Zn(II) ion in its deprotonated form. The azomethine band is shifted to 1584  $\text{cm}^{-1}$  due to binding with the metal ion. A new band of medium intensity is found at 1649  $\text{cm}^{-1}$  which is due to the formation of a new  $-\text{C}=\text{N}$  bond formed during the formation of the complex *via* enolization.

The IR spectrum of the compound  $[\text{Zn}_2(\text{Ac4Cy})_2]\cdot \text{H}_2\text{O}$  (27), (Figure 6.4) exhibits a band at 3297  $\text{cm}^{-1}$  indicating the presence of water in the molecule.  $\nu(^4\text{N}-\text{H})$  vibrations are observed at 3017  $\text{cm}^{-1}$ . The azomethine band is shifted to 1576  $\text{cm}^{-1}$  due to binding with the metal ion. The  $\nu(\text{C}=\text{S})$  band shifts to lower wavenumber and that may be due to the formation of

strong metal-sulfur bonds [20]. The cyclohexyl stretching vibrations typical of the ligand moiety appear at 2931 and 2841  $\text{cm}^{-1}$ .

Table 6.6. Infrared spectral assignments ( $\text{cm}^{-1}$ ) of ligands and their Zn(II) complexes

Compound	$\nu(\text{C}=\text{N})$	$\nu/\delta(\text{C}-\text{S})$	$\nu(\text{M}-\text{N})$	$\nu(\text{N}-\text{N})$	py(ip)
$\text{H}_2\text{Ac4Ph}$	1597	1322,808	-	1028	628
$[\text{Zn}_2(\text{Ac4Ph})_2]\cdot\text{H}_2\text{O}$ ( <b>26</b> )	1584	1229,725	415	1062	672
$\text{H}_2\text{Ac4Cy}$	1596	1307, 857	-	1013	601
$[\text{Zn}_2(\text{Ac4Cy})_2]\cdot\text{H}_2\text{O}$ ( <b>27</b> )	1576	1207,735	407	1062	638
$\text{H}_2\text{Ac4Me}$	1549	1353,869	-	1045	607
$[\text{Zn}_2(\text{Ac4Me})_2]\cdot\text{H}_2\text{O}$ ( <b>28</b> )	1534	1225,737	447	1062	622
$\text{H}_2\text{Ac4Et}$	1541	1307, 857	-	1050	639
$[\text{Zn}_2(\text{Ac4Et})_2]\cdot\text{H}_2\text{O}$ ( <b>29</b> )	1526	1205,747	415	1062	656

The IR spectrum of compound  $[\text{Zn}_2(\text{Ac4Me})_2]\cdot\text{H}_2\text{O}$  (**28**), (Figure 6.5) reveals a broad band with low intensity around 3392  $\text{cm}^{-1}$ , which can be attributed to the presence of non-hydrogen bonded lattice water content in the sample. The band at 1601  $\text{cm}^{-1}$  is assigned to the  $-\text{C}=\text{N}-\text{N}=\text{C}-$  moiety, newly formed as a result of deprotonation of the ligand for coordination. This spectrum supports the coordination of ligand to metal through azomethine nitrogen atom by shifting the  $\nu(\text{C}=\text{N})$  band to lower frequency. Band at 1062  $\text{cm}^{-1}$  is assigned to  $\nu(\text{N}-\text{N})$ .

IR spectrum of  $[\text{Zn}_2(\text{Ac4Et})_2]\cdot\text{H}_2\text{O}$  (**29**), (Figure 6.6) shows band around 3290  $\text{cm}^{-1}$  corresponds to  $\nu(^4\text{N}-\text{H})$ . A band at 3438  $\text{cm}^{-1}$  is assigned for lattice water. A shift towards lower frequency of  $\nu(\text{C}=\text{N})$  at 1526  $\text{cm}^{-1}$  suggests bonding through azomethine nitrogen. Absence of any band in the region 2600-2800  $\text{cm}^{-1}$  suggests the coordination through thiolato sulfur.

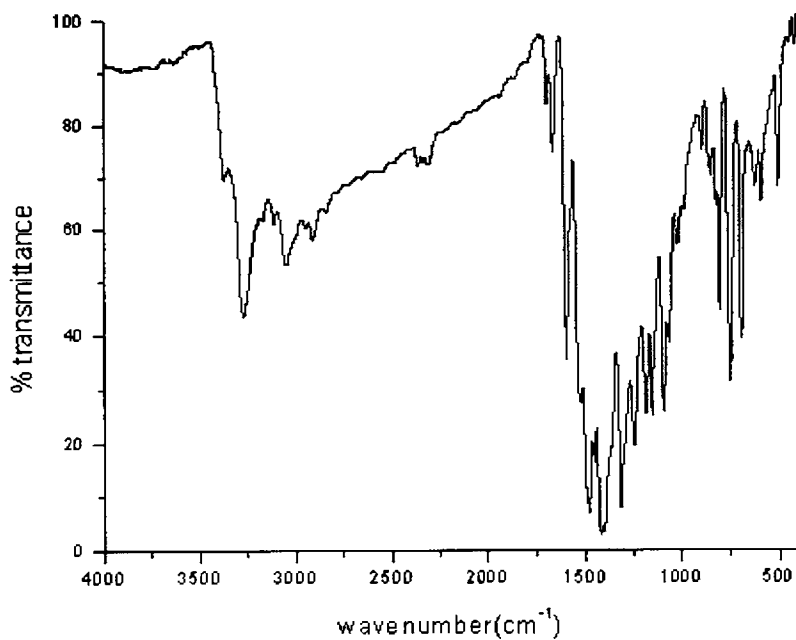


Figure 6.3. IR spectrum of compound  $[\text{Zn}_2(\text{Ac4Ph})_2] \cdot 2\text{H}_2\text{O}$  (26)

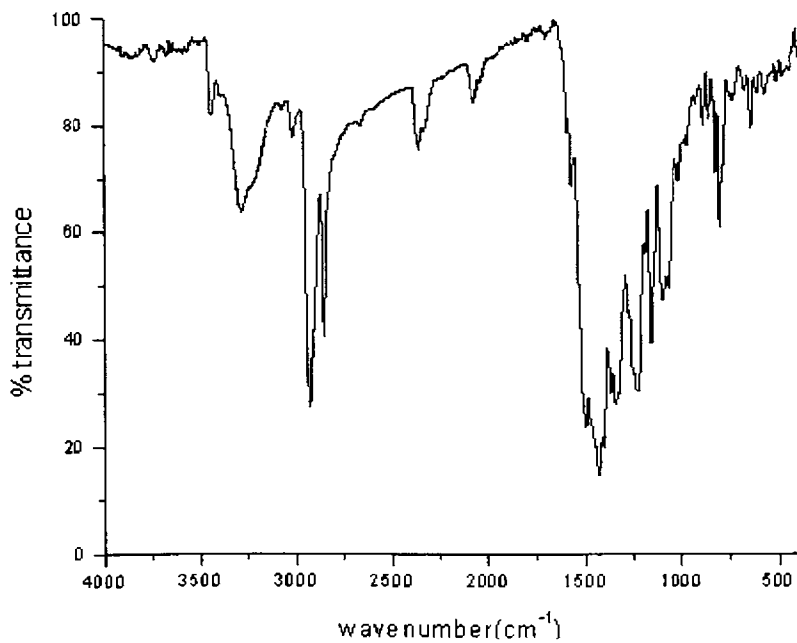


Figure 6.4. IR spectrum of compound  $[\text{Zn}_2(\text{Ac4Cy})_2] \cdot \text{H}_2\text{O}$  (27)

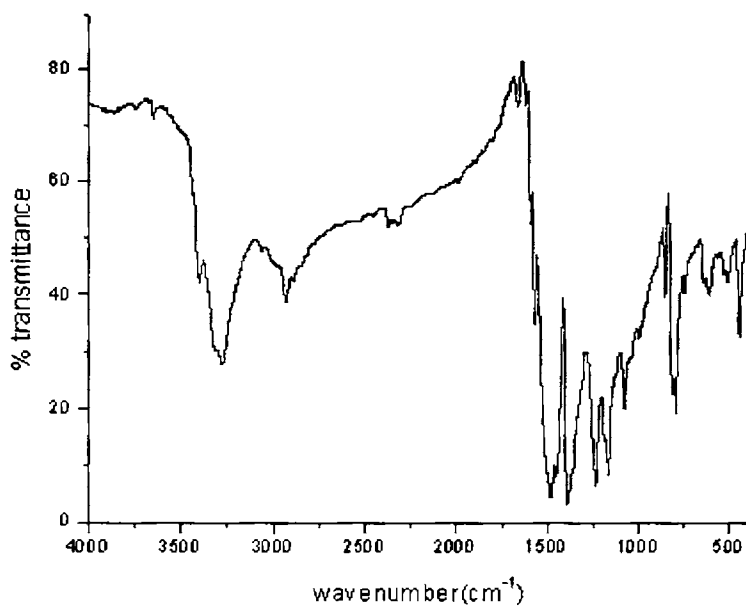


Figure 6.5. IR spectrum of compound  $[\text{Zn}_2(\text{Ac4Me})_2] \cdot \text{H}_2\text{O}$  (28)

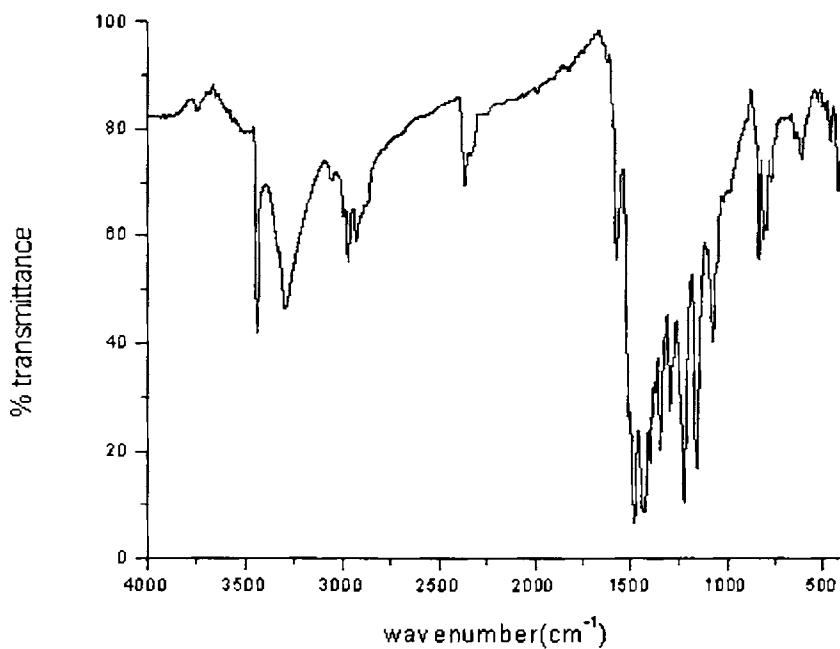


Figure 6.6. IR spectrum of compound  $[\text{Zn}_2(\text{Ac4Et})_2] \cdot \text{H}_2\text{O}$  (29)

### 6.4.2b. Electronic spectral studies

For zinc(II) systems no *d-d* transitions are expected since the d shell is completely filled (Figure 6.7). All the zinc complexes were found to be yellow in color. This color arises due to charge transfer transitions. Table 6.7 lists the various intra-ligand and charge transfer transitions in the zinc(II) complexes. Ligands show bands at  $\sim 32,340$  and  $29,190 \text{ cm}^{-1}$  attributable to the  $\pi \rightarrow \pi^*$  transitions of the phenyl ring [21-23] and  $n \rightarrow \pi^*$  transitions of the azomethine and thioamide functions respectively [24, 25]. The energy of these bands is slightly shifted on complexation. The shift showing donation of a lone pair of electrons to the metal by the coordination of azomethine nitrogen. The shift of the  $\pi \rightarrow \pi^*$  bands to longer wavelength region in complexes is the result of the C=S bond being weakened and the conjugation system enhanced on complexation [26, 27]. In addition to this intraligand band, a new band at *ca*  $24,470 \text{ cm}^{-1}$  is observed in the spectra of all Zn(II) complexes. This band can safely be assigned to Zn  $\rightarrow$  S charge transfer band.

Table 6.7. Electronic spectral assignments ( $\text{cm}^{-1}$ ) for the ligands and their Zn(II) complexes

Compound	$\pi \rightarrow \pi^*$	$n \rightarrow \pi^*$	MLCT
H <sub>2</sub> Ac4Ph	32,250	28,900	-
[Zn <sub>2</sub> (Ac4Ph) <sub>2</sub> ] $\cdot$ 2H <sub>2</sub> O ( <b>26</b> )	32,150	28,560	24,150
H <sub>2</sub> Ac4Cy	32,450	29,210	-
[Zn <sub>2</sub> (Ac4Cy) <sub>2</sub> ] $\cdot$ H <sub>2</sub> O ( <b>27</b> )	32,250	29,130	24,040
H <sub>2</sub> Ac4Me	32,050	29,620	-
[Zn <sub>2</sub> (Ac4Me) <sub>2</sub> ] $\cdot$ H <sub>2</sub> O ( <b>28</b> )	32,010	29,230	24,810
H <sub>2</sub> Ac4Et	32,240	29,390	-
[Zn <sub>2</sub> (Ac4Et) <sub>2</sub> ] $\cdot$ H <sub>2</sub> O ( <b>29</b> )	32,190	29,330	24,880



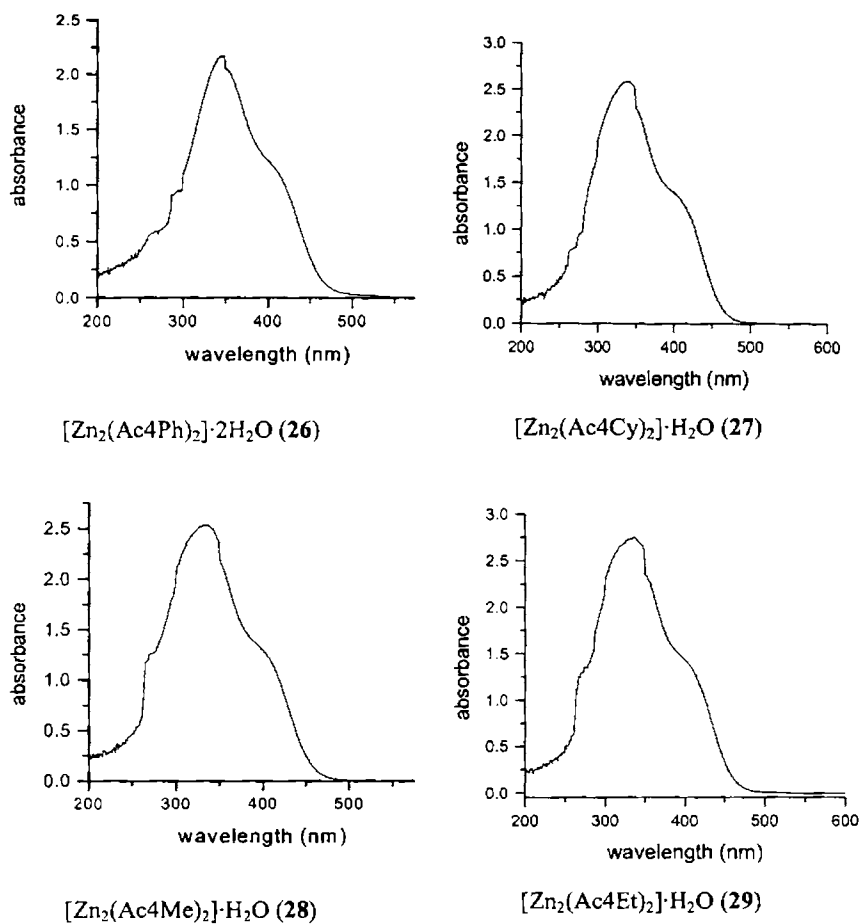


Figure 6.7. Electronic spectra of Zn(II) complexes

#### 6.4.2c. $^1\text{H}$ NMR spectral studies

The  $^1\text{H}$  NMR spectrum of compound  $[\text{Zn}_2(\text{Ac}4\text{Ph})_2] \cdot 2\text{H}_2\text{O}$  (26) (Figure 6.8) recorded in DMSO displayed a signal at 9.21 corresponds to N(4) and N(5) protons which are having same environment. The anionic coordination of the ligand is evidenced by the disappearance of a signal at 10.24 corresponding to N(3) and N(6) protons. A sharp singlet, which

integrates as six hydrogens at  $\delta=2.50$  ppm is assigned to methyl protons attached to C(7) and C(11) which are chemically and magnetically equivalent. Aromatic protons appear at 7.01-8.08 ppm. A triplet observed at 7.25 is assigned to pyridyl ring C(3)-H proton. The assignments of the remaining aromatic protons are rather difficult. There is downfield shifting of the signals for the pyridyl ring protons in the spectra of complexes compared to the uncomplexed bis(thiosemicarbazone). This may be due to the loss of electron density *via* coordination of the ligand to metal centre. In the spectrum of compound  $[\text{Zn}_2(\text{Ac}4\text{Cy})_2]\cdot\text{H}_2\text{O}$  (**27**) (Figure 6.9), a doublet observed at 7.58 ppm is assigned to protons at N(4) and N(5) which are having the same environment. Signal at  $\delta=3.36$  is assigned to methyl protons attached to N(4) and N(5). Protons attached to cyclohexyl groups appear at 1.1-3.7 ppm.

The  $^1\text{H}$  NMR spectrum of compound  $[\text{Zn}_2(\text{Ac}4\text{Me})_2]\cdot\text{H}_2\text{O}$  (**28**) and  $[\text{Zn}_2(\text{Ac}4\text{Et})_2]\cdot\text{H}_2\text{O}$  (**29**), recorded in DMSO has no signals corresponding to N(3) and N(6) protons implying the coordination of the ligand is in enolate form. Two signals at *ca* 8.43 and 8.74 corresponds to N(4) and N(5)H which are having different environment on coordination. A doublets observed at  $\delta=7.51$  is assigned to C(2)H and C(4)H protons and C(3)H proton of the pyridyl ring appear as a triplet at  $\delta=7.94$  ppm. A triplet at  $\delta=1.03$  ppm is assigned to the signal corresponding to six protons attached to  $-\text{CH}_2$ . The remaining aliphatic protons of two  $-\text{CH}_3$  groups and two  $-\text{CH}_2$  groups are observed as multiplet in the region 2.23-3.16 ppm where the chemical shift values are very close and hence it is very difficult to be resolved.

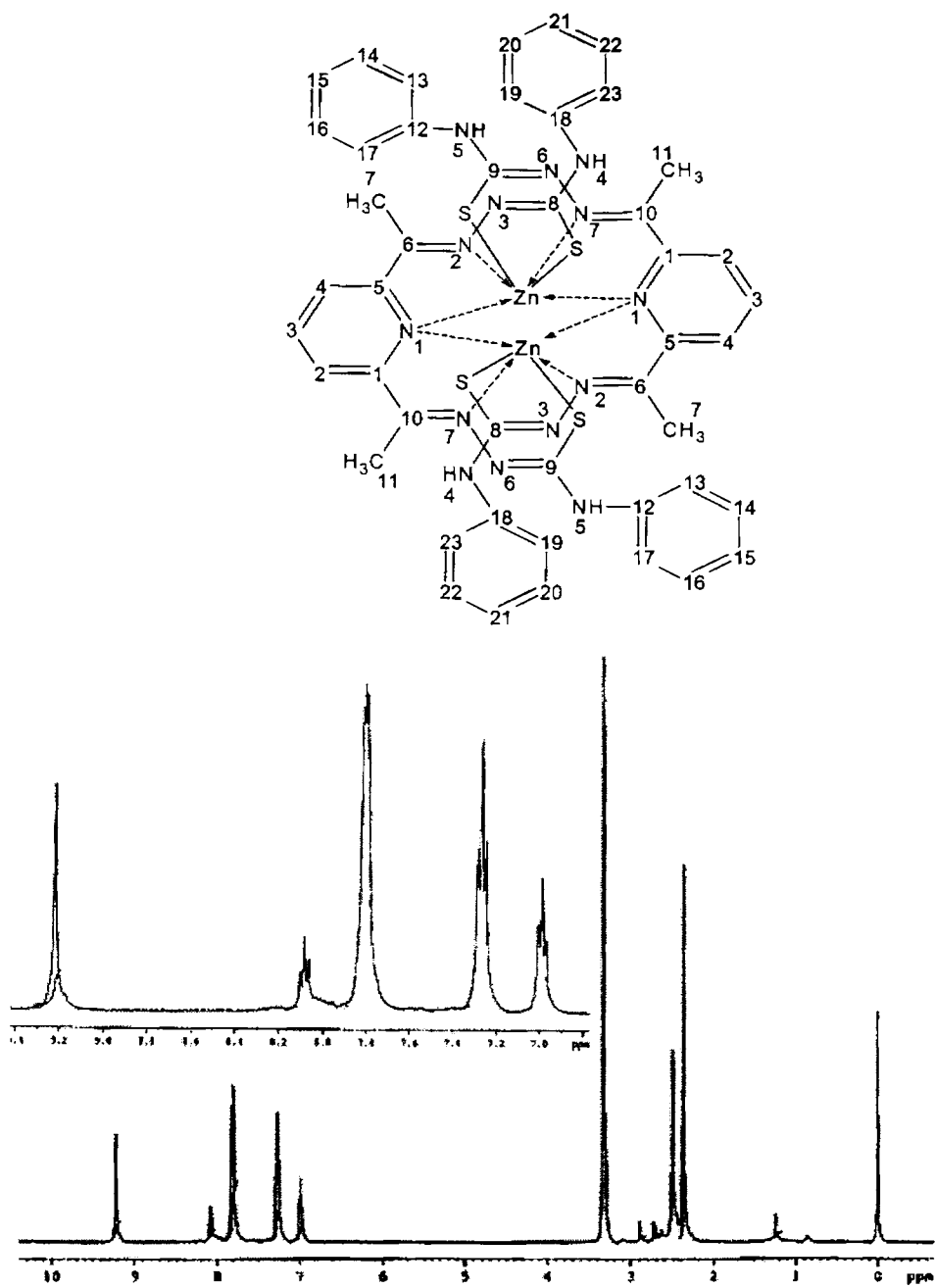


Figure 6.8.  $^1H$  NMR spectrum of compound  $[Zn_2(Ac_4Ph)_2] \cdot 2H_2O$  (26)

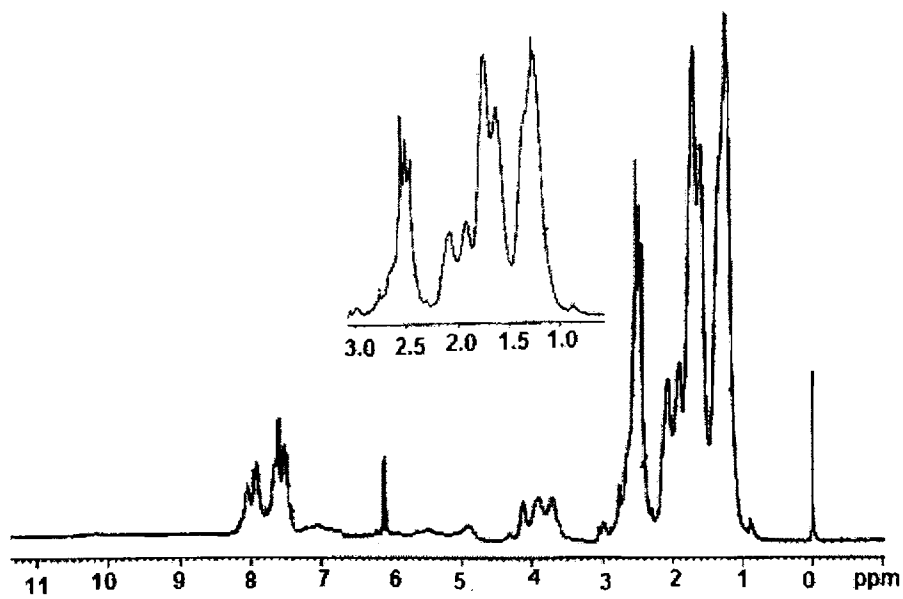
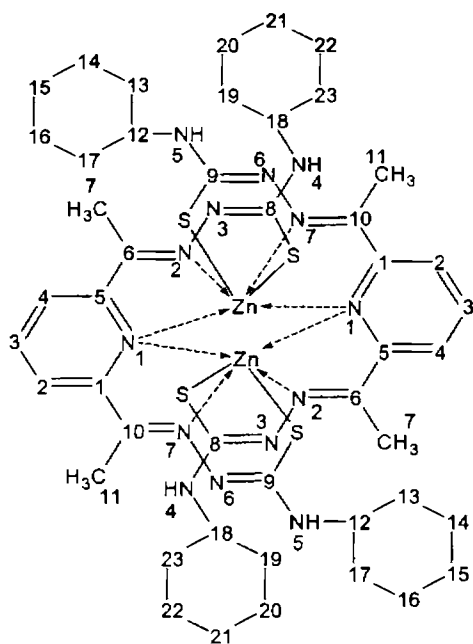


Figure 6.9.  $^1\text{H}$  NMR spectrum of compound  $[\text{Zn}_2(\text{Ac}_4\text{Cy})_2]\cdot\text{H}_2\text{O}$  (27)

### 6.4.3. Spectral characteristics of cadmium complexes

#### 6.4.3a. IR spectral studies

The significant bands obtained in the vibrational spectra of the four ligands and their Cd(II) complexes and their tentative assignments are presented in Table 6.8. The IR spectrum of the ligand in its uncoordinated form shows bands in the 3300-3000  $\text{cm}^{-1}$  region, attributable to stretching modes of NH groups. The hydrate nature of most of complexes makes it difficult to observe the  $\nu(\text{N-H})$  bands due to the presence of neutral ligand, as found for similar complexes where the ligand was not completely deprotonated [28]. The bands corresponding to  $\nu(\text{C-N})$  and  $\nu(\text{C=N})$  modes appear slightly shifted in all complexes and overlapped with  $\nu(\text{C=C})$  absorptions which is indicative of coordination of the metal to the pyridine and imine nitrogen atoms. The pyridine nitrogen coordination is again evidenced by the shift of pyridine ring deformation mode from a higher to lower frequency region in all the complexes.

Compound  $[\text{Cd}(\text{HAc4Ph})\text{Cl}]\cdot\text{H}_2\text{O}$  (**30**) (Figure 6.10) consisting of chloro ligand, shows two bands at 3033 and 3168  $\text{cm}^{-1}$  corresponds to the  $\nu(^2\text{N-H})$  and  $\nu(^4\text{N-H})$  vibrations of the monoanionic ligand. A band with low intensity around 3365  $\text{cm}^{-1}$ , which can be attributed to the presence of non-hydrogen bonded lattice water content in the sample. The band at 1607  $\text{cm}^{-1}$  is assigned to the  $-\text{C=N-N=C}-$  moiety, newly formed as a result of monodeprotonation of the ligand for coordination. The azomethine band suffered a negative shift and is observed at 1568  $\text{cm}^{-1}$ .

Table 6.8. Infrared spectral assignments ( $\text{cm}^{-1}$ ) of ligands and their Cd(II) complexes

Compound	$\nu(\text{C}=\text{N})$	$\nu/\delta(\text{C}-\text{S})$	$\nu(\text{M}-\text{N})$	$\nu(\text{N}-\text{N})$	$\nu(\text{ip})$
$\text{H}_2\text{Ac4Ph}$	1597	1322,808	-	1028	628
$[\text{Cd}(\text{HAc4Ph})\text{Cl}]\cdot\text{H}_2\text{O}$ (30)	1568	1307,790	423	1062	680
$[\text{Cd}_2(\text{Ac4Ph})_2]\cdot 2\text{H}_2\text{O}$ (31)	1590	1221,725	407	1062	688
$\text{H}_2\text{Ac4Cy}$	1596	1307, 857	-	1013	601
$[\text{Cd}(\text{H}_2\text{Ac4Cy})\text{Cl}]\cdot\text{H}_2\text{O}$ (32)	1558	1290,846	415	1070	622
$[\text{Cd}_2(\text{Ac4Cy})_2]\cdot\text{H}_2\text{O}$ (33)	1558	1207,737	409	1080	638
$[\text{Cd}(\text{H}_2\text{Ac4Cy})\text{NO}_3]\cdot\text{H}_2\text{O}$ (34)	1558	1292,827	410	1052	656
$\text{H}_2\text{Ac4Me}$	1549	1353,869	-	1045	607
$[\text{Cd}_2(\text{Ac4Me})_2]\cdot 2\text{H}_2\text{O}$ (35)	1534	1250,756	407	1070	638
$\text{H}_2\text{Ac4Et}$	1541	1307, 857	-	1050	639
$[\text{Cd}_2(\text{Ac4Et})_2]\cdot\text{H}_2\text{O}$ (36)	1534	1231,753	410	1078	650
$[\text{Cd}(\text{H}_2\text{Ac4Et})\text{Br}]\cdot\text{H}_2\text{O}$ (37)	1538	1290,810	415	1086	664
$[\text{Cd}(\text{HAc4Et})\text{Cl}]\cdot 4\text{H}_2\text{O}$ (38)	1537	1285,813	410	1094	680

The IR spectrum of the compound  $[\text{Cd}_2(\text{Ac4Ph})_2]\cdot 2\text{H}_2\text{O}$  (31) (Figure 6.11) reveals a band with low intensity around  $3365\text{ cm}^{-1}$ , which can be attributed to the presence of lattice water in the sample. A band at  $3033\text{ cm}^{-1}$  is assigned to  $\nu(\text{N-H})$  vibration of the deprotonated ligand. Absence of any band in the region  $2600\text{--}2800\text{ cm}^{-1}$  suggests the coordination through thiolato sulfur. The aromatic ring vibrations occur at  $1476$  and  $1419\text{ cm}^{-1}$ .

Compound  $[\text{Cd}(\text{H}_2\text{Ac4Cy})\text{Cl}]\text{Cl}\cdot\text{H}_2\text{O}$  (32) (Figure 6.12) consisting of two chloro ligands, shows two bands at  $3039$  and  $3185\text{ cm}^{-1}$  corresponds to the  $\nu(\text{N-H})$  vibrations of the neutral ligand. A band at  $3480\text{ cm}^{-1}$  is assigned for lattice water. The cyclohexyl stretching vibrations typical of the ligand moiety appear at  $2934$  and  $2849\text{ cm}^{-1}$ . A negative shift of  $\nu(\text{C=N})$  band at  $1590\text{ cm}^{-1}$  suggests the coordination through azomethine nitrogen.

In the IR spectrum of compound  $[\text{Cd}_2(\text{Ac4Cy})_2]\cdot\text{H}_2\text{O}$  (33) (Figure 6.13), a broad band observed at  $3430\text{ cm}^{-1}$  indicates the presence of lattice water in the molecule. The cyclohexyl stretching vibrations appear at  $2919$  and  $2849\text{ cm}^{-1}$ . Absence of any band in the region  $2600\text{--}2800\text{ cm}^{-1}$  suggests the coordination through thiolato sulfur. A shift towards lower frequency of  $\nu(\text{C=N})$  at  $1558\text{ cm}^{-1}$  suggests bonding through azomethine nitrogen.

In the IR spectrum of compound  $[\text{Cd}(\text{H}_2\text{Ac4Cy})\text{NO}_3]\text{NO}_3\cdot\text{H}_2\text{O}$  (34) (Figure 6.14), a broad band observed at  $3473\text{ cm}^{-1}$  indicates the presence of lattice water in the molecule. For nitrate complexes, the unidentate and bidentate  $\text{NO}_3$  groups exhibit three NO stretching bands. The separation of two highest-frequency bands is  $115\text{ cm}^{-1}$  for unidentate complex whereas it is

186  $\text{cm}^{-1}$  for bidentate complex. Here in this complex, the three bands observed at 1478, 1362 and 1070  $\text{cm}^{-1}$  indicates the bands of the nitrate group [29]. The fact that the nitrate group is terminally bonded in this case is understood from the separation of 116  $\text{cm}^{-1}$  between the two highest frequency bands just mentioned above.

The IR spectrum of compound  $[\text{Cd}_2(\text{Ac}_4\text{Me})_2]\cdot 2\text{H}_2\text{O}$  (35), reveals a broad band with low intensity around 3457  $\text{cm}^{-1}$ , which can be attributed to the presence of non-hydrogen bonded lattice water content in the sample.

The IR spectrum of the compound  $[\text{Cd}_2(\text{Ac}_4\text{Et})_2]\cdot \text{H}_2\text{O}$  (36) (Figure 6.15), exhibits a band at 3407  $\text{cm}^{-1}$  indicating the presence of non-coordinated water in the molecule. A negative shift of  $\nu(\text{C}=\text{N})$  band at 1534  $\text{cm}^{-1}$  suggests the coordination through azomethine nitrogen.

IR spectrum of compound  $[\text{Cd}(\text{H}_2\text{Ac}_4\text{Et})\text{Br}]\text{Br}$  (37) (Figure 6.16), shows bands at 3207 and 3340  $\text{cm}^{-1}$  corresponds to  $\nu(^2\text{N}-\text{H})$  and  $\nu(^4\text{N}-\text{H})$  vibrations of the protonated ligand. The azomethine band is shifted to 1538  $\text{cm}^{-1}$  due to binding with the metal ion. Bands at 1086 and 452  $\text{cm}^{-1}$  are assigned to  $\nu(\text{N}-\text{N})$  and  $\nu(\text{Cd}-\text{N})$  respectively.

In the IR spectrum of compound  $[\text{Cd}(\text{HAc}_4\text{Et})\text{Cl}]\cdot 4\text{H}_2\text{O}$  (38), a broad band observed at *ca* 3200  $\text{cm}^{-1}$  and this is due to water molecule and the N-H group. This spectrum supports the coordination of ligand to metal through azomethine nitrogen atom by shifting the  $\nu(\text{C}=\text{N})$  band to lower frequency. Band at 1094  $\text{cm}^{-1}$  is assigned to  $\nu(\text{N}-\text{N})$ .



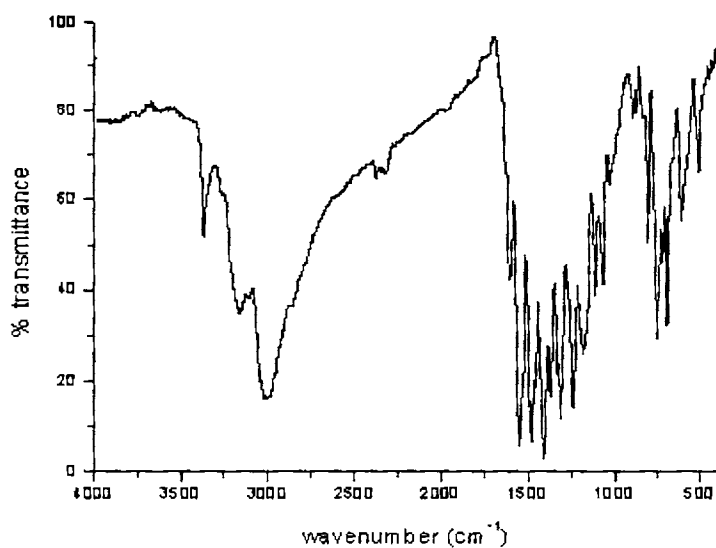


Figure 6.10. IR spectrum of compound  $[\text{Cd}(\text{HAc4Ph})\text{Cl}] \cdot \text{H}_2\text{O}$  (30)

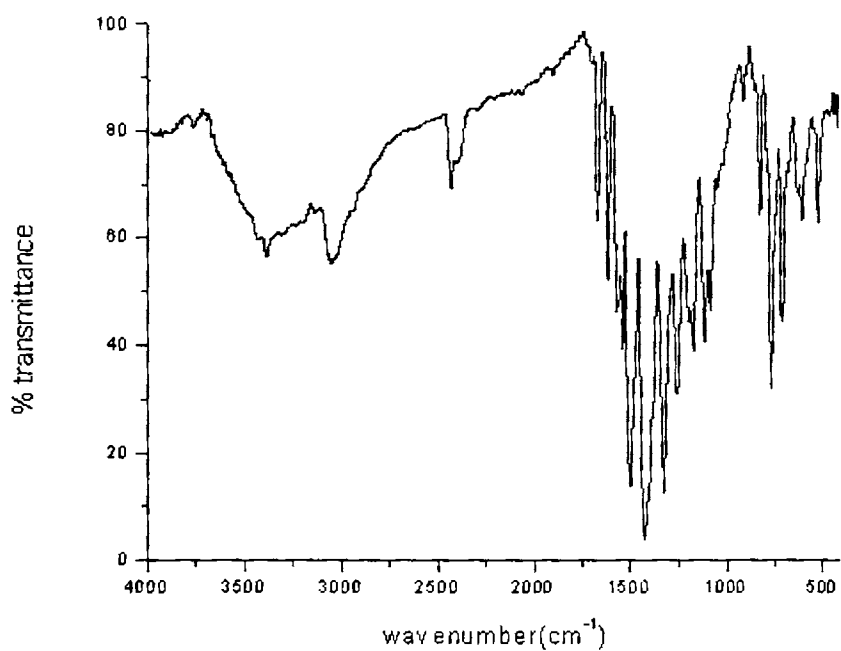


Figure 6.11. IR spectrum of compound  $[\text{Cd}_2(\text{Ac4Ph})_2] \cdot 2\text{H}_2\text{O}$  (31)

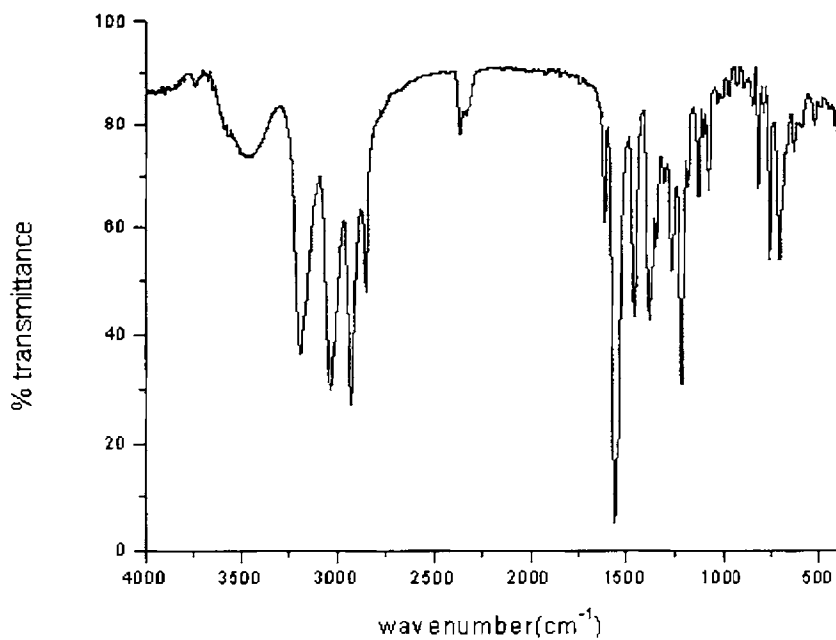


Figure 6.12. IR spectrum of compound  $[\text{Cd}(\text{H}_2\text{Ac}_4\text{Cy})\text{Cl}]\text{Cl}\cdot\text{H}_2\text{O}$  (32)

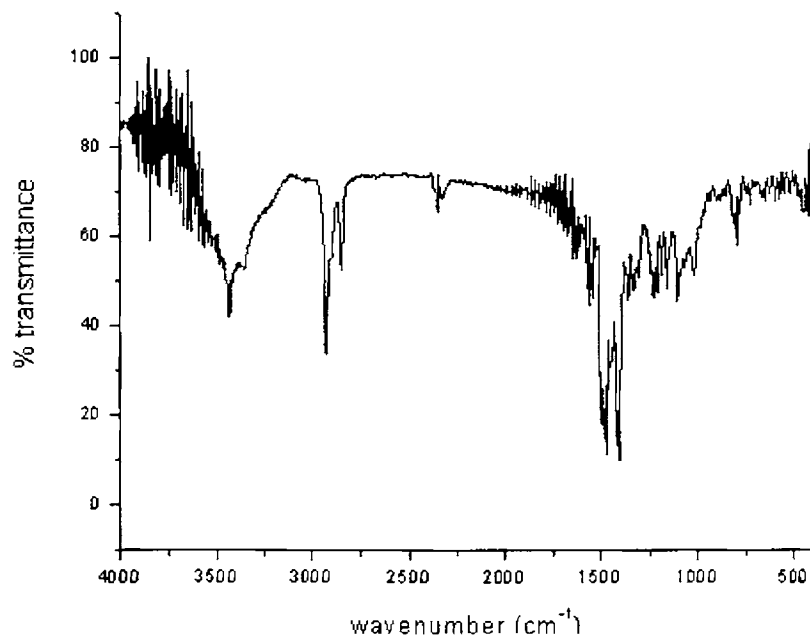


Figure 6.13. IR spectrum of compound  $[\text{Cd}_2(\text{Ac}_4\text{Cy})_2]\cdot\text{H}_2\text{O}$  (33)

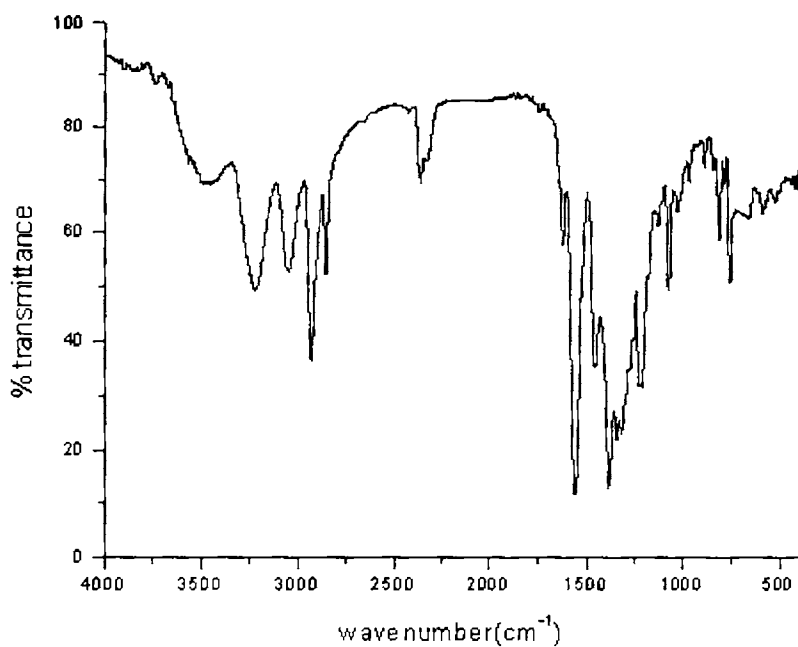


Figure 6.14. IR spectrum of compound  $[\text{Cd}(\text{H}_2\text{Ac}_4\text{Cy})\text{NO}_3]\text{NO}_3 \cdot \text{H}_2\text{O}$  (34)

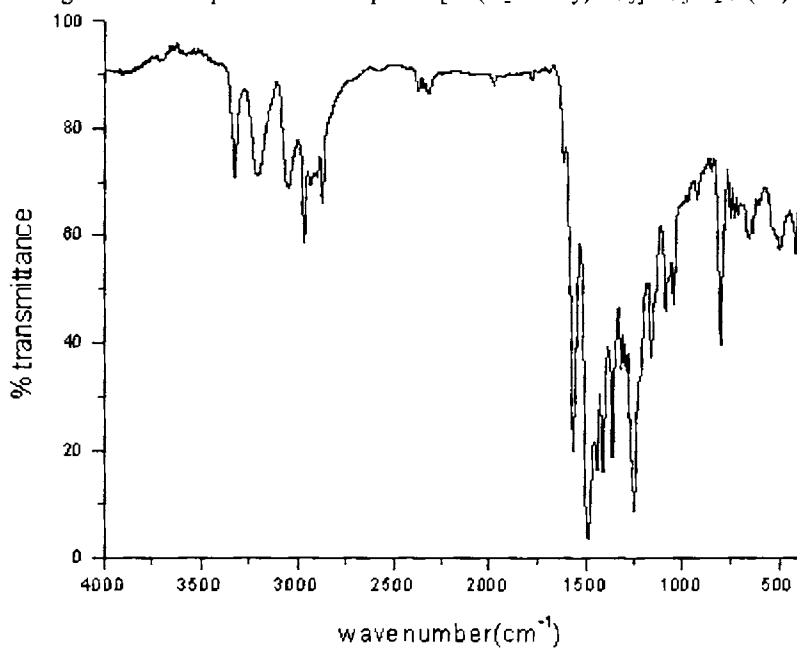


Figure 6.15. IR spectrum of compound  $[\text{Cd}_2(\text{Ac}_4\text{Et}_2)] \cdot \text{H}_2\text{O}$  (36)

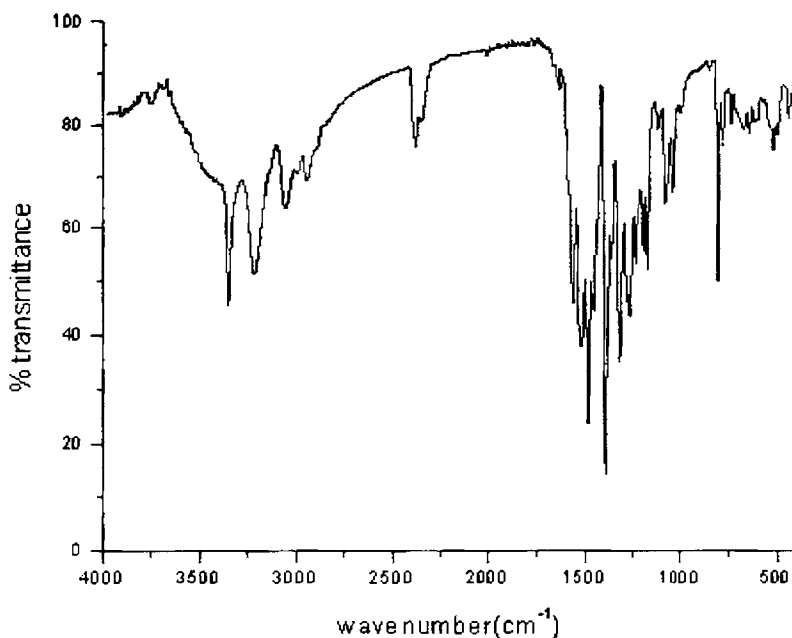
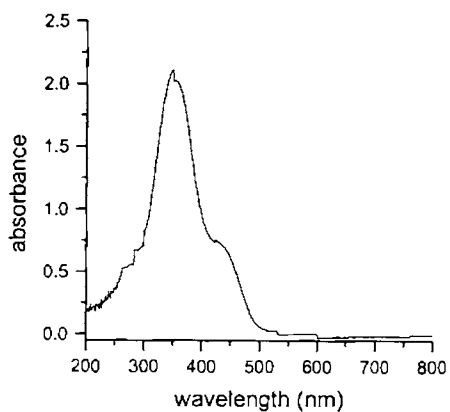


Figure 6.16. IR spectrum of compound  $[\text{Cd}(\text{H}_2\text{Ac}_4\text{Et})\text{Br}]\text{Br}$  (37)

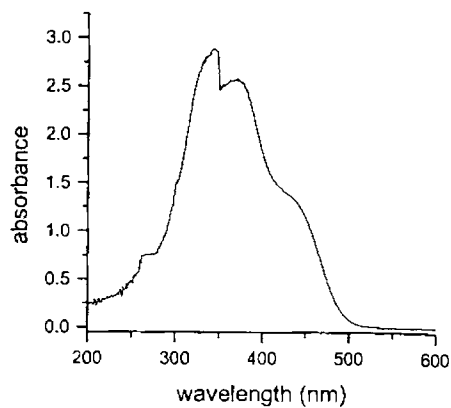
#### 6.4.3b. Electronic spectral studies

For the Cd(II) complexes also, no  $d-d$  transitions are expected. The ligand and charge transfer transitions found are listed in Table 6.9 and representative spectra are in Figure 6.17. The electronic spectra of the ligands recorded in DMF show bands at  $\sim 37,340$  and  $30,187 \text{ cm}^{-1}$  assignable to  $\pi \rightarrow \pi^*$  transitions of the phenyl ring [18-20] and  $n \rightarrow \pi^*$  transitions of the azomethine and thioamide functions respectively [21, 22]. The energy of these bands is slightly shifted upon complexation. The shift of the  $\pi \rightarrow \pi^*$  bands to longer wavelength region in complexes is the result of the  $\text{C}=\text{S}$  bond being weakened and the conjugation system enhanced on complexation [23, 24]. The  $n \rightarrow \pi^*$  bands in the complexes have shown a blue shift due to donation of lone pair of electrons to the metal and hence the coordination of azomethine with a

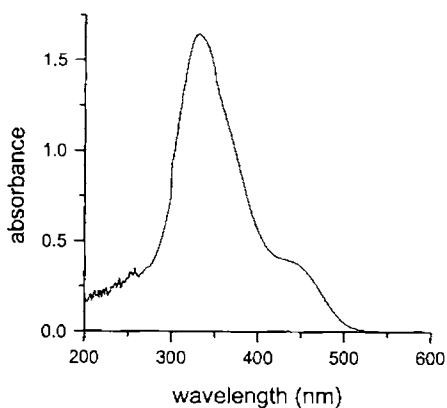
reduction of intensity. A moderately intense broad band for the complexes in the region 22,080-26,750  $\text{cm}^{-1}$  is assigned to  $\text{Cd} \rightarrow \text{S}$  transitions.



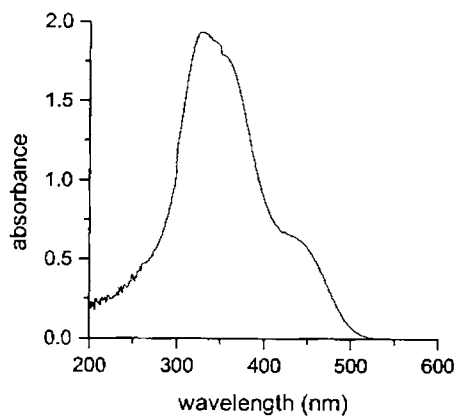
[Cd(HAc4Ph)Cl]·H<sub>2</sub>O (30)



[Cd<sub>2</sub>(Ac4Ph)<sub>2</sub>]·2H<sub>2</sub>O (31)



[Cd(H<sub>2</sub>Ac4Cy)Cl]·Cl·H<sub>2</sub>O (32)



[Cd<sub>2</sub>(Ac4Cy)<sub>2</sub>]·H<sub>2</sub>O (33)

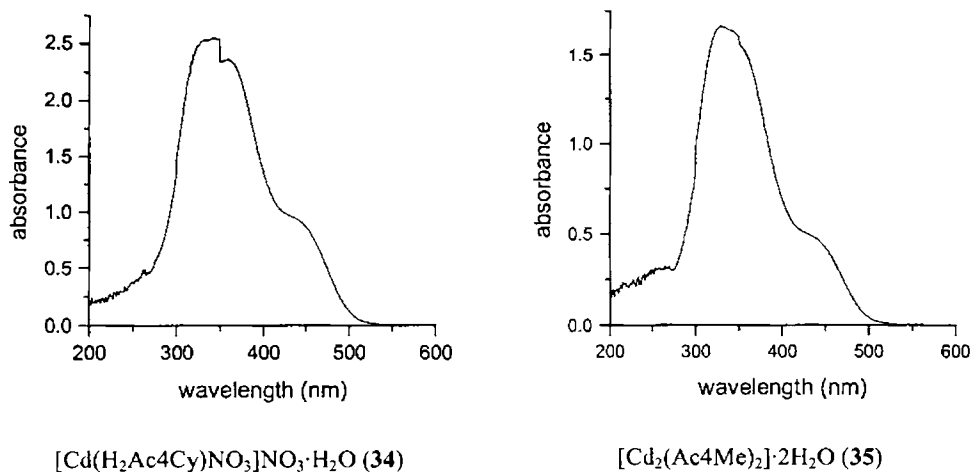


Figure 6.17. Electronic spectra of Cd(II) complexes

Table 6.9. Electronic spectral assignments ( $\text{cm}^{-1}$ ) for the ligands and their Cd(II) complexes

Compound	$\pi \rightarrow \pi^*$	$n \rightarrow \pi^*$	MLCT
$\text{H}_2\text{Ac4Ph}$	32,250	28,900	-
$[\text{Cd}(\text{HAc4Ph})\text{Cl}] \cdot \text{H}_2\text{O}$ (30)	32,060	28,260	24,330
$[\text{Cd}_2(\text{Ac4Ph})_2] \cdot 2\text{H}_2\text{O}$ (31)	32,210	28,530	26,600
$\text{H}_2\text{Ac4Cy}$	32,450	29,210	-
$[\text{Cd}(\text{H}_2\text{Ac4Cy})\text{Cl}]\text{Cl} \cdot \text{H}_2\text{O}$ (32)	32,140	28,960	22,420
$[\text{Cd}_2(\text{Ac4Cy})_2] \cdot \text{H}_2\text{O}$ (33)	31,960	29,200	22,730
$[\text{Cd}(\text{H}_2\text{Ac4Cy})\text{NO}_3]\text{NO}_3 \cdot \text{H}_2\text{O}$ (34)	32,320	29,150	26,740
$\text{H}_2\text{Ac4Me}$	32,050	29,620	-
$[\text{Cd}_2(\text{Ac4Me})_2] \cdot 2\text{H}_2\text{O}$ (35)	32,00	29,500	22,830
$\text{H}_2\text{Ac4Et}$	32,240	29,390	-
$[\text{Cd}_2(\text{Ac4Et})_2] \cdot \text{H}_2\text{O}$ (36)	31,980	28,890	24,130
$[\text{Cd}(\text{H}_2\text{Ac4Et})\text{Br}]\text{Br}$ (37)	32,210	29,230	22,080
$[\text{Cd}(\text{HAc4Et})\text{Cl}] \cdot 4\text{H}_2\text{O}$ (38)	32,030	29,180	24,810

#### 6.4.3c. $^1\text{H}$ NMR spectral studies

Elemental analysis of the compound  $[\text{Cd}(\text{HAc4Ph})\text{Cl}]\cdot\text{H}_2\text{O}$  (**30**) suggested a partial deprotonated ligand, implying the coordination of one arm of the ligand in enolate form. A signal at  $\delta=10.21$  ppm is assigned to the proton at either N(3) or N(6). Such a signal is not present in the case of  $[\text{Cd}_2(\text{Ac4Ph})_2]\cdot 2\text{H}_2\text{O}$  (**31**) indicating the coordination of ligand in the deprotonated form. A signal observed at  $\delta=10.70$  is assigned to N(4) and N(5) protons in both the compounds. Pyridyl ring protons at C(2) and C(4) appear as doublets at *ca*  $\delta=8.65$  and  $8.82$ , while proton at C(3) appears as a doublet of a doublet at *ca*  $7.90$  ppm. Aromatic protons appear in the region  $7.22$ - $8.60$  ppm. The triplet observed at  $7.6$  ppm corresponding to two protons at C(20) and C(22).

$^1\text{H}$  NMR spectra of complexes  $[\text{Cd}(\text{H}_2\text{Ac4Cy})\text{Cl}]\text{Cl}\cdot\text{H}_2\text{O}$  (**32**) and  $[\text{Cd}(\text{H}_2\text{Ac4Cy})\text{NO}_3]\text{NO}_3\cdot\text{H}_2\text{O}$  (**34**) are very similar. In both cases, the signal of hydrogen atoms of the secondary amine (N(3) and N(6) H) has appeared at  $10.23$  ppm and the signal corresponding to the terminal amine hydrogen atoms (N(4) and N(5) H) is shifted to upfield, and it is inside the multiplet of the aromatic hydrogen atoms. In the case of  $[\text{Cd}_2(\text{Ac4Cy})_2]\cdot\text{H}_2\text{O}$  (**33**) there is no signal corresponding to N(3) and N(6)H indicate that in this complex the ligand is dideprotonated. In these compounds **32**, **33** and **34**, signals corresponding to all the aliphatic protons of methyl group and the cyclohexyl moiety appeared in the range  $\delta=1.14$ - $2.92$  ppm.

The  $^1\text{H}$  NMR spectrum of  $[\text{Cd}_2(\text{Ac4Me})_2]\cdot 2\text{H}_2\text{O}$  (**35**) shows the absence of the NH hydrazine protons (N(3) and N(6)), present in the free

ligand. This is in agreement with the bis-deprotonation of the ligand in the complexes and the coordination to the metals.

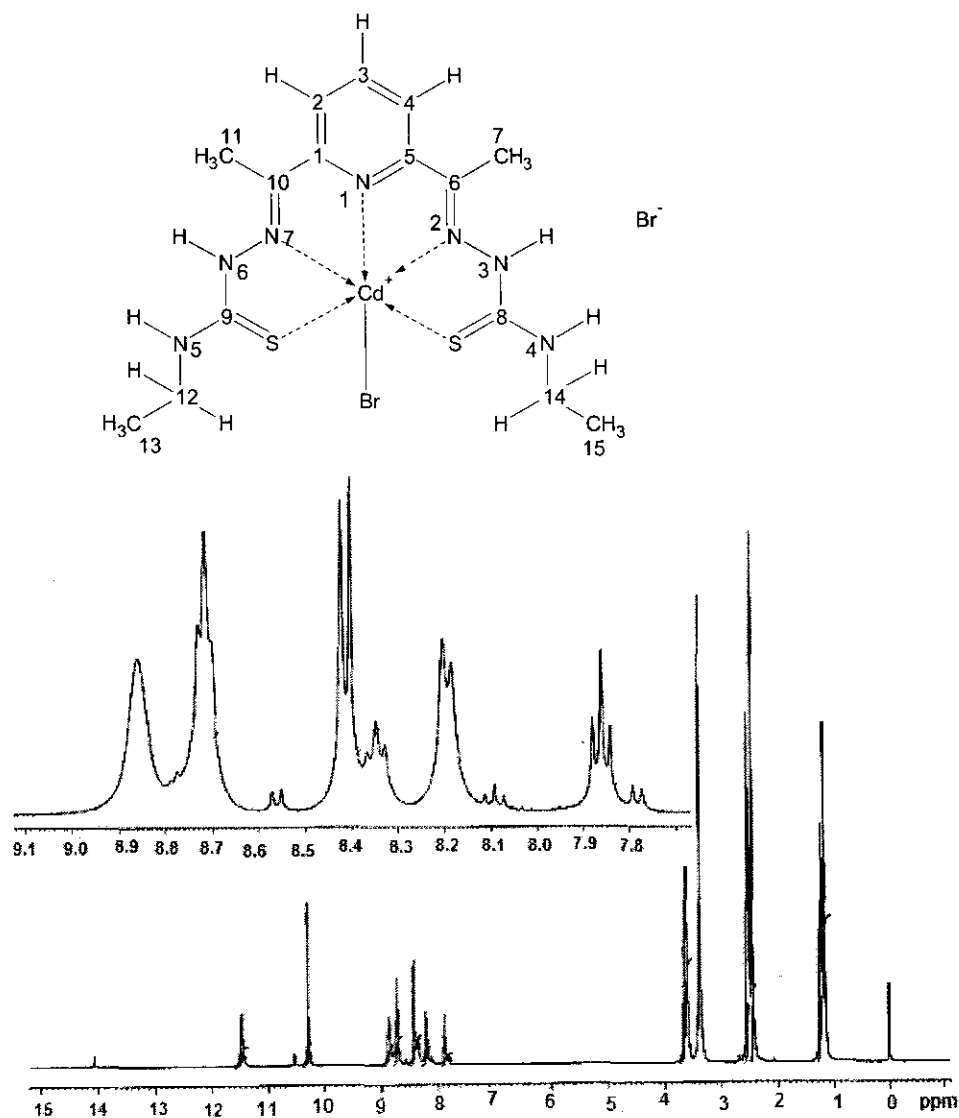
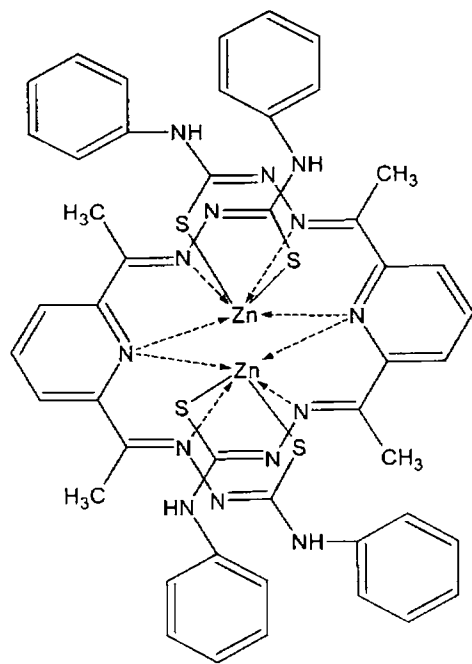


Figure 6.18.  $^1H$  NMR spectrum of compound  $[Cd(H_2Ac_4Et)Br]Br$  (37)

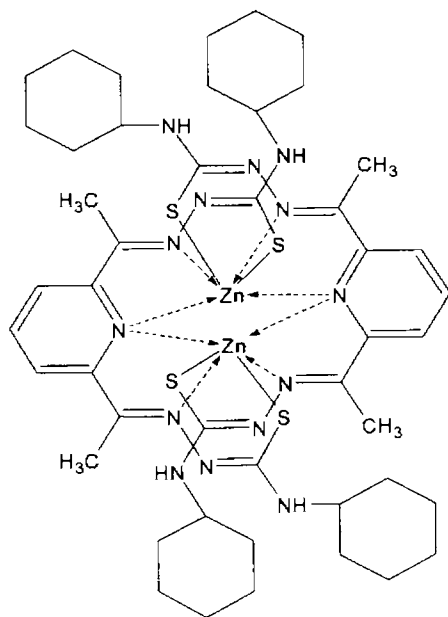


The signal due to NH-Me groups (N(4) and N(5)) is slightly shifted upfield in this complex from 8.65 to 8.48 although these groups are not bound to metal center. A signal observed at 8.42 corresponds to H which are having the same environment. Besides, the complexation provokes important changes in the aromatic region. Signals of the pyridine protons are shifted with respect to the ligand, their positions being exchanged. This is an indication of the coordination of the metal to the pyridine nitrogen atom. Aliphatic region shows two signals corresponding to the methyl groups, which do not undergo significant changes.

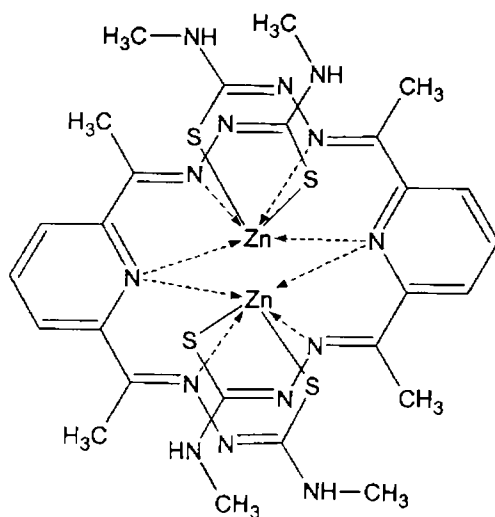
Based on the elemental analyses and spectral studies, following tentative structures were assigned for the complexes. Solvent molecules are not included in structures for clarity. Single crystals of one of the Zn(II) compound (**27a**) of X-ray diffraction quality were grown from its solution in DMF and dichloromethane in 1:1 ratio by slow evaporation over a period of 5 days. Such types of compounds are reported earlier with different geometry [30-32]. Despite repeated attempts, we were unable to obtain the cadmium(II) complex in a suitable crystalline form for X-ray study. However, in view of its very low solubility in most of the common polar and non-polar organic solvents a monomeric five-coordinate geometry for [Cd(SNNNS)] is very unlikely. Because of the tendency of the cadmium(II) ion to form six-coordinate complexes, it is likely that the complex has a pyridine-nitrogen-bridged dimeric structure.



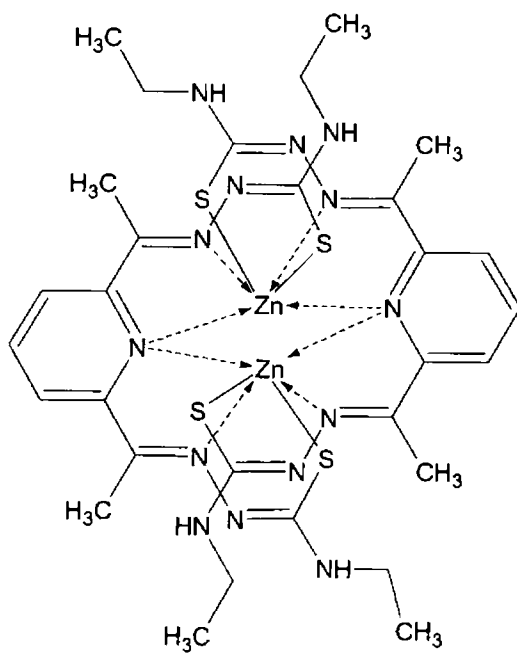
**[Zn<sub>2</sub>(Ac<sub>4</sub>Ph)<sub>2</sub>]·2H<sub>2</sub>O (26)**



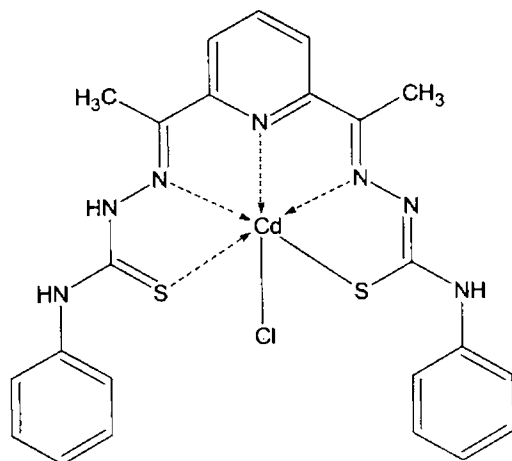
**[Zn<sub>2</sub>(Ac<sub>4</sub>Cy)<sub>2</sub>]·H<sub>2</sub>O (27)**



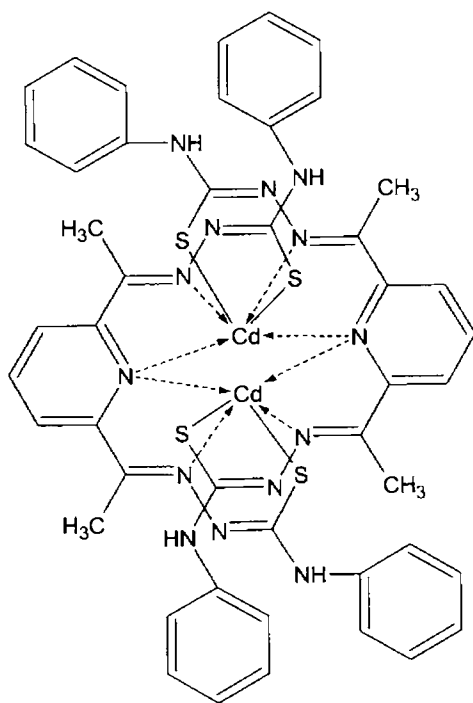
$[\text{Zn}_2(\text{Ac4Me})_2] \cdot \text{H}_2\text{O}$  (28)



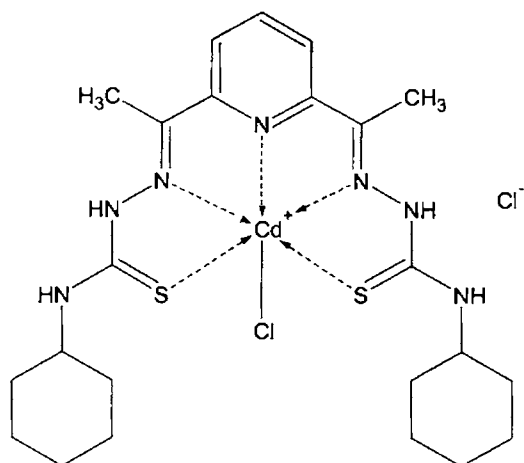
$[\text{Zn}_2(\text{Ac4Et})_2] \cdot \text{H}_2\text{O}$  (29)



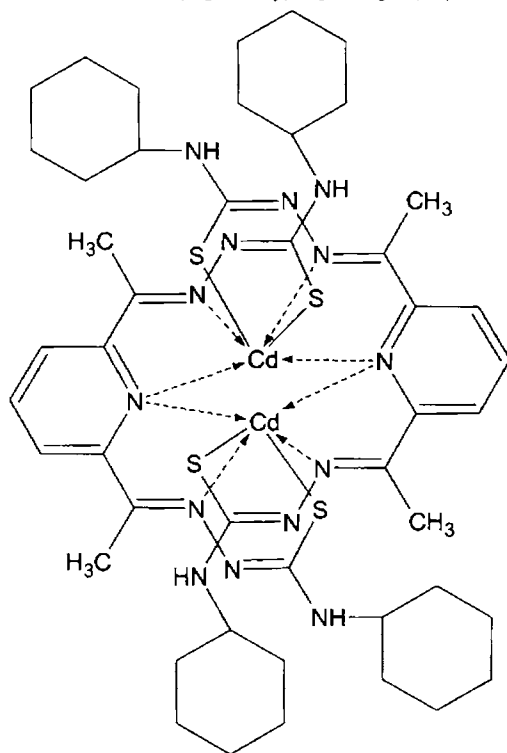
**[Cd(HAc4Ph)Cl]·H<sub>2</sub>O (30)**



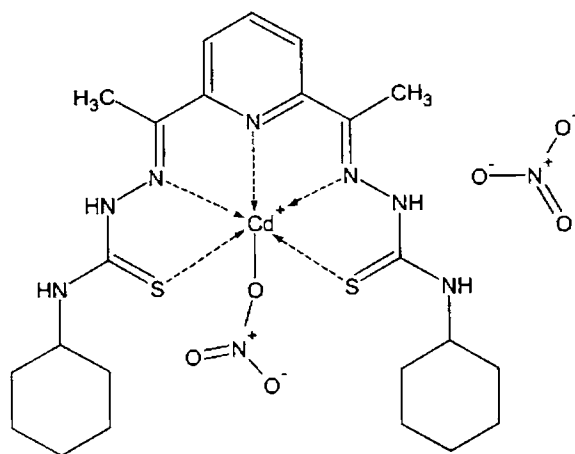
**[Cd<sub>2</sub>(Ac4Ph)<sub>2</sub>]·2H<sub>2</sub>O (31)**



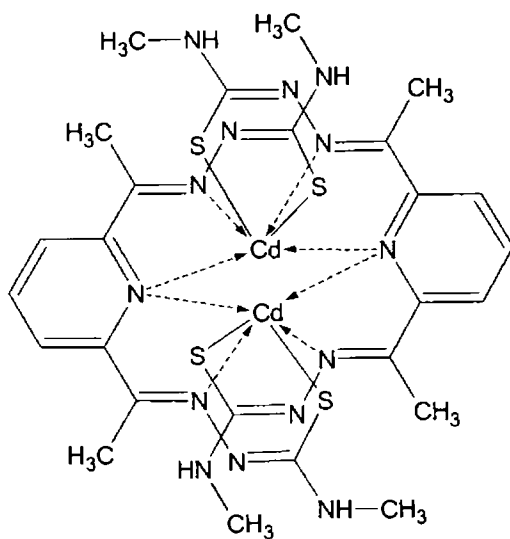
$[Cd(H_2Ac_4Cy)Cl]Cl \cdot H_2O$  (32)



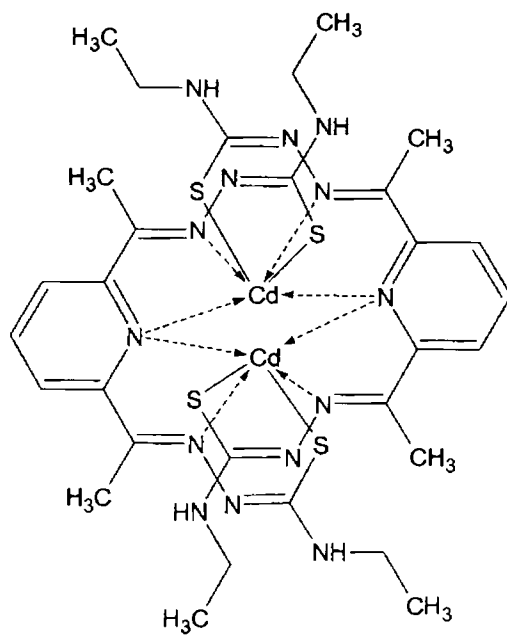
$[Cd_2(Ac_4Cy)_2] \cdot H_2O$  (33)



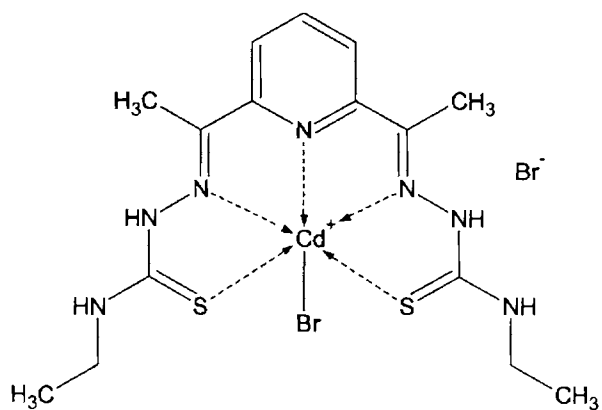
**[Cd(H<sub>2</sub>Ac<sub>4</sub>Cy)NO<sub>3</sub>]NO<sub>3</sub>·H<sub>2</sub>O (34)**



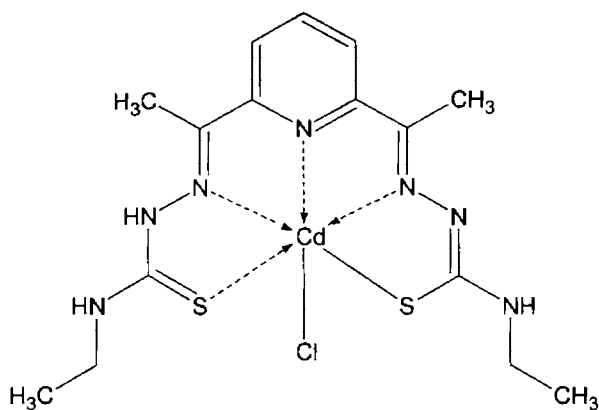
**[Cd<sub>2</sub>(Ac<sub>4</sub>Me)<sub>2</sub>]·2H<sub>2</sub>O (35)**



$[\text{Cd}_2(\text{Ac4Et})_2] \cdot \text{H}_2\text{O}$  (36)



$[\text{Cd}(\text{H}_2\text{Ac4Et})\text{Br}] \text{Br}$  (37)



[Cd(HAc4Et)Cl]·4H<sub>2</sub>O (38)

### Concluding remarks

This chapter deals with the synthesis and spectral characterization of four zinc(II) complexes and nine cadmium(II) complexes of four ligands viz. 2,6-diacetylpyridine bis(*N*<sup>4</sup>-phenylthiosemicarbazone) [H<sub>2</sub>Ac4Ph], 2,6-diacetylpyridine bis(*N*<sup>4</sup>-cyclohexylthiosemicarbazone) [H<sub>2</sub>Ac4Cy], 2,6-diacetylpyridine bis(*N*<sup>4</sup>-methylthiosemicarbazone) [H<sub>2</sub>Ac4Me], 2,6-diacetylpyridine bis(*N*<sup>4</sup>-ethylthiosemicarbazone) [H<sub>2</sub>Ac4Et]. Both the zinc complexes and cadmium complexes were characterized by partial elemental analyses, molar conductivity and IR, electronic and NMR spectral studies. Yellow colored single crystals suitable for X-ray analysis were obtained in the case of compound 27. This reveals a novel structure for this compound. Two dimers present in one asymmetric unit are having four zinc atoms with different coordination mode. The structures proposed for the remaining complexes are tentative because of the lack of X-ray crystal structure data.



## References

1. R.H. Prince, *Adv. Inorg. Radiochem.* 22 (1979) 349.
2. L.S. Sarma, J.R. Kumar, K.J. Reddy, T. Thriveni, A.V. Reddy, *J. Braz. Chem. Soc.* 17 (2006) 463.
3. T. Walsh, H. Sandstead, A.S. Prasad, P.M. Newberne, J. Pamela . *Zinc: Health Effects* Carol Boston University School of Medicine, Boston, 1990.
4. H. Sakurai, Y. Kojima, Y. Yoshikawa K. Kawabe, H. Yasui. *Coord. Chem. Rev.* 226 (2002) 187.
5. M.B. Ferrari, G.G. Fava, C. Pelizzi, P. Tarasconi, *J. Chem. Soc., Dalton Trans.* (1992) 2153.
6. G.D. Munno, S. Mauro, T. Pizzino, D Viterbo, *J. Chem. Soc., Dalton Trans.* (1993) 1113.
7. H.P. Srivastava, D. Tiwari, *J. Indian Chem. Soc.* 70 (1993) 499.
8. M.D. Walker, D.R. Williams, *J. Chem. Soc., Dalton Trans.* (1974) 1186.
9. G. Faraglia, R. Graziani, Z. Guo, U. Casellato, S. Sitran, *Inorg. Chim. Acta* 192 (1992) 17.
10. J.S. Casas, A. Sanchez, J. Bravo, S. Garcia-Fontan, E.E Castellano, M.M. Jones, *Inorg. Chim. Acta* 158 (1989) 119.

11. M.A. Romero-Molina, M.D. Gutierrez-Valuro, R. Lopez-Garzon, J.M. Salas-Peregrin, M.I. Arriortua, F.J. Zufiiga, *Inorg. Chim. Acta* 136 (1987) 87.
12. G. Atassi, P. Dumont, J.C. Harteel, *Eur. J. Cancer* 15 (1979) 451.
13. G.M. Sheldrick, *Acta Crystallogr. A* 46 (1990) 467.
14. G.M. Sheldrick, SHELXS-97 Program for the solution of Crystal Structures, University of Göttingen, Göttingen, Germany, 1997.
15. A.L. Spek, PLATON, A Multipurpose Crystallographic Tool, Utrecht University, Utrecht, The Netherlands, 1999.
16. R.C. De Conti, B.R. Toftner, K.C. Agrawal, R. Tomchick, J.A.R. Mead, J.R. Bertino, A.C. Sartorelli, W.A. Creasy, *Cancer Res.* 32 (1972) 455.
17. M. Mohan, A. Agarawal, N.K. Jha, *J. Inorg. Biochem.* 34 (1988) 41.
18. A. Bino, N. Cohen, *Inorg. Chim. Acta* 210 (1993) 11.
19. W.J. Geary, *Coord. Chem. Rev.* 7 (1971) 81.
20. R.P. John, A. Sreekanth, M.R.P. Kurup, H.-K. Fun, *Polyhedron* 24 (2005) 601.
21. R.P. John, A. Sreekanth, M.R.P. Kurup, A. Usman, I.A. Razak, H.-K. Fun, *Spectrochim. Acta A* 59 (2003) 1349.
22. M. Nazimuddin, M.A. Ali, F.E. Smith, *Polyhedron* 10 (1991) 1327.

23. E. Bermejo, R. Carballo, A. Castineiras, R. Dominguez, A. E. Liberta, C. Maichle-Mossmer, D.X. West, *Z. Naturforsch., B. Chem. Sci.* 54 (1999) 777.
24. A. Castineiras, E. Bermejo, D.X. West, L.J. Ackerman, J.Valde-Martinez, S. Hernandez-Ortega, *Polyhedron* 18 (1999) 1463.
25. A.D. Naik, V.K. Revankar, *Proc. Indian Acad. Sci (Chem. Sci.)* 113 (2001) 285.
26. V. Philip, V. Suni, M. Nethaji, M.R.P. Kurup, *Polyhedron* 25 (2006) 1931.
27. I.-X. Li, H.A. Tang, Yi-Zhi Li, M. Wang, L.-F. Wang, C.-G. Xia, *J. Inorg. Biochem.* 78 (2000) 167.
28. M.C. Rodriguez-Arguelles, M.B. Ferrari, F. Bisceglie, C. Pelizzi, G. Pelosi, S. Pinelli, M. Sassi, *J. Inorg. Biochem.* 98 (2004) 313.
29. K. Nakamoto, *Infrared and Raman spectra of Inorganic and Coordination compounds*, 5<sup>th</sup> ed., Wiley, New York, 1997.
30. R. Pedrido, M.R. Bermejo, M.J. Romero, M. Vázquez, A.M.González-Noya, M. Maneiro, M.J. Rodríguez, M.I. Fernández, *Dalton Trans.* (2005) 572.
31. G.F. de Sousa, D.X. West, C.A. Brown, J.K. Swearingen, J.Valdés-Martínez, R.A. Toscano, S. Hernández-Ortega, M. Hörner, A.J. Bortoluzzi, *Polyhedron* 19 (2000) 841.
32. E. Labisbal, A. Castineiras, C.A. Brown, D.X. West, *Z. Naturforsch* 56b (2001) 229.

Transition metal complexes of bis(thiosemicarbazone) (btsc) ligands have been investigated as metallodrugs for a number of years. Recent studies of metal complexes of tetradentate bis(thiosemicarbazones) have included a number of structural, as well as biological studies. Coordination of heterocyclic bis(thiosemicarbazones) as neutral, monoanionic and dianionic ligands is possible depending on the metal center and the particular metal salt selected for complex preparation. To date, these ligands have been shown to coordinate as planar pentadentate and tetradentate ligands to one metal center or bridging ligands in binuclear complexes.

Further structural studies of complexes of these ligands will likely expand the field with new modes of coordination. Substitution on the thiosemicarbazone moieties will help to achieve these new modes of coordination. Spectral and structural studies have been carried out on metal complexes of 2,6-diacetylpyridine bis{N(4)-substituted thiosemicarbazones}. However considerable interest has been shown in 2,6-diacetylpyridine bis(thiosemicarbazone), and its metal complexes.

Chapter 1 deals with an extensive literature survey relating the applications and recent developments in the field of bis(thiosemicarbazones) and their transition metal complexes. The objectives of the present study and a brief introduction to the various analytical methods are also included in this chapter.

Chapter 2 deals with the syntheses and characterization of four bis(thiosemicarbazone) ligands. The ligands synthesized are:

- 1) 2,6-diacetylpyridine bis(*N*<sup>4</sup>-phenylthiosemicarbazone) [H<sub>2</sub>Ac4Ph]
- 2) 2,6-diacetylpyridine bis(*N*<sup>4</sup>-cyclohexylthiosemicarbazone) [H<sub>2</sub>Ac4Cy]

- 3) 2,6-diacetylpyridine bis(*N*<sup>4</sup>-methylthiosemicarbazone) [H<sub>2</sub>Ac4Me]
- 4) 2,6-diacetylpyridine bis(*N*<sup>4</sup>-ethylthiosemicarbazone) [H<sub>2</sub>Ac4Et]

The ligands consist of three nitrogens and two sulfur atoms capable of coordination with the metal ion. The four ligands were characterized by <sup>1</sup>H NMR, IR and electronic spectral studies.

Chapter 3 gives a view of the nine Cu(II) compounds synthesized and characterized by various spectroscopic techniques such as IR, electronic spectral studies and EPR. The ligands are found to coordinate in the neutral form and in enolate form. The magnetic susceptibility measurements are also done. Mononuclear Cu(II) complexes exhibit magnetic moments in the range 1.5-1.9 B.M., which are close to the spin only value. The magnetic moments of the binuclear Cu(II) complexes were found to be in the range 1.15-1.40 B.M. In the electronic spectral studies, the d-d transitions are found to be broad. So the three *d-d* transitions could not be assigned. The IR spectral studies revealed that the azomethine bands are found to be shifted as a result of its coordination to the metal centre. The molar conductivity values indicate that all the complexes are non-electrolytes, with values at high end of the non-electrolyte range suggesting that the anion and the ligand are coordinated to the central copper(II). EPR spectra of all the Cu(II) complexes were recorded both in polycrystalline state at 298 K and at solution in DMF at 77 K. The g values and the various EPR spectral parameters are calculated. The EPR spectra of some complexes exhibit a half field signal *ca* 1500 gauss and it is a useful criterion for dipolar interaction from the presence of some dinuclear or trinuclear complex formation. Unfortunately instead of repeated attempts we were unable to obtain X-ray quality single crystals for structural studies of these metal complexes.

Chapter 4 deals with the synthesis and characterization of five Mn(II) compounds. Elemental analyses suggested different stoichiometries for all the five complexes. The compounds were characterized by various spectral studies. In all the complexes except [Mn(Ac4Ph)H<sub>2</sub>O], the ligands act as pentadentate neutral molecules and coordinate to Mn(II) ion through two thione sulfur atoms, two azomethine nitrogens and the pyridine nitrogen, suggesting a heptacoordination. While in compound [Mn(Ac4Ph)H<sub>2</sub>O], the dianionic ligand is coordinated to the metal by losing its amide protons from the two thiosemicarbazone moieties, suggesting six coordination in this case. The magnetic moments of the five Mn(II) complexes are calculated from the magnetic susceptibility measurements are found in the range 5.78-6.08 B.M., indicating the presence of five unpaired electrons. The EPR spectral studies showed that in some compounds there is appreciable zero-field splitting. The six hyperfine splittings observed correspond to coupling of unpaired electron with that of Mn nucleus with  $I=5/2$ . In one case five  $g$  values are obtained corresponding to five transitions with different energy, appear at different positions, each with six hyperfine splittings. The IR and electronic spectral studies are also done.

Chapter 5 deals with that of eight Ni(II) and three Pd(II) compounds. The compounds were characterized by various spectral studies. The mode of coordination is different for all the four bis(thiosemicarbazone) ligands. In some of the compounds it coordinates as a dianionic ligand and in some other cases it coordinate as neutral ligand. It is very interesting to note that in compounds [Ni(HAc4Cy)OAc]·C<sub>2</sub>H<sub>5</sub>OH and [Ni(HAc4Et)OAc]·CH<sub>3</sub>OH the ligand coordinate both as thiol form *via* deprotonation of the S-H group and as thione form. Magnetic susceptibility measurements of Ni(II) complexes indicated the presence of two unpaired electrons. In the Pd(II) complexes,

ligands are coordinated both in thione form and in thiolate form. The binding of the ligand in monodeprotonated form is evidenced by NMR spectral studies by the observance of the –NH peak. The IR spectral studies also support this. Unfortunately single crystals suitable for X-ray diffraction were not obtained.

Chapter 6 describes the synthesis and characterization of Zn(II) and Cd(II) compounds using various spectral studies and by single crystal X-ray diffraction studies. All the Zn(II) complexes are yellow in color and the ligands are found to be coordinated in the enolate form. The single crystal X-ray diffraction study of the compound  $Zn_4(Ac_4Cy)_4 \cdot 4DMF$  was done. This crystal is monoclinic in nature with  $C2/c$  symmetry and having two dimers in one asymmetric unit. Bis(thiosemicarbazones) on reaction with cadmium(II) salts has been shown to be very interesting in that, three different types of complexes were obtained, independent of the nature of cadmium(II) salts. In some compounds the ligand acts as mono anionic by losing one of its amide protons while in some other compounds the ligand acts as a neutral molecule suggesting six coordination in both cases. But in the case of the remaining Cd(II) complexes ligands act as dianionic and are coordinated in enolate form and these complexes may probably suggest a dimeric structure having a six coordinate geometry since five coordination is less common in the case of Cd(II) complexes. All the complexes are found to be diamagnetic as expected due to the  $d^{10}$  configuration of the metal ion.

\*\*\*\*\*

## ***Curriculum Vitae***

### **PERSONAL PROFILE**

Date of Birth	27 <sup>th</sup> June 1979
Permanent address	Shreyas Pakkil P.O Kottayam 686 012, Kerala Ph.No. 0481- 2361964

### **EDUCATION**

1994	SSLC B.I.G.H.S, Pallom, Kottayam (88.5 %)
1994-1996	Pre-Degree BCM College, Kottayam (71.2%)
1996-1999	B.Sc. Chemistry CMS College, Kottayam (75.7%)
1999-2001	M.Sc. Pure Chemistry CMS College, Kottayam (60.7%)
2001-2002	B.Ed. (Physical Science) St.Joseph's Training College Mannanam, Kottayam (65.9 %)
2003-2004	M.Phil. (Chemistry) Dept. of Applied Chemistry CUSAT Kochi – 682022 (67.7 %)